New insights into subglacial meltwater drainage pathways from the ArcticDEM

Emma La Marre Lewington

A thesis submitted in partial fulfilment of the requirements for the Doctor of Philosophy

The University of Sheffield
Faculty of Social Sciences
Department of Geography

September 2020

ABSTRACT

Subglacial hydrology has been linked to some of the most dynamic ice sheet behaviour and is likely a key regulator of the impacts of climate change on ice sheet mass balance. Evidence of palaeo-meltwater drainage on the beds of former ice sheets enables a large-scale assessment of the distribution and nature of the subglacial hydrological system, which helps to contextualise spatio-temporally limited observations from contemporary ice masses.

In this thesis I develop a new fully-automatic mapping method to detect and map meltwater tracks. I use this as a starting point for holistic meltwater feature mapping (i.e. incorporating a range of erosional to depositional signatures) to investigate the nature and evolution of the subglacial drainage system across the former Keewatin sector of the Laurentide Ice Sheet. I map a range of meltwater features (i.e. eskers and associated assemblages, tunnel valleys and meltwater tracks) and propose the grouping of tunnel valleys and meltwater tracks under the term 'meltwater corridor'. I then propose a formation theory for meltwater corridors based on the repeated interaction between a conduit and the surrounding hydraulically-connected distributed drainage system driven by variable surface meltwater inputs. This is a process known to occur in contemporary settings and is able to account for the observations made from the holistic landform map. This provides new insight into the distribution and nature of the subglacial hydrological system over a large area. Results within also contribute to a better understanding of temporal relationships through the use of eskers beads and fans as a time-transgressive signature, provide a mechanism for sediment access and entrainment at the bed and links the presence of meltwater pathways to the formation and preservation of other subglacial bedforms (e.g. drumlins and ribbed moraines) and overlying ice sheet dynamics. This thesis has benefited enormously from the recent release of freely available, widespread high-resolution digital elevation data – the ArcticDEM – which has enabled the identification and mapping of meltwater drainage signatures.

CONTENTS

Chapter 1: Introduction

Chapter 2: An automated method for mapping geomorphological expressions of former subglacial meltwater pathways from high resolution digital elevation data

Chapter 3: A model for interaction between conduits and surrounding hydraulically connected distributed drainage based on morphological evidence from Keewatin, Canada

List of figures

List of tables

ACKNOWLEDGEMENTS

CHAPTER 1: INTRODUCTION

1.1 Significance and Rationale

1.1.1 Ice sheet hydrology and dynamics

The subglacial hydrological system is key to understanding ice sheet mass balance regulation (Williams et al. 2020) and some of the most dynamic ice sheet behaviour (e.g. Zwally et al. 2002; Joughin et al. 2008; Sole et al. 2011; Rennermalm et al. 2013; Nienow et al. 2017), which ultimately influences future sea level rise, ocean circulation and climate (Cazenave and Llovel, 2010; Rignot et al. 2011; Gillet-Chaulet et al. 2012; Bamber and Aspinall, 2013; Nick et al. 2013). The presence of water at the bed has been linked to enhanced basal sliding and deformation facilitating faster ice motion (e.g. Alley et al. 1986; Englehardt and Kamb, 1997) as well as reduced motion in response to water re-routing, basal freeze-on and substrate stiffening (e.g. Alley et al. 1994; Anadakrishnan and Alley, 1997; Tulaczyk et al. 2000; Bougamont et al. 2003; Bell, 2008) at centennial and longer timescales. Additionally, variations in water pressure at the bed - largely controlled by the configuration of the drainage system and its ability to accommodate water inputs - are key regulators of dynamic shorter term changes in ice motion (i.e. decadal and less) with the presence of an efficient drainage system reducing basal water pressure and thus motion (e.g. Schoof, 2010; Hewitt, 2013) and an inefficient system increasing water pressure and facilitating fast ice flow (e.g. Kamb, 1987; Zwally et al. 2002; Williams et al. 2020). The distribution and nature of the subglacial drainage network is therefore a crucial control on ice sheet dynamics and long term ice sheet mass balance.

This thesis utilises geomorphological evidence from the bed of the Laurentide Ice Sheet (LIS) to explore the nature and distribution of subglacial drainage at an ice sheet scale. Much of the literature used to explore the processes involved in generating these geomorphic signatures is based on examples from the Greenland Ice Sheet (GrIS) where a lot of the large-scale (i.e. ice sheet) contemporary research on hydro-dynamics has been undertaken (see Nienow et al. (2017) for a review). Much of the Greenlandic research has focussed on the south-western margins where the ice sheet is land terminating, situated on resistant Precambrian shield and

experiencing rapid surface melt and resultant melt-induced ice velocity fluctuations over various spatial and temporal scales. This is expected to be the best analogue for the rapidly deglaciating Keewatin sector of the LIS studied here (see Greenwood et al. (2016) for a discussion).

Nonetheless, ice sheet scale research at the GrIS remains a relatively recent development and much of this has been inspired by pioneering work based on mountain glaciers (e.g. Hubbard and Nienow, 1997; Fountain and Walder, 1998; Irvine-Fynn et al. 2011) which I have also drawn on in places to explore processes in more detail. The Antarctic Ice Sheet (AIS) has traditionally been thought to have a rather different ice sheet hydrological system with limited surface meltwater inputs and drainage at the bed dominated by slow, distributed drainage networks (e.g. Ashmore and Bingham, 2014). Nevertheless, research suggests that AIS hydrology still influences ice sheet dynamics and mass loss (e.g. Nitsche et al. 2013), for example through the active drainage and refill of numerous subglacial lakes, often over significant distances (e.g. Fricker et al. 2007; Stearns et al. 2008; Carter et al. 2009; Flament et al. 2014). Furthermore, there is increasing evidence to support the widespread development of surface lakes around the margins of the AIS during the melt-season (e.g. Langley et al. 2016; Kingslake et al. 2017; Lenaerts et al. 2017; Stokes et al. 2019; Tuckett et al. 2019; Moussavi et al. 2020), with these shown to impact ice shelf stability (e.g. Scambos et al. 2000, 2004; Banwell et al. 2013b; Langley et al. 2016) and more recently, grounded ice dynamics (Tuckett et al. 2019). As such, examples from the Antarctic literature are also drawn on in places, specifically with regards to the role of hydrology on ice stream dynamics and for examples of modern analogues for landform formation at the subglacial bed and ice front.

Meltwater can be generated directly at the ice bed by pressure melting, geothermal heating and / or frictional melting. In areas where air temperatures are high enough to facilitate surface melting, water can also be delivered indirectly in much larger amounts - approximately four orders of magnitude more per year (1,000 – 10,000 mm (Boulton et al. 1995)) - from the surface i.e. supraglacially. Observations from the early 2000s identified a positive relationship between surface meltwater production and ice sheet acceleration at the GrIS (Zwally et al. 2002). This was

subsequently confirmed by Das et al. (2008) who observed the creation of a pathway via hydrofracture from the surface through cold, thick ice delivering water to the bed. This revealed a mechanism for the rapid response of ice flow to changes in climate on less than decadal timescales (Das et al. 2008), representing a paradigm shift as previous work assumed that the GrIS responded to enhanced surface melt through changes in surface mass balance over longer timescales.

Ice sheet hydrology and motion are linked by variations in effective pressure (defined as ice overburden pressure minus subglacial water pressure). Importantly, an increase in basal water pressure results in ice-bed separation (i.e. partial flotation) and reduced ice bed friction and / or enhanced subglacial sediment deformation (where sediments are present) (e.g. Lliboutry, 1968; Engelhardt et al. 1978; Hodge, 1979; Bindschadler, 1983; Iken and Bindschadler, 1986; Fowler, 1987; Iverson et al. 1999; Bingham et al. 2008) causing acceleration of the overlying ice (Bartholomew et al. 2010; Hoffman et al. 2010). Although the overall magnitude of meltwater delivery to the bed is important, the key control on basal water pressure is the variability in meltwater inputs (e.g. Schoof, 2010; Bartholomew et al. 2012) and the system's ability to accommodate it (e.g. Irvine-Fynn et al. 2011; Hall et al. 2013; Flowers et al. 2015). Unlike basal meltwater production, supraglacial meltwater inputs are highly variable over space and time. This results in rapid ice velocity increases associated with increased surface melt events (e.g. Shepherd et al. 2009; Tedstone et al. 2013), supraglacial lake drainages (e.g. Das et al. 2008; Hoffman et al. 2011; Joughin et al. 2013) or even precipitation events (e.g. Doyle et al. 2015; Horgan et al. 2015).

Zwally et al. (2002) identified a direct correlation between surface meltwater production and periods of accelerated ice flow (i.e. periods of enhanced melt coinciding with larger ice sheet accelerations), with the speed-up typically occurring within weeks of melt onset. The recognition of this link caused concern that predicted increases in melt extent and duration would give rise to enhanced mass loss and a positive feedback whereby ice flow acceleration in the ablation zone would cause dynamic thinning (i.e. drawing down ice from the interior), exposing more ice to higher temperatures and enhanced ablation (e.g. Zwally et al. 2002; Krabill et al. 2004; Bell, 2008; Pritchard et al. 2009), resulting in significant mass loss (Parizek and Alley, 2004). However, studies since have found no significant correlation between surface

melt and ice flow when considering annual rather than seasonal patterns, showing that the additional early melt season speed-up during high melt years is offset by a corresponding winter extra slow-down (e.g. Sole et al. 2013; Tedstone et al. 2015; Williams et al. 2020). As the efficiency of the subglacial hydrological system evolves in response to sustained inputs throughout the melt season (e.g. Röthlisberger, 1972), water pressure will decrease, increasing effective pressure and subsequently enhancing ice-bed coupling and reducing ice motion (Röthlisberger, 1972; Schoof, 2010). As the widespread, large channels take some time to close down at the end of the melt season, water from the surrounding distributed drainage system is drawn in and removed resulting in enhanced ice-bed coupling and annual minimum ice velocities (e.g. Sole et al. 2013; Tedstone et al. 2013; van de Wal et al. 2015; Stevens et al. 2016).

On multi-annual timescales a sustained decrease in ice sheet velocity has been observed across the GrIS ablation zone over the past three decades despite a contemporaneous increase in melt (van de Wal et al. 2008; Tedstone et al. 2015; Stevens et al. 2016; Williams et al. 2020). For example, Tedstone et al. (2015) noted a 12 % slow down in a large land terminating sector of the GrIS between 2007 - 2014 and 1985 - 1994 despite a 50 % increase in surface meltwater production (Wilton et al. 2017). While changes in thickness and ice slope could explain ~ 30 % of this (Tedstone et al. 2015), an additional mechanism is also required. Many of the mechanisms relating surface meltwater inputs and ice dynamics are not yet fully understood but regional ice slow-downs have been linked to increasingly large and prevalent channels extending across a greater proportion of the bed (at the expense of the distributed drainage system) which draw in water from the surrounding distributed drainage system (e.g. Sole et al. 2013; Hoffman et al. 2016). This process reduces the pressure within the surrounding distributed drainage network, increasing effective pressure and enhancing ice-bed coupling (Bartholomew et al. 2012; Sole et al. 2013; Tedstone et al. 2015; Cowton et al. 2016). While this occurs annually (i.e. at the end of the melt-season contributing to the annual minimum), it is also proposed to have a cumulative effect with year-on-year enhanced drainage contributing to a net regional slow down as the distributed network is not fully re-pressurised during intervening winters (Pritchard et al. 2009; Helm et al. 2014; Tedstone et al. 2014; van de Wal et al. 2015). However, as would be expected from this mechanism, recent

cooling (2013 – 2019) and a subsequent reduction in meltwater production has resulted in a recent increase in ice velocity likely associated with smaller channels that close faster allowing the surrounding distributed drainage system to re-pressurise (Williams et al. 2020).

Surface meltwater induced speed-ups extend inland throughout the melt season as meltwater supplies increase and changes to the hydrological system propagate gradually upstream (e.g. Nienow et al. 1998; Bartholomew et al. 2010; Chandler et al. 2013; Andrews et al. 2014). However, the inland limit of this at the GrIS is not yet fully known with research suggesting channelisation becomes limited by low ice surface slopes (and thus limited potential energy for melting (e.g. Meierbachtol et al. 2013; Dow et al. 2014)), lower and later melt generation and high overburden pressure (causing increased creep closure), and that the drainage of surface meltwater inputs to the bed further inland may have a different effect (e.g. Phillips et al. 2013; Sole et al. 2013; Doyle et al. 2014). Current work puts this limit at ~ 50 km inland from the margin (Bartholomew et al. 2011; Chandler et al. 2013).

There is growing evidence to suggest that reorganisation of the subglacial hydrological system occurs over centennial and longer timescales and can influence ice stream dynamics and mass balance at both the GrIS and AIS (Bell, 2008; Christianson et al. 2014; Christoffersen et al. 2014; Chu et al. 2016). Changes to the size and location of subglacial catchments in response to variations in basal water pressure and ice surface slope can impact subglacial water routing (e.g. Livingstone et al. 2013; Lindbäck et al. 2015; Chu et al. 2016). These changes to the subglacial drainage network may direct water away from some areas (i.e. 'water piracy' - Anadakrishnan and Alley, 1997; Vaughan et al. 2008; Carter et al. 2013) and towards others, impacting ice sheet dynamics. This is supported by physical experiments which suggest that subglacial hydrology plays a role in ice stream 'lifecycles' and that ice streams can develop, progress and decay in response to interactions between ice flow, subglacial water drainage and basal erosion (Lelandais et al. 2018).

1.1.2 Geomorphological relevance of ice sheet hydrology and dynamics

Subglacial hydrological systems are a key geomorphic agent for eroding, transporting and depositing sediment beneath ice sheets and glaciers (Alley et al. 1997, 2003; Swift et al. 2002). This has ice dynamical implications as, for instance, the thickness and distribution of basal sediments controls the pattern and rate of sediment deformation (Swift et al. 2005a). The type, rate and effectiveness of subglacial meltwater erosion is determined by the nature of the basal sediment, the source, magnitude and variability of the meltwater supply, the drainage system configuration and its access to sediment (Brennand, 1994; Swift et al. 2005a). Subglacial drainage systems with large surface meltwater inputs are identified as key sediment transport systems (Swift et al. 2005a, 2005b; Cook et al. 2020). Cowton et al. (2012) suggest that large volumes of surface meltwater accessing the ice base, as well as efficient evacuation of meltwater, thick ice and rapid ice flow around the margins of the GrIS provide the ideal conditions for generating and evacuating large volumes of subglacial sediment.

Subglacially-produced landforms exposed after retreat provide a rich record for reconstructing palaeo-ice sheets through the process of glacial inversion (Kleman and Borgström, 1996; Kleman et al. 2006). Given the ease of viewing palaeo-meltwater landforms, they have been fundamental in inspiring and guiding conceptual and numerical models of how water organises itself into drainage systems beneath present day ice masses. Such landforms are key to contextualising spatially and temporally limited observations from contemporary ice sheets - where the bed cannot be directly observed and the configuration and evolution of the subglacial drainage network is largely inferred from tracer and borehole monitoring studies and the use of ice dynamic proxies (e.g. Chandler et al. 2013; Andrews et al. 2014; Tedstone et al. 2015) - and are commonly used to support and develop the theory of ice sheet hydrological systems (e.g. Shreve, 1985; Clark and Walder, 1994; Boulton et al. 2007a, 2007b; 2009; Beaud et al. 2018a; 2018b; Hewitt and Creyts, 2019).

The distribution of subglacial meltwater landforms allows former ice sheet extent, relative thickness and retreat patterns to be reconstructed (e.g. Dyke and Prest, 1987; Boulton and Clark, 1990; Clark et al. 2004, 2012; Evans et al. 2005; Ottessen et al.

2008) and provides insight into ice sheet dynamics, thermal regime and subglacial hydrology (e.g. Kleman, 1992; Clark and Walder, 1994; Kleman and Borgstrom, 1996; Stokes and Clark, 1999; Kleman and Glasser, 2007; Margold et al. 2013, 2015; Storrar, et al. 2014a, 2014b; Stokes et al. 2015; Livingstone et al. 2016; Kuhn et al. 2017; Simkins et al. 2017). Eskers, meltwater channels and tunnel valleys which indicate channelised subglacial drainage (i.e. location and direction of former drainage) have typically been the focus of palaeo-meltwater studies (e.g. Shreve, 1985; Brennand, 1994, 2000; Clark and Walder, 1994; Punkari, 1997; Boulton et al. 2007a, 2007b, 2009; Storrar et al. 2014a, 2014b; Livingstone and Clark, 2016); likely due to the lack of appropriate analogues for detecting distributed drainage or its lack of preservation (Greenwood et al. 2016).

1.2 Background

While some surface melt is retained for multiple years in firn at the ice sheet surface, delaying delivery to the bed (e.g. Forster et al. 2014; Kuipers Munneke et al. 2014; Poinar et al. 2019), on bare ice – which is extensive in western Greenland in the boreal summer – a large amount of surface meltwater is transported across the surface in supraglacial stream networks where channels become incised as a result of enhanced heat transfer caused by turbulent water flow (Karlstrom et al. 2013). If these streams intersect with crevasses or moulins (which are themselves formed by a supraglacial stream flowing into a crevasse), water is transported through ice up to several-kilometres thick and delivered to the bed (Fig. 1.1). Together drainage of surface water through crevasses and moulins accounts for ~ 62 % (~ 47 % and ~ 15 % respectively) of ice sheet runoff in west Greenland (Koziol et al. 2017). Crevasses are surface fractures on the ice sheet, which may be extended to the bed by meltwater induced propagation (i.e. hydrofracturing) (Weertman, 1972; van der Veen, 1998; Alley et al. 2005; Krawczynski et al. 2009). Instead of being transferred directly to the bed, surface water may also be stored – often temporarily – within surface lakes. Lakes which do not freeze over may either spill slowly over the surface of the ice sheet (e.g. Tedesco et al. 2013; Kingslake et al. 2015; Koziol et al. 2017) or rapidly drain if there is an initial crack and enough meltwater to drive hydrofracture to the bed (e.g. Das et al. 2008; Krawczynski et al. 2009; Banwell et al. 2012; Doyle et al. 2013; Clason et al. 2015; Koziol et al. 2017). Drainage can occur in less than a day with peak

discharges of up to ~ 8,700 m^3 s^{-1} (Das et al. 2008). Surface lakes drain ~ 3 % during the hydrofracture event itself and a further ~ 21 % from the subsequent pathway developed to the bed (Koziol et al. 2017). Supraglacial lakes are common around the fringes of the GrIS and their coverage is extending inland with increasing surface melt and the inland extension of the ablation zone (Fig. 1.1) (e.g. Howat et al. 2013; Carravick and Quincey, 2014; Fitzpatrick et al. 2014; Ignéczi et al. 2016; Cooley and Christoffersen, 2017). The resulting impact of lake drainages on ice sheet dynamics is determined by whether or not the lake drains entirely (or partially), the rate of drainage (e.g. Tedesco et al. 2013; Kingslake et al. 2015), and the efficiency of the drainage system encounters at the bed.
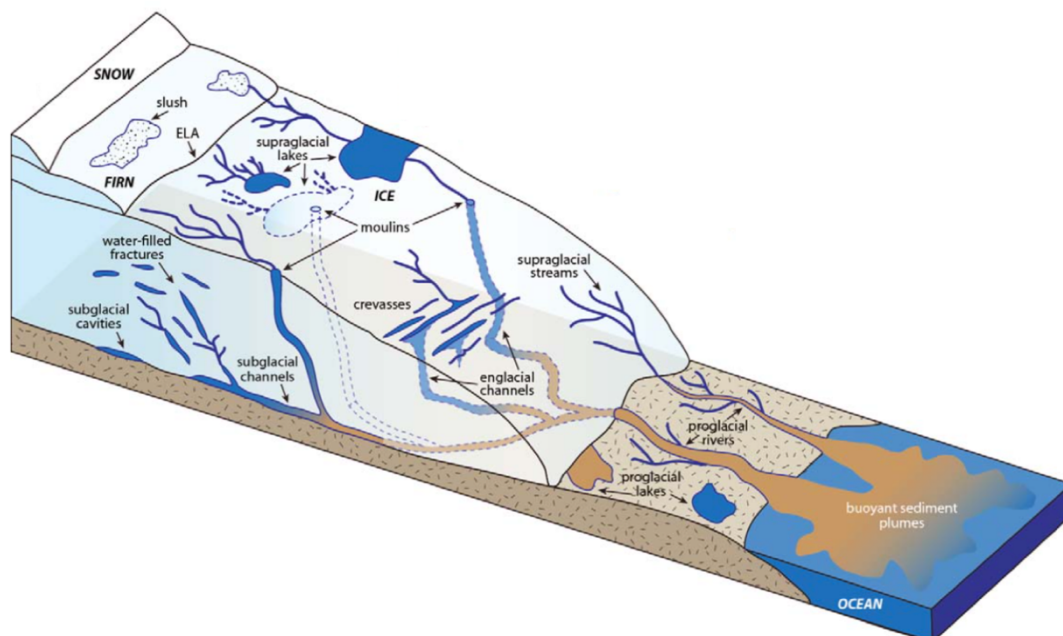
Figure 1.1 Hydrological elements of a land terminating ice sheet (Chu et al. 2014; Modified from Cuffey and Paterson, 2010).

The exact morphology of moulins and surface-to-bed connections are not fully known but contemporary evidence and theory suggest they are near vertical (van der Veen, 2007; Das et al. 2008; Catania and Neumann, 2010; Doyle et al. 2013). Once developed, they likely stay open as long as frictional heat dissipation of the flowing water is greater than the rate of ice creep closure (Fountain and Walder, 1998), potentially sustaining rapid delivery of water directly to the bed throughout the melt

season (Smith et al. 2015). Longer term stability of surface-to-bed connections has also been considered. Surface lakes form in surface depressions largely controlled by underlying topography (e.g. Sergienko, 2013; Ignéczi et al. 2018). Given that there is no significant ice sheet thinning which will alter the transfer of basal topography to the surface (Gudmundsson, 2003; Ignéczi et al. 2018), surface lakes are likely to form in the same location year-on-year. The distribution of crevasses and moulins is thought to be controlled by the tensile stress regime of the ice (often calculated using the von Mises criterion (Vaughan, 1993)) (e.g. Catania et al. 2008; Price et al. 2008; Colgan et al. 2011; Clason et al. 2015; Poinar et al. 2015). Similarly, crevasses and moulins will form in approximately the same location each year given a similar spatial distribution of stress and strain and sufficient surface meltwater (e.g. Poinar et al. 2015). As a result, secondary hydrofracture (i.e. the reactivation of a surface-to-bed connection year-on-year) occurs, contributing to persistent drainage down the same routeway (e.g. Catania and Neumann, 2010; Gulley et al. 2012; Doyle et al. 2013; Stevens et al. 2015; Chudley et al. 2019). The spatial pattern of surface-to-bed connections and their stability is important as this determines where water is injected to the bed and ultimately impacts the organisation of subglacial channels (e.g. Banwell et al. 2016).

Once surface meltwater inputs reach the bed, groundwater flow can remove a certain amount of water at the ice-bed interface but additional drainage structures are often required to prevent water accumulating (Boulton et al. 2007a, 2007b, 2009) and to maintain ice sheet stability. Traditionally the subglacial hydrological system has been conceptualised as a binary model comprising: (a) 'slow', inefficient distributed drainage - taking the form of thin films of water (Weertman, 1972), linked cavities (Lliboutry, 1986; Walder, 1986; Kamb, 1987) and / or groundwater flow (Boulton et al. 1995); and (b) 'fast', efficient channelised drainage with conduits cut either up into the ice (Rothlisberger-channel) or down into the bed (Nye-channel) (e.g. Rothlisberger, 1972; Shreve, 1972; Nye,1973; Hooke et al. 1990) (Fig. 1.2). Wide, shallow sedimentary canals (Walder and Fowler, 1994) are often considered inefficient; however, at times they are able to evacuate water efficiently (Ng, 2000) and are therefore classified as intermediate forms here (Fig. 1.2).
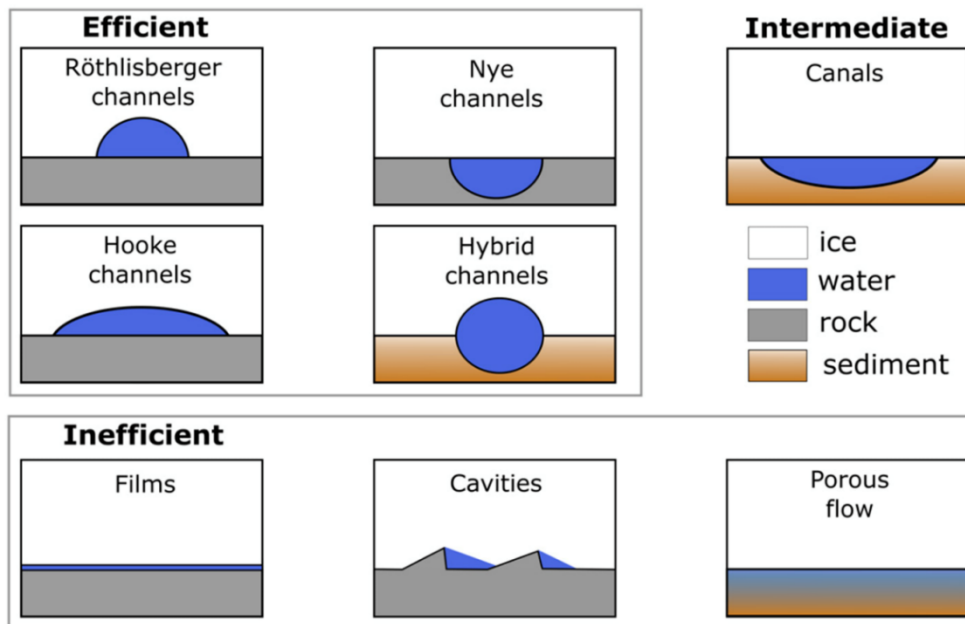
Figure 1.2. Conceptualised efficient, inefficient and intermediate subglacial drainage modes. Ice flow is into the page except for the cavities where it is left to right. (Davison et al. 2019).

The dominant form of inefficient drainage is thought to be cavities which are created in the lee of basal obstacles as ice slides over an irregular bed (e.g. Walder, 1986; Kamb, 1987). Larger cavities form in response to greater sliding, viscosity and discharge rates and lower effective pressure (Walder, 1986; Kamb, 1987) as well as an increase in meltwater supply (Iken et al. 1983; Bartholomaus et al. 2011; Cowton et al. 2016). Cavities may be completely isolated from surface meltwater inputs and other cavities (e.g. Weertman, 1964; Iken and Truffer, 1997) or small orifices may create interconnections between adjacent features. Alternatively, Weertman (1964) predicted a thin, continuous water film (mm's thick) beneath ice with an impermeable bed. However, theory suggests that films greater than several millimetres are unlikely to be stable (Walder, 1982; Weertman and Birchfield, 1983) and are unlikely to contribute much to subglacial water transport.

Exactly how conduits are initiated is poorly understood and typically avoided in numerical models by assigning an initial conduit geometry (e.g. Colgan et al. 2012; Banwell et al. 2013a; Meierbachtol et al. 2013; Dow et al. 2014). Nevertheless, numerical modelling that does incorporate the transition suggests that discharge

variability is a critical control when switching between a cavity and conduit system (Schoof, 2010; Hewitt, 2011). In efficient conduits cut up into the ice (R-channels) or down into the bed (N-channels), increased discharge results in decreased water pressure when in steady state (Röthlisberger, 1972; Hooke, 1984). This is the opposite relationship to that experienced by the distributed system. The capacity of a conduit is determined by the balance between channel expansion caused by turbulent melting and channel closure caused by ice creep (Röthlisberger, 1972; Shreve, 1972). Any energy generated from turbulence above what is required to maintain water temperature at the pressure melting point will contribute to conduit enlargement. Conduits thus become unstable with a low discharge, resulting in closure over the winter when surface inputs are reduced / non-existent and flow does not balance out creep closure (Walder, 1986; Fountain and Walder, 1998; Chandler et al. 2013).
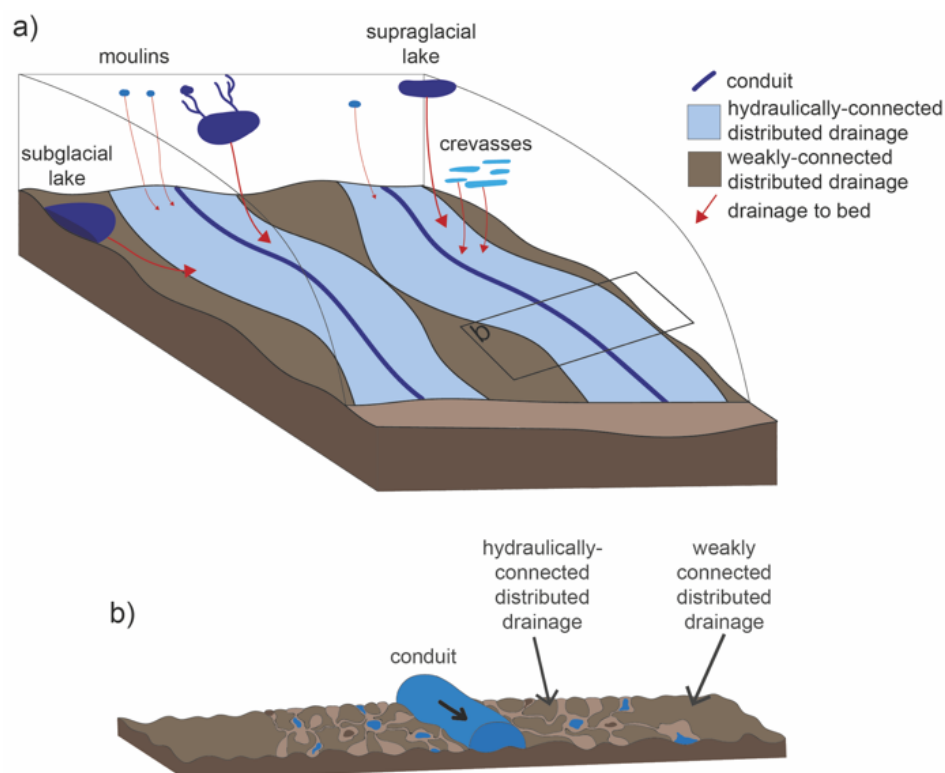
Figure 1.3 Ice sheet hydrological system with varying surface and basal inputs (a) and a three-system drainage model (b). In the three-system drainage model, the hydraulically connected distributed drainage system (light blue in a), is influenced regularly by surface meltwater inputs through the conduit. The weakly-connected distributed drainage system (dark brown) is largely isolated and rarely or never impacted by surface meltwater inputs. At present, the relative

coverage of each is not yet known, nor the precise configuration or relation between each component.

The cross-sectional shape of subglacial conduits has been discussed in the literature with early work assuming a semi-circular shape (e.g. Röthlisberger, 1972); however, others have suggested that it is more likely that conduits are broad and low (i.e. H-channels (Hooke et al. 1990)) (Fig. 1.2). While conduits have typically been classified as R- (i.e. cut up into the ice) or N- (i.e. cut down into the bed), it is also possible that there are 'hybrid' channels (i.e. partly eroded up into the ice and down into the bed (Fig. 1.2)). For example, water within an N-channel may melt the overlying ice and persistent routing within an R-channel will eventually result in downward incision into the bed (Davison et al. 2019).

While the above drainage configurations form the conceptual building-blocks of the subglacial hydrological system, a growing body of research supports the idea that the traditional conception of a binary system is an over-simplification of reality. Instead the dominant mode of drainage is likely to vary over time and space with different modes frequently and extensively connected (e.g. Hubbard et al. 1995; Andrews et al. 2014; Hoffman et al. 2016; Downs et al. 2018; Davison et al. 2019). As a result, a new model has been proposed (Fig. 1.3) comprising: (a) a moulin-connected channelised system which remains hydraulically connected to surface meltwater inputs throughout the melt season; (b) an active hydraulically connected distributed system strongly influenced by the moulin-connected channelised system (and therefore surface inputs across a range of spatial and temporal scales (e.g. Hubbard et al. 1995)) and; (c) a weakly-connected distributed system largely isolated from the channelised system and only rarely – if ever – affected by surface meltwater inputs (Andrews et al. 2014; Hoffman et al. 2016; Rada and Schoof, 2018).

In theory, in a steady-state system, water flows from surrounding high pressure distributed regions into lower pressure conduits. Borehole measurements of subglacial water pressure, modelling and ice velocity proxy data (e.g. Hubbard et al. 1995; Gordon et al. 1998; Bartholomaus et al. 2008; Werder et al. 2013; Tedstone et al. 2014) suggest; however, that given a sufficiently large and rapid spike in water delivery

to a subglacial conduit, the hydraulic gradient can be reversed such that water is forced out of and laterally away from the conduit into the hydraulically connected distributed drainage system. This has been variously termed a Variable Pressure Axis (VPA) (Hubbard et al. 1995), efficient subsystem (Rada and Schoof, 2018), efficient core (e.g. Davison et al. 2019) etc. In this thesis, I use the term hydraulically connected distributed drainage which is considered to be the lateral limit of the influence of pressure variations that originate in a subglacial conduit and cause the flow of water in or out of the conduit. This mechanism has implications for overlying ice sheet dynamics, for example, over pressurisation overwhelms the conduit and can elicit ice flow acceleration and ice sheet surface uplift (e.g. van de Wal et al. 2008; Bartholomew et al. 2011; Doyle et al. 2013; Tedstone et al. 2015). The extent of this dynamic effect is much greater than the area of the bed directly affected by the meltwater.

Beyond the hydraulically connected distributed drainage system, the remaining distributed drainage system – likely composed of cavities – is largely isolated or disconnected from surface meltwater inputs (e.g. Andrews et al. 2014; Hoffman et al. 2016; Rada and Schoof, 2018). This section may still exhibit some slow leakage into the efficient subsystem outlined above (Hoffman et al. 2016; Rada and Schoof, 2018), with the relative amount and locations of water transfer between system components likely determined by the spacing and location of moulins and the conduits they feed (Hoffman et al. 2016). In this thesis I refer to this area as 'weakly connected' following Hoffman et al. (2016). It is possible that pressure spikes – as well as forcing water out from the conduit into the surrounding distributed system – also increase connections between weakly connected drainage and the efficient core (e.g. Davison et al. 2019). This interaction is expected to increase throughout the melt season (Chandler et al. 2013; Hoffman and Price, 2013; Hoffman et al. 2016).

1.2.1 Subglacial palaeo-landforms

Below I detail the key characteristics of a series of common subglacial palaeo-landforms, their formational hypotheses and their use for determining hydrological properties and reconstructing ice sheets.

1.2.1.1 Eskers

Eskers are linear depositional landforms made up of glaciofluvial sand and gravel, metres to tens of metres in width and height. They are typically inferred to represent the former position and morphology of Röthlisberger conduits (R-channels) thermally eroded up into the base of the ice by turbulent water flow (Banerjee and McDonald, 1975; Brennand, 2000), although, eskers can also form englacially and supraglacially (e.g. Price, 1969; Gustavson and Boothroyd, 1987). They exist as individual segments that often align to form networks extending up to several hundreds of kilometres (e.g. Shreve, 1985; Aylsworth and Shilts, 1989; Brennand, 2000; Storrar et al. 2014a; Stroeven et al. 2016). Most long eskers exhibit gaps along their length which may be the result of non-deposition or post-depositional erosion (Banerjee and McDonald, 1975). Eskers are widespread across the beds of the former Laurentide and Fennoscandian ice sheets (e.g. Prest et al. 1968; Aylsworth and Shilts, 1989; Brennand, 2000; Boulton et al. 2001; Storrar et al. 2013; Stroeven et al. 2016) and while some eskers appear relatively isolated, others form dendritic networks with up to fourth-order tributaries (Shilts et al. 1987; Storrar et al. 2014a).

Morphological variations are common along individual esker ridges (Banerjee and McDonald, 1975; Rust and Romanelli, 1975; Hebrand and Amark, 1989; Gorrell and Shaw, 1991; Warren and Ashley, 1994; Brennand, 2000; Mäkinen, 2003; Burke et al. 2015; Perkins et al. 2016; Storrar et al. 2020). Unravelling these variations and categorising eskers based on their morphology and sedimentology (e.g. Brennand, 2000; Perkins et al. 2016) has the potential to reveal further insight into the conditions under which eskers formed and the portion of the hydrological system they represent (e.g. Burke et al. 2015).
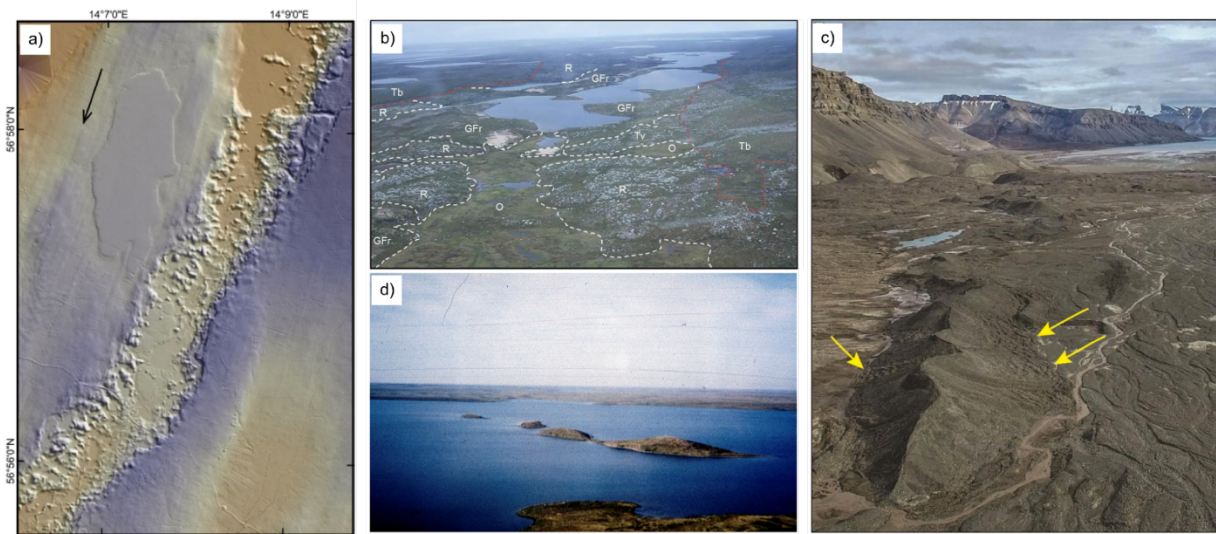
Figure 1.4 Varying expressions of subglacial meltwater landforms; (a) meltwater track in southern Sweden (former ice flow direction marked by the arrow) (Peterson and Johnson, 2018); (b) looking down a meltwater track in northern Canada (Haiblen, 2017); (c) an esker ridge in the glacial foreground, Iceland (Storrar et al. 2020 – courtesy of Jakub Ondruch) and; (d) esker beads, Meliadine Lake, Canada (courtesy of Isabelle McMartin).

While eskers are commonly reduced to a single crest-line during mapping (especially at a large-scale) and are typically described as single, straight-to-sinuous undulating ridges (Fig. 1.5a), additional esker morphologies and associated deposits (Fig. 1.5) have been identified reflecting a wide range of depositional environments and processes (e.g. Banerjee and McDonald, 1975; Rust and Romanelli, 1975; Hebrand and Åmark, 1989; Gorrell and Shaw, 1991; Warren and Ashley, 1994; Brennand, 2000; Mäkinen, 2003; Cummings et al. 2011a; Perkins et al. 2016; Prowse, 2017; Storrar et al. 2020). These will now be briefly discussed.

Beaded eskers (Fig. 1.5b) are characterised as a series of aligned mounds ranging in expression from roughly conical hills to more triangular and fan-shaped deposits. Successive beads may be quasi-regularly spaced, separated by gaps and form long chains over the landscape or they may overlap and merge locally into longer ridge segments. Although a subglacial origin has been proposed (e.g. Brennand, 1994), they are generally interpreted to represent sequential deposition at the mouth of a conduit in subaqueous locations in response to a back-wasting ice front (De Geer,

1897, 1910; Banerjee and McDonald, 1975; Saunderson, 1977; Cheel, 1982; Ringrose, 1982; Diemer, 1988; Hebrand and Åmark, 1989; Ashley et al. 1991; Livingstone et al. 2020).
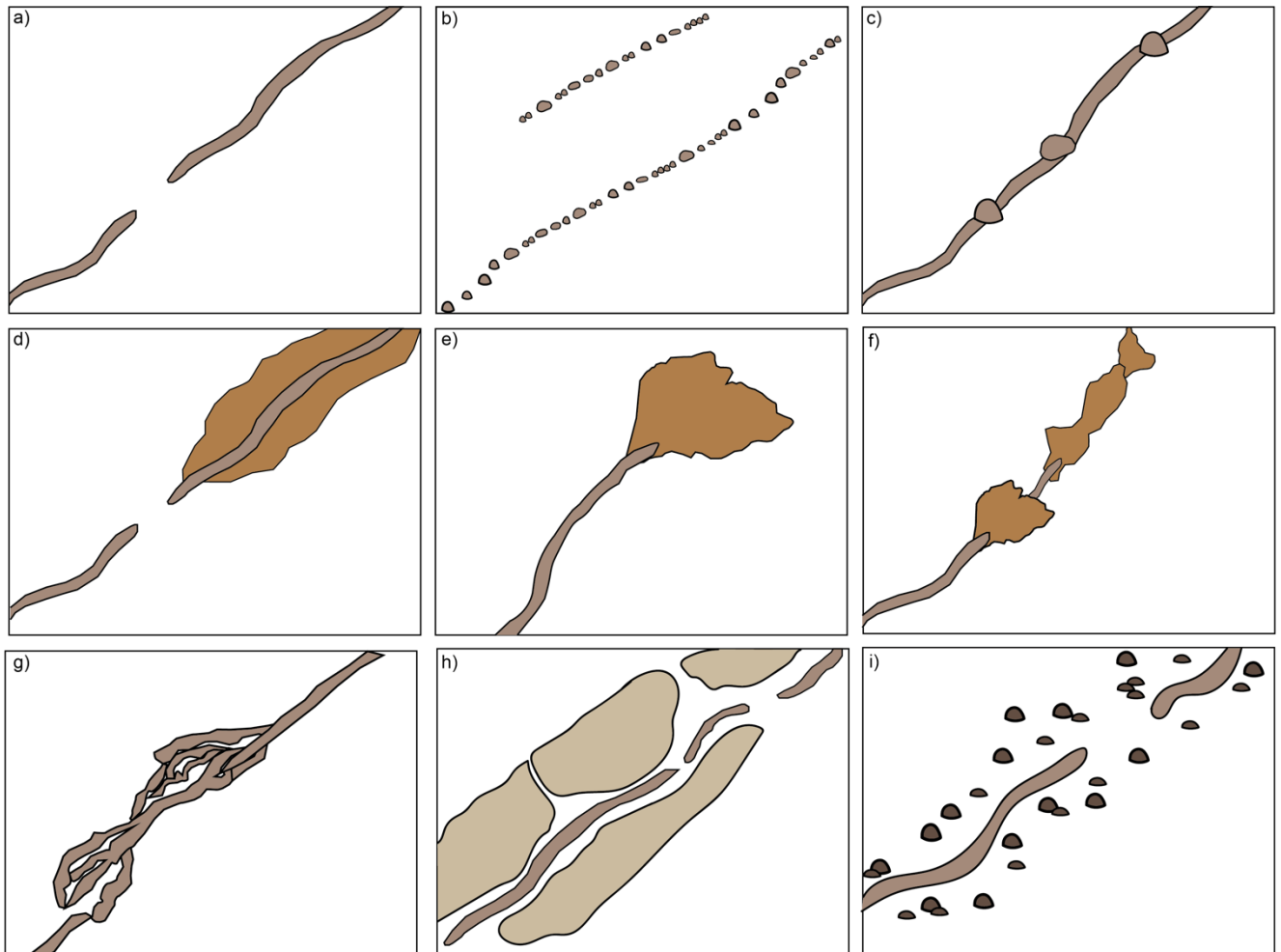
Figure 1.5 Esker assemblages and extended esker deposits: (a) esker ridge; (b) beaded eskers; (c) expansions along esker ridge; (d) lateral esker fans (splays); (e) single, large terminal esker fan; (f) multiple terminal esker fans; (g) esker nets (i.e. section of multiple ridges along an esker); (h) extended glaciofluvial deposits (often within erosional corridors); (i) hummocky terrain. Ice flow direction is from lower left to upper right in all panels.

Esker fans are identified in both lateral (Fig. 1.5d) and terminal (Fig. 1.5e) positions. Fans are often repeated along the main ridge (Fig. 1.5f) and are likely composed of glaciofluvial sand and gravel (e.g. Cummings et al. 2011a). Lateral fan-

shaped sediments or esker splays adjacent to the coarse central ridge are typically the same height as the main ridge but an order of magnitude wider and gently sloped, thinning away from the central ridge (Cummings et al. 2011a, 2011b). They have been interpreted as: (a) subaqueous outwash deposited by a sediment laden jet (Powell, 1990; Hoyal et al. 2003) potentially after esker deposition (Burke et al. 2012); (b) supraglacial deposits resulting from the flooding of a central channel resulting in fine sediment deposition akin to an overbank splay deposit in fluvial systems (Prowse, 2017) or; (c) subglacial deposits related to a high intensity flow event resulting in localised hydraulic lifting alongside the main conduit (Brennand, 1994). Terminal fans vary in size and shape from triangular mounds to flat-topped hills and may be superimposed over or extend from the central core (e.g. Sharpe, 1988; Gorrell and Shaw, 1991). They are typically found at the end of esker segments and often at former moraine margins. Terminal fans have been associated with deposition into standing water (Brennand, 2000), recording ice frontal or grounding line sedimentation as meltwater flow velocity rapidly decreases on exiting the subglacial conduit (Gorrell and Shaw, 1991). If retreat is slow or at a stand-still, fans may build up to the water surface forming deltas (Martini, 1990). Alternatively, ice-frontal retreat may result in a series of fans forming in the direction of ice recession (Banerjee and McDonald, 1975).

Esker nets or ribs (Fig. 1.5g) consist of anastomosing sections of eskers typically up to 1 km in length and much wider than a single esker ridge. Esker nets may be located at the end of an esker segment or may re-join downstream into a single esker ridge. A variety of mechanisms have been invoked for their formation including; (a) sediment choking in response to changes in sediment supply, ice surface slope, retreat rate or other unknown factors, causing conduit avulsion (Shilts et al. 1987; Menzies and Shilts, 1996); (b) the establishment of a broad zone of minor conduits alongside the main conduit in response to enhanced water flow (Gorrell and Shaw, 1991; Brennand, 1994) or; (c) supraglacial sedimentation within abandoned supraglacial channels with successive shifts in supraglacial stream position generating a series of ridges which are superimposed on one another as the ice ablates (Bennett and Glasser, 1996; Bennett et al. 2009) – an analogous process has been observed in Svalbard (Huddart et al. 1999). Nonetheless, Storrar et al. (2020) highlight the fact that increased sediment supply could also just produce a large single ridge and so is probably not the sole reason for complex esker formation. They suggest that a

dynamically evolving drainage system is required in addition to high volumes of sediment and meltwater and that there is a degree of chaos in determining where esker complexity will arise.

In addition to complex esker assemblages, several extended deposits have also been associated with eskers. For example, broad meltwater valley fills (Fig. 1.5h) – flat, sandy sediment, corridor like tracts – are often found alongside eskers. These are typically located within erosional corridors (Rampton, 2000; Utting et al. 2009) and may be pitted due to the melt-out of ice blocks (kettle holes) (e.g. Burke et al. 2015). Meltwater valley fill deposits are hypothesised to form where conduits drain into standing open water (MacDonald et al. 2009; Prowse, 2017) or in subglacial positions owing to their association with eskers (St-Onge, 1984). Similarly, pads and splays which comprise elevated detached bodies of sediment, have been interpreted as supraglacial fan deposits formed by the re-routing of sediment-laden meltwater from a main conduit onto the adjacent surface of the glacier where sediment accumulates in water-filled depressions or fractures on the surface (Prowse, 2017). Finally, hummocky terrain (Fig. 1.5i) has also been identified alongside eskers. Brennand (1994) suggests that a rapid increase in water and sediment input may result in subglacial conduit breaching, forcing water and sediment out and into surrounding conduits, thus forming the hummocky terrain. Alternative formation mechanisms have also been identified and these will be discussed in more detail in association with meltwater tracks in Section 1.2.1.3.

A key uncertainty is whether esker networks represent synchronous deposition in long subglacial meltwater conduits (e.g. Shreve, 1985; Brennand, 1994) or time-transgressive formation at the downstream terminus of short R-channels or at re-entrants at the ice sheet margin (e.g. De Geer, 1987; Hebrand and Åmark, 1989; Mäkinen, 2003; Beaud et al. 2018a; Hewitt and Creyts, 2019; Livingstone et al. 2020) (Fig. 1.6).
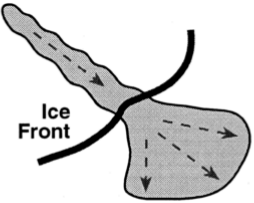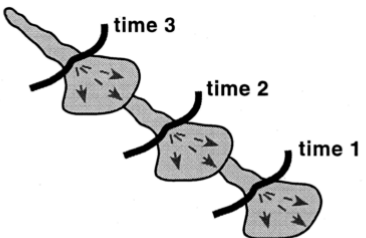
SEDIMENTATION IN EXTENSIVE, SYNCHRONOUS R-CHANNELS	SEGMENTAL SEDIMENTATION IN R-CHANNELS OR REENTRANTS CLOSE TO THE ICE FRONT AS THE ICE FRONT RETREATED
Esker Morphology: • relatively continuous ridge with gaps • fans in a terminal position or superimposed **Esker Sedimentology:** • coarse ridge with fines mostly in terminal or superimposed fans • low paleoflow variability except in terminal superimposed fans • regional trend in clast characteristics (e.g. lithology and roundness)	**Esker Morphology:** • ridge segments punctuated by fans **Esker Sedimentology:** • segmental trends in sediment texture and structure consistent with flow deceleration on entry into a standing water body • higher overall paleoflow variability due to presence of fans • segmental trends in clast characteristics (e.g. roundness)

Figure 1.6 Morpho-sedimentary diagnostic criteria for determining the genesis of long, dendritic eskers formed synchronously in R-channels or re-entrants that terminated in standing water (in Brennand, 2000; derived from Banerjee and McDonald, 1975; Shreve, 1985; Brennand, 1994; Brennand and Shaw, 1996).

a) Synchronous formation

Relatively unbroken, long esker ridges consisting of single, continuous facies are interpreted to have been deposited synchronously in long conduits extending 100s km beneath stagnant ice (e.g. Brennand, 1994, 2000; Brennand and Shaw, 1996). Brennand (2000) suggest that eskers formed via this mechanism would: (a) generate coarse ridges with terminal or superimposed fans containing fines at the down-glacier end only rather than along the full length of the esker; (b) exhibit evidence of low palaeo-flow variability measured from sand structures and gravel fabrics; and (c) present regional rather than segmental trends in clast lithology and roundness indicative of a conduit increasing in size down-flow beneath a thinning margin (Fig. 1.6a).

b) Time-transgressive formation

Time-transgressive formation has been invoked for eskers consisting of a series of beads or morpho-sequences with each segment related to a separate depositional event (e.g. De Geer, 1897, 1910; Hebrand and Åmark, 1989; Mäkinen, 2003; Livingstone et al. 2020). These are thought to have been deposited within segments in shorter R-channels or at re-entrants at the ice sheet margin, aligning to form long chains as the ice front retreats following a pattern set by dendritic subglacial drainage pathways (Boulton et al. 2009), supraglacial streams (Shilts, 1984) or the development of surface-to-bed connections and resulting tree-shaped conduits (Hooke and Fastook, 2007). Eskers formed in this manner are expected to display segmental trends in sediment texture, structure and clast roundness as well as more variable palaeo-flow indicators (Brennand, 2000). Sequences may comprise multiple fans, (Fig 1.6b) (Hebrand and Åmark, 1989) or esker beads (De Geer et al. 1897, 1910).

Recent modelling efforts support a time-transgressive origin for the deposition of eskers (e.g. Livingstone et al. 2015; Beaud et al. 2018a; Hewitt and Creyts, 2019); however, that is not to say that synchronous deposition does not occur in some scenarios (e.g. Brennand, 1994; Brennand and Shaw, 1996). For example, observations of eskers formed during jökulhlaups in Iceland indicate rapid backfilling of conduits by the deposition of large volumes of sediment, forming long, near-synchronous eskers (e.g. Burke et al. 2008). A similar mechanism has been proposed to explain eskers deposited downstream of palaeo-subglacial lakes (Livingstone et al. 2016).

1.2.1.2 Meltwater channels and tunnel valleys

Within the literature there are inconsistencies and a lack of clarity surrounding terminology with various researchers referring to 'tunnel channels', 'tunnel valleys', 'channels', 'conduits' etc. Often these are subject-specific (e.g. geomorphology, glaciology, engineering). In this thesis I use the term (meltwater) channel to refer to palaeo-evidence of erosional channelised flow of water preserved on the ice sheet bed (i.e. the outline of the path the water took) at all scales from N-channels through to tunnel valleys. I reserve the term conduit to refer to active channelised flow beneath

a contemporary ice mass (i.e. the enclosed sediment or ice walled pipe carrying water at the ice-bed interface).

Subglacial meltwater channels, or N-channels, incised into bedrock or sediment substrate 10s of metres to 400 m deep (e.g. Mooers, 1989; Ehlers and Linke, 1989) range from metres to tens of metres wide (e.g. Sissons, 1961; Glasser and Sambrook Smith, 1999; Piotrowski, 1999) to large tunnel valleys several kilometres in width and tens of kilometres long (e.g. Kehew et al. 2012; van der Vegt et al. 2012; Livingstone and Clark, 2016). Their formation has been linked to subglacial meltwater erosion at the ice-bed interface (Ó Cofaigh, 1996; Kehew et al. 2012; van der Vegt et al. 2012) which is supported by: (a) their orientation quasi-parallel to former glacier flow i.e. following the hydropotential gradient; (b) undulating long profiles indicative of erosion by basal meltwater under high hydraulic pressures; (c) termination at or near former ice margins; and (d) the presence of eskers within them. Although there are some examples of tunnel valleys on crystalline bedrock, most are carved into soft or lithified sediments (Ó Cofaigh, 1996; Janszen et al. 2012; Ravier et al. 2014) and tunnel valleys are often considered the soft bed equivalent of eskers (Boulton et al. 2009). Tunnel valleys are characteristically orientated roughly parallel to former ice flow; however, they have also been observed to join, split and cross-cut each another – perhaps indicating multiple periods of drainage and formation (e.g. Wright, 1973; Mooers, 1989; Kehew et al. 1999; 2005; Fisher et al. 2005). Tunnel valleys have been identified at various developmental stages from well-developed valleys with vertical sides and well defined valley sides to indistinct valleys often associated with hummocky terrain and even as a series of aligned depressions (e.g. Kehew et al. 1999; Sjogren et al. 2002).

Tunnel valleys are considered an important part of the subglacial hydrological system, responsible for the evacuation of large amounts of sediment and water, yet, their precise mechanism of formation is still debated. While large bedrock tunnel valleys have been hypothesised to form as a result of repeated water flow over multiple glacial cycles (e.g. Kirkham et al. 2020a), this thesis focuses on those predominantly eroded into sediment during one glacier cycle. The debate around tunnel valley genesis hinges on gradual steady-state formation (Fig. 1.7a) (e.g. Boulton and Hindmarsh, 1987; Mooers, 1989; Praeg, 2003; Boulton et al. 2009) versus formation

due to floods (Fig. 1.7 b-d) (e.g. Piotrowski, 1994; Cutler et al. 2002; Hooke and Jennings, 2006; Jørgensen and Sandersen, 2006). Flood hypotheses rely on the sudden release of a large volume of meltwater at the bed relative to the system's existing capacity (e.g. Wright, 1973; Piotrowksi, 1994; Shaw, 2002, 2010; Hooke and Jennings, 2006). However, these hypotheses vary in the required flood magnitude, regularity of the meltwater flow, the source of the meltwater input, whether a flood is responsible for creating single or multiple tunnel valleys and whether a tunnel valley is the result of a single or multiple flood event(s). These will now be discussed in more detail:

a) Steady-state formation

In this hypothesis (Fig. 1.7a), tunnel valleys form headwards by the erosion of soft sediments into low pressure channels (e.g. Boulton and Hindmarsh, 1987; Moeers, 1989; Praeg, 2003; Boulton et al. 2009). Due to lower water pressure within the conduit – initiated by piping at the ice sheet margin (Shoemaker, 1986; Boulton and Hindmarsh, 1987; Hooke and Jennings, 2006) – subglacial water flows towards the conduit and enlarges it (Boulton and Hindmarsh, 1987; Boulton et al. 2007a, 2007b, 2009). Flow into the conduit erodes and transports sediments which are then evacuated to the margin (Boulton and Hindmarsh, 1987), gradually widening and deepening the tunnel valley. In this manner, large tunnel valleys could be formed under relatively low discharge conditions (e.g. Kehew et al. 2012).

b) Flood formation

Outburst floods (Fig. 1.7b) have been invoked to explain the synchronous occupation and incision of entire tunnel valley networks (e.g. Wright, 1972; Shaw and Gorrell, 1991; Brennand and Shaw, 1994; Shaw, 2002; Sjogren et al. 2002). While this is unlikely owing to the unrealistically large amounts of water that would be required to achieve this (Ó Cofaigh et al. 1996; Clarke, 2005), it is possible that lower magnitude, repeated discrete outburst floods could result in the formation of individual tunnel valleys (e.g. Wright, 1973; Boyd et al. 1988; Wingfield, 1990; Piotrowksi, 1994; Cutler et al. 2002; Hooke and Jennings, 2006; Jorgensen and Sandersen, 2006). The water required for such outburst events may be sourced from surface or subglacial

lake drainages (e.g. Mooers, 1989) or may involve ponding of water at the bed, perhaps behind a marginal permafrost ridge or a frozen toe, which when released results in the rapid erosion of tunnel valleys terminating at the margin (e.g. Attig et al. 1989; Piotrowski, 1994; Cutler et al. 2002, Hooke and Jennings, 2006).
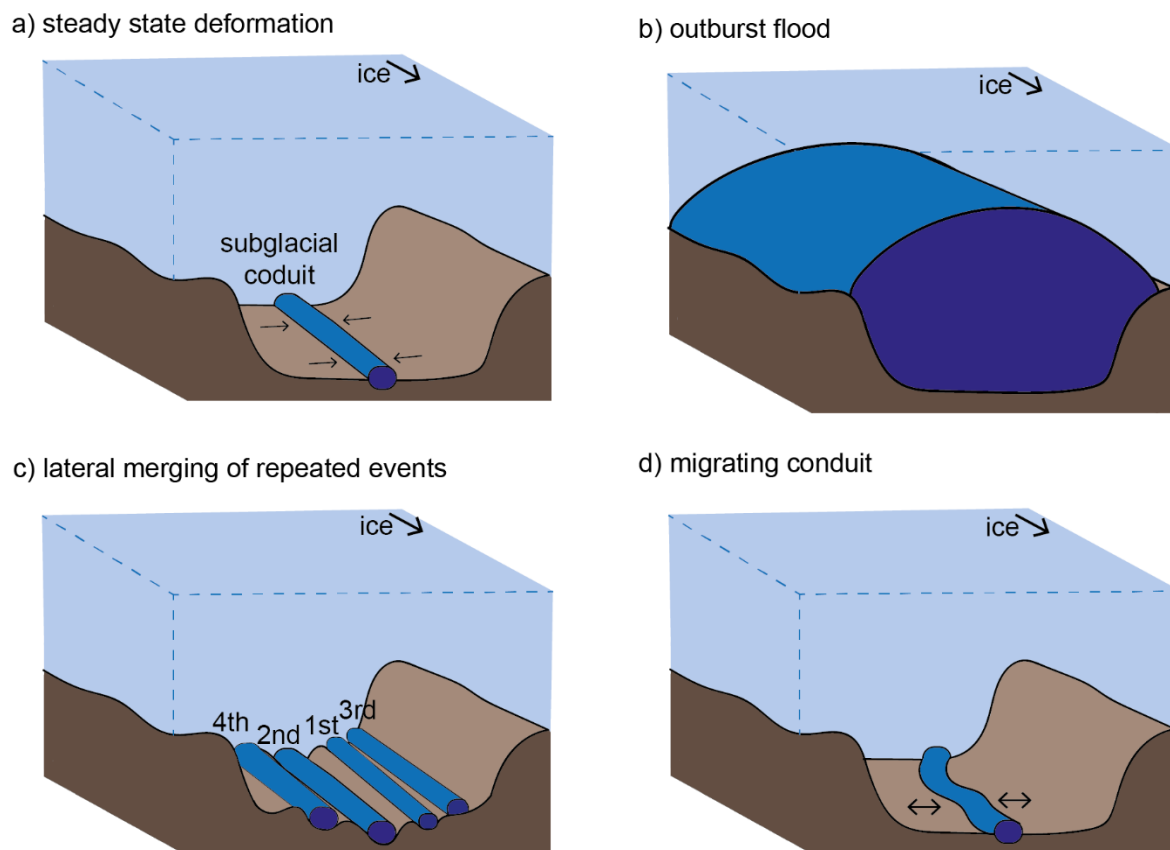
Figure 1.7 Proposed formation theories for meltwater channels as a result of subglacial conduits; (a) the tunnel valley is formed by the flow of subglacial material into a subglacial conduit that is much smaller than the resulting tunnel valley; (b) tunnel valley is eroded by a subglacial conduit as large as the tunnel valley (e.g. a large flood event); (c) the tunnel valley is formed as a result of merging signatures of multiple events (based on Clayton et al. (1999) and Kehew et al. (2012)) and; (d) the tunnel valley is eroded by a laterally migrating conduit smaller than the resulting valley.

Observations of some tunnel valleys suggest that they are composed of multiple cut and fill sequences whose dimensions are often much smaller than the dimensions

of the resulting tunnel valley (Kehew et al. 2012). This led to the proposition that tunnel valleys may represent the lateral merging of multiple erosional events (e.g. Fig. 1.7c) (e.g. Jorgensen and Sanderson, 2006). In this way, tunnel valleys may form from repeated flood events over multiple years (e.g. Beaud et al. 2018b) or glacial cycles (e.g. Jorgensen and Sanderson, 2006) with flood drainages following similar routes at the bed. An alternative hypothesis to explain the greater width of tunnel valleys relative to observed conduits is the lateral migration of individual or multiple conduits flowing either parallel to one another or in anastomosing networks (e.g. Nordmann, 1958; Smed, 1962, 1998; Kruger, 1989). In this scenario (Fig. 1.7d), conduits migrate across an area wider than their diameter, accessing and eroding greater volumes of sediment. At present, not much is known about how conduits migrate at the bed beneath contemporary ice sheets; however, conduit migration may be expected in response to temporal variations in ice thickness, subglacial topography and regional and local basal water pressure causing lateral movement in a manner analogous to a central river in a floodplain.

1.2.1.3   Meltwater tracks

Detailed mapping in northern Canada and Scandinavia has revealed the presence of linear tracks variously termed 'hummock corridors', 'glaciofluvial corridors', 'washed zones' and 'esker corridors', typically a few hundred metres to several kilometres wide and a few kilometres to hundreds of kilometres long (e.g. St-Onge, 1984; Dredge et al. 1985; Rampton, 2000; Utting et al. 2009; Burke et al. 2012; Kerr et al. 2014a, 2014b; Sharpe et al. 2017; Peterson et al. 2017; Peterson and Johnson, 2018; Lewington et al. 2019). In this thesis to avoid mixing of terminology, I refer to all these features as meltwater tracks.

Some meltwater tracks exhibit sharp lateral boundaries with significant vertical relief while others are more diffuse and characterised by subdued relief. These features often contain eskers and hummocks (Peterson and Johnson, 2018) as well as 'patches' of glaciofluvial deposits and areas of exposed bedrock. The individual hummocks within the meltwater tracks vary in size (10s to 100s m in width / length in plan-view), shape (mostly irregular) and relief (1 to 10s of m) (Peterson and Johnson, 2018). In general, hummocks tend to show no consistent plan-form shape, although

triangular-shaped hummocks have been identified in Finland (Mäkinen et al. 2017) and Sweden (Peterson et al. 2017).

Table 1.1 Metrics of meltwater tracks reported in the literature.

Location	Source	Term used	Frequency	Length (km)	Width (km)	Spacing (km)
Southwestern Finland	*Makinen et al. (2017)*	Triangular-shaped landforms within distinguishable route	Single feature(s) selected for purpose	40 (longest feature)	1 – 2.5 (most distinct features)	1 – 4 (most distinct features)
Southern Swedish Uplands (SSU), Sweden	*Peterson and Johnson (2018)*	Hummock corridor	76 hummock tracts	1.5 – 11.8 (mean 5.2)	0.2 – 4.9 (mean 1.1)	0.8 – 54.5 (mean 14.5)
Southern Fraser Plateau, Canada	*Burke et al. (2011)*	Erosional corridor	Single	~ 40	~ 0.25 - 1	-
Southern Slave Province, Canada	*Rampton (2000)*	Meltwater corridor	-	-	0.5 - >2	-
East Arm Area, Great Slave Lake, Canada	*Sharpe et al. (2017)*	Meltwater erosional corridor	Approx. 22 corridors	80 - 120	~0.3 - 3	5 - 15
East-central Alberta and South-central Michigan	*Sjogren et al. (2002)*	Incipient tunnel channel	-	-	0.2 - 4	-
Redrock Lake Area, Canada	*St-Onge (1984)*	Glaciofluvial meltwater corridor	>15 (estimated from map)	Commonly > 20 (estimated from map)	Up to 1	12 – 15
Kivalliq region, Nunavut, Canada	*Storrar and Livingstone (2017)*	Corridor-like tracts of glaciofluvial deposits	-	-	Up to 6	•
Walker Lake, Canada	*Utting* et al. *(2009)*	Glaciofluvial corridor	>20 (estimated from map)	~ 5 - 12	~0.2 - ~ 0.7	5 – 10

While some meltwater tracks can be traced over long distances (> 100 km), often they are discontinuous with intervening segments of smoother terrain, tunnel valleys or eskers connecting them. At a regional scale – i.e., a horizontal scale exceeding the size of individual meltwater tracks and approaching the size of the collection of multiple meltwater tracks and / or the ice sheet – meltwater tracks appear to exhibit a radial pattern (e.g. Peterson and Johnson, 2018) indicative of a larger divergent network

(Utting et al. 2009) and seem to be quasi-regularly spaced. Locally, meltwater tracks display a high degree of parallel conformity with each other and with other subglacial bedforms such as drumlins and lineations suggesting a relationship with palaeo-ice flow.

A subglacial meltwater origin is largely agreed upon for meltwater tracks based on adverse and undulating long profiles, orientations roughly parallel to former glacier flow, termination at or near former ice margins and their association with eskers; however, exactly how these features formed is not yet known (e.g. St-Onge, 1984; Rampton, 2000; Utting et al. 2009; Peterson and Johnson, 2018). Proposed formation theories have invoked similar mechanisms as for tunnel valleys, specifically time transgressive formation (e.g. St-Onge, 1984) or subglacial floods of varying magnitude and duration (e.g. Rampton, 2000; Utting et al. 2009; Burke et al. 2011; Haiblen, 2017). Due to their similarities, it has been suggested that meltwater tracks may be related to tunnel valleys and represent an earlier stage of formation prior to the formation of fully developed tunnel valleys, perhaps limited by time, sediment thickness or water availability (e.g. Sjogren, 2002; Peterson et al. 2018).

1.2.2 Controls on meltwater landform formation and expression

The distribution of meltwater landforms on palaeo-ice sheet beds appears to be almost ubiquitous; however, landform expression is seen to vary and has been linked to a range of controlling factors. A fundamental question in unravelling the hydrological imprint then, is determining whether different meltwater landform patterns and expressions represent different hydrological regimes or the same hydrological regime experiencing different glaciological or background controls.

1.2.2.1 Glaciological controls

The subglacial bed has been conceptualised as a complex, evolving mosaic of cold (frozen) and warm based (at or above the pressure melting point) patches with drainage prevented in frozen areas and promoted in warm based sectors (e.g. Kleman and Glasser, 2007). The thermal organisation of the bed therefore ultimately dictates the capacity for subglacial drainage at any point in time and space. However,

observations of the palaeo-bed are complicated by the superposition of mass wasting signatures and younger deglacial signatures on top of earlier indicators (e.g. eskers superimposed on ribbed moraines).

Shreve (1972) proposed that the hydraulic potential gradient (estimated from ice thickness and basal topography) can predict subglacial drainage patterns at the ice sheet scale. This method has been used to estimate drainage beneath Greenland (e.g. Lewis and Smith, 2009; Bamber et al. 2013; Banwell et al. 2013a; Livingstone et al. 2013; Karlsson and Dahl-Jensen, 2015), Antarctica (e.g. Wingham et al. 2006; Wright and Siegert, 2012; Wolovick et al. 2013) and for palaeo-ice sheets in Canada (Livingstone et al. 2013, 2015) and Europe (Shackleton et al. 2018). While this approach has had some success in predicting the location of drainage pathways, its accuracy and precision remain largely untested and it is limited by assumptions of uniform meltwater production and delivery, and constant water pressure (Gulley et al. 2012).

A connection between surface meltwater inputs and subglacial meltwater landforms has been hypothesised (e.g. Banerjee and McDonald, 1975; St-Onge, 1984; Mooers, 1989) but is yet to be definitively confirmed. Surface meltwater plays an important role in conduit formation and landform development, contributing significantly to erosion, transport and deposition rates in ablation areas (Cook et al. 2020). We may therefore expect meltwater landforms to reflect the locations and density of surface meltwater delivery points to the bed and their expressions to be modulated by the relative frequency and magnitude of meltwater delivery, i.e. coupling landform distribution and expression with spatio-temporal variations in climatically-driven meltwater availability.

At the large scale across northern Canada, Storrar et al. (2014b) proposed that an increase in esker spatial density (and therefore channelisation of the subglacial drainage system) throughout deglaciation was linked to a pronounced warming after the Younger Dryas between 12.5 - 9 kyr B.P. which resulted in increased surface meltwater production and delivery to the bed (Carlson et al. 2009). In southern Sweden, Peterson and Johnson (2018) similarly suggested that an increase in spatial frequency of hummock corridors can be correlated with the relatively warm Bølling-

Allerød interstadial. Furthermore, at the landform scale, variations in landform morphology have also been hypothesised to exhibit a climate signal with Lundqvist (1999) linking esker sedimentation rates to the 11-year sunspot cycle and moraine sequences in Iceland linked to above-average temperatures (e.g. Chandler et al. 2019). Variable rates of retreat also have the potential to influence the expression of subglacial meltwater landforms (e.g. the development and size) as well as their spatial density based on how long ice remains stable in a particular location. For example, it is possible that slower retreat rates facilitate the development of wider and deeper incisional features (e.g. Livingstone and Clark, 2016).

1.2.2.2   Background controls

Background controls such as basal substrate and geology determine the erodibility, drainage capacity and strength of the bed and the nature of the ice-bed coupling (Greenwood and Clark, 2010). Bedrock substrates are typically simplified into crystalline (i.e. 'hard') versus sedimentary (i.e. 'soft') beds. Crystalline beds are assumed to be more resistant to erosion, generating a thinner, discontinuous till which is more easily drained and therefore stiffer (e.g. Freeze and Cherry, 1979; Boulton, 1987; Boulton and Hindmarsh, 1987; Piotrowski, 1987; Clark, 1994; Clark and Walder, 1994; Evans et al. 2006). Conversely, sedimentary beds are more easily eroded forming thick and continuous till cover and a smooth ice-bed contact (Clark, 1994) with poor drainage and greater till deformation. The literature tends to correlate eskers with areas of hard bed (e.g. over shield areas - Clark and Walder, 1994) where erosion of the ice is relatively easier than down into the bed (i.e. R-channels), while conduits preferentially eroded down into the bed (i.e. N-channels and tunnel valleys) are considered the soft bed equivalent (Nye and Frank, 1973; Boulton et al. 2009). Some large-scale observations support this generalisation (e.g. Clark and Walder, 1994), but there are also exceptions. These include eskers formed in soft bed areas with thick sediments (Greenwood and Clark, 2008; Storrar et al. 2014b; Burke et al. 2015) and tunnel valleys incised into hard bedrock (Clapperton, 1968; Sugden et al. 1991; Nitsche et al. 2013; Jansen et al. 2014).

Till characteristics reflect the underlying bedrock material (Clark and Walder, 1994) and are an important control on landform creation and expression. For example,

esker expression has been correlated with underlying local till characteristics, with thicker more pervasive till enabling larger well-developed eskers to form and thin, discontinuous, clast-poor till generating fewer (if any) smaller eskers (Wilson, 1939; Burke et al. 2015). Complex eskers (e.g. esker 'nets' or anabranching and enlarged sections) have also been correlated with regions of significant sediment supply (Brennand, 1994, 2000; Brennand and Shaw, 1996; Burke et al. 2008; Burke et al. 2010; Storrar et al. 2020). Similarly, variations in the expression of incisional features – in particular, their width to depth ratio – have been linked to variations in sediment thickness. Investigations of channel morphology have shown that those in areas of thick till are generally deeper and narrower while those in areas of thin to absent till cover are typically less deep and wider (e.g. Sjogren et al. 2002; Peterson and Johnson, 2018).

1.3 Key uncertainties and issues

1.3.1 The large-scale drainage configuration, the connectivity of different drainage elements and its response to meltwater perturbations

The configuration of the subglacial drainage network has been inferred from contemporary observations such as tracer studies (e.g. Willis et al. 1990; Nienow et al. 1996, 1998; Bingham et al. 2005; Cowton et al. 2013), borehole water pressure measurements (e.g. Fountain, 1994; Hubbard et al. 1995; Mair et al. 2003; Fudge et al. 2008), surface velocity patterns (e.g. Iken and Bindshadler, 1986; Jansson, 1996; Mair et al. 2002; Bartholomew et al. 2012), meltwater landforms on palaeo-beds (e.g. Shilts et al. 1987; Aylsworth and Shilts, 1989; Brennand, 2000; Burke et al. 2012; Storrar et al. 2014a; 2014b; Livingstone and Clark, 2016; Livingstone et al. 2016; Perkins et al. 2016; Peterson et al. 2018; Ojala et al. 2019), glaciohydrological theory (e.g. Röthlisberger, 1972) and modelling (e.g. Andrews et al. 2014; Hoffman et al. 2016). However, despite widespread acceptance that the subglacial drainage system is heterogeneous, a lack of direct observations limits our understanding of how these systems interact and over what spatial and temporal scales different systems operate.

The large-scale drainage configuration is largely based on R-channel theory which predicts a low pressure dendritic network of conduits that capture water from

their surroundings. Evidence from palaeo-ice sheet beds indicate the widespread occurrence of eskers (i.e. conduits) suggesting long-distance operational connectivity (e.g. Aylsworth and Shilts, 1978; Storrar et al. 2014a) and thus a high degree of channelisation. However, evidence in contemporary settings suggests channelisation is generally limited to the marginal zone of an ice sheet ~ 50 km inland at the GrIS (e.g. Chandler et al. 2013; de Fleurian et al. 2016; Koziol and Arnold, 2018). An exception to this may be rapid drainage of subglacial lakes further inland which facilitates conduit development (e.g. Wingham et al. 2006; Carter et al. 2017).

There are several limitations to using the distribution of eskers to infer contemporary drainage configurations. Eskers exhibit a range of morphologies that may not all represent deposition in low pressure R-channels (Greenwood et al. 2016). Increasing evidence suggests that (most) eskers are likely to form at the margin (e.g. Livingstone et al. 2015, 2020; Beaud et al. 2018a; Hewitt and Creyts, 2019). This implies that eskers represent a composite record of subglacial drainage close to the ice-marginal rather than subglacial drainage deep into the ice sheet where there may be different conduit dimensions and behaviours (e.g. migration, sinuosity etc.). Indeed, there are very few direct observations of the morphology of conduits beneath ice (Gulley et al. 2012) and much of what we do know is based on observations of ice-marginal conduits which may have been subject to partial collapse or different glaciological conditions (Greenwood et al. 2016). Finally, eskers are a product of deglaciation and we do not yet know over what timescales they are formed or how they have been modified since. As a result, we cannot say for sure that adjacent eskers were formed at the same time, therefore limiting confidence in inferences about contemporary hydrological system based on the spacing of eskers.

Much of the ice bed is expected to have inefficient non-dendritic channel networks comprising poorly connected linked cavities under high pressure. This drainage mode is thought to typically occur under thicker ice with limited surface inputs towards the interior of the GrIS and beneath much of the AIS (e.g. Ashmore and Bingham, 2014) and in areas isolated from surface melt inputs between channelised drainage within the ablation area. Distributed drainage in the ablation area is believed to be key in controlling overlying ice sheet dynamics (e.g. Andrews et al. 2014; Hoffman et al. 2014). Furthermore, there are suggestions that high pressure, non-

channelised, efficient distributed pathways can develop towards the interior of the ice sheet (e.g. Meierbachtol et al. 2013) suggesting that additional drainage modes may be in play. While conduits and distributed drainage likely occur in different settings, it is becoming increasingly important to view the system as having a range of modes which may interact. The most realistic drainage configuration is likely to be one that is highly variable over space and time, responding to transient inputs of surface water from daily to multi annual timescales and with episodic events superimposed on this.

1.3.2 Difficulties linking landforms to processes

While early studies used palaeo-meltwater features as simple indicators of palaeo-ice sheet extent or flow direction (e.g. Boulton et al. 2001), they are now increasingly being used to gain deeper insight into hydrological properties and the dynamic response of ice sheets to these (e.g. Bell, 2008; Nitsche et al. 2013; Storrar et al. 2014b; Livingstone et al. 2015, 2020; Mäkinen et al. 2017; Storrar and Livingstone, 2017; Ojala et al. 2019). Nonetheless, this is still somewhat limited due to what Kleman et al. (2006) refer to as the 'genetic problem' – landforms cannot be fully used to understand conditions beneath the ice sheet until we are certain of the processes under which landforms (and variations in expression of these) were created. More research is needed into linking meltwater landforms to the processes which formed them before we can have confidence in our interpretations of their distribution, morphology, presence / absence etc.

This is likely to be improved by bridging the disconnect between observations of contemporary and palaeo landforms and modelling disciplines which have tended to progress in relative isolation of each other (Greenwood et al. 2016). There are many difficulties associated with this approach such as: different scales, conditions, research methods, stages of glaciation / deglaciation and environments (climatic and topographic). One way of addressing these difficulties is through using modern analogues to help link specific processes in contemporary settings to particular landforms and morphological expressions and to help assess landform modification following deglaciation. This is being done for drumlins in Antarctica where landforms have been observed beneath the contemporary ice sheet and repeat surveys revealed the first example of active drumlin formation (King et al. 2007, 2016; Smith et al. 2007).

This allowed existing formation theories to be assessed and certain hypotheses discounted based on site specific conditions (Smith et al. 2007). Although there are limited observations of contemporary eskers (e.g. Price, 1966; Howarth et al. 1971; Huddart et al. 1999; Russell et al. 2001; Burke et al. 2009; Bennett et al. 2010; Drews et al. 2017; Storrar et al. 2020) and tunnel valleys (e.g. Russell et al. 2007) forming, further identification of analogues may help better understand the timescales of landform formation and specific glaciological and background conditions.

It is also useful to consider processes occurring in contemporary settings when interpreting landforms and considering potential formation hypotheses. If something is being observed at contemporary ice sheets, uniformitarianism would suggest that similar processes may also have occurred in the palaeo-setting and thus have left a geomorphic signature. For example, conduit development inland is expected to be limited to ~ 50 km from the ice sheet margin (Bartholomew et al. 2011; Chandler et al. 2013); however, water rapidly inputted to the bed further inland may still be removed efficiently via alternative drainage mechanisms such as a transient turbulent sheet and / or efficient distributed pathways (e.g. Meierbachtol et al. 2013; Dow et al. 2015). The recently characterised 'murtoo' – a triangular till landform – has been hypothesised to represent such drainage towards the ice sheet interior under high pressure and upstream of the development of conduits (and eskers) closer to the margin (Mäkinen et al. 2017; Ojala et al. 2019).

Modelling is also useful for determining the physical plausibility of a process occurring and generating a landform. For example, process understanding has been enhanced by the modelling of Hewitt (2011) who coupled channelised and distributed flow and showed that water pressure perturbations could be 'felt' in the distributed system around a channel on a flat bed and that this can be used to give a rough approximation of conduit spacing (~ 10 km). Numerical models which incorporate sediment erosion and transport as well as hydrology have also been useful for understanding the physical processes behind landform formation. For example, Beaud et al. (2018a) used a one-dimensional numerical model to investigate whether subglacial water flow from frequent surface melt events was sufficient to explain the formation of tunnel valleys over long periods of time without the need for large floods. Beaud et al. (2018b) showed that sediment accumulation near the margin (and thus

the formation of incipient eskers) occurs due to the dynamics of channelised flow and the creation of a bottleneck. Finally, physical modelling such as that by Lelandais et al. (2018) – which uses a silicon putty 'ice sheet' and a sand 'bed' – allows the formation and evolution of drainage features to be monitored and for their morphometrics and spatial organisation to be compared with palaeo-landforms recorded on former ice sheet beds. This facilitates experimentation with different parameters to try and recreate different formation scenarios and resulting expressions.

1.3.3 Ability to identify and separate signals

Channelised drainage signatures appear ubiquitously on the bed of palaeo-ice sheets and are the focus of most palaeo-meltwater studies (Greenwood et al. 2016). However, contemporary observations and glacial theory suggest that low pressure R-channels should be relatively limited (e.g. Bartholomew et al. 2012; Chandler et al. 2013). The seeming lack of widespread distributed drainage systems in the palaeo-record may be the result of limited potential for landform creation due to less energetic water flow, or if landforms are created; poor preservation and / or poorly developed templates for their identification (Greenwood et al. 2016) or insufficient resolution data used to detect them (e.g. Mäkinen et al. 2017; Ojala et al. 2019).

The absence of a geomorphic signature does not necessarily indicate the absence of drainage in a particular location. As discussed above, the palaeo-record is the combined product of hydrological processes, sedimentological and geomorphic work (Burke et al. 2015; Greenwood et al. 2016). A lack of water flow velocity or sediment starvation may result in a lack of erosion or deposition respectively resulting in no signature; however, this does not mean that water did not flow there. As such, subglacial meltwater landform maps – particularly when only considering one landform type (i.e. eskers (depositional) or tunnel valleys (erosional)) - should be viewed as a minimum map.

Preservation of eskers is likely favoured in areas where they contain enough sediment to remain considerable topographical features after any ice contained within them has melted, are situated on and bounded by several km on either side by relatively flat ground which minimises their risk of erosion by the proglacial drainage

system, and where retreat continues backwards without any subsequent ice re-advances (Storrar et al. 2020). This explains why eskers are abundant on the beds of the former Laurentide and Fennoscandian ice sheets. Evidence of tunnel valleys may also be hidden due to partial or complete infilling following their formation. Several different erosional and sedimentary processes (not just glacial) can contribute to infilling and this may limit their surface identification.

Finally, there is the issue of equifinality whereby multiple mechanisms may explain the formation of the same geomorphic signature (e.g. Livingstone and Clark, 2016; Möller and Dowling, 2018; Storrar et al. 2020). For example, studies have found evidence to support different hypotheses for tunnel valley formation suggesting that care must be taken to avoid generalising support for one theory based on one location alone and that a polygenetic origin is possible (e.g. Hooke and Jennings, 2006; Livingstone and Clark, 2016). Similarly, eskers are understood to record a variety of meltwater sources and depositional environments and thus not all of them can be interpreted as the casts of R-channels (e.g. Perkins et al. 2016).

1.3.4 Mapping of single subglacial meltwater landform types

Meltwater landform types are typically mapped and interpreted individually (e.g. Clark and Walder, 1994; Brennand, 2000; Storrar et al. 2013; Burke et al. 2015; Livingstone and Clark, 2016; Mäkinen et al. 2017) rather than as a holistic drainage signature (c.f. Storrar and Livingstone, 2017). However, meltwater landforms are often associated with one another; for example, eskers within tunnel valleys or meltwater tracks (e.g. Wright, 1973; Attig et al. 1989; Mooers, 1989) or eskers transitioning downstream to / from tunnel valleys and meltwater tracks (e.g. Livingstone et al. 2016). As such, it is not yet clear whether or how differing expressions of subglacial drainage are interrelated and to what extent variations in drainage or background conditions (e.g. bed substrate, geology and local topography) control the preserved geomorphic signature. This has important implications for using palaeo-meltwater landforms to represent ice sheet hydrology in models (i.e. a map of an individual landform type may not account for different drainage modes) and for testing numerical models, which predict the configuration of the subglacial hydrological system (e.g. Hewitt, 2011; Werder et al. 2013). Mapping of all meltwater drainage features while retaining

information about each landform type is likely to yield important information for understanding the nature and evolution of the hydrological system and for gaining insight into potential controls on the formation of each.

1.4 Motivation

This PhD has benefited from the release of the ArcticDEM https://www.pgc.umn.edu/data/arcticdem/ (Fig. 1.8) to address some of the key research questions surrounding the functioning and geomorphic signature of the subglacial hydrological system. The ArcticDEM is a 2 - 10 m resolution digital elevation model for the whole of the Arctic (above 60° north), and all of Greenland, Alaska and the Kamchatka Peninsula (Porter et al. 2018). Data started to be released gradually as I began my PhD in September 2016. I initially used the 5 m resolution data product mosaiced into 50 x 50 km tiles. Later in my PhD when they became available (release 7) I used 10 m resolution tiles which had fewer missing data and high enough resolution for large-scale mapping of meltwater landforms. For detailed manual mapping (e.g. of esker beads) I used the 2 m resolution release which was the final data product to be released.

Prior to the release of the ArcticDEM the existing data for Canada was the Canadian Digital Elevation Model (CDEM). This provided data at 50 m resolution for much of the country. The release of the ArcticDEM thus generated a data explosion with huge potential to assess palaeo-subglacial meltwater landforms at a large scale and an unprecedented resolution. By allowing me to carry out a consistent survey of meltwater landforms across a large area, use of the ArcticDEM ensured that a wide range of different features (i.e. eskers, esker beads, meltwater tracks, meltwater channels etc.) were captured across my study area and that these covered a range of 'background' conditions (e.g. glaciological, sedimentological, geological, topographical etc.). This allowed me to explore controls on the underlying processes responsible for landform formation and the associations between different landform types. A large-scale approach not only allows a wide selection of geomorphic expressions to be captured but also prevents coincidental or 'cherry-picked' findings from small, local study areas.

Figure 1.8 The ArcticDEM domain (black), including all land area north of 60º (Porter et al. 2018). Data were available in 50 x 50 km tiles at a 5 m resolution when I started my PhD and now at 2 m and 10 m resolutions. Data are freely available at https://www.pgc.umn.edu/data/arcticdem/.

1.5 Aims and Objectives

The aim of this thesis is to investigate the distribution, morphology and formation of subglacial hydrological systems using geomorphological signatures recorded in the ArcticDEM at the ice sheet scale.

1.5.1 Objectives

O1) Ice sheet scale automatic mapping of subglacial meltwater tracks

I develop the first automatic method for identifying and mapping subglacial meltwater tracks from newly released high resolution ArcticDEM data. This method, based on image processing techniques, aims to separate individual features from their background based on several predefined criteria relating to size, parallel conformity and elongation. The development of an automatic method facilitates the rapid

detection of features across large areas and removes the subjectivity associated with manual mapping. The method is tested regionally at 3 sites where the output is quantitatively compared to manual mapping to determine the accuracy and precision of the outputs. Following this, the method is run over a large section of northern Canada. The data generated here confirm the pervasiveness of meltwater tracks in the Keewatin sector of the LIS. While meltwater tracks have been identified previously in this area (e.g. Rampton, 2000; Utting et al. 2009; Sharpe et al. 2017), it was not known whether these were a local occurrence or how they related to other subglacial meltwater features (i.e. eskers and tunnel valleys).

O2) Detailed manual mapping of all visible traces of subglacial meltwater drainage across the Keewatin sector of the Laurentide Ice Sheet (LIS).

The output of O1 is used alongside existing mapping of eskers (Storrar et al. 2014a) to inform detailed manual mapping of all visible traces of subglacial meltwater flow across the Keewatin sector of the LIS (O2). Here, I create the first large-scale map of all visible subglacial meltwater traces. Mapping and analysing the system as a holistic drainage network influences interpretation of the drainage system's nature and evolution. It allows me to assess the range of different geomorphic expressions of meltwater flow including depositional eskers to erosional features ranging from deeply incised, clear incisional features to less well defined elongated tracks of hummocks. While these features have traditionally been treated separately, work here demonstrates the extra information that can be obtained by combining these into a holistic map. Due to similarities in spacing, widths and associations with other subglacial features, I propose grouping the erosional features under the term 'meltwater corridor' and suggest viewing these features as a continuum, potentially caused by different magnitude or duration of a similar process.

O3) Investigating controls on the distribution and geomorphic expression of subglacial meltwater drainage routes.

I use the mapping completed in O2 to explore the spatial coincidence between meltwater routes of varying geomorphic expression and background controls (e.g. topography, geology, surface substrate). This helps me to assess whether changes in

the mode of drainage or background conditions control feature expression, which will be informative for understanding the nature and evolution of the palaeo-drainage network as well as assessing formation theories. This is done at a large scale to increase confidence in any associations found. The exploration of controls is based on a number of hypotheses proposed in the literature; for example, that eskers form preferentially on hard beds while erosional signatures are more likely to occur on soft beds or that subglacial bed roughness controls the distribution of surface lakes and thus the locations of meltwater inputs to the bed.

O4) Linking process and form to better understand how differing geomorphic expressions are related and the conditions they represent within the drainage system

Here, I apply recent improved understanding of modern contemporary subglacial drainage systems to palaeo-settings to offer insights into their evolution and impact on ice sheet dynamics. While there is often a disconnect between the different fields of studies, this is an important part of better understanding the processes which resulted in palaeo-geomorphological signatures and thus how we interpret them. In the process of mapping and exploring potential links between different drainage signatures, I also identify new serendipitous meltwater feature associations which I also explore here with the aim of further unravelling subglacial drainage processes and the controls on variations in expression.

1.6 Study Location

Keewatin, Nunavut was selected as the main focus of this thesis for a number of reasons. Firstly, it represents an important location for understanding the history of the LIS which was the largest ice sheet to grow and decay during the last glacial cycle (Fig. 1.9). Knowledge of its deglaciation is key to understanding rates, magnitude and mechanisms of ice sheet decay and associated impacts on sea level change (e.g. Carlson et al. 2008; Kleman and Applegate, 2014; Stokes et al. 2015) which are important for contextualising current changes and predicting the future of contemporary ice sheets (Clark et al. 2009; Carlson and Clark, 2012; IPCC, 2013).
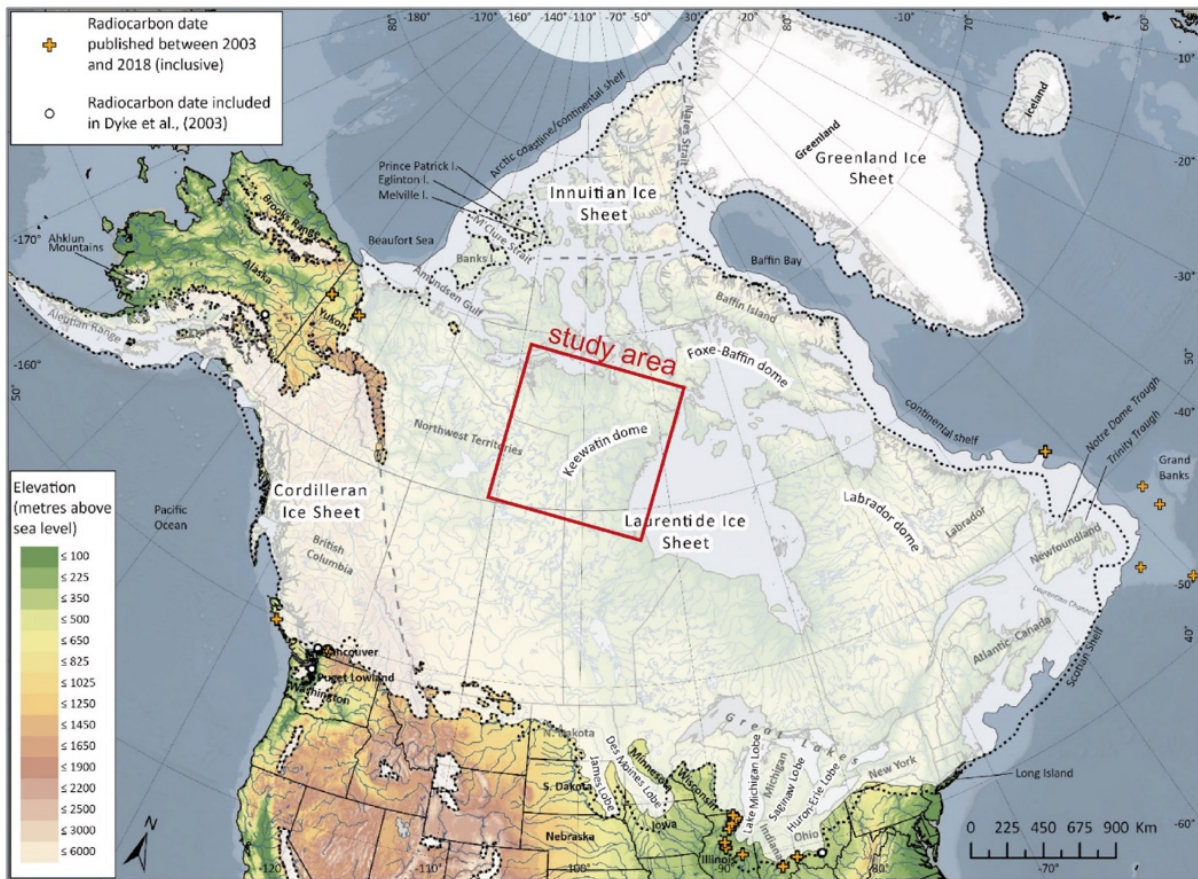
Figure 1.9 Laurentide Ice Sheet at its maximum extent (Dalton et al. 2020) with the approximate location of the study area outlined in red.

The LIS reached its Last Glacial Maximum (LGM) extent at ~ 21 - 20 ka (Marshall et al. 2000) (Fig. 1.9) with the final stages of deglaciation occurring during the early to mid-Holocene (11.5 - 6 ka) coincident with increased summer insolation and atmospheric carbon dioxide concentrations (Carlson et al. 2007, 2008; Marcott et al. 2013). This study focusses on an area (Fig. 1.9) approximately 1 million km^2 to the west of Hudson Bay in northern Canada (Fig. 1.10). An ice dome was centred over Keewatin and acted as a major ice dispersal centre (Lee et al. 1957; Dyke and Prest, 1987; McMartin and Henderson, 2004). This area records the final stages of deglaciation between ~ 10 – 7 ka (Fig. 1.10).
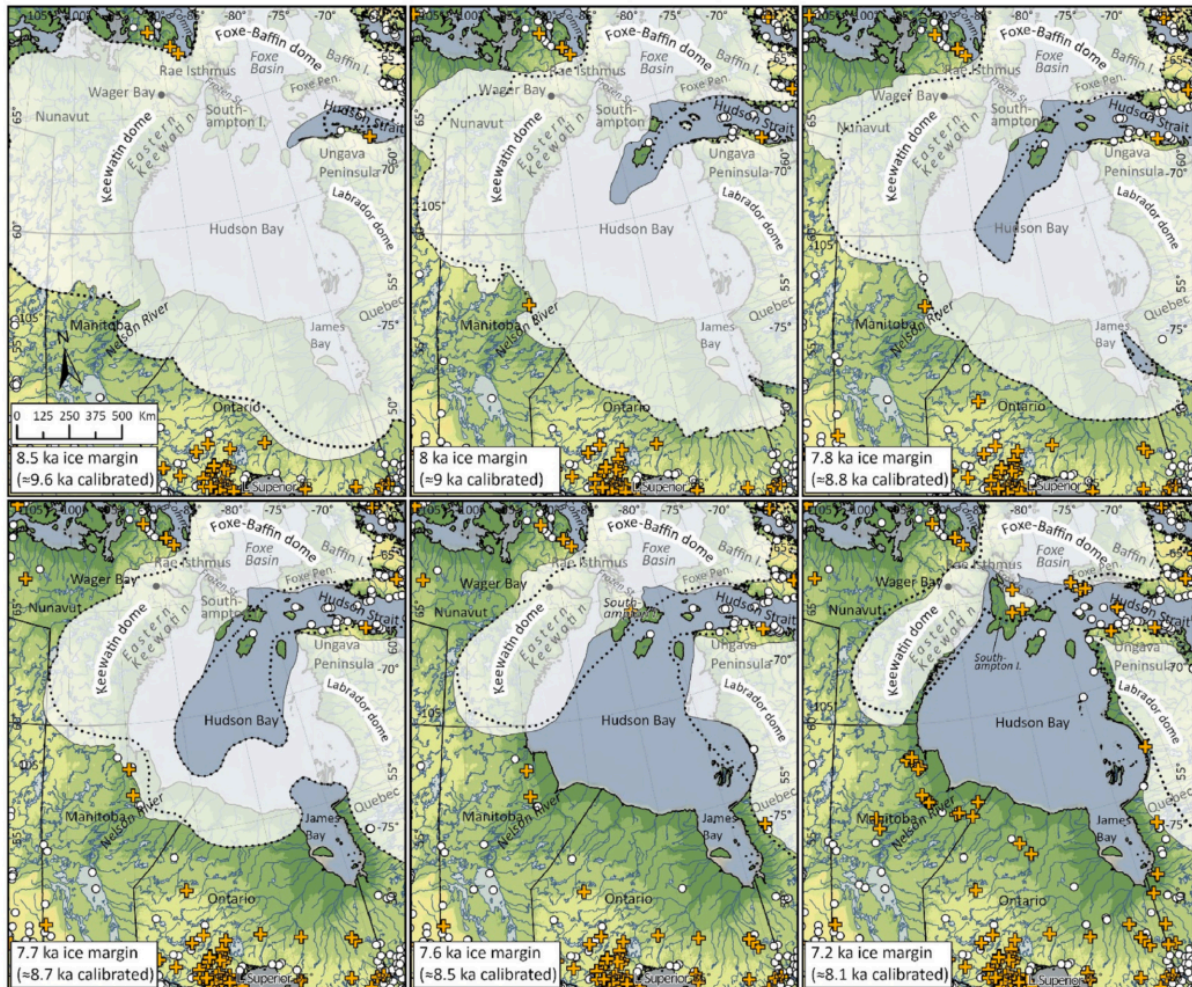
Figure 1.10. Ice margins showing the deglaciation of the study area (Keewatin) at selected time intervals. Ice margins are based on extensive fieldwork and deglacial radiocarbon ages (Dalton et al. 2020).

The Keewatin area exhibits widespread evidence of subglacial meltwater activity and traditionally eskers have been identified as the predominant meltwater landform (Fig. 1.11). Their widespread occurrence has been linked to the fact that the area is broadly flat with negligible relief and is underlain by resistant Precambrian bedrock that is either exposed or covered by till ranging from thin and discontinuous (typically < 2 m) to thick and pervasive (typically > 2 m) (e.g. Clark and Walder, 1994). This has been thought to favour depositional as opposed to erosional geomorphic work. However, meltwater tracks (e.g. St-Onge, 1984; Aylsworth and Shilts, 1989; Rampton, 2000; Utting et al. 2009; Sharpe et al. 2017) and meltwater channels (e.g. Storrar and Livingstone, 2017) have also been recorded in this area. At a large scale, eskers

radiate out from the ice divide, directly beneath which they are rare (Shilts et al. 1987; Aylsworth and Shilts, 1989; Storrar et al. 2013, 2014a). At a local to regional scale, they exhibit a dendritic pattern and 12 - 15 km quasi-uniform spacing (e.g. Banerjee and McDonald, 1975; St-Onge, 1984; Shilts et al. 1987; Bolduc, 1992; Storrar et al. 2014a). Esker formation here has been linked to increased surface meltwater inputs associated with rapid melting of the LIS towards the end of deglaciation (Storrar et al. 2014b).
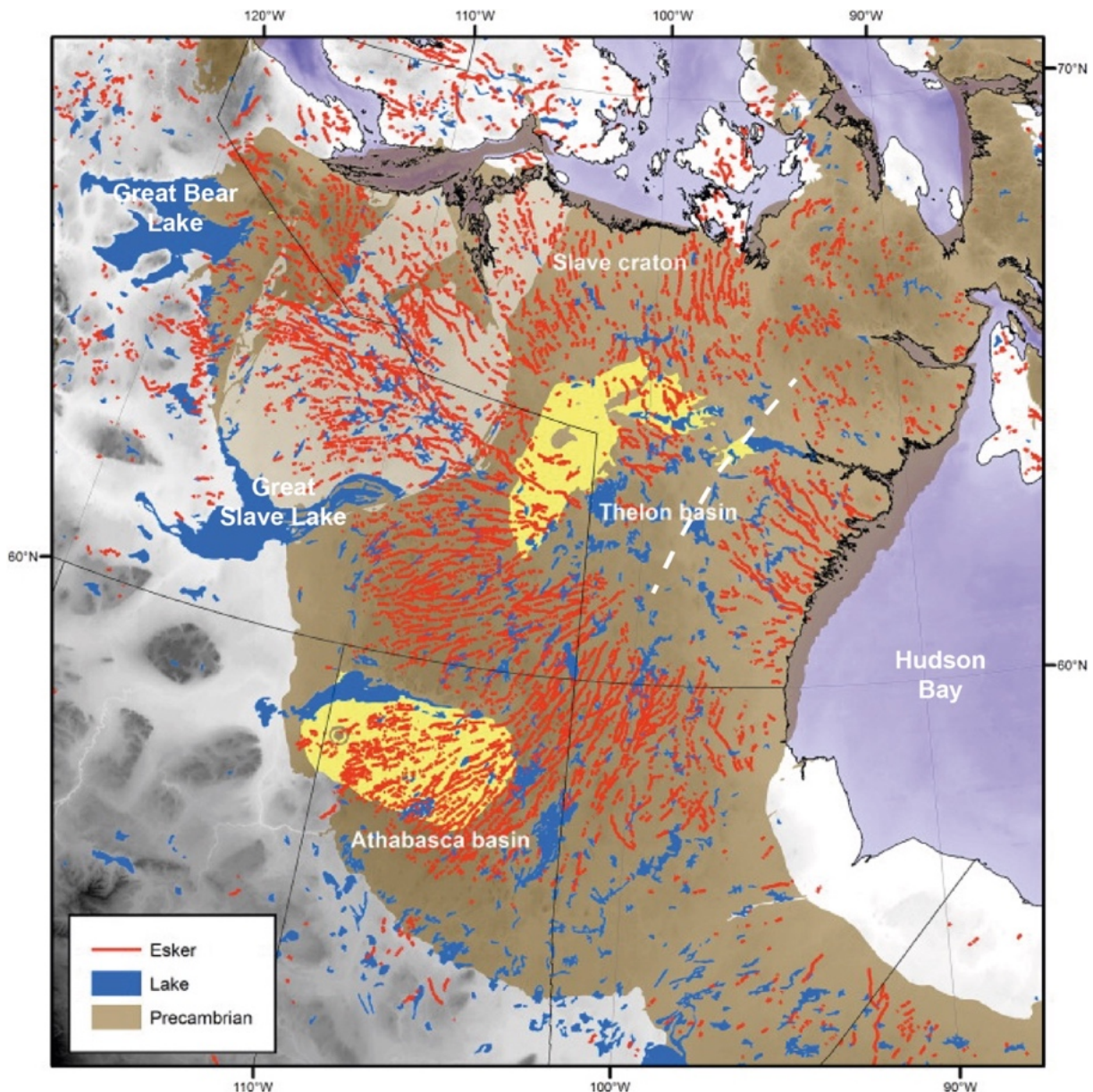
Figure 1.11 Esker distribution around the Keewatin ice divide (yellow polygons represent the Thelon and Athabasca sedimentary basins) with the approximate location of the Keewatin ice divide marked by the white dashed line (modified from Storrar et al. 2014a).

As a result of the above, this area is perhaps one of the closest analogues to the rapidly melting contemporary margins of the GrIS. Furthermore, as mentioned in section 1.4, this study has been motivated by the release of freely available high-resolution ArcticDEM which covers this area. While higher resolution work has been previously undertaken in the wider area (e.g. Utting et al. 2009; Haiblen, 2017), this has largely been restricted to smaller sample sites. This new dataset facilitate a large-scale study of finer-scale features whose wider distribution have yet to be determined. Finally, despite a large body of previous work in this area, the deglacial history of Keewatin remains poorly constrained owing to limited moraines and the remoteness of the area which limits geochronological constraints (Dalton et al. 2020). There is therefore an opportunity to increase understanding of ice sheet dynamics and retreat style across this glaciologically important area by unravelling the meltwater and deglaciation signatures left behind on the ice sheet bed.

1.7 Thesis structure, relation to previous publications and workflow

I will now outline how the above 4 objectives will be achieved within the next 3 chapters. In Chapter 2 I explore automatic mapping as a means of rapidly and objectively obtaining a large-scale dataset of hummock corridors (O1). This work has been published in Lewington et al. (2019). Within the paper the code is developed and tested on three test sites. This is extended further within Chapter 2 by using the method over a large area of northern Canada including the entire study area of this thesis.

In Chapter 3 I use the output from the automatic detection method alongside existing mapping of eskers (Storrar et al. 2013) as a starting point for detailed manual mapping of all visible meltwater traces. This is used to create a holistic map of subglacial drainage at the bed of an ice sheet (O2). I also investigate spatial associations between each drainage expression and background controls and attempt to link the geomorphic signature to observed processes occurring at contemporary ice sheets (O3). This work is published in Lewington et al. (2020).

For the above first author papers (Lewington et al. 2019, 2020), I designed and undertook the data analysis myself with input from my supervisors on project design.

I then designed and drafted the figures and text for the paper with input from my supervisors and two additional co-authors. Although both of these published papers (Lewington et al. 2019, 2020) are relevant to this thesis, I do not cite them as the results are presented herein.

In Chapter 4 I explore serendipitous findings identified during the mapping campaign which have the potential to further understanding of the nature and evolution of the subglacial hydrological system, its relationship with ice sheet dynamics and deglaciation and landform genesis (O4). This includes an investigation into the large-scale distribution of esker beads, fans and nets. I initially identified an area of dense esker bead 'chains' with striking parallel conformity and similarity in spacing. Dr Stephen Livingstone undertook detailed manual mapping in this area and noticed an association between individual beads and v-shaped moraine ridges, interpreted as De Geer moraines (i.e. annual deposits at a grounding line) which was used as evidence for time transgressive formation at a marine terminating ice front. This work was published in Livingstone et al. (2020) and I was second author. In Chapter 4, I tested the hypothesis presented in Livingstone et al. (2020) using a larger sample size from across the whole study area. I also explored the relationship between drumlin length and distance from meltwater corridors after noticing that in a specific location, length did not appear to be uniform or random but instead clustered with shorter eskers more commonly adjacent to meltwater corridors. Finally, I present additional observations of ribbed moraine tracts influenced by subglacial meltwater flow, which have potential to reveal additional insight into the processes occurring at the subglacial bed and add context to the hypothesis developed within Chapter 3.

In Chapter 5, I present the main conclusions from Chapters 2 - 4 and contextualise these within the overall scope of the study and wider literature. I also consider potential limitations of the study and identify areas which could be the focus of future research.

CHAPTER 2: AN AUTOMATED METHOD FOR MAPPING GEOMORPHOLGICAL EXPRESSIONS OF FORMER SUBGLACIAL MELWATER PATHWAYS FROM HIGH RESOLUTION DIGITAL ELEVATION DATA

2.1 Introduction

This chapter has been published in a shorter form in Lewington et al. (2019) but is extended here by applying the automatic method at an ice sheet scale across Canada (~ 2.5 million km^2). The objective of this chapter is to describe and demonstrate the utility of a new automatic method for mapping the large-scale distribution of meltwater tracks from high-resolution DEMs. Meltwater tracks have been identified in sample areas across northern Canada (e.g. St-Onge, 1984; Rampton, 2000; Utting et al. 2009); however, until recently their widespread occurrence had not been confirmed. Initial surveillance of the newly released ArcticDEM suggests these features are common across the Keewatin sector of the LIS. Similar features are also prevalent across the southern Swedish uplands (Peterson et al. 2017), an area comparable to Keewatin in that both the LIS and Fenno-Scandinavian ice sheet experienced rapid deglaciation during a warmer period and both were situated over Precambrian Shield bedrock.

Traditionally information on subglacial bedform distribution and morphology has been obtained by visual identification and onscreen digitization of feature boundaries (e.g. Clark et al. 2004; Greenwood and Clark, 2008; Hughes et al. 2010; Storrar et al. 2013; Livingstone and Clark, 2016). However, several issues are apparent with this approach including its time-consuming nature, the subjectivity of landform and boundary identification, concerns over visualisation / illumination techniques (e.g. Smith and Clark, 2005; Hughes et al. 2010) and uncertainty regarding whether different practitioners produce the same consistent results (e.g. Hillier et al. 2015). The increasing availability and resolution of DEMs and remote sensing imagery and the immensity of data analysis required to manually explore and map large regions at such fine resolution has meant that manual mapping has become a bottleneck in rapidly obtaining information about the presence or absence and characteristics of multiple landforms over wide areas.

Automatic or semi-automatic image analysis methods offer an alternative means of rapidly mapping and extracting quantitative information directly from DEMs (see Evans, 2012 and Bishop et al. 2012 for discussions). Several studies have attempted to employ semi-automatic or automatic techniques for mapping subglacial bedforms, particularly drumlins. These methods typically rely on an object based image analysis approach (OBIA) (e.g. Saha et al. 2011; Evans, 2012; Jorge and Brennand, 2017; Yu et al. 2015; Foroutan and Zimbelman, 2017; Middleton et al. 2020) which uses a multi-resolution algorithm (Baatz and Schäpe, 2000) to group pixels into image objects and classify them based on predetermined rules (e.g. elevation, slope, axis, length, entropy and eccentricity).

2.2 Methods

When visually assessing a landscape by eye a range of factors are considered such as texture, size, shape, association with other landforms etc. By determining the key characteristics of the meltwater tracks through an initial exploration of the terrain, key criteria could be identified and included in the automatic mapping process to help isolate meltwater tracks from their background. These included:

a) Texture (Fig. 2.1 a-c) – while depth was considered as an initial discriminating factor because many meltwater tracks exhibit negative relief (Fig. 2.1 e-f), this was not ubiquitous. However, it became clear from observing these features across the multi-directional hillshaded DEM that they could be isolated based on a 'textural' difference largely due to the presence of hummocks at the bed. In quantitative terms the combination of the specific wavelength and magnitude of variations in the surface elevation data meant that they stand out from their surroundings which are often smooth and streamline. In some examples, this is the only way that meltwater tracks could be identified as a faint trace of former subglacial meltwater flow (Fig. 2.1 a) or as an elongated tract of hummocks (Fig. 2.1 b).

b) Parallel conformity (Fig. 2.1 f) – Like eskers, meltwater tracks typically closely follow the former ice flow direction. As a result, adjacent corridors – at least at a local scale - exhibit a high degree of parallel conformity.
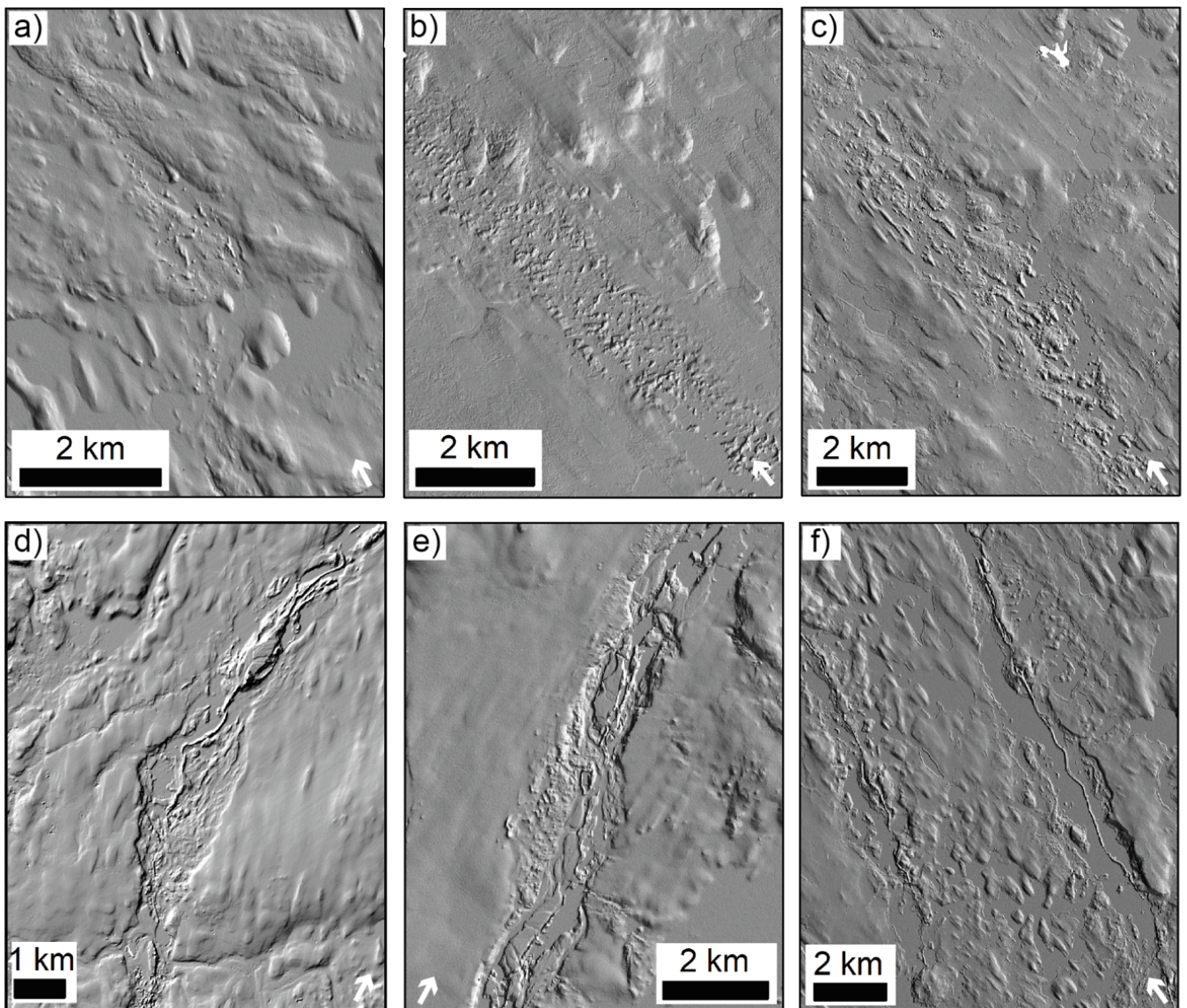
Figure 2.1 Examples of highly variable meltwater track morphologies; a) and b) subtle signatures of palaeo-meltwater flow largely identified due to differences in texture; c) a meltwater track containing hummocks and an esker as well as flatter sections; despite some negative relief the boundary between the meltwater track and its surroundings is not sharp; d and e) meltwater tracks with negative relief, and containing an esker, hummocks and sediment deposits; f) adjacent meltwater corridors clearly distinguished from the surrounding streamlined terrain exhibiting variable relief, containing hummocks and eskers and in places 'scalloped' edges.

c) Elongation (Fig. 2.1 a-f) – meltwater tracks are typically highly elongated features. Although they are sometimes fragmented in places (although far less commonly than eskers), sections are typically far longer (at least 1.5 times) than they are wide.

d) Size (Fig. 2.1 a-f) – using the high-resolution data, meltwater tracks are clearly noticeable features on the palaeo-bed and owing to their fairly continuous nature, individual meltwater track segments are typically above a certain area. Thus removing smaller features (< 1.6 km^2) is likely to remove a large amount of 'noise'.

The DEM tiles used come from the freely-available ArcticDEM dataset (https://www.pgc.umn.edu/data/arcticdem) which provides 50 x 50 km tiles at 5 m resolution for all land area above 60°N. To develop and test the automatic method, three test sites were selected from the ArcticDEM (Fig. 2.3). These were chosen to ensure a range of meltwater track morphologies and background conditions were sampled (e.g. varying relief, presence / absence of fluvial features etc.). At test site 1 meltwater tracks typically exhibit strong positive or negative relief with well-defined edges and are qualitatively clearly distinguished from their surroundings (Fig. 2.4 a). The site includes relatively straight meltwater tracks extending significant distances across the bed. At test site 2 the background topography is more complex and meltwater tracks tend to curve across the landscape, exhibit less pronounced relief and have poorly defined boundaries (Fig. 2.4 b and c). The meltwater tracks at test site 3 are typically discontinuous and have less noticeable relief and the surrounding landscape is characterised by a strong fluvial network and significant vertical relief in the south-west of the site (Fig. 2.4 d).
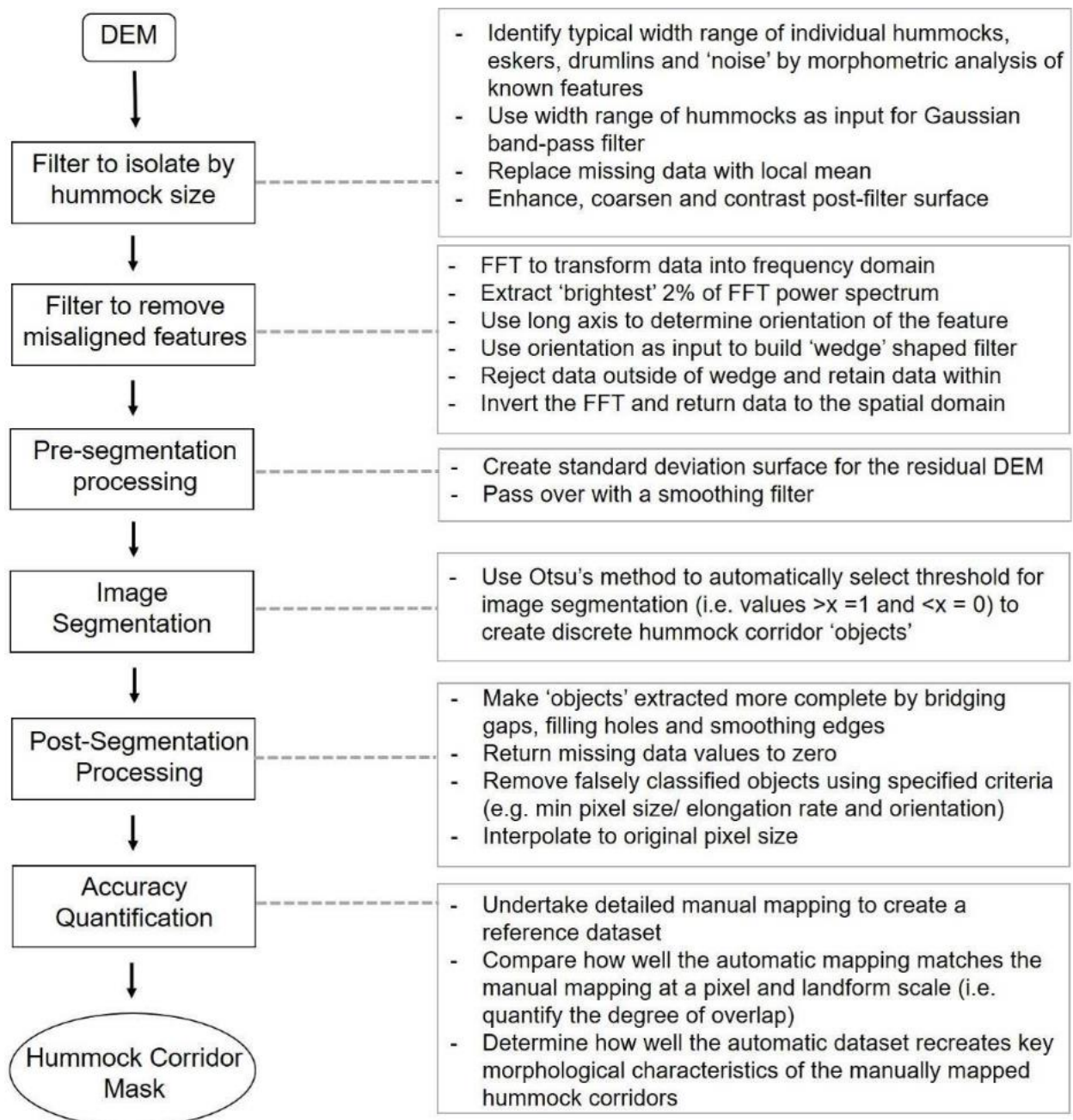
Figure 2.2 Main steps of the automatic method to identify and extract meltwater tracks (left-hand sequence) with details about each step expanded on (right).
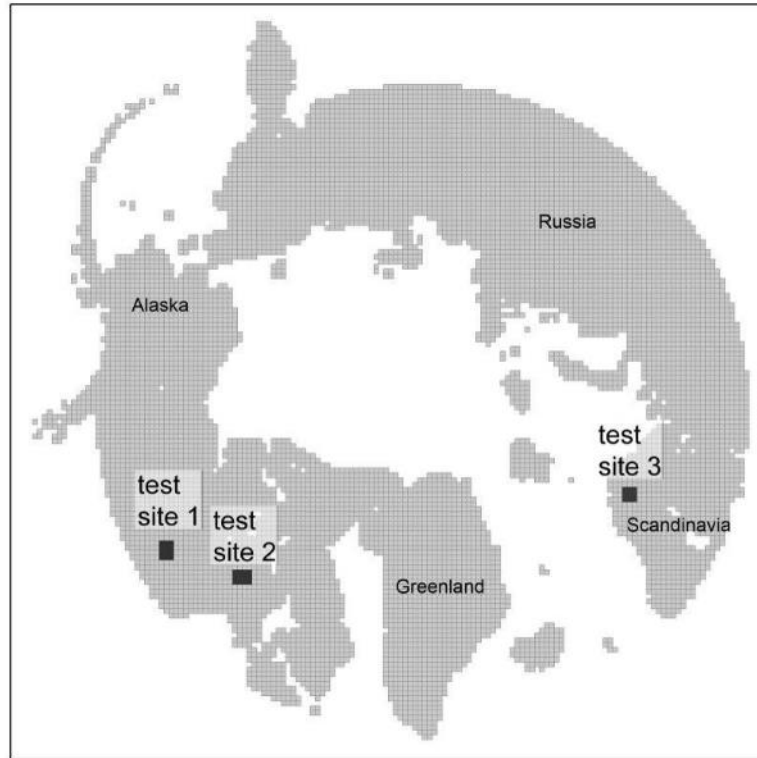
Figure 2.3 Location of the three test sites used in this chapter: (1) Northwest territories, Canada (30,000 km^2), (2) Nunavut, Canada (30,000 km^2) and (3) Northern Scandinavia (22,500 km^2). Grey background indicates the total extent of Arctic DEM data. See Fig. 2.4 for example of typical terrain from each test site.

2.2.1 Processing Step One: Filter to isolate hummocks by size

Elevation values in a DEM vary significantly, depending on the presence of large-scale topographic features (e.g. valleys, hills, mountains etc.) and / or the type of landforms present. Typically, landforms fall within a definable length-scale and amplitude of topographic variability. In theory, mathematical operations can be applied to a DEM to isolate a particular feature based on this knowledge. Using length-scales to separate morphological features of interest from background topography is well established within the earth sciences (e.g. Wessel, 1998; Hillier and Watts, 2004; Hillier and Smith, 2008) and has been used within glacial geomorphology to enhance the detection of subtle features such as lineations (Hillier and Smith, 2008).
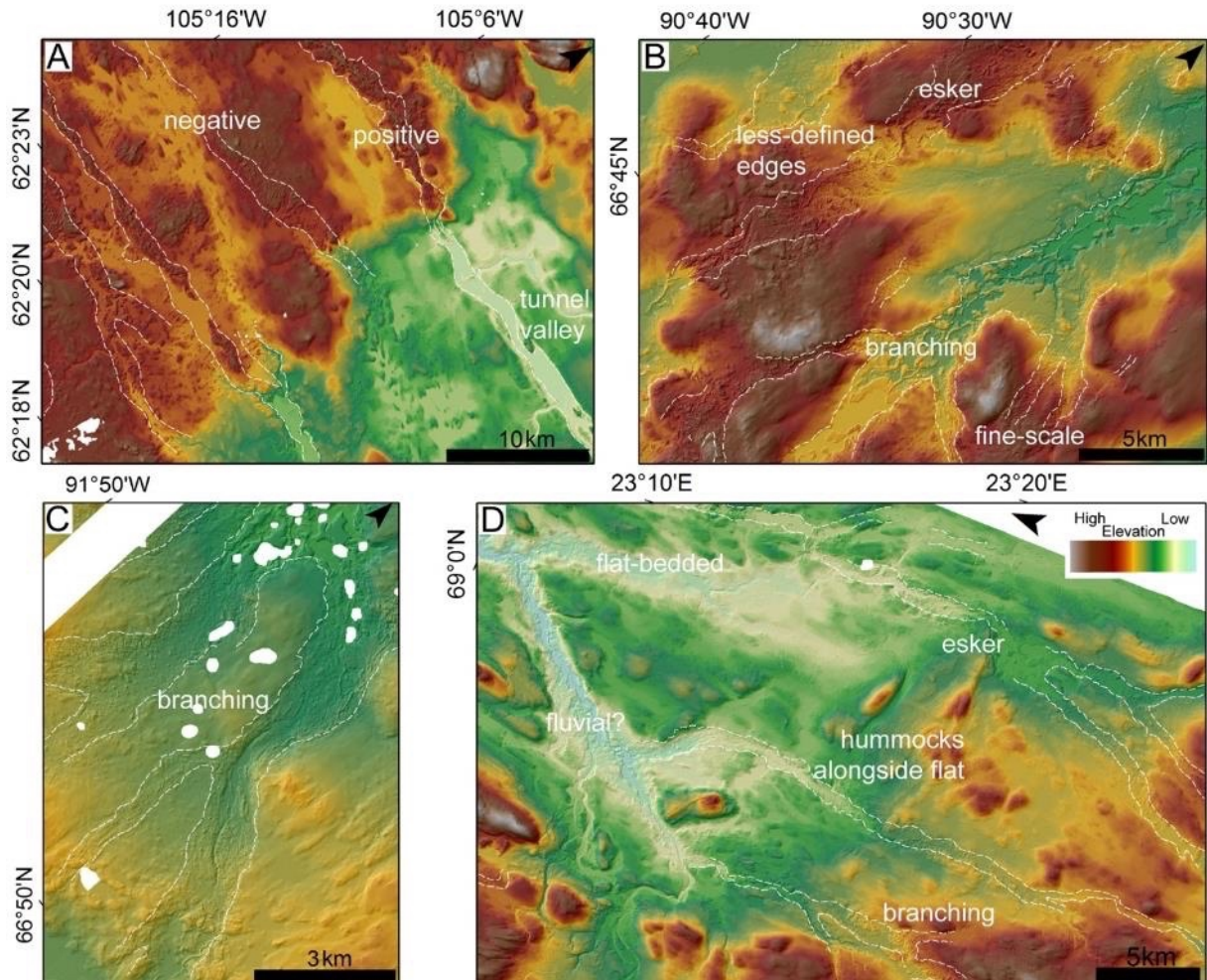
Figure 2.4 Example of meltwater tracks (outlined in white dashed lines) from each of the test sites with locations identified in Fig. 2.11 - 2.13 (a) Test site 1 - note the transition down-flow (inferred ice flow from east to west) from tunnel valley to meltwater track associated with an increase in elevation and the alternating positive and negative meltwater tracks. (b) and (c) Test site 2 – note the more complex meltwater tracks that branch and can be difficult to identify on the bed owing to their more subdued relief. (d) Test site 3 – example of meltwater tracks branching off a large central channel with few/ no hummocks in places.

Individual hummocks from the three test sites were randomly selected, measured (long axis) and recorded to determine their typical length-scale range (Fig. 2.5). To minimise overlap with features which tend to co-occur with meltwater tracks, drumlins, eskers and background 'noise' in the DEM (artefacts which often occur in elongate patches) were also sampled (their minor axis). The results (Fig. 2.6) reveal a typical length-scale of 40 - 180 m for hummocks. This is distinguishable from the 'noise' and

the drumlins at the lower and upper bounds. Although eskers display a similar length-scale as hummocks, their low spatial density largely precludes their classification as meltwater tracks at later stages of processing.
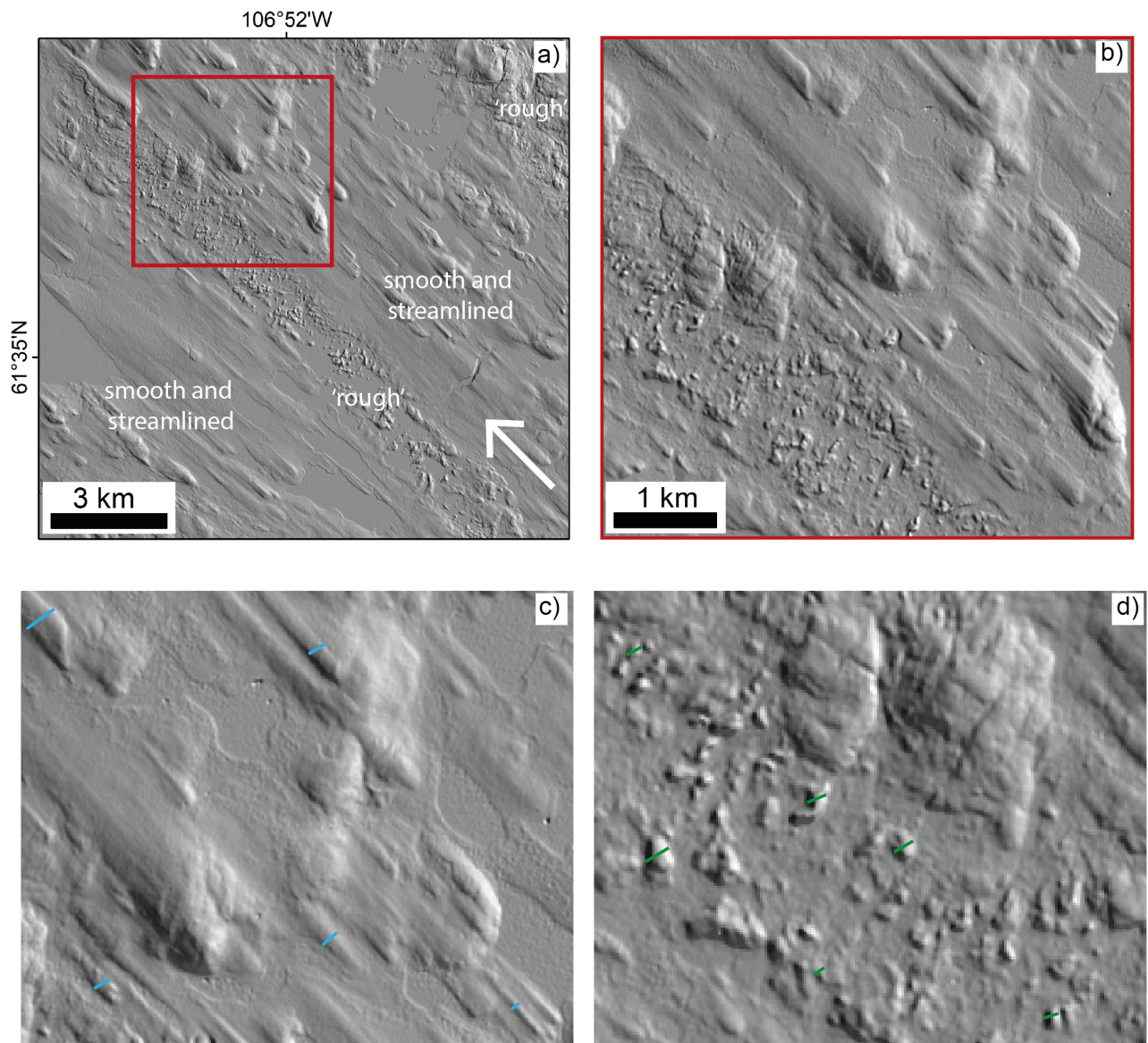
Figure 2.5 Example of textural difference between meltwater corridors and surrounding smooth, streamlined terrain. This was used to develop a method for the delineation of drumlins (c – blue) and hummocks (d – green). Hummocks were clearly differentiated from drumlins based on their size (considerably smaller), shape (typically not elongated and non-uniform) and their location (i.e. within meltwater tracks or along meltwater pathways).

The length-scale range was used to determine the upper and lower bounds of a 2D Gaussian-weighted band-pass filter (filt2: written by Chad A. Greene of the University of Texas Institute for Geophysics for use in Matlab - freely available at: https://uk.mathworks.com/matlabcentral/fileexchange/61003-filt2-2d-geospatial-data-filter). The band-pass filter suppresses spatial frequencies outside the specified length-scale range, thus attenuating (although not eliminating) a large amount of the topographic variation associated with other features on the bed. Values of 40 and 150 m were selected as the lower and upper bounds as this struck the best balance between retaining information whilst preventing false detections. This resulted in a residual surface with a large amount of background topographies removed, emphasising areas with features within the length-scale of individual hummocks.
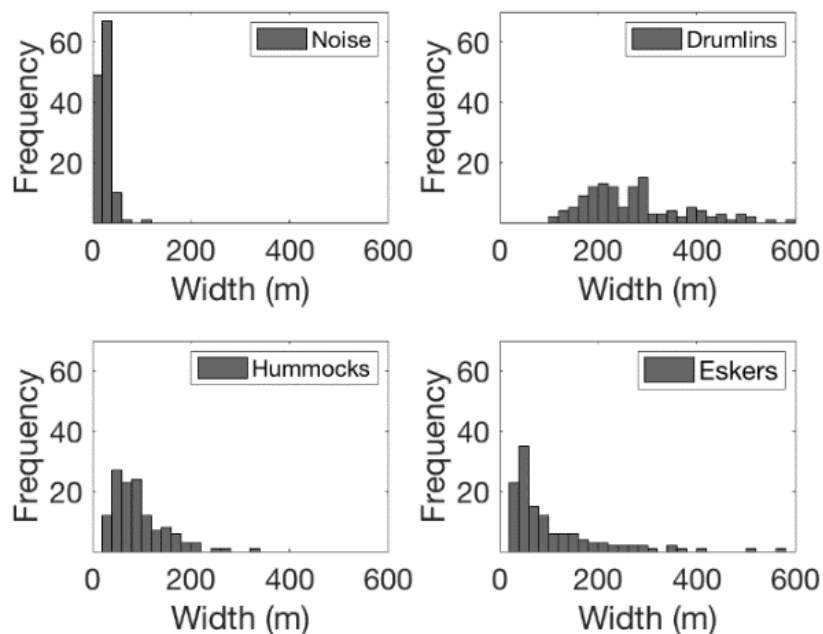
Figure 2.6 Histograms showing the horizontal widths of 'noise', drumlins, hummocks and eskers (n = 130) randomly selected and measured from the three test sites. Note that the hummocks form their own population with only a small overlap at the upper and lower ends. A large amount of the 'noise' (artefacts in the DEM that sometimes occur in linear zones) was smaller than 10 m thus preventing accurate measurement.

For some hydrological features (e.g. lakes and rivers) and in areas of cloud cover or shadows, the ArcticDEM tiles contain no elevation data and were coded as

NaN (i.e. Not a Number). While the 2D Gaussian-weighted band-pass filter is designed to work on data with NaNs, several of the subsequent processing steps require continuous data so a method to fill in the NaNs was implemented. Standard interpolation or smoothing methods (e.g. inpaint_nans - https://uk.mathworks.com/matlabcentral/fileexchange/4551-inpaint_nans) can be used to fill NaNs with realistic values over smaller areas; however, the large size of some missing data patches here (up to ~ 480 km^2) would result in the introduction of artefacts and thus render this approach inappropriate. To address this a method for 'flooding' isolated NaN patches with their individual local mean was developed. Firstly, a mask of contiguous patches of NaNs was created. The mean elevation of a 100-pixel wide buffer around each patch was then used to replace the NaNs within. This was carried out after the initial filtering which removed a large amount of elevation variations, creating more uniform values within the NaN buffers and reducing the likelihood of steep jumps in elevation across short distances. While this approach precluded the detection of meltwater tracks within these areas, it effectively blended the missing data with its surroundings preventing spurious artefacts. NaN values in the original data were returned to zero at the final stage to ensure that no areas were falsely classified.

To further enhance the contrast in relief at the length-scale retained by the band-pass filter the residuals were converted to absolute values and each pixel replaced with the maximum of the adjacent pixels if the original value was greater than the tile median or replaced with the minimum of the adjacent pixels if the original value was less than the median. This process is analogous to 'contrast stretching' in the processing of grey-scaled images. The 'enhanced' residual surface was then normalised by rescaling the data so values fell between 0 and 255 (i.e. unsigned 8-bit integers) to ensure consistency between different tiles and to minimise memory requirements for storing data (Fig. 2.7).
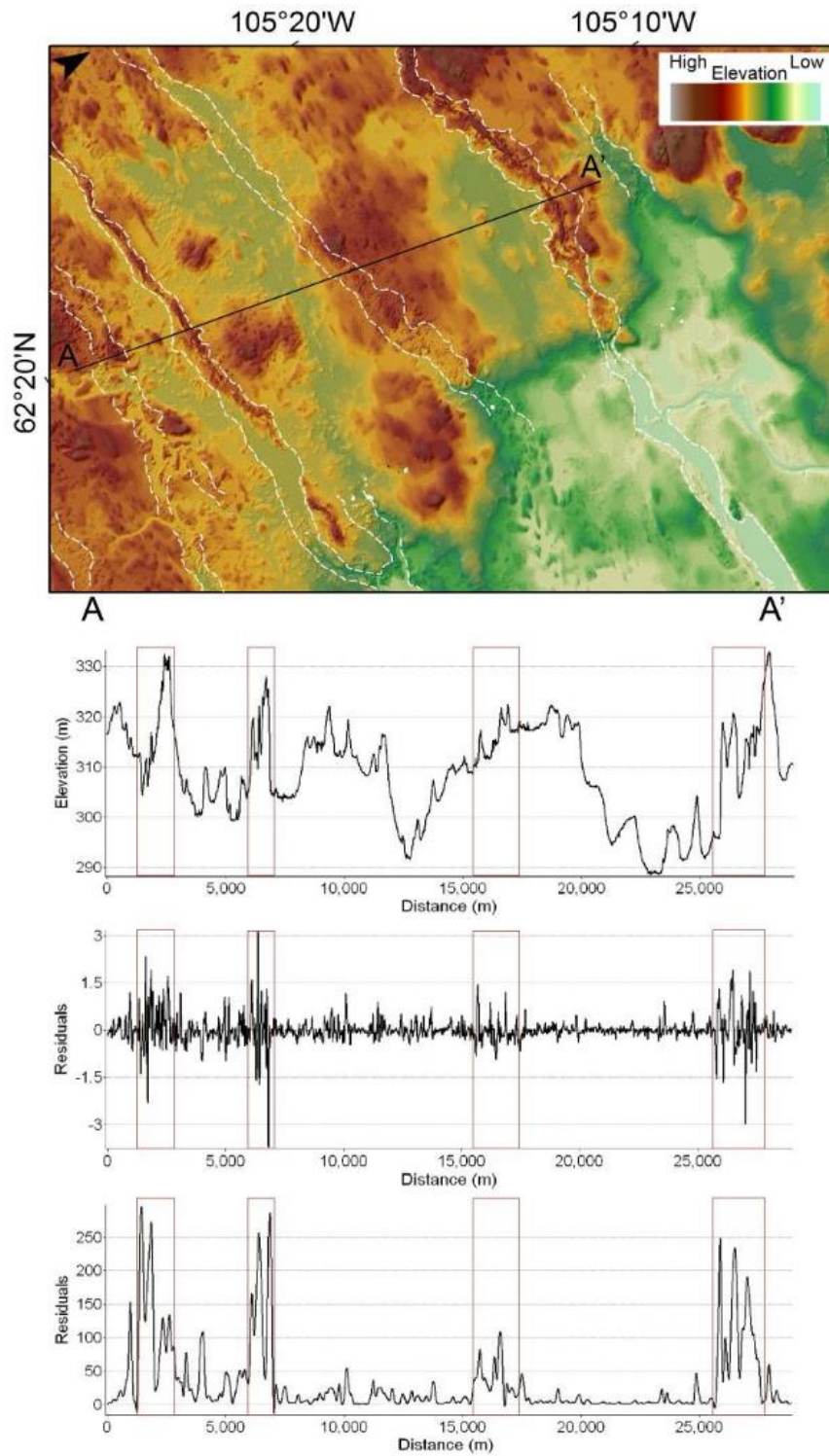
Figure 2.7 Cross-profiles across four meltwater tracks (red boxes) showing top to bottom: (i) original elevation data with significant elevation variations, (ii) residual surface created post band-pass filter and (ii) residual surface created following enhancement. The 2D output of this process for the same area can be seen in Figure 2.8.

2.2.2   Processing Step Two: Filter to remove misaligned features

Fast Fourier Transforms (FFTs) are commonly used in image analysis to identify and remove interference or artefacts and to analyse repeating patterns and extract features (e.g. Van Buren, 1987; Tsai and Hsieh, 1999; Jordan and Schott, 2005; Arrell et al. 2008; Munch et al. 2009). In glaciology, FFTs have been used to map crevasses from remotely sensed images (e.g. Williams et al. 2018) and to automatically derive the spectral signature of mega-scale glacial lineations (MSGLs) (Spagnolo et al. 2017). At regional scales, long axes of meltwater tracks are typically observed to have a (sub-) parallel arrangement (e.g. Peterson et al. 2017). A FFT was therefore applied to each enhanced DEM tile to identify the dominant orientation of meltwater tracks and remove misaligned features.

The FFT produces a power spectrum array of the enhanced DEM in the frequency domain with the zero-frequency component (measuring the 'average' elevation) located at the centre of the array. In the frequency domain directional features are identified as a concentration of high-intensity pixels (i.e. bright areas), reaching out from the centre and perpendicular to the direction of the feature in the spatial domain (Fig. 2.8 b). A 'wedge-shaped' filter was then applied to the FFT of the enhanced DEM to extract features aligned with the dominant direction of the image and reject misaligned features. To automate this process and allow the width and orientation of the wedge filter to vary with each input tile, the highest 2% of the power spectrum was extracted, creating a binary mask (Fig. 2.8 c). The shape of this mask varied depending on the 'strength' of the directionality in the image. The amplitude distribution of a tile's FFT (in the 2D frequency domain) generated an ellipse-shaped mask when there were well-defined meltwater tracks while less well-defined / no meltwater track resulted in a circular shape. Identifying the start and end points of the long axis of the mask allowed the use of trigonometry to determine its angle relative to the x-axis (tan(x) = change in x / change in y) and this was used as the orientation input for the wedge-filter. Next, the length of the minor-axis was calculated and divided by three – based on sensitivity analysis – to determine the wedge filter width (i.e. how far it could deviate from the centreline Fig. 2.8 d). Once the filter had been applied and the misaligned features removed, the FFT was inverted to return the filtered data back into the spatial domain (e.g. Fig. 2.8 e).
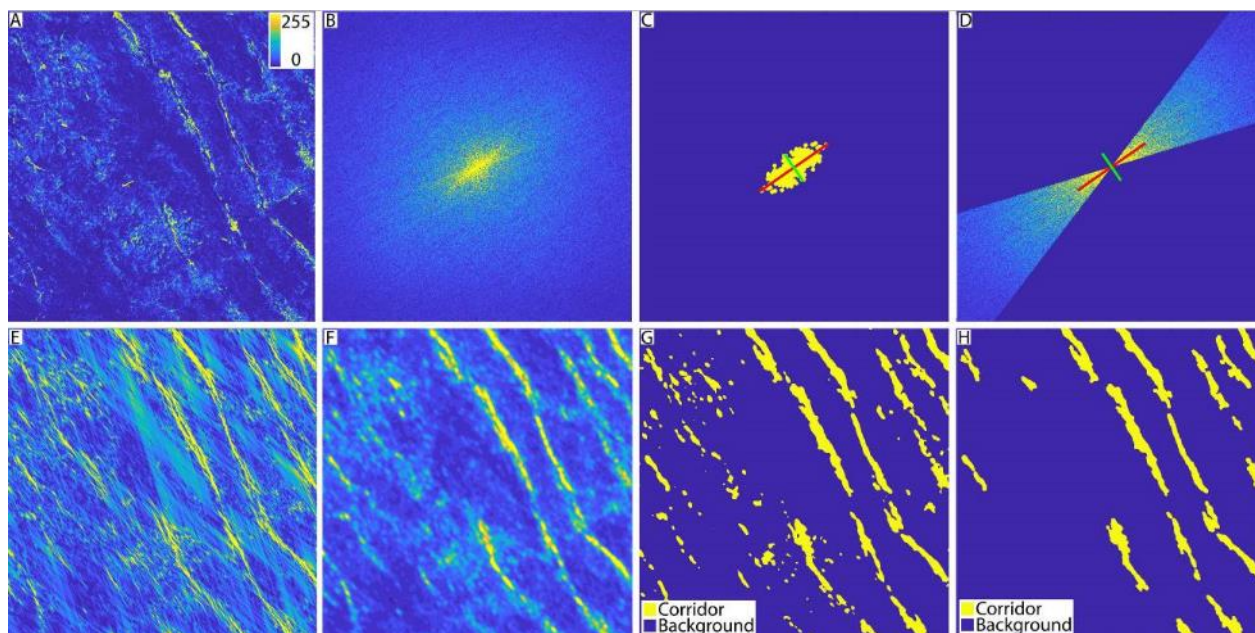
Figure 2.8 2D output of the method stages outlined so far in the text for the same area as Figure 2.7; (a) DEM tile post-spatial filter and enhancement (but pre FFT filter) with scale bar representing intensity. (b) FFT power spectrum in the frequency domain with the 'average' at the centre and the directional trend evident from the peaks reaching out. (c) FFT mask i.e. highest 2% of the power spectrum with long (red) and short (green) axes identified. (d) 'Wedge' shaped filter overlain on the FFT – inside the wedge information is retained whilst outside (blue) is rejected. (e) Tile post spatial and FFT filtering i.e. data returned to the spatial domain (colour scale limited to intensity of 50 to highlight meltwater track). (f) Tile post standard deviation and smoothing (colour scale limited to intensity of 20 to highlight meltwater track). (f) Tile post segmentation. (h) Tile post clean up i.e. a binary image where meltwater track have a value of 1 (yellow) and the background has a value of 0 (blue).

2.2.3   Processing Step Three: Image Segmentation

Image segmentation is the final processing stage used to extract meltwater tracks. It is commonly used in image processing to divide an image into distinct regions, each containing pixels with similar characteristics e.g. colour or texture (e.g. Haralick and Shapiro, 1985; Ryherd and Woodcock, 1996; Baatz and Schape, 2000). Thresholding is the simplest image segmentation technique and produces a binary image with two sements each containing solely pixels with intensity values either

greater or smaller than the threshold. Here, a threshold was selected which separated pixels which likely contain meltwater tracks (high values) from those which do not (low values). The above steps were designed to enhance the contrast between these two areas.

To minimise user input an automatic method for selecting the threshold was chosen. Here, the approach of Otsu (1979) which detects a threshold based on a histogram of pixel intensity values was selected. Otsu's method is optimal when the foreground is distinctly different from the background (e.g. a white object on a black background) and when there is limited intensity variation within each of the two regions. To ensure the best output, the difference between meltwater tracks and their background was further enhanced. Standard deviation was used as a measure of topographic roughness, highlighting areas with a high degree of local variations (i.e. 'rough' sections of the bed within the meltwater tracks where topographic variations had been retained). A 12-by-12 moving average filter was then passed over the residual surface to homogenise the meltwater track (Fig. 2.6 f).

The image was then segmented using the threshold determined by the Otsu (1979) method creating a binary image of meltwater track (with a value of 1) and background (with a value of 0) (Fig. 2.8 g). Next, several post-processing methods were applied to improve the segmentation output (Fig. 2.6 h). To improve the meltwater tracks longitudinal completeness, a series of morphological operations available in Matlab were used to bridge gaps ('bwmorph, bridge') in the data. Any interior holes were then filled ('imfill, holes') and the edges smoothed (imopen with a disk structuring element). False classifications were recognisable in the data as small 'speckles', objects with low elongation values or objects which did not conform to the dominant orientation. To remove these, several criteria were specified. Firstly, individual objects in the final mask must have (a) an area exceeding 40,000 pixels (1 pixel = 5 x 5 m), (b) an elongation ratio greater than 1.5 (comparison with manual mapping suggests that rough regions with a value less than this are not meltwater tracks), and (c) they must be aligned within +/- 40° of the dominant direction. The last criterion removed erroneous 'patches' since 'real' misaligned features had already been removed by the FFT.

2.2.4 Accuracy Quantification

Finally, to quantify how well the automatic output captured 'reality' an accuracy assessment was undertaken. Detailed manual mapping of meltwater tracks at the three test sites were used as a reference dataset to compare with the automatic output. Meltwater tracks were mapped as polygons to allow for direct comparison with the automatic output through on-screen digitization in ArcGIS 10.4. (Fig. 2.9). Meltwater tracks were identified as regions of hummocks which stood out from the surrounding smooth, streamlined bed, often exhibiting a positive / negative relief and an association with eskers.

The spatial scale selected for accuracy assessment is important and will likely influence the results (e.g. Dungan, 2002; Stehman and Wickham, 2011). As a first-order measure of accuracy the manual and automatic datasets were compared at the pixel-scale. More detailed analysis at the landform-scale was then performed to assess the method's utility in reproducing the spatial distribution, pattern and morphology of meltwater tracks at an ice-sheet scale. The landform scale accuracy assessment is considered the more appropriate measure for determining the method's ability to provide insight into the formation and evolution of subglacial meltwater pathways.
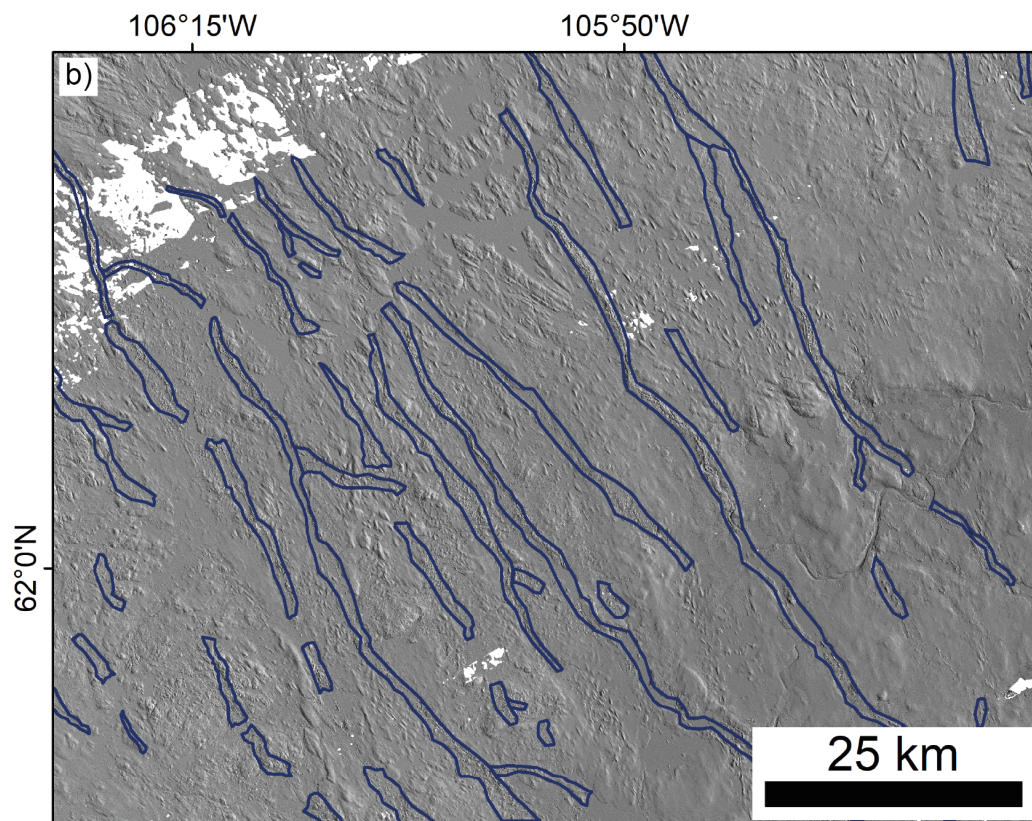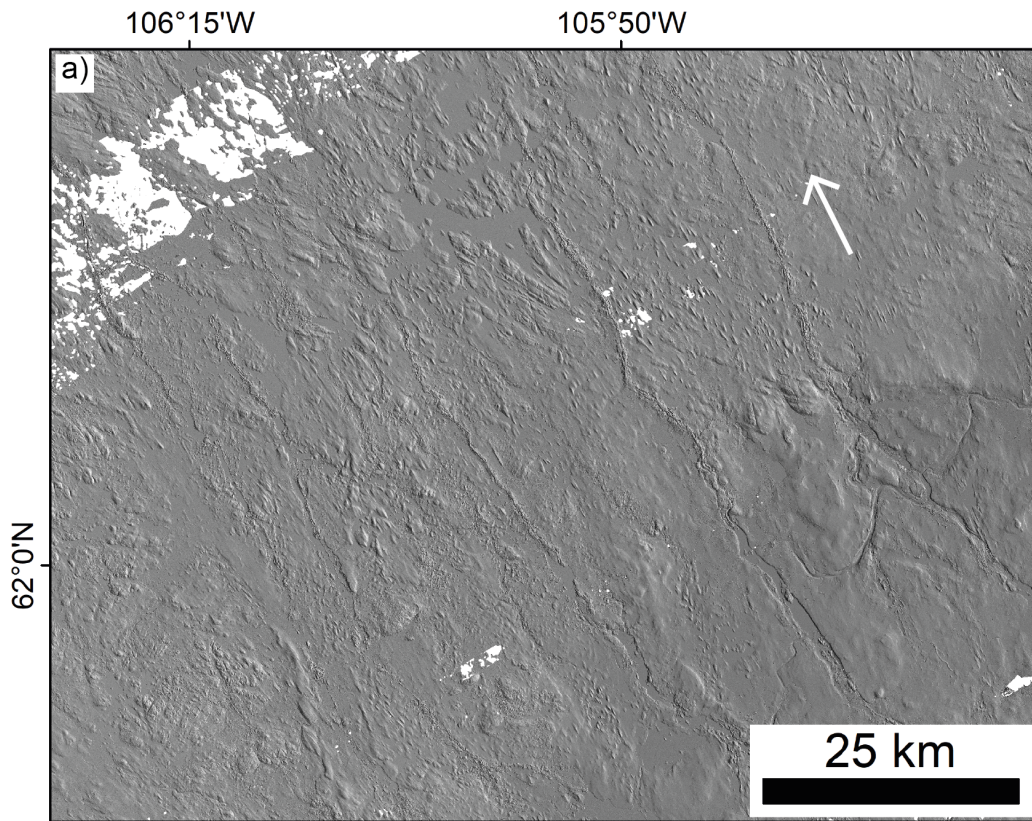
Figure 2.9 Meltwater corridors in test site 1 and an example of their detailed manual mapping (b).

2.2.4.1 Pixel-scale

To compare the datasets at a pixel-scale the manual and automatic output were overlain and each pixel classified as either:

- True Positive (TP) – positive in the reference and automatic output
- False Positive (FP) – negative in the reference and positive in the automatic output
- True Negative (TN) – negative in the reference and automatic output
- False Negative (FN) – positive in the reference and negative in the automatic output

where TP represents the location of pixels classified as meltwater tracks using both methods, FP represents pixels classified as meltwater tracks in the automatic but not in the reference (i.e. over-estimation), TN represents background pixels in both data and FN represents pixels classified as meltwater tracks in the manual but not in the automatic (i.e. under-estimation). This information was recorded in an error matrix.

Using this information, more specific measures of quality were calculated:

$$\text{recall} = \frac{\text{TP}}{(\text{TP}+\text{FN})} * 100 \qquad\qquad (\text{equation } 1)$$

$$\text{precision} = \frac{\text{TP}}{(\text{TP}+\text{FP})} * 100 \qquad\qquad (\text{equation } 2)$$

where recall indicates how much of the reference data are captured by the automatic output (i.e. 'completeness') and precision indicates how much of the automatic output matches the reference data (i.e. 'correctness'). These measures have been used in remote sensing and OBIA accuracy assessments (e.g. Hillier et al. 2015; Zhang et al. 2015; Pratomo et al. 2017).

2.2.4.2 Landform-scale

To quantify landform-scale accuracy, region-based precision and recall indicators were used. The approach was similar to the pixel-scale method described

in Section 2.2.4.1 but instead of overlaying and comparing individual pixels, individual meltwater tracks were compared. To achieve this, the match criteria and mapping direction were determined first. A match criteria specifies the minimum overlap required between the manual and automatic mapping before a 'match' is confirmed. This criterion varies in the literature; d'Oleire-Otmanns et al. (2013) consider any overlap a success, Eisank et al. (2014) select a minimum of 50% overlap and Jorge and Brennand (2017) use two criteria (a) a 'morphometric detection rate' requiring a 50% minimum overlap and additional divergence criteria and (b) a 'general detection rate' requiring a 10% minimum overlap. Here, a minimum overlap of 25% was selected. While this is lower than the 50% often used, the size of many of these features is significantly greater than those in the literature above (which is focussed on drumlins) and visual assessment suggests that a minimum 25% match is able to capture the meltwater tracks sufficiently.

The mapping direction determines which way the two datasets are compared – i.e. manual to automatic or automatic to manual. This alternates when calculating recall and precision for region-based measures (Zhang et al. 2015). For recall (i.e. 'completeness') the automatic segments are matched to the reference. Conversely, for precision (i.e. 'correctness') the reference polygons are matched to the automatic segments. For both recall and precision, meltwater tracks which overlapped by greater than the minimum overlap (25%) were classified as true positives while meltwater tracks which were overlapped by less than the minimum overlap or with no overlap, were classified as false positives and false negatives respectively.

2.2.4.3 Morphology

To gain meaningful information from about the morphometry of meltwater tracks from the automatic output, it is important to assess how well the automatic mapping matches the morphometric characteristics of the manually mapped dataset. Metrics (length and width) for each corridor were extracted automatically from both datasets. To obtain the most representative results, pre-processing of the manual and automatic mapping were undertaken to separate corridor networks and individual meltwater tracks into discrete features. This was done manually in ArcGIS with care taken to avoid bias in the results by splitting features only where there was obvious evidence

of trunk / tributary meltwater tracks, merging (e.g. small pixel bridges), clear change in orientation of features or evidence of elongated sections joining falsely classified 'patches'. The overall clarity of the output may be further improved by separating the 'patches' (i.e. falsely classified sections) from the elongated data (i.e. the meltwater tracks) and selectively removing them.

The length of each corridor was calculated automatically by identifying the furthest two boundary pixels and measuring the straight-line distance between them. As meltwater tracks can be long width was measured using perpendicular transects at 5% intervals along each corridor. An average value was then assigned ensuring that variations in width were captured for all meltwater tracks regardless of their length. Finally, 'real-length' was approximated by dividing the area of the meltwater track by its mean width (henceforth referred to simply as 'length').

2.3 Results

The automatic method provided maps of meltwater tracks across the three test sites (Fig. 2.10). Importantly, mapping of meltwater tracks was consistent across individual input tiles and allowed the detection of relatively continuous meltwater tracks. Figure 2.10 shows how the automatic output is able to pick out the dominant direction of meltwater tracks and the location of individual features.
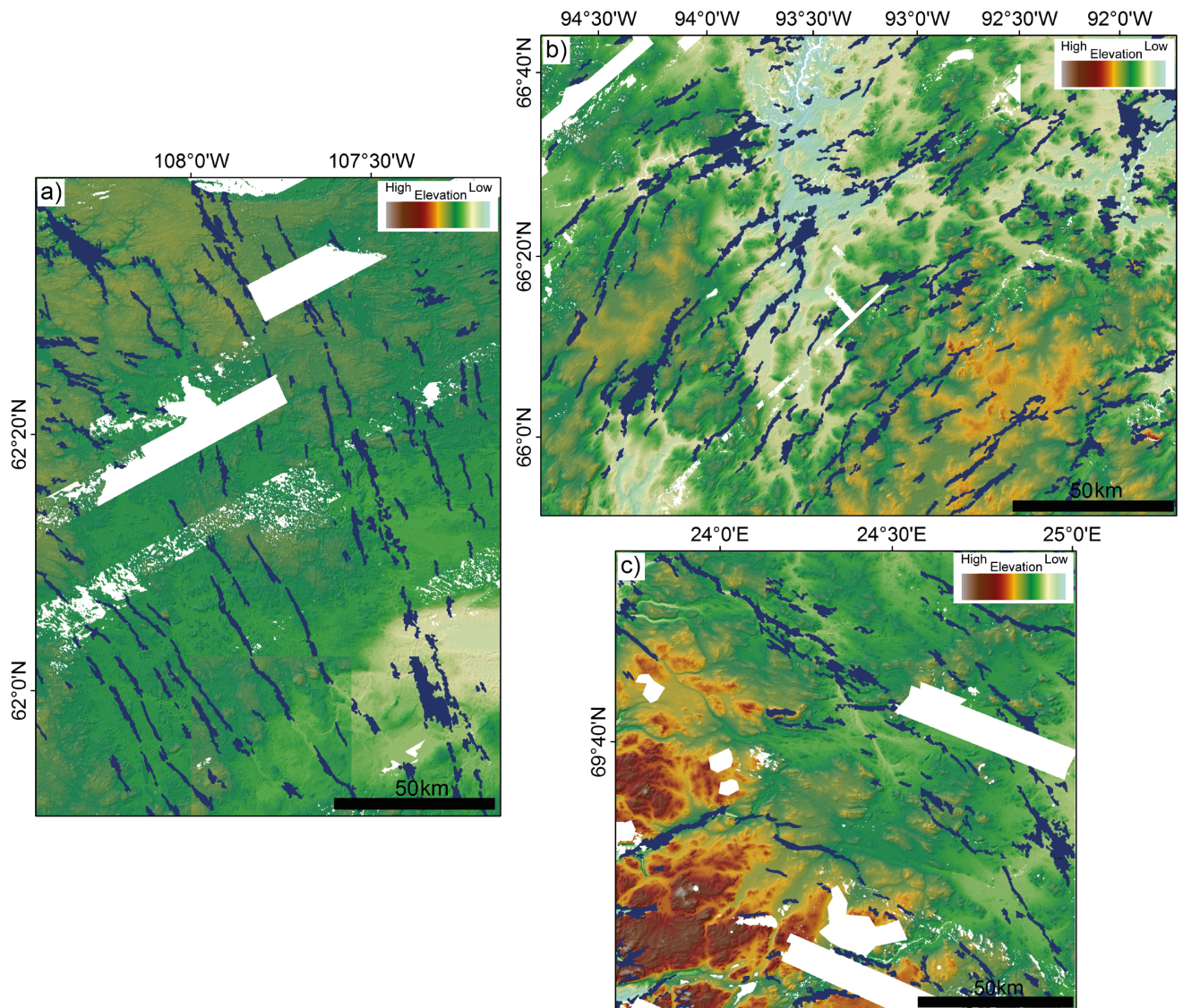
Figure 2.10 Automatic mapping output for test site 1 (a), test site 2 (b) and test site 3 (c).

2.3.1 Automatic method performance

2.3.1.1 Pixel-scale assessment

At test site 1 (Table 2.1) recall is 45 % and precision 33 %. This was the highest recall value of the three test sites and likely reflected the fact that test site 1 contained the longest, widest meltwater tracks with the most pronounced relief and clear boundary edges. Test site 2 has a 42 % recall and 36 % precision. This was the highest precision value of the test sites, indicating the lowest percentage of 'false'

classifications. At test site 3 recall is 16 % and precision 6 %. This was significantly lower than the other two sites and visual inspection confirms this was because the automatic method misidentifies several large valleys as meltwater tracks.

Table 2.1 Error matrix showing the number of correctly/ incorrectly identified pixels at each test site. These values were used to calculate further measures of accuracy i.e. precision and recall (equations 1 and 2).

		Automatic: *Yes*	Automatic: *No*
TS 1	**Manual: *Yes***	31001304 (TP)	37947732 (FN)
	Manual: *No*	62046071 (FP)	1061300000 (TN)
TS2	**Manual: *Yes***	46188919 (TP)	63775215 (FN)
	Manual: *No*	81485389 (FP)	1008300000 (TN)
TS3	**Manual: *Yes***	4057104 (TP)	21866102 (FN)
	Manual: *No*	63649814 (FP)	810426980 (TN)

2.3.1.2 Landform-scale assessment

2.3.1.2.1 Region-based recall and precision

The number of meltwater tracks correctly / incorrectly identified at each test site is summarised in table 2.3. These values were used to produce a measure of precision and accuracy (equations 1 and 2).

Table 2.2 Error matrix showing the number of correctly/ incorrectly mapped meltwater tracks at each test site. Results for both matching directions are included i.e. manual to automatic (for calculating recall) and automatic to manual (for calculating precision) as manual and automatic datasets do not always have the same number of meltwater tracks.

		Automatic: *Yes*	Automatic: *No*	*Total Manual*
TS 1 **Recall**	Manual: *Yes*	118 (TP)	106 (FN)	*224*
	Manual: *No*			
	Total Automatic			
TS 1 **Precision**	Manual: *Yes*	108 (TP)		
	Manual: *No*	115 (FP)		
	Total Automatic	*223*		
TS 2 **Recall**	Manual: *Yes*	194 (TP)	371 (FN)	*565*
	Manual: *No*			
	Total Automatic			
TS 2 **Precision**	Manual: *Yes*	153 (TP)		
	Manual: *No*	153 (FP)		
	Total Automatic	*306*		
TS 3 **Recall**	Manual: *Yes*	64 (TP)	105 (FN)	*169*
	Manual: *No*			
	Total Automatic			
TS 3 **Precision**	Manual: *Yes*	43 (TP)		
	Manual: *No*	150 (FP)		
	Total Automatic	*193*		
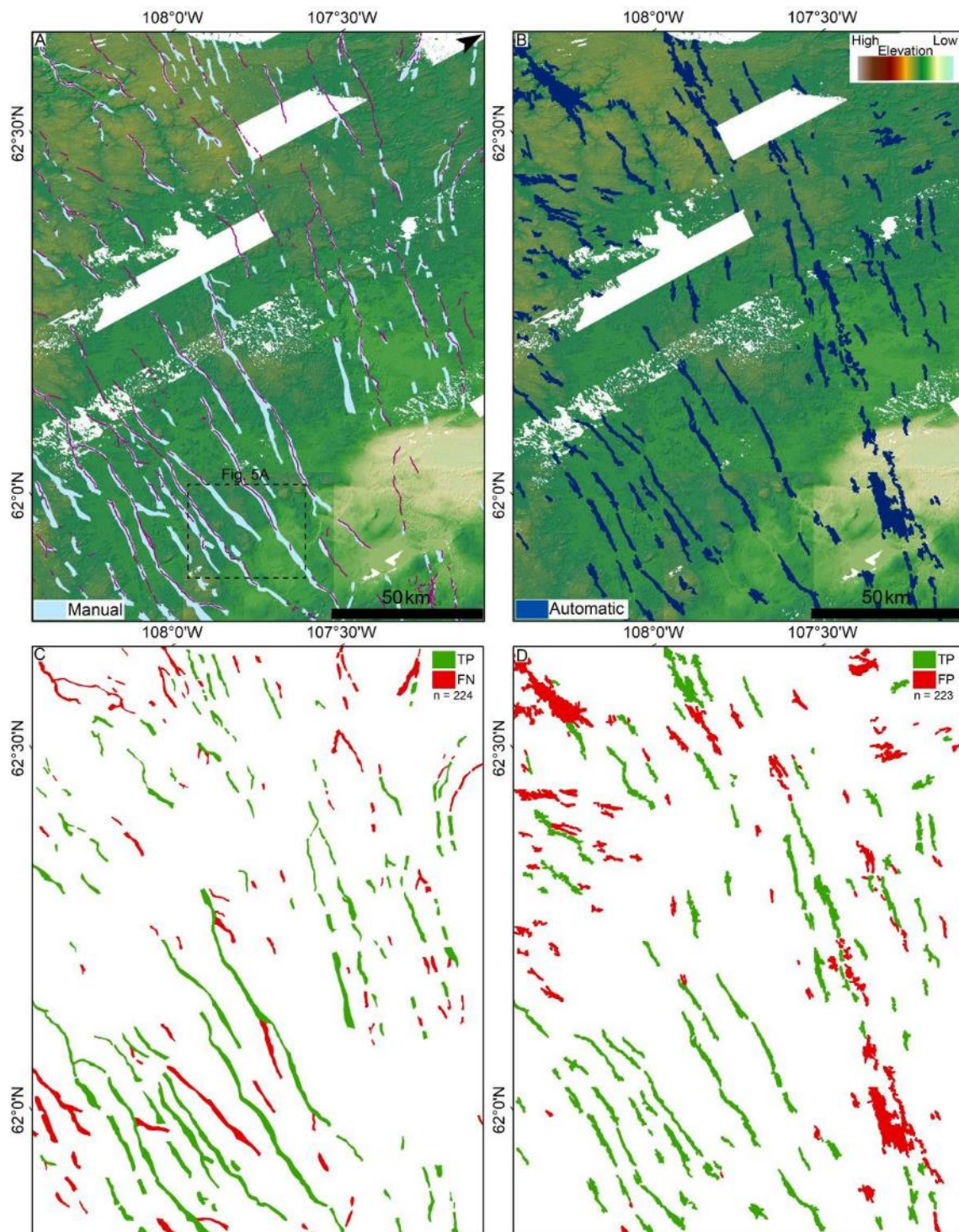
Figure 2.11 Large-scale manual (a) and automatic (b) mapping of meltwater tracks in test site 1 (near Dubawnt Lake, Canada - former ice-flow from E to W). Manually mapped eskers are also shown in (a) as pink lines. The success of the method is assessed in (c) and (d). Meltwater tracks which exhibit a > 25% minimum overlap are coloured green (i.e. True Positives – match in the manual and automatic) while meltwater tracks with < 25% minimum overlap are coloured red. In (c) these are False Negatives (i.e. manual meltwater tracks

missed) and in (d) False Positives (i.e. incorrectly identified automatic meltwater tracks). N = the total number of meltwater tracks in each group.

Comparison of the manual and automatic outputs (table 2.4) indicates a combined recall of 39 % and precision of 42 %. However, there is considerable inter-test site variation with site 1 giving the highest recall (53%) and site 2 the lowest (34 %). The highest precision is at site 2 (50 %) and the lowest at site 3 (22 %). In general the quality of the automatic mapping is improved when compared at the landform scale rather than per pixel particularly in more complex regions (e.g. site 3 – Fig. 2.4 d).

Table 2.3 Summary of region-based recall and precision measures (equations 1 and 2) by test site using a > 25 % minimum overlap criteria.

	Recall (%)	Precision (%)
TS1	53	48
TS2	34	50
TS3	38	22
Combined Results	39	42

Manual and automatic mapping for each test site can be seen in Figures 11, 12 and 13 (a) and (b) respectively. The outcome of the accuracy assessment can be visualised in (c) and (d) with meltwater tracks with > 25 % overlap coloured green and those with < 25 % overlap coloured red.
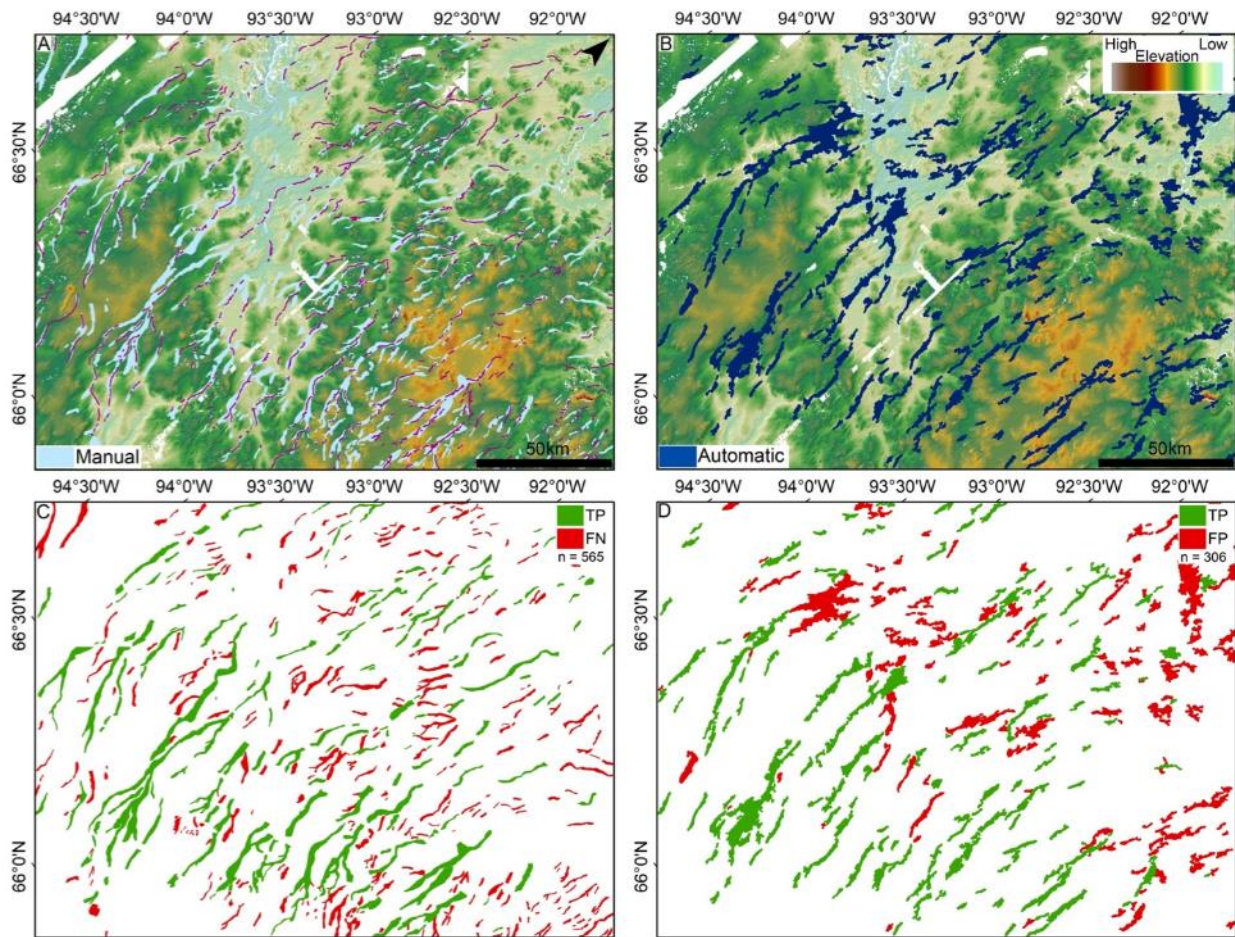
Figure 2.12 Large-scale manual (a) and automatic (b) mapping of meltwater tracks in test site 2, Nunavut, Canada (former ice-flow from S to N). Manually mapped eskers are also shown in (a) as pink lines. The success of the method is assessed in (c) and (d). Meltwater tracks which exhibit a > 25 % minimum overlap are coloured green (i.e. True Positives – match in the manual and automatic) while meltwater tracks with < 25 % minimum overlap are coloured red. In (d) these are False Negatives (i.e. manual meltwater tracks missed) and in (d) False Positives (i.e. incorrectly identified automatic meltwater tracks). N = the total number of meltwater tracks in each group.

Results indicate that the automatic method can capture meltwater tracks of varying morphology including those with positive and negative relief and branching networks. Automatically detected meltwater tracks can be traced over significant distances even when the features curve across the landscape or cross DEM tile boundaries. However, it is also clear that the meltwater tracks missed in the automatic output are often narrower and 'finer-scale' in expression i.e. they have more subdued

relief, fewer, more widely distributed or smaller individual hummocks, or they are separated by bounding sections of flat-bed that are unlikely to be detected.
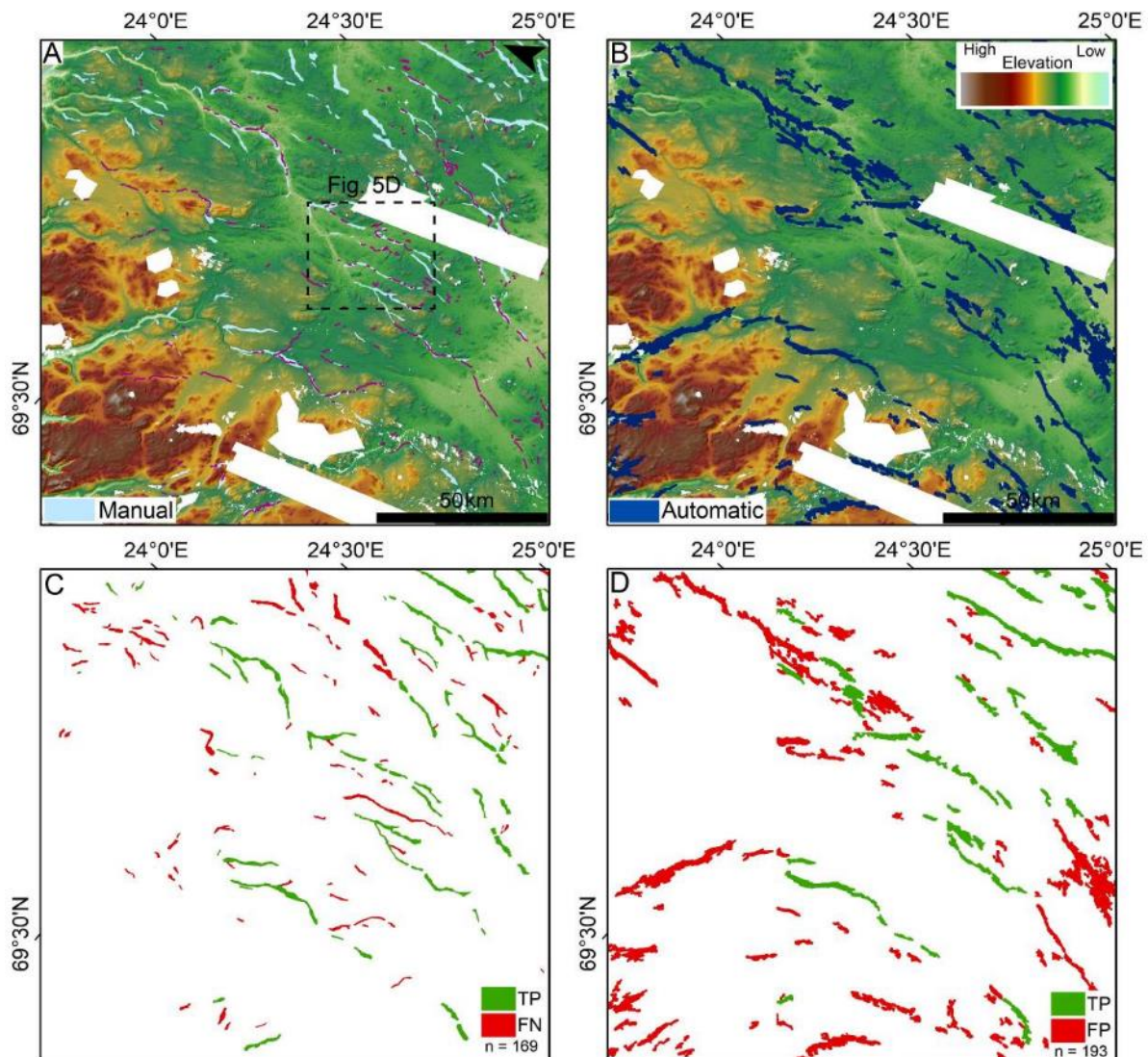
Figure 2.13 Large-scale manual (a) and automatic (b) mapping of meltwater tracks in test site 3, northern Scandinavia (former ice-flow from S to N). Manually mapped eskers are also shown in (a) as pink lines. The success of the method is assessed in (c) and (d). Meltwater tracks which exhibit a > 25 % minimum overlap are coloured green (i.e. True Positives – match in the manual and automatic) while meltwater tracks with < 25 % minimum overlap are coloured red. In (c) these are False Negatives (i.e. manual corridors missed) and in (d) False Positives (i.e. incorrectly identified automatic meltwater tracks). N = the total number of meltwater tracks in each group.

Given that the automatic method under-detects narrower corridors, I explored whether there was a critical value below which the method was less able / unable to detect features. This was investigated by evaluating the recall value (i.e. percentage of the manually mapped meltwater tracks correctly identified) as minimum meltwater track width was increased (Fig. 2.14). Meltwater track detection rate increased from 39 % for all corridors to 80 % when just meltwater tracks wider than 1.4 km were considered. Recall values increased roughly linearly with meltwater track width at test sites 1 and 2. At test site 3 recall values increased up until ~ 0.6 km whereupon they started to drop again. This is attributed to the narrower meltwater tracks at this site, with only two meltwater tracks wider than 1.2 km.
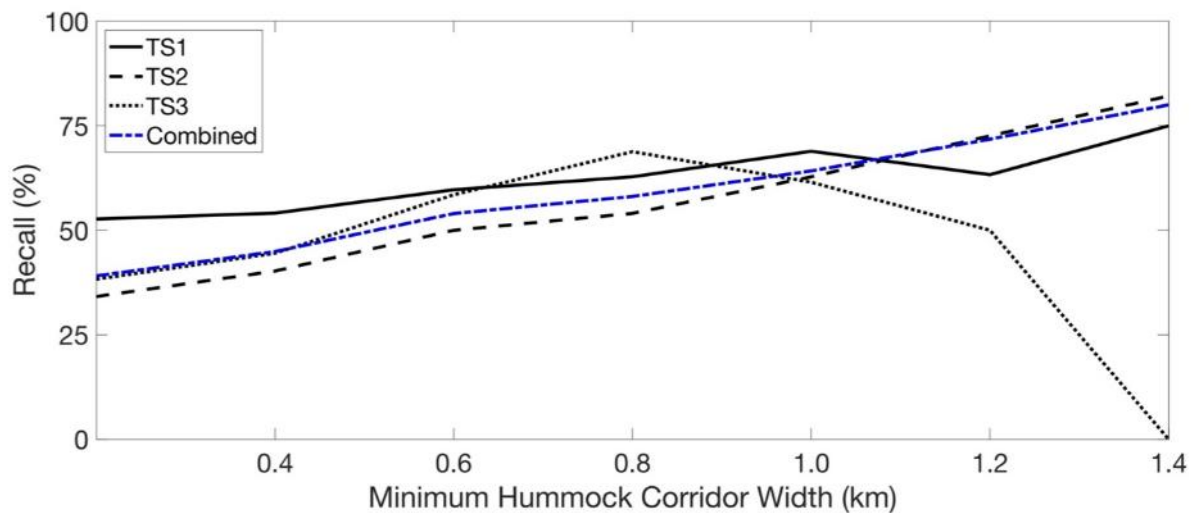
Figure 2.14 Change in recall value as minimum width of meltwater tracks included in the calculation increases (all to only > 1.4 km).

As the automatic output does a better job at detecting wider meltwater tracks, I also calculated the overall area of correctly identified corridors. At test site 1 the meltwater tracks identified as true positives account for 71 % of the total area of manually mapped meltwater tracks. Similarly, the meltwater tracks identified as true positives account for 64 % and 59 % of the total area for test sites 2 and 3 respectively. Therefore, while 50 – 60 % of the meltwater tracks were missed by the automatic approach (Table 2.4), the meltwater tracks that matched represent a higher proportion of the overall area. This suggests that the automatic method is capable of

approximating the large-scale distribution and pattern of meltwater tracks even though some of the finer-scale detail is lost.

2.3.1.2.2 Morphology

The length and width of meltwater tracks in the manual and automatic outputs are first compared by investigating their frequency distributions (Fig. 2.15) and descriptive statistics (Table 2.5). The manual mapping and automatic mapping display similarity in these distributions including a positive skew indicating a high abundance of shorter (less than 10 km) and narrower (less than 2 km) meltwater track segments. In general, the mean and median are similar particularly for the combined data set (~ 1,000 corridor segments for all 3 sites) and for corridor length.
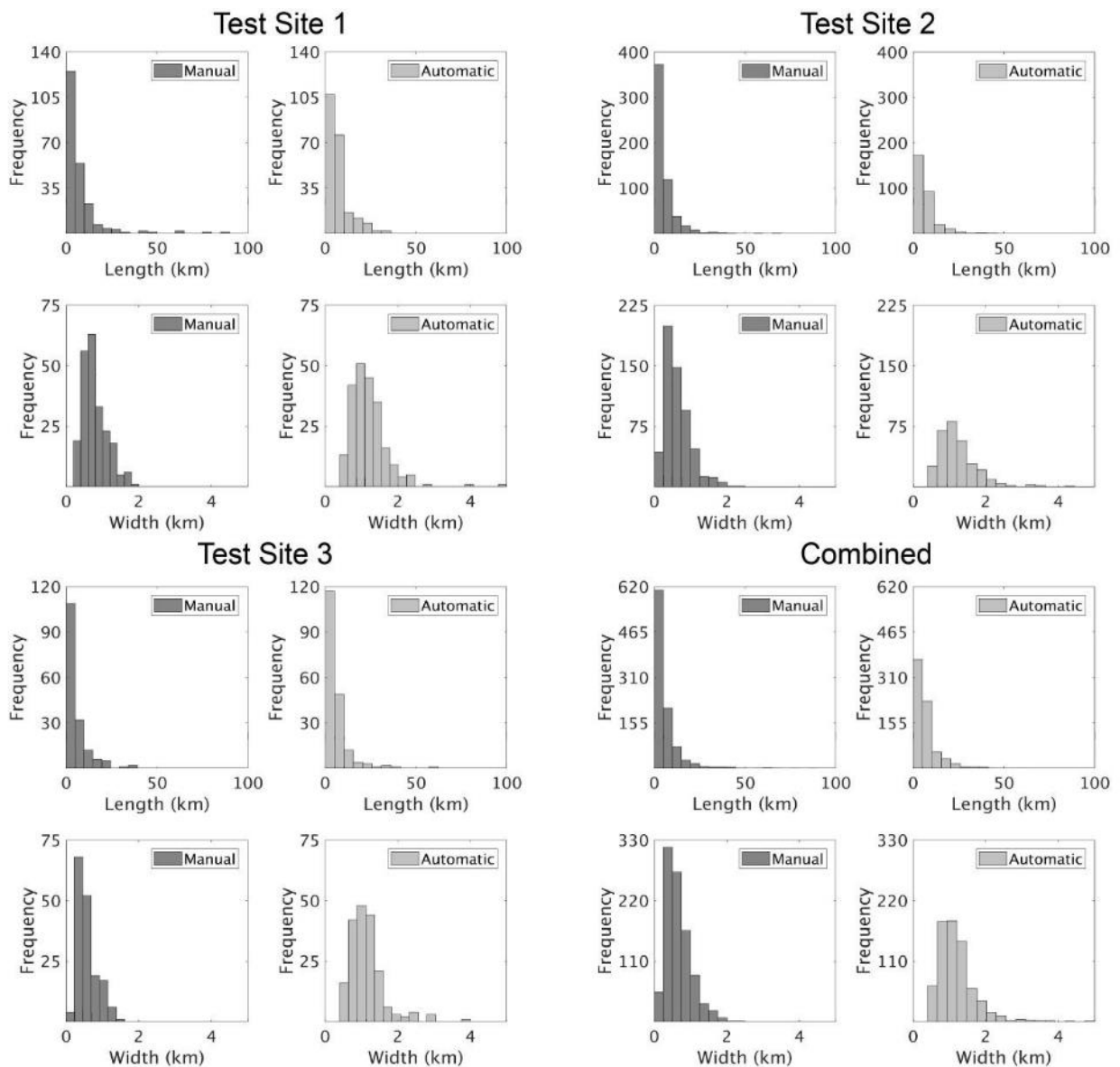
Figure 2.15 Frequency distribution of automatic and manually mapped meltwater track real-length and width for each test site. (Width bins of 5 km for length and 0.2 km for width.)

Nonetheless, there are also some differences between the manual and automatic metrics; noticeably, a lack of data in the narrowest width bins in the automatic output which helps explain the overall higher mean and median widths of meltwater tracks at each test site (Table 2.5). In Section 2.3.1.2.1, above, I demonstrate that this systematic under-estimation occurs because the automatic method struggles to identify narrower corridors.

The automatic output fails to capture the longest manually mapped segments as is shown by significantly lower maximum lengths (Table 2.5). However, in general the mean and median values for manual and automatic lengths are much closer than the widths (only varying by 0.7 km and 0.5 km for the combined dataset: n = 958 for the manual meltwater tracks and n = 722 for the automatic). This suggests that the automatic method does a better job at capturing length than width. A Wilcoxon Rank Sum Test (equivalent to Mann-Whitney U-Test) was used to test the similarity of the automatic and manual measurements at each test site. The null hypothesis (i.e. that the automatic and manual measurements were from distributions with the same median) was rejected at the 5% significance level for all comparisons excluding the automatic and manual lengths at test site 1 (p-value = 0.2056).

Table 2.4 Descriptive statistics for manual and automatic mapping (length and width (km)) for each test site and combined across all three.

		Test Site 1		Test Site 2		Test Site 3		Combined	
		Length (km)	*Width (km)*	*Length (km)*	*Width (km)*	*Length (km)*	*Width (km)*	*Length (km)*	*Width (km)*
Mean	*manual*	8.1	0.8	5.7	0.6	5.7	0.6	6.3	0.7
	automatic	7.4	1.2	7.1	1.2	6.4	1.1	7.0	1.2
Median	*manual*	4.6	0.7	3.8	0.6	3.7	0.5	4.0	0.6
	automatic	5.4	1.1	5.3	1.1	4.2	1.1	5.0	1.1
Standard Dev.	*manual*	11.3	0.3	6.3	0.4	6.2	0.3	7.8	0.3
	automatic	6.2	0.5	6.0	0.5	7.0	0.5	6.3	0.5
Min	*manual*	1.1	0.2	0.7	0.1	0.8	0.0	0.7	0.0
	automatic	1.1	0.5	1.2	0.5	1.1	0.5	1.1	0.5
Max	*manual*	90.0	1.9	69.0	2.5	39.2	1.6	90.0	2.5
	automatic	35.9	4.9	46.4	4.4	61.3	3.9	61.3	4.9

2.4. Discussion

2.4.1   Overall performance

This new approach has facilitated the identification and mapping of almost 1,000 meltwater track segments across 82,500 km^2, largely reproducing their overall distribution (i.e. successfully capturing 71 %, 64 % and 59 % of their total area at each test site) and morphometry compared to manual mapping (i.e. largely reproducing the length / width distributions). The output of this provides insight into the expression and variation of these features and contributes to an increasing body of literature on them (e.g. St-Onge, 1984; Rampton, 2000; Utting et al. 2009; Sharpe et al. 2017; Peterson and Johnson, 2018).

The output of the automatic method has created a near-continuous map of meltwater tracks which aligns meltwater track segments across adjacent ArcticDEM tile boundaries and is able to recreate the general pattern across a large area. While some of the finer detail is lost, this method nevertheless has value for rapidly (< 80 seconds per 50 x 50 km^2 5 m resolution tile, run on the University of Sheffield High Performance Computer cluster – Iceberg – with a specified memory of 32 GB) assessing significant volumes of data and providing information on meltwater track distribution and spatial arrangement and extracting information on morphometry. Furthermore, assessing many meltwater tracks across significant areas makes it more likely that we will capture a more representative dataset and allows assessment of their association with other bed features.

2.4.2   Limitations

2.4.2.1 Meltwater track morphology

Despite progress in the automatic detection and mapping of subglacial bedforms, several limitations exist which need to be acknowledged before assessing and using the output. The automatic method fails to identify all the manually mapped meltwater tracks across the three test sites. While this does not appear to influence understanding of the general location nor the large-scale trends of meltwater tracks

(i.e. general direction, length and width) or their association with other bedforms, it does suggest that some detail is being lost.

Further exploration of the reasons for this suggest that meltwater track morphology influences whether they are detected and retained in the final output. The automatic output is sensitive to meltwater track width with detection rates increasing as corridor width increases (from 39 % when all meltwater tracks are included to 64 % for meltwater tracks wider than 1 km and up to 80 % for meltwater tracks greater than 1.4 km). It is likely that narrower meltwater tracks are removed during the filtering stages or when the data resolution is reduced and the results smoothed. Many of the wider meltwater tracks are also longer and this highlights issues related to the discontinuous nature of meltwater tracks. Meltwater track segments detected automatically likely represent parts of a larger meltwater track / network of meltwater tracks, fragmented because of 'real' gaps in the meltwater track (e.g. areas of flat bed or areas with too few hummocks to be detected / retained) or because of the side-effects of processing prior to metric extraction (i.e. separating trunk / tributary meltwater tracks). This means that they should be taken as a minimum meltwater track length and should we choose to interpolate between segments, it is likely that the meltwater tracks would reach greater lengths and form more complete networks. Assessing the automatic map of meltwater tracks without interpolating between the segments, means that the full length of the manual mapping is unlikely to be captured by the automatic method as a single, complete feature. The gaps along flow may be a possible reason for not detecting more complete meltwater tracks despite increased widths.

2.4.2.2 Background conditions

As meltwater track morphology cannot fully explain why meltwater tracks were / were not detected, other possible causes for imperfect detection (rates below 100%) must also be considered. One such consideration is differences in surface roughness across the bed. Meltwater tracks display variations in expression (e.g. relief, definition, hummock density) both within and across sites and this makes it difficult to develop a method which can automatically detect all of them whilst also minimising false classifications. Despite efforts to filter out the background, confounding roughness

elements are sometimes retained. Large sections of the bed surrounding test site 3 in northern Scandinavia have greater variation in relief than those in Canada and there is more likely to be evidence of human activities (e.g. the presence of roads). These areas of confounding roughness may be classified as meltwater tracks regardless of their possible lack of exposure to subglacial meltwater flow, especially if they exhibit characteristics comparable with the pre-defined criteria for meltwater tracks. Similarly, other background features such as fluvial channels and geologically controlled landforms may also be classified as meltwater tracks. This is a particular problem when these features have a 'stronger' directional trend than any meltwater tracks in the same tile skewing the FFT wedge filter and thus inadvertently removing meltwater tracks. It is possible that these features are part of the same subglacial hydrological network (e.g. Fig. 2.4 d); however, if they are not, inclusion of additional steps such as overlying the automatic output on the DEM / geology map would allow the user to manually identify erroneous areas (often by shape and size) and assess case by case whether these should be deleted or retained.

2.4.2.3 Mapping and accuracy quantification methods

It is important to acknowledge the subjectivity and limitations of manually mapping meltwater tracks in general, especially those on complex backgrounds or those which form part of a larger glaciofluvial complex where boundaries are unlikely to be discrete. Some of the meltwater tracks observed across the study sites are less pronounced in terms of their overall relief and / or the relief / number of the hummocks within them making them difficult to manually map (e.g. Fig. 2.1). It is therefore unlikely that the automatic method will be able to capture these either given that the filtering and coarsening steps remove some detail. It is also likely that individual manual mappers would map these differently. As such, manual mapping is not necessarily 'true' nor should the automatic method be expected to reproduce it perfectly.

Furthermore, instead of just missing meltwater tracks, there are examples from the test sites where the automatic method can differentiate meltwater tracks from complex backgrounds, even identifying some which were missed / incompletely mapped by the manual mapping. Ultimately, the automatic method relies on a series of decision-making criteria based on the key characteristics of meltwater tracks and their

relationship with the surrounding topography. These ultimately determine the eventual mapping of corridors and the overall success of the output. This means that the results are consistent, repeatable and defensible (Saha et al. 2011). However, it is important to consider the implications of the parameter selection on results. Decisions such as how much topographic variation was retained, how far feature orientation was allowed to vary and the minimum threshold size of features are all likely to have influenced the overall results. This was largely a balancing act between retaining detail and avoiding noise and as there are no hard limits on meltwater track morphology, likely introduced a certain amount of subjectivity into the automatic output. Future analysis may experiment with varying these parameters and testing the impact on the output.

Finally, it is also important to consider how the accuracy measures are interpreted when determining how well the automatic output fits the reference data. While it is useful for providing a quantitative summary of how many meltwater tracks are detected at each site, it does not consider additional factors which are relevant here. For example, individual inspection of meltwater track segments suggests that in some cases, using a minimum of 25 % meant that some 'real' meltwater tracks were incorrectly missed. Furthermore, the method gives equal weighting to every meltwater track, regardless of its size.

2.4.3 Large-scale application of the new automatic method in Canada

The automatic method developed within this chapter was run over a large section of northern Canada (Fig. 2.16). The output shows the ubiquity of meltwater tracks across this section of the ice sheet confirming the findings of localised studies (e.g. Rampton, 2000; Utting et al. 2009). Here, they exhibit a clear radial pattern around the former Keewatin ice divide. This matches and adds to previous mapping of eskers (e.g. Aylsworth and Shilts, 1989; Storrar et al. 2013) which are known to form as a result of subglacial meltwater activity, thus adding confidence in the general pattern and interpretation as former meltwater routes.

Visual assessment of the results (Figs. 2.11 - 2.13) suggests that misidentification is typically associated with narrower features or additional features on the bed exhibiting strong directional trends, such as fluvial channels, geology or in

some cases linear tracts of drumlins (Fig. 2.9). To identify and remove misclassified features in the output, I manually 'cleaned up' the results (Fig. 2.16 b). This was achieved by comparing the output to geological maps (i.e. to identify bedrock patches) and maps of water bodies. Large 'blocky' areas were identified by eye and removed. The output was also compared to existing glacial geomorphological mapping to ensure that other fields of features (e.g. ribbed moraines, drumlins etc.) were not misclassified as meltwater tracks. Future work may reduce these effects automatically by trialling the code on different resolution data or by using different sized sample tiles. Determining the scale at which the meltwater tracks remain aligned may allow the user to alter the input tile size as a way of reducing the likelihood of additional directional features influencing the FFT filter. Furthermore, issues with connectivity along meltwater tracks can also be addressed through manual mapping as this will enable interpolation and joining up features which appear linked along-flow but which have not been fully identified automatically (e.g. due to a more subtle feature expression).
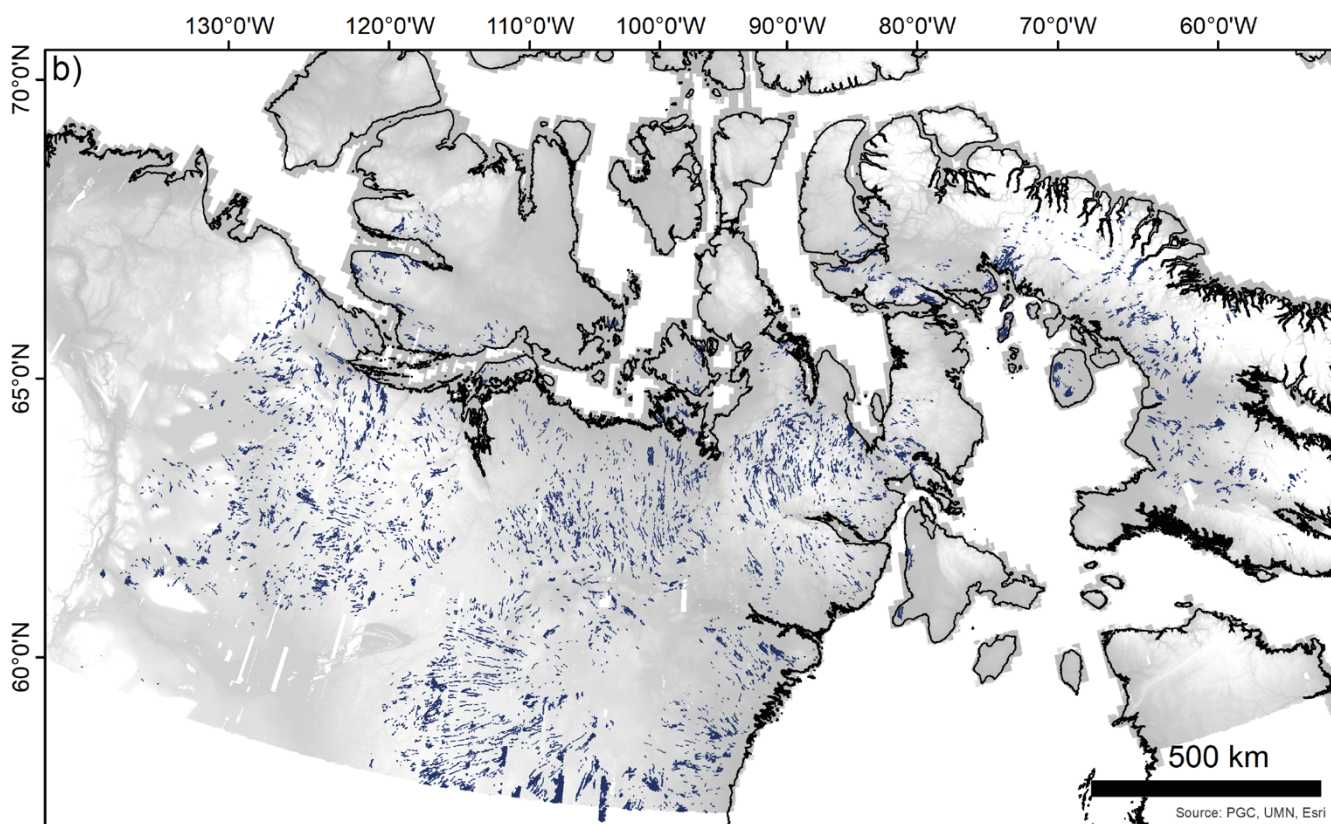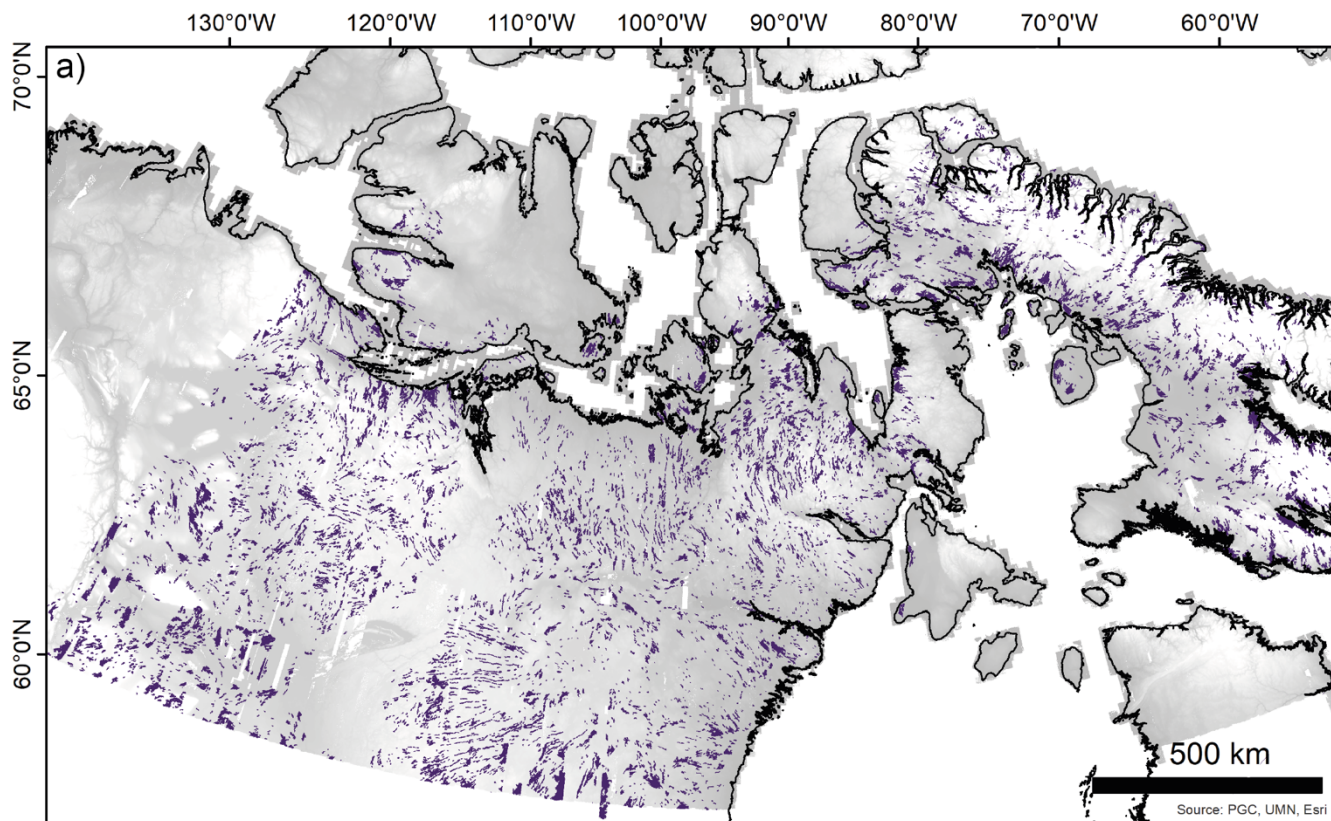
Figure 2.16 Large-scale output of automatic mapping technique (a) original (purple) and (b) cleaned up version (blue) (i.e. large patches of clearly misclassified pixels removed).

2.5   Conclusions

This work has been motivated by the release of large-scale high resolution ArcticDEM data which allows subglacial bedforms to be mapped at an unprecedented spatial scale. Meltwater tracks have been widely identified on the beds of palaeo-ice sheets, and the results of my automated mapping method offer the potential to rapidly gain a large amount of information on the morphological characteristics and large-scale distribution of meltwater tracks. This will add to the existing literature on meltwater tracks and can be used to inform the development of hypotheses for meltwater track formation.

Given the increasing availability of high-resolution data, there is a need to develop new methods which can rapidly obtain meaningful information directly from DEMs. Automatic mapping techniques aim to increase reproducibility in landform detection and mapping by using predefined criteria to produce the same result for the same area every time. While automatic methods aim to reduce subjectivity (e.g. by facilitating the detection of features which conform to the criteria and which may be missed by a visual assessment), a certain amount of subjectivity remains owing to the parameter selection. Nonetheless, while automatic mapping may never reach the same level of detail and precision as manual mapping by skilled practitioners for individual bedforms, it has potential when the priority is to quantify the large-scale, broad-brush pattern of landforms. This method adds to an increasing body of literature on the development of automatic methods for the identification and mapping of palaeo-subglacial bedforms by developing the first automatic method for extracting spatial information on meltwater tracks. The method is tested on three areas across the ArcticDEM and demonstrates that meltwater tracks with varying expressions and varying background conditions can be identified automatically. Results suggest that the new method can capture the general location and spatial pattern and distribution of meltwater tracks and provides a decent 'first pass' map which can later be refined manually depending on the desired output. For this study, the ability to correctly identify each hummock is less important than the method's ability to capture the location and overall pattern of meltwater tracks and when considering a large sample size, the results (Fig. 2.16 b) suggest that the automatic method can accurately capture their presence and distribution across regional areas. Finally, it is possible that

in the future, parameters within the automatic method could be adapted to automatically identify other bedforms which also share a predefined horizontal size range and orientation. This may allow the code to be applied to other problems inside glacial geomorphology (e.g. drumlins and eskers) or beyond

CHAPTER 3: A MODEL FOR INTERACTION BETWEEN CONDUITS AND SURROUNDING HYDRAULICALLY CONNECTED DISTRIBUTED DRAINAGE BASED ON MORPHOLOGICAL EVIDENCE FROM KEEWATIN, CANADA

3.1 Introduction

The output of Chapter 2 revealed the widespread presence of meltwater tracks across the study area. In this chapter - published in Lewington et al. (2020) - I identify and map all visible traces of subglacial meltwater drainage around the former Keewatin Ice Divide in Canada, including meltwater tracks, to create the first holistic drainage map for this area. A holistic mapping approach was selected to facilitate the detection of meltwater landforms at both ends of the geomorphic spectrum (i.e. erosional and depositional). Geomorphic work can vary significantly over time and space depending on the mode of drainage as well as external background (e.g. sediment thickness and underlying geology) and glaciological (e.g. distance from the ice sheet margin, ice surface slope or thermal regime) conditions. By mapping all traces of meltwater drainage this holistic approach will provide a more representative picture of the 'true' drainage system which will better enable me to identify process-form relationships and underlying controls on the drainage system geometry and expression. Better understanding of exactly what each landform expression represents will allow for more accurate interpretations of the palaeo-hydrological system which is vital for enhancing understanding of the nature and impacts of contemporary drainage and contextualising limited spatio-temporal observations.
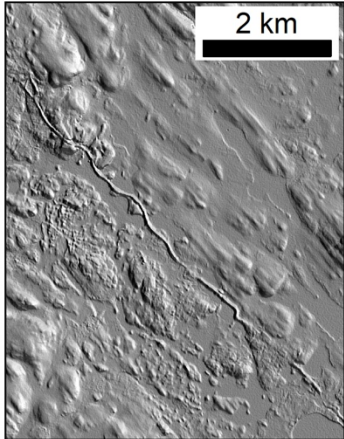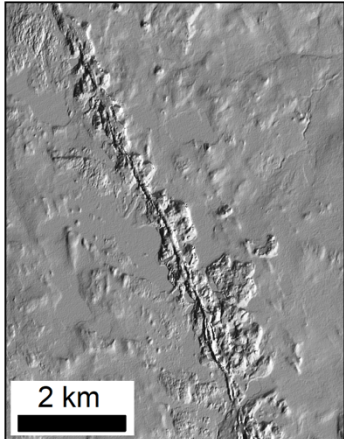
3.2 Methods

In this chapter I used the output of the automatic method (Fig. 2.16 b) alongside an esker map produced from 30 m resolution Landsat ETM+ multispectral imagery (Storrar et al. 2013) as a starting point for detailed manual mapping of all visible meltwater landforms from the ArcticDEM. I created an integrated map of meltwater routes by manually mapping centrelines of all visible traces of subglacial meltwater drainage including eskers, meltwater tracks and meltwater channels (see Table 3.1 for mapping criteria and examples). Multiple orthogonal hillshades were generated (45 and 135 degrees) to avoid azimuth bias (Smith and Clark, 2005) and mapping was

undertaken at a range of spatial scales to maximise the number of features captured (Chandler et al. 2018). Features were mapped directly into ArcGIS.

Given the large-scale nature of the project, a balance had to be struck between acquiring a sufficient volume of data to explore large-scale distributions and patterns etc. and the level of detail in the mapping. This resulted in generalisations such as mapping features as polylines (i.e. the centreline) and not differentiating between different expressions of drainage (Table 3.1).

Table 3.1 Mapping criteria for meltwater landforms which make up the meltwater routes map presented in figure 3.1.

Feature	Geomorphic criteria	Example
Esker	- Straight to sinuous ridge - May be a single strand or exhibit double (adjacent) or multiple (anastomosing) ridges - Typically fragmented in places along its length - Generally parallel to palaeo-ice flow direction	
Esker with splay	- An esker ridge surrounded by lateral fans - Lateral fans typically wider than the esker itself and sloping away from the esker ridge	

Meltwater track	- Differentiated largely based on textural differences between the meltwater track and the surrounding bed - May exhibit variable sized and shaped hummocks, broad valley fill deposits and / or exposed bedrock - Variable relief – some are incised and exhibit a negative relief while others exhibit little to no relief - Variable definition of edges – boundary between feature and surroundings may be sharp and easily delineated or not - A spatial association with eskers (which they often contain) - A spatial association with tunnel valleys (often transitioning along-flow into or occurring closely alongside) - Parallel conformity with each other, other meltwater features and palaeo-ice flow	 Significant variations in expression - see Fig. 2.1 for examples of varying morphology
Meltwater channel	- Generally a more pronounced negative relief than meltwater tracks - Beds typically flat and are more U-shaped in appearance - Typically straight valley edges with a clear boundary between feature and surrounding - Aligned in the direction of palaeo-ice flow - Often contain eskers	
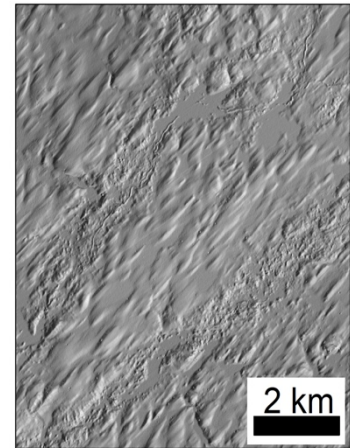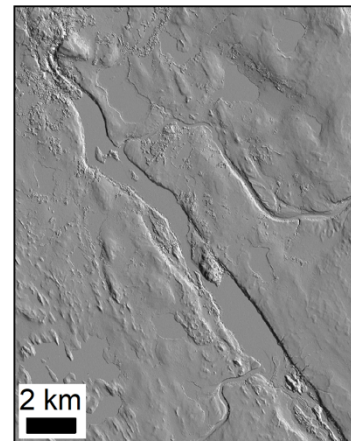
3.2.1 Classification and morphometry

The meltwater routes were used to explore the occurrence and morphology of different types of meltwater landforms. As mentioned in section 3.2, when mapping meltwater routes different landform expressions (i.e. eskers, meltwater tracks and meltwater channels) were not differentiated. Therefore, to assess variations sampling of meltwater landform expression was carried out. Former ice-margin estimates from Dyke et al. (2003) were used as transects (Fig. 3.1) with the intersection of each

transect and a meltwater route determining the location of a sample point. The overall study area was split into three test sites incorporating an area ~ 256,000 km^2 (~ 35 % of the total study area) and capturing a majority (~ 60 %) of the overall meltwater routes (Fig. 3.1. This method resulted in the sampling of 444 meltwater route widths and 554 spacings. It is acknowledged that some variations in feature morphology may have been missed using this method; however, this approach provided a balance between time and sample size and was deemed to provide sufficient insight.

Using former ice margin estimates (Dyke, 2003) ensured that transects were approximately evenly spaced (~ 30 - 40 km apart) and distributed around the ice sheet divide. This chronology is based on approximately 4,000 (mostly radiocarbon) data points. The samples came from an area covering ~ 1,000 years of deglaciation between 9.7 and 8.6 ka. This period encompasses the final stages of deglaciation when the ice sheet was experiencing a strongly negative surface mass balance with associated increasing rates of meltwater production (e.g. Carlson et al. 2008, 2009). Retreat rates were generally between 100 - 200 m yr^{-1} from 13 to 9.5 ka increasing rapidly between 9.5 and 9 ka to around 400 m yr^{-1} after which the retreat rate decreased briefly before another increase from ~ 8.5 ka (Dyke et al. 2003).
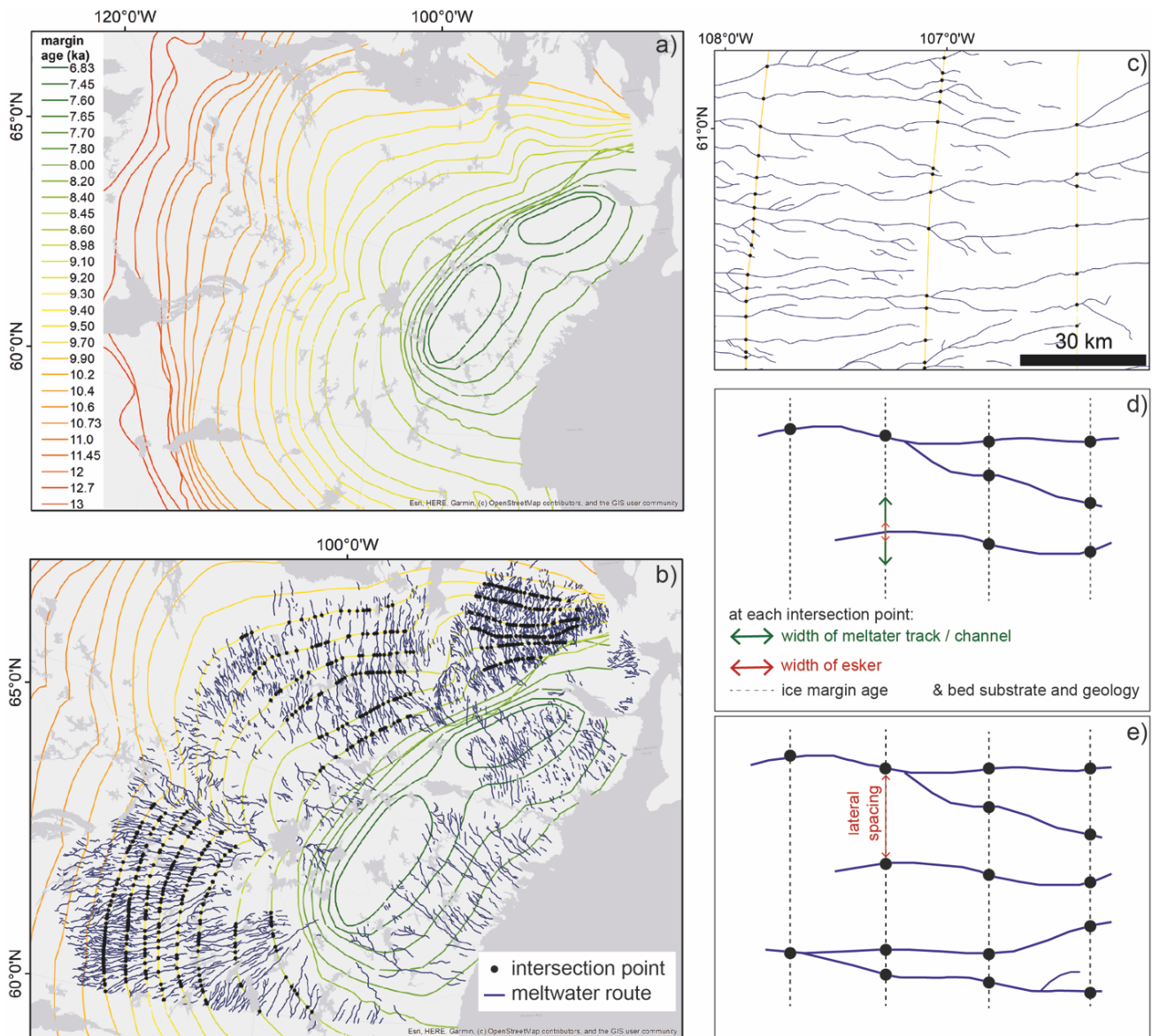
Figure 3.1. (a) Ice-margin estimates (Dyke et al. 2003) for the Keewatin sector of the LIS; (b) intersection points between mapped meltwater routes and ice-margin estimates used for sample locations; (c) a zoomed in example of meltwater routes, margin isochrones and intersections from the SW of the study area; (d) method for recording meltwater route characteristics and; (e) lateral spacing.

When a meltwater route intersected a transect, an intersection point was added, and the following information recorded (Fig. 3.2):

- Landform type - esker ridge, esker with lateral splay, meltwater track or meltwater channel.

- Width of landform (or landforms if an esker ridge was present within a meltwater track, meltwater channel or surrounded by a lateral splay).
- Bed substrate and geology (Fulton, 1995; Wheeler et al. 1996).

Spacing between adjacent meltwater route centrelines was calculated along each transect with centrelines at the end of each transect and those separated by clear breaks, such as the coincidence of lakes, discounted. The total length of meltwater route centrelines was calculated automatically in a Geographic Information System (GIS). While the precision of the isochrone dates is not likely to be very high owing to poor geochronological constraints in the area (Dalton et al. 2020) and thus numerous assumptions in their construction, the transect date was also recorded during the sampling. This allowed for relative changes in width and spacing of the meltwater routes over time to be explored as the ice sheet retreated towards the ice divide.

a)

b)

c)

- ● sample point (intersection)
- ── age isochrone (transect)
- ── mw route width
- ── esker width
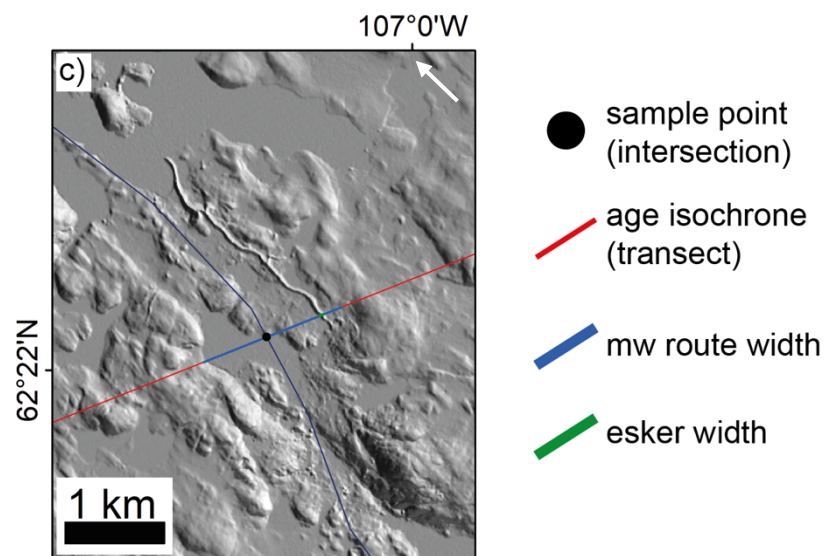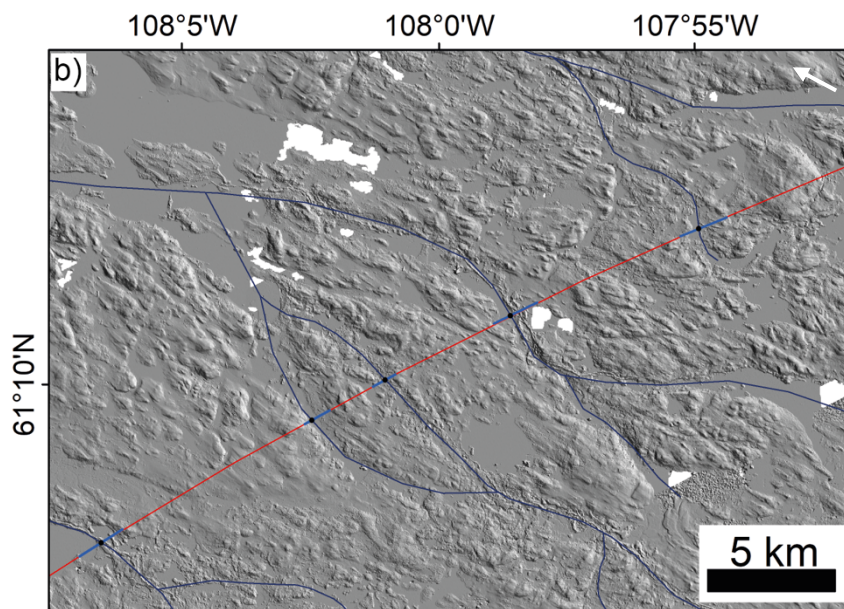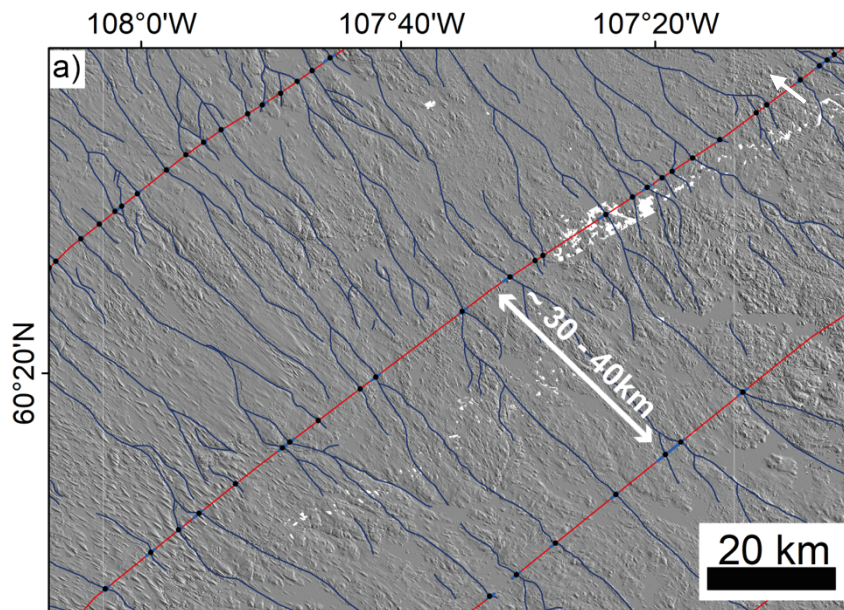
Figure 3.2 (above). Sampling method for obtaining information on meltwater route width, expression, relative age and basal substrate / surface material. Note that in c) the esker is situated to the right (looking down flow); this off-centre alignment is not uncommon. White arrows represent inferred palaeo-ice flow direction.

3.2.2 Testing controls on meltwater route width and expression

This study takes a large-scale approach to exploring controls on meltwater route width and expression. While this approach results in a compromise in terms of data resolution available for the surface substrate and geology maps, it also increases statistical confidence in the results due to the larger sample size. Before the analysis was undertaken, three test sites (Figs. 3.3 and 3.4) were selected from the study area to allow for more detailed mapping and comparisons.

To explore substrate and geological controls on meltwater route occurrence, distribution and properties, the overall length of meltwater routes overlying each substrate type (Fulton, 1995) and geology (Wheeler et al. 1996) within the three test sites was calculated (Figs. 3.3 and 3.4). The total area of each basal unit within the test sites was also calculated and values were converted to percentages. Following this, the percentage area was subtracted from the percentage of meltwater routes for each individual substrate and geology type, giving a positive (over-represented) or negative (under-represented) value. Next, meltwater routes were split and classified by feature type (i.e. esker, esker with lateral splay, meltwater channel and meltwater track). The above analysis was then repeated by feature type to explore whether geomorphological expression is controlled by surface substrate or geology. It is important to note that categorisations along meltwater routes were not always independent as the same section was sometimes coded as a meltwater track and an esker with splay as often positive features are situated within wider erosional corridors.
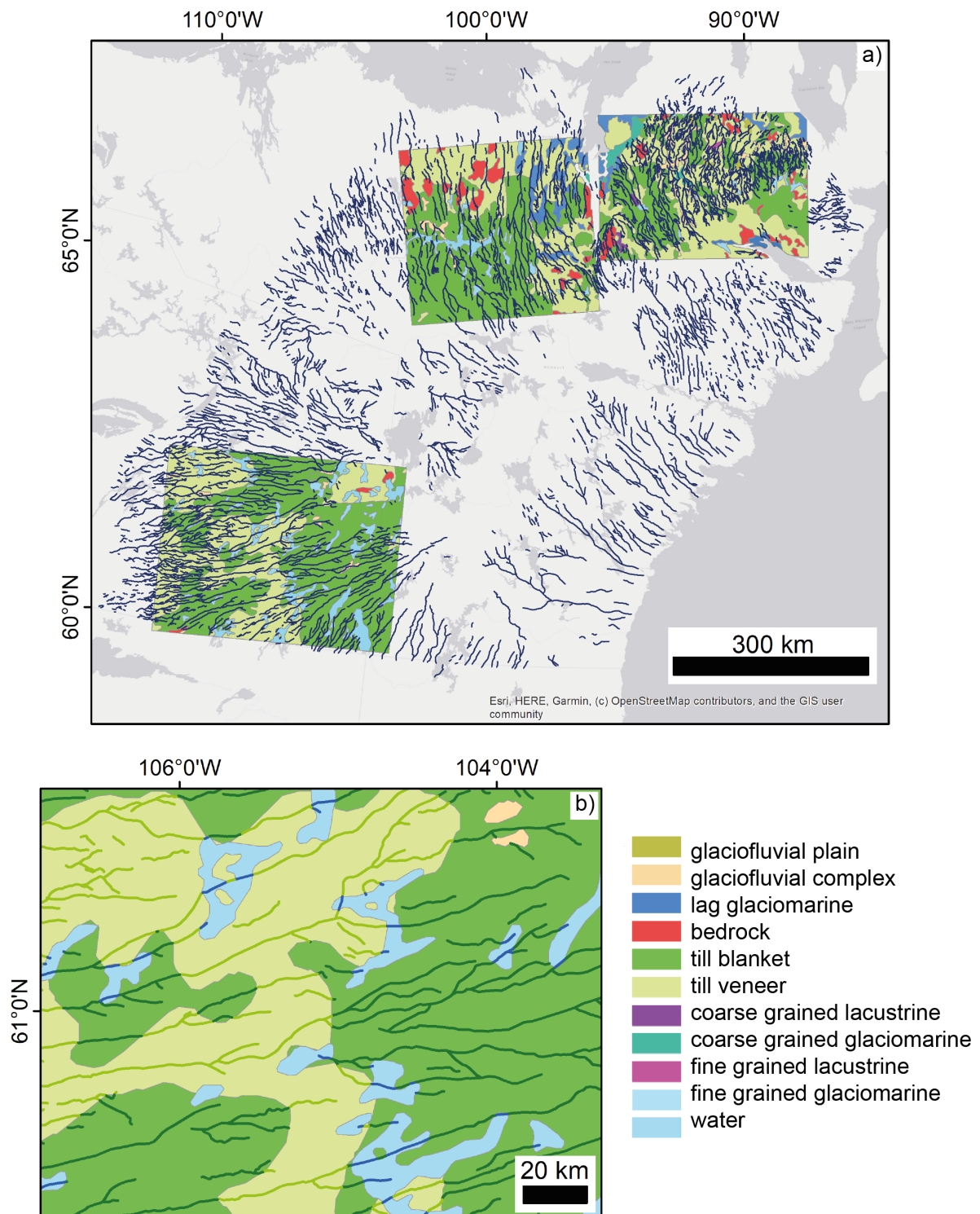
Figure 3.3 a) Meltwater routes overlain on surface material at three sites around the ice sheet and; b) Example of how meltwater routes were split up according to the underlying surface material.
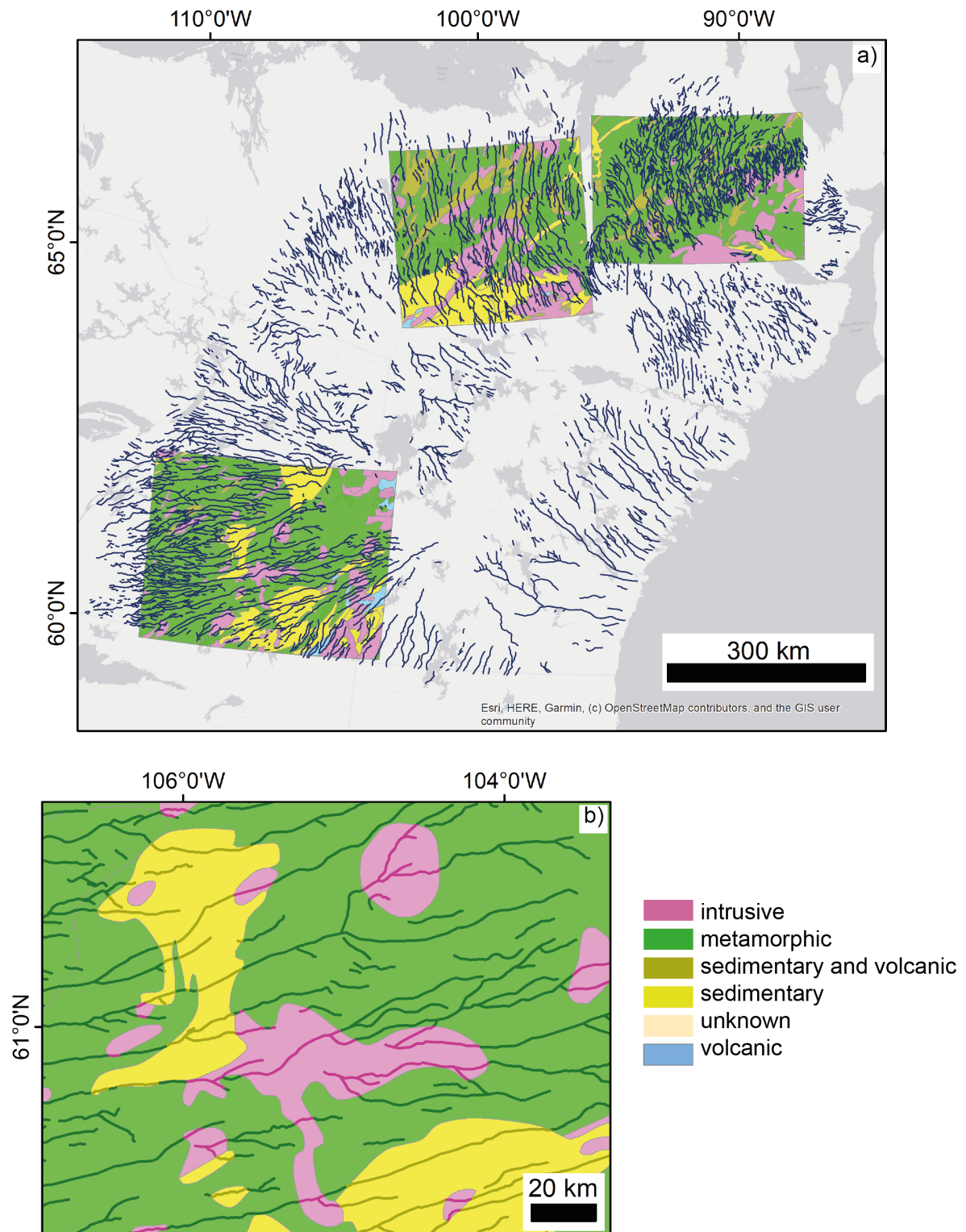
Figure 3.4 a) Meltwater routes overlain on the underlying geology at three sites around the ice sheet and; b) Example of how meltwater routes were split up according to the geology.

It was noted that landform type varies both across adjacent meltwater routes and along individual meltwater route centrelines. To assess any potential relationship between landform type and background controls in more detail (i.e. at a higher resolution than the 30 – 40 km spaced transects), four of the mapped meltwater routes were selected at random and sampled with a higher frequency (at 1 km intervals (Fig. 3.5)). At each sample location the width of the meltwater track or meltwater channel, the presence or absence of an esker (and its width if present), surface substrate, bed geology and elevation were recorded.
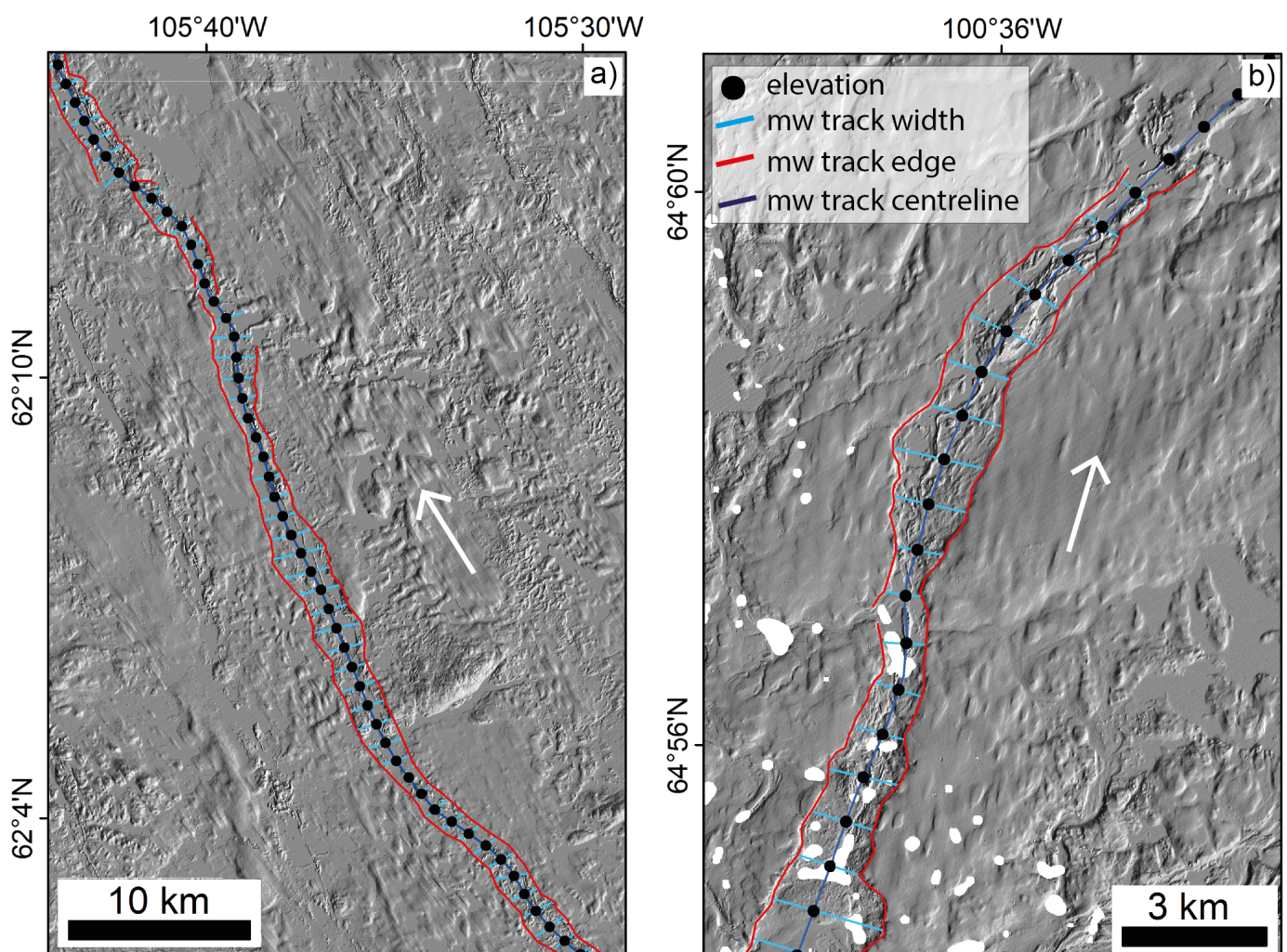
Figure 3.5 Detailed sampling (every 1 km) of randomly selected meltwater tracks. White arrows represent inferred palaeo-ice flow direction.

The transfer of surface meltwater to the bed via moulins is thought to be strongly controlled and largely fixed by bed topography which preconditions the surface drainage network. This suggests that likely locations of surface crevassing – caused by elevated tensile stresses as ice flows over bedrock ridges (Catania and Neumann, 2010) – and supraglacial lakes – which form where water collects within surface depressions – can be directly predicted from basal topography (Gudmundsson, 2003; Karlstrom and Yang, 2016; Crozier et al. 2018; Ignéczi et al. 2018).

Ignéczi et al. (2018) predict the large-scale pattern of surface relief from basal topography for the GrIS using a non-stationary integral method (Ng et al. 2018) and Gudmundsson's (2003) linearized transfer functions. Their method is based on the idea that topographic variations within a specific range (i.e. 1 – 3 times ice thickness) are most likely to be transferred to the surface; the exact wavelength is modulated by ice thickness, surface slope and basal slippiness. Although the direct application of this method is beyond the scope of this work, I apply a simplified roughness calculation (standard deviation) refined using the findings of Ignéczi et al, (2018) to target the relevant basal topographic wavelengths transferred to the surface. I then compare the spatial coincidence between subglacial meltwater pathway density and basal roughness based on the understanding that basal roughness should be directly associated with; a) an increased density of surface meltwater input points due to enhanced crevassing; and b) a greater magnitude of meltwater being delivered to the bed via the drainage of surface lakes fixed in surface depressions directly above basal undulations.

To capture the relevant bed roughness elements Ignéczi et al. (2018) found that the size of the smoothing window should not exceed 10 times the ice thickness (Gudmundsson, 2003) while still capturing longer scale variations and dampening rapid changes in local topography (Ng et al. 2018). To remove finer-scale local topographic relief I first resampled the ArcticDEM to 100 m and then applied a circular median filter with a 2 km diameter. As the LIS was typically 500 – 2000 m thick, a standard deviation window of 20 km was then chosen to identify areas of greatest 'relevant' topographic variability (i.e. greatest standard deviation values).

Next, ice stream locations (Margold et al. 2015) were quantitatively compared to the distribution of meltwater routes. This allowed exploration of whether or not there was a difference in expression of subglacial meltwater pathways between ice stream and non-ice stream areas. This was based on the understanding that subglacial hydrological conditions, and therefore the formation and expression of meltwater landforms, are likely to have been different in ice stream areas due to shallower surface slopes, lower basal hydraulic gradients, higher ice velocity and soft deforming sediments. Livingstone et al. (2015) compared modelled subglacial drainage routes – although limited to subglacial meltwater inputs and not surface contributions - with eskers in this area. They found a lower density of eskers on the bed of former palaeo-ice streams despite these being the locations of major subglacial drainage routes, which likely contributed to the ice streams flow (Engelhardt and Kamb, 1997; Kamb, 2001). Possible explanations include: (i) eskers preferentially occur on hard beds and are less common over soft sediments more typical of ice stream beds and / or; (ii) increased ice creep as a result of high basal velocities and poor preservation potential due to erosion by fast ice flow. I focus on the integrated drainage network on the Dubawnt Lake ice stream bed, the major palaeo-ice stream within my study area, to investigate signatures of drainage in these areas when not looking at eskers alone.

Finally, I explore the potential role of subglacial lake drainage events in forming the meltwater pathways. Palaeo-subglacial lake identification is based on hydraulic potential modelling to predict the likely locations of former subglacial lakes (e.g. Evatt et al. 2006; Livingstone et al. 2013; Shackleton et al. 2018) and geomorphic criteria such as evidence of channelised flow (e.g. meltwater channels and eskers) linked to flat-spots upstream (e.g. Livingstone et al. 2016; Kirkham et al. 2020a). Previous research has also made use of the geological record based on sediment facies, landform-sediment associations and biogeochemical tracers (e.g. Livingstone et al. 2012; Kuhn et al. 2017); however, this is not achievable here without field sampling.

Subglacial lakes are thought to be widespread beneath ice sheets, with more than 400 documented beneath the AIS (Siegert et al. 2016), over 50 beneath the GrIS (Bowling et al. 2019) and many others beneath both ice caps (e.g. Björnsson, 2003, Rutishauser et al. 2018) and valley glaciers (Capps et al. 2010). Therefore,

unsurprisingly, hundreds of subglacial lakes have been predicted to occur beneath the LIS (e.g. Livingstone et al. 2013) with some confirmed from geological evidence (Christoffersen et al. 2008; Livingstone et al. 2016).

Livingstone et al. (2013) used hydraulic potential calculations (following Shreve et al. 1972) derived from an ensemble of models to predict palaeo-subglacial meltwater routes and locate likely ponding sites during deglaciation of the North American Ice Sheet, including across my study area. Two different flotation criteria (F) were used; F = 1 and F = 0.75. In reality, the flotation criteria varies over time and space depending on the drainage system configuration, ice temperature, ice-overburden pressure and underlying geology (Clarke, 2005). While the 'true' value is likely to be nearer 1 (e.g. Kamb, 2001), the less conservative predictions produced using the lower value of 0.75 were used here as this effectively generated an upper bound, identifying all the topographic depressions capable of forming a subglacial lake (Livingstone et al., 2013). The meltwater routes map was overlain on the lake prediction maps (Livingstone et al. (2013), F = 0.75) to identify any spatial associations between mapped meltwater routes and upstream subglacial lakes.

Geomorphic criteria have also been used to identify how meltwater landforms or landform assemblages were created. For example, Perkins et al. (2016) used the crest shape (cross-sectional area) of eskers to help differentiate between depositional settings and Livingstone et al., (2016) identified a downstream transitional landform association (i.e. flat spot -> meltwater channel -> esker), which they suggested could be a characteristic of subglacial lake drainages. During mapping I searched for examples of these transitions.

3.3 Results

3.3.1 An integrated drainage signature

Mapping all traces of meltwater drainage reveals the ubiquity of former subglacial drainage across the study area (Fig. 3.6). A total of ~ 3,000 meltwater routes were mapped over a ~ 1 million km^2 area with a total length of almost 55,000 km. The meltwater routes exhibit a similar overall pattern to earlier esker maps (e.g. Aylsworth

and Shilts, 1989; Storrar et al. 2013) radiating out from the former Keewatin Ice Divide. More than 90 % of mapped esker ridges in this region are estimated to occur along a meltwater route and therefore form part of the same network.

The large-scale pattern of meltwater routes (Fig. 3.7a) indicate a slight increase in width throughout deglaciation (from 9.7 ka to 8.6 ka) for this sector of the LIS. The spacing of the meltwater routes appears to increase until ~ 9.3 ka, which together with the change in widths suggests that the relative coverage of meltwater across the bed may not have been changing that much (i.e. as meltwater routes width increased, the relative spacing decreased). However, after 9.3 ka the spacing decreased. This suggests that the relative coverage of meltwater at the bed increased after 9.3 ka with wider meltwater routes spaced more closely together.
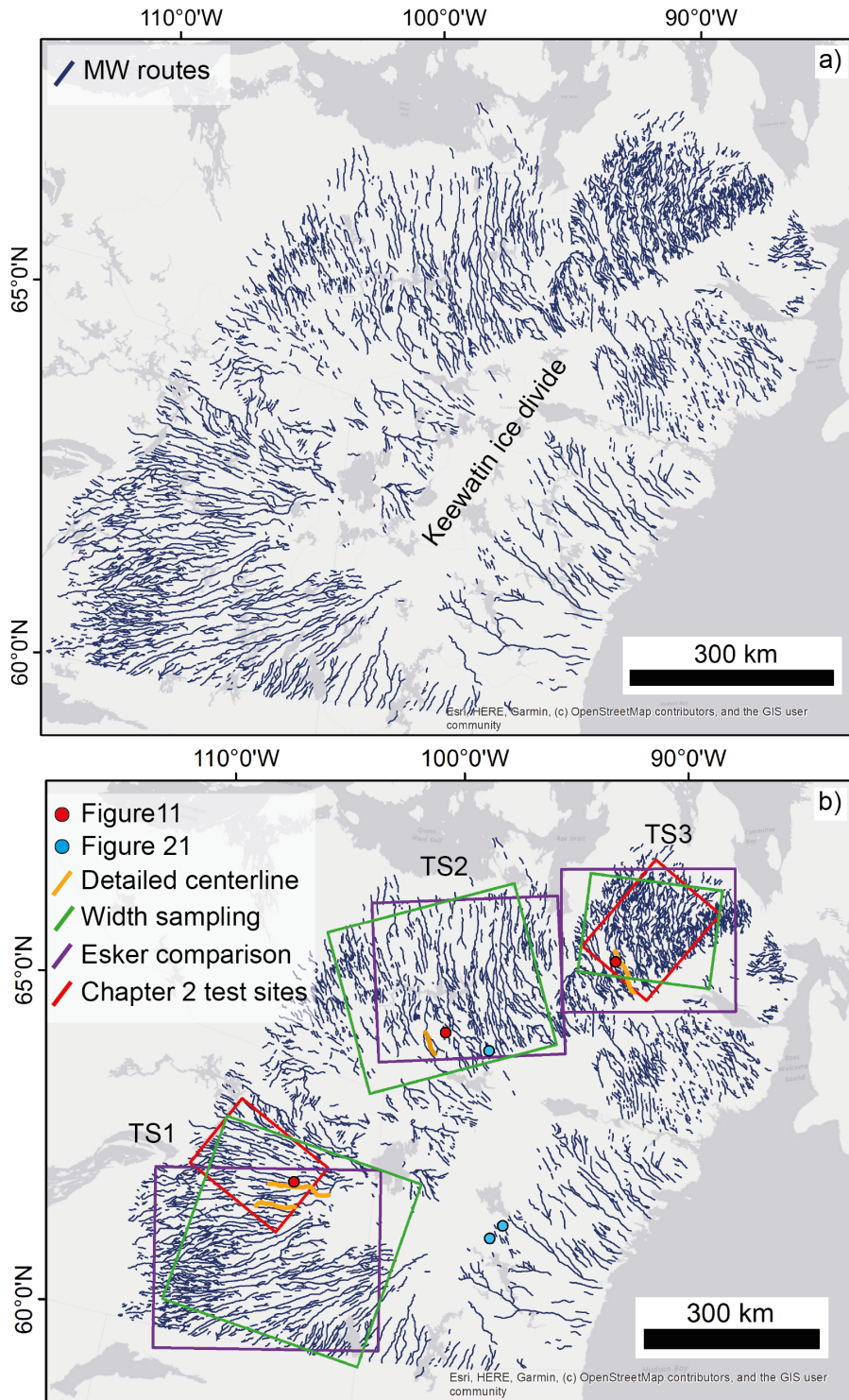
Figure 3.6 a) Integrated map of meltwater routes around the Keewatin ice divide; b) Locations of other figures relative to the overall study area. The study area was broadly split into three areas of interest – test site 1, test site 2 and test site 3. All the precise location and extent of these varied slightly throughout the study, they generally coincide with the same sector of the ice sheet as outlined in this figure. Locations used to develop the automatic method (red boxes) in chapter 2 are also identified to demonstrate their relative extent.
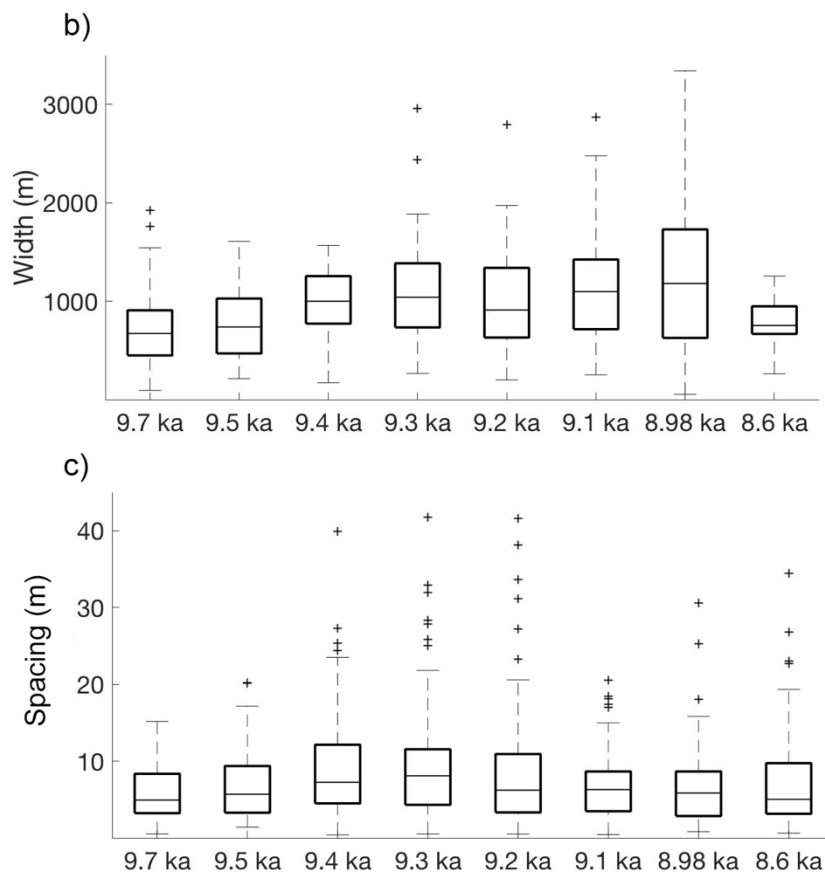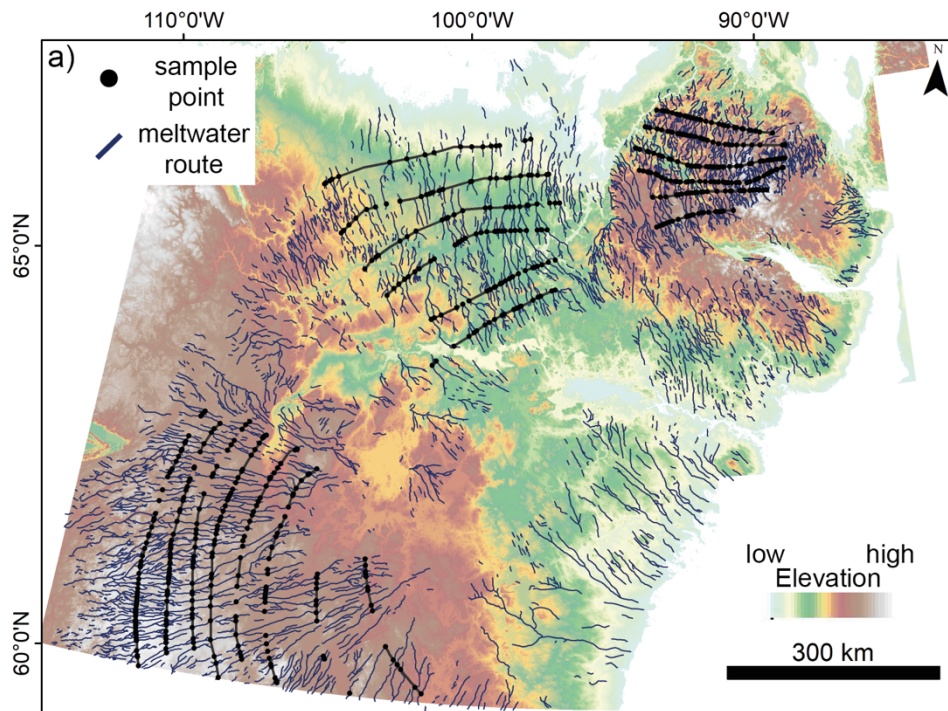
Figure 3.7 Combined width (sample size = n) and spacing (sample size = n2) from the three test sites measured at 9.7 ka (n = 57, n2 = 53), 9.5 ka (n = 50, n2 = 46), 9.4 ka (n = 41, n2 = 71), 9.3 ka (n = 57, n2 = 90), 9.2 ka (n = 60, n2 = 89), 9.1 ka (n = 83, n2 = 89), 8.98 ka (n = 55, n2 = 57) and 8.6 ka (n = 42, n2 = 59).

To investigate whether changes in meltwater coverage is occurring uniformly around the ice sheet or whether the occurrence of meltwater corridors with different characteristics are skewing the overall results, the width and spacing data for each test site were plotted individually (Fig. 3.8). Results illustrate differences in meltwater route characteristics around the ice sheet divide. Meltwater routes at test site 3 are generally more closely spaced than those at test sites 1 and 2. There is also a difference in meltwater route widths with test site 1 showing a general increase over time while test sites 2 and 3 show more subtle changes i.e. increase -> decrease -> increase. Test sites 2 and 3 capture shorter periods of time though with points starting later than they do at test site 1. At the regional scale the overall trends are less clear.
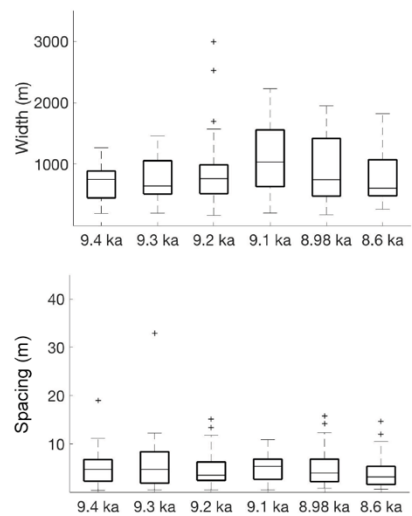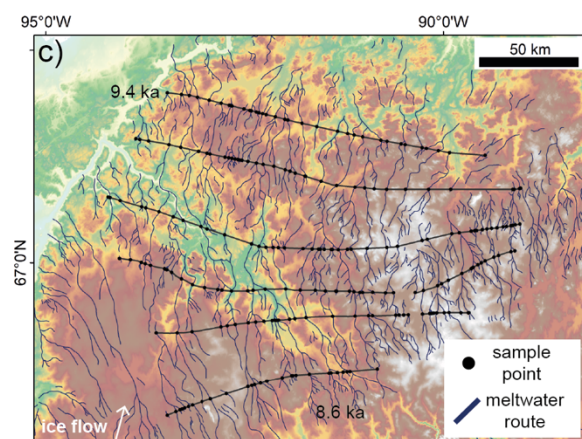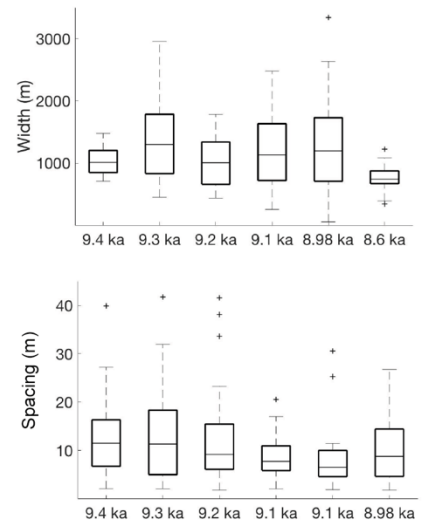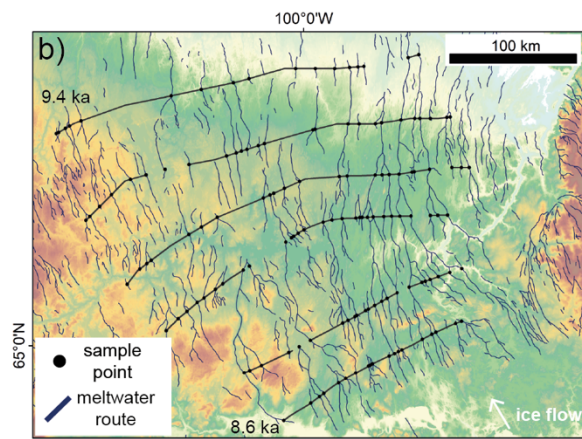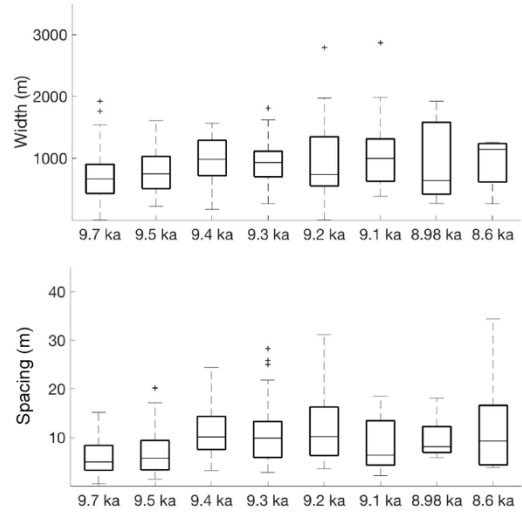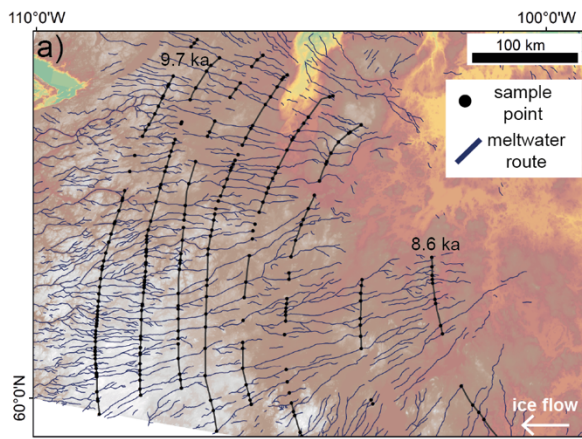
Figure 3.8 Width (sample size = n) and spacing (sample size = n2) for individual test sites. Test site 1 (n = 58, 49, 28, 34, 25, 27, 9 and 6; n2 = 53, 46,23, 31, 21, 24, 7 and 14); Test site

2 (n = 7, 12, 18, 28, 23, 18; n2 = 14, 23, 22, 23, 19 and 19); Test site 3 (n = 34, 36, 43, 43, 33 and 26; n2 = 33, 36, 46, 42, 31, and 26). It is important to note that some of these are based on small sample sizes.

Of the sample points taken along the transects at the three test sites (Fig. 3.6 and 3.7), 84 % of sample locations captured a meltwater track (65 %) or meltwater channel (19 %). The remaining samples captured an esker ridge alone (6 %), captured an esker ridge with a lateral splay (6 %) or were deemed unclassified (4 %). However, subglacial meltwater signatures were not always mutually exclusive and often esker ridges or sometimes even eskers with lateral splay, were recorded within the meltwater tracks and channels. Esker mapping by Storrar et al. (2013) was updated in the study area. Due to the higher resolution data available and the smaller spatial area covered, smaller features which may have been missed could be included. A comparison between the updated esker map and the new meltwater routes map confirms the large-scale association between eskers and wider meltwater features which often flank and connect intervening segments. Eskers were recorded at 43 % of all sample locations. Where they were recorded, 87 % of the time they were flanked by a meltwater track, channel or splay.

Table 3.2 Summary statistics for meltwater routes

	Length (km) (all features)	Width (km) (based on the 3 test sites)	Centreline spacing (km) (based on the 3 test sites)
Min	0.7	0.05	0.4
Lower quartile	4.8	0.5	3.3
Upper quartile	20.1	1.1	10.1
Max	339.9	3.3	77.9
Mean	18.1	0.9	8.1
Std dev.	26.5	0.6	7.4

Meltwater routes reach a maximum of 3.3 km in width and 340 km in length (Table 3.1), but are noted to reach up to 760 km when they extend beyond the limits of the study area (Storrar et al. 2014a). Meltwater channels and meltwater tracks are

typically an order of magnitude wider (mean width: 900 m) than the eskers which they often contain (mean width: 97 m). Meltwater routes appear to vary in width across the study area and along individual centrelines but show no clear trend from the ice divide towards the margin. If these landforms are assumed to have formed time-transgressively, this would suggest no clear trend in width during deglaciation. Within the study area, adjacent centrelines are spaced on average 8 km apart (Table 3.1). This is at the lower end of the range reported in the literature (Fig. 3.9) (e.g. Banerjee and McDonald, 1975; St-Onge, 1984; Shilts et al. 1987; Hebrand and Åmark, 1989; Bolduc, 1992; Boulton et al. 2009; Hewitt, 2011). This is not surprising given that all traces of subglacial meltwater flow including meltwater tracks not containing eskers were mapped. Like variations in width, there appears to be no coherent change in spacing during deglaciation (Fig. 3.7 and 3.8) if a time transgressive formation is assumed.
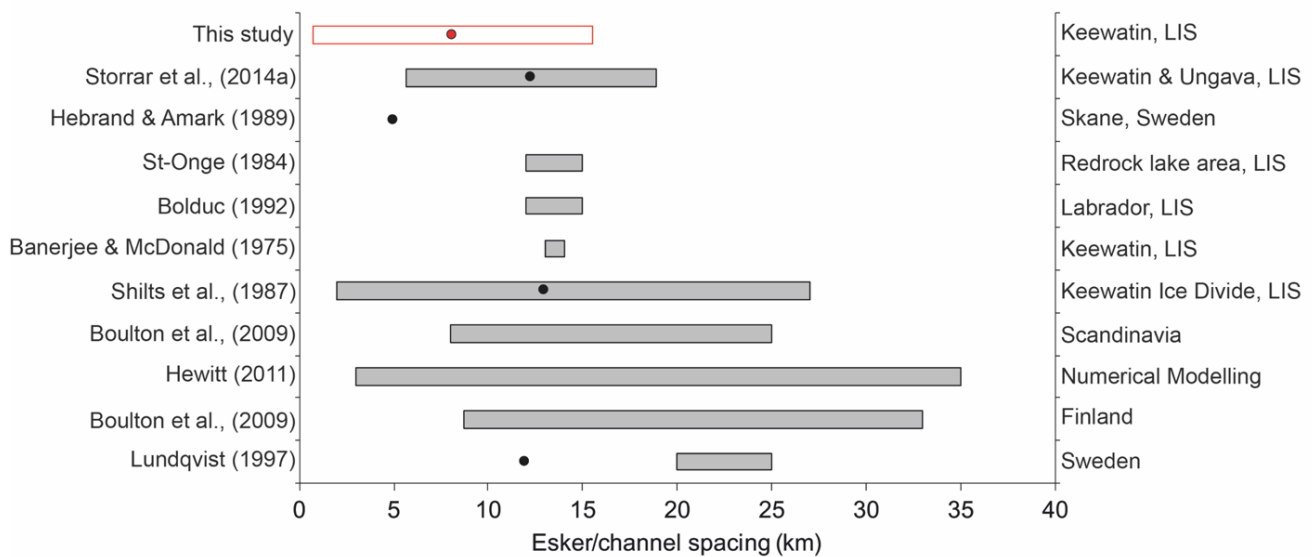
Figure 3.9 Examples of esker and subglacial channel spacing quoted in the literature with bars representing maximum and minimum and the points the mean (Storrar et al. 2014a). The top two bars represent a large-scale esker sample taken from an area which includes this study (Storrar et al. 2014a) and the spacing recorded by all visible traces of subglacial meltwater (i.e. eskers and meltwater corridors). For these two, the bars represent standard deviation and the points the mean. (Modified from Storrar et al. 2014a).

Eskers have previously been widely mapped in northern Canada. Initial mapping was largely undertaken by the Geological Survey of Canada using aerial photography and field observations (e.g. Aylsworth and Shilts, 1989). This included mapping of 'esker systems' – comprising a series of hummocks or short, flat-topped segments which phase downstream into relatively continuous esker ridges or occasionally beaded eskers – across 1.3 million km^2 of the Keewatin sector of the LIS (Aylsworth and Shilts, 1989; Aylsworth et al. 2012). Discontinuous esker ridges are connected to areas of outwash, meltwater channels or belts of bedrock stripped free of drift. More recently, increasing availability of remotely sensed data allowed Storrar et al. (2013) to digitise eskers at an ice sheet scale for the LIS (including the Keewatin sector) using Landsat 7 ETM+ imagery. From this, a secondary dataset was derived by interpolating a straight line between successive aligned esker ridges, creating a continuous pathway, which reflects the location of the major conduits in which the eskers formed (Storrar et al. 2014a). This chapter extends earlier work, which recognises links between eskers and broader traces of subglacial meltwater flow but does not explicitly describe or formally quantify them (e.g. Aylsworth and Shilts, 1989; Storrar et al. 2014a). It is encouraging that despite different datasets and mapping procedures, the overall patterns are similar (Fig. 3.10).
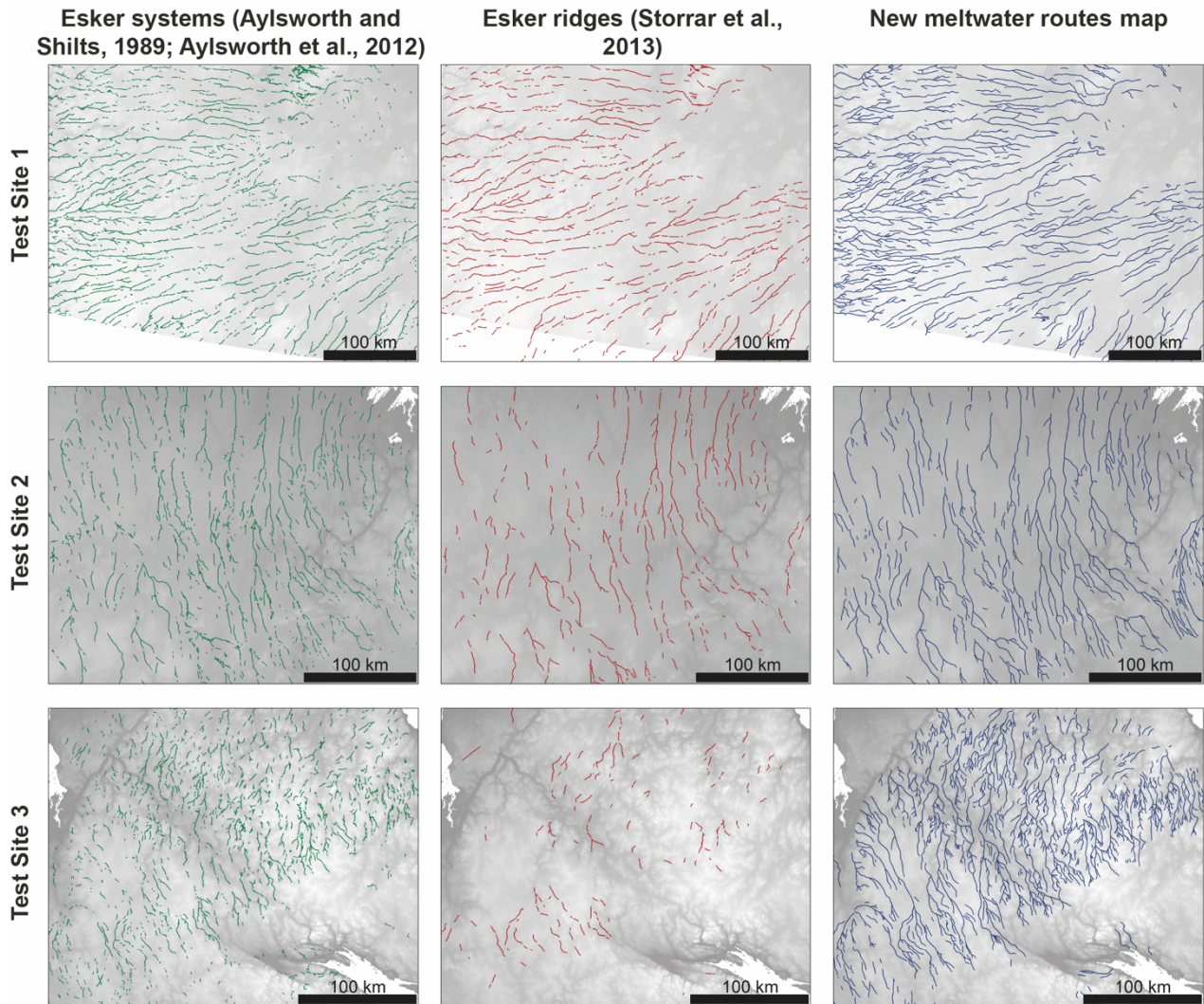
Figure 3.10 Comparison of existing maps of 'esker systems' (green) from air photo interpretation (Aylsworth and Shilts, 1989; Aylsworth et al. 2012), esker ridges (red) from Landsat imagery (Storrar et al. 2013) and the new meltwater routes from the ArcticDEM (blue). Mapping of meltwater routes includes all traces of subglacial meltwater flow (eskers, eskers with lateral splays, meltwater tracks and meltwater channels). The new map does not include any interpolation between geomorphic features. Mapping all meltwater features resulted in more continuous meltwater pathways. The locations of test site 1, test site 2 and test site 3 are identified in Fig. 3.6. DEM(s) created from the Canadian Digital Elevation Model (CDEM). Ottawa, ON: Natural Resources Canada. [2015]

3.3.2 Geomorphological variations

Landforms along meltwater routes exhibit a high degree of geomorphic variability and each of the palaeo-meltwater landforms outlined in Section 1.2.1 (eskers, meltwater channels and meltwater tracks) are identified in the study area. Meltwater channels exhibit negative relief down to ~ 30 m below their immediate surroundings. Meltwater tracks exhibit less pronounced or even negligible relief, being identified instead due to the presence of elongated tracts of hummocks (Fig. 2.1 b-c). Meltwater route edges vary from straight to crenulated and may be discontinuous along sections (Fig. 2.1 d-f). A variety of landforms are found within the meltwater tracks and channels. These include hummocks of varying size, shape, and relief as well as eskers and associated glaciofluvial material (Fig. 2.1). In places, till may be entirely eroded, revealing patches of bedrock. Eskers display a high degree of variability along the meltwater routes with single, continuous ridges the exception rather than the norm. Meltwater routes vary in geomorphological expression both across flow, between adjacent routes, and along flow, with multiple transitions to and from 'different' feature types (Fig. 3.11).

![Meltwater channel]	Meltwater channel
![Meltwater track]	Meltwater track
![Esker with lateral splay]	Esker with lateral splay
![Esker]	Esker
![Mapped meltwater routes]	Mapped meltwater routes
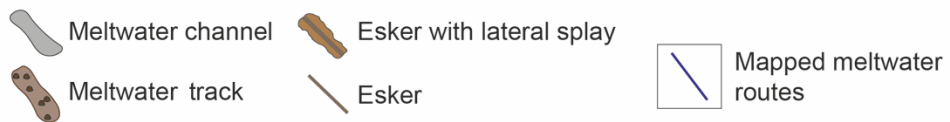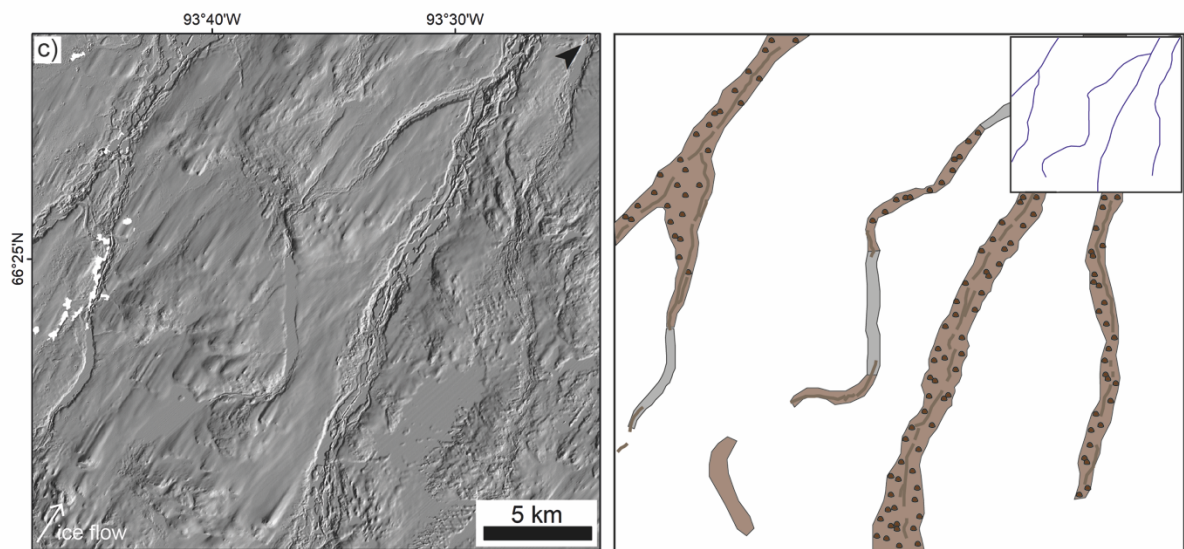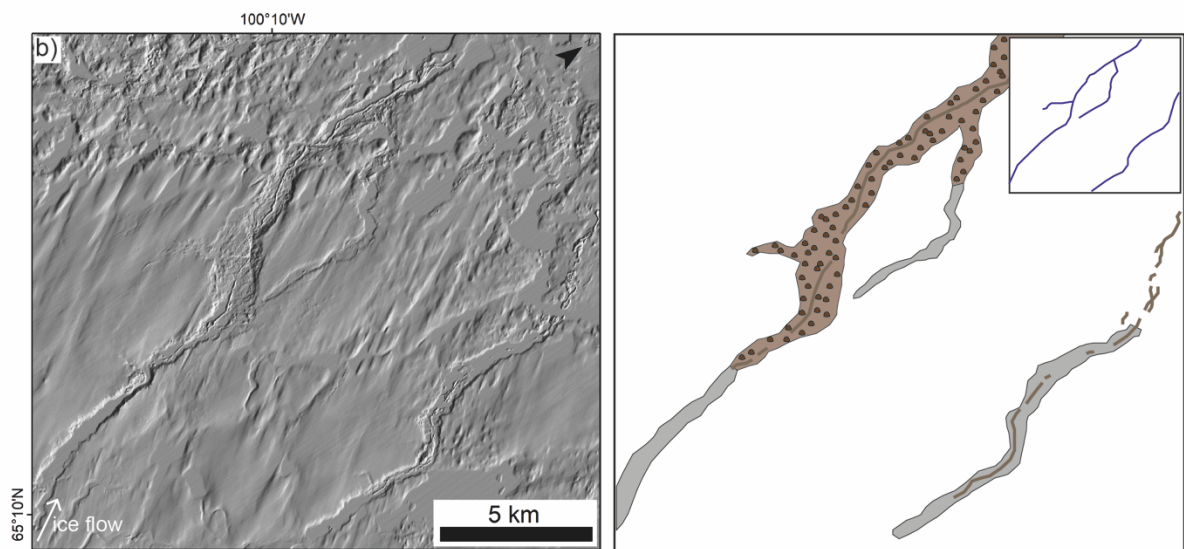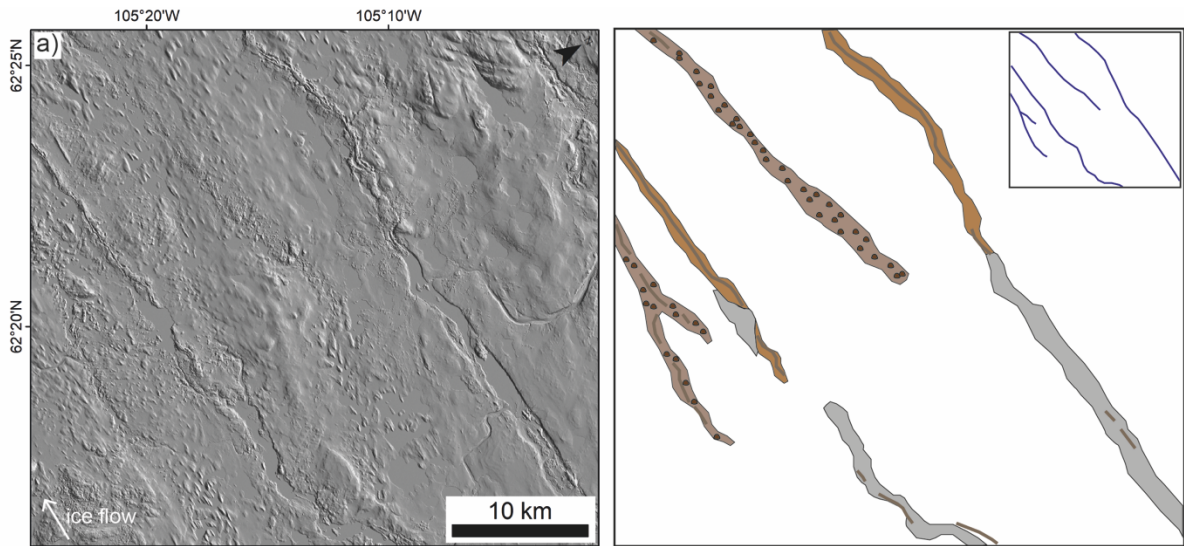
Figure 3.11 (above). Examples of transitions and associations along meltwater routes. The left panel shows the DEM and the right panel shows an interpretation of the feature types with an inset (top right) showing how meltwater routes are mapped as single lines through all types. White patches in the DEM represent areas of missing data due to the presence of hydrological features (e.g. lakes and rivers) or in areas of cloud cover and shadow. DEM(s) created by the Polar Geospatial Center from DigitalGlobe, Inc. imagery.

Despite variations in expression (e.g. relief, definition and the presence or absence of hummocks, glaciofluvial material and eskers), meltwater tracks and meltwater channels are both associated with eskers and form an integrated and coherent large-scale spatial pattern (Fig. 3.6). Furthermore, both meltwater tracks and meltwater channels have a qualitatively similar width range of several hundred metres to ~3 kilometres (Fig. 3.12). The relationship between the two distributions was quantitatively compared using the two-sample Kolmogorov-Smirnov test and the null hypothesis that the two datasets were from the same continuous distribution could not be rejected at the 5 % significance level.
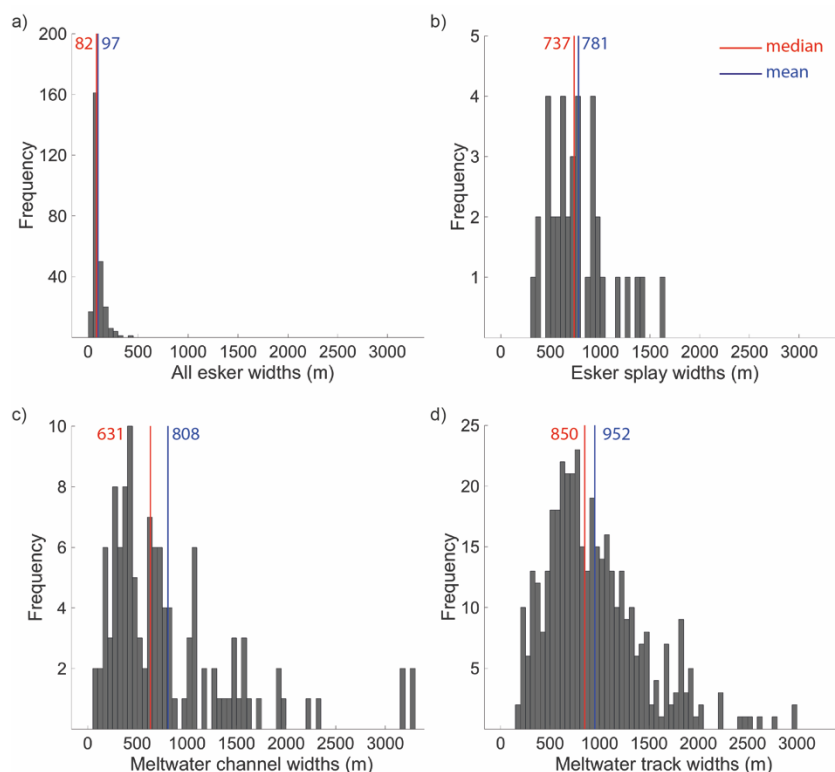
Figure 3.12 Width distributions (in metres) of (a) all esker ridges (n = 259), (b) eskers with lateral splays (n = 37), (c) meltwater channels (n = 118) and (d) meltwater tracks (n = 408) from the whole study area. The median is marked on in red and the mean in blue.

3.3.3 Controls on the large scale distribution of meltwater landforms

Most subglacial meltwater landforms occur within areas of till (Fig. 3.13). Meltwater tracks, meltwater channels and eskers with lateral splays are overrepresented in areas of till blanket, while esker ridges are strongly underrepresented. Meltwater features appear most commonly over areas of metamorphic bedrock, although meltwater channels (incisional features) are overrepresented on more erodible sedimentary rocks.

Figure 3.14 reveals high topographic variability in the NE of the study area. This coincides with the highest density of meltwater routes. Palaeo-ice streams are rare in the Keewatin District region (Stokes and Clark, 2003a, 2003b; Margold et al. 2018), but where they do occur, meltwater routes are noticeably sparser (Fig. 3.15). Comparing the spatial density of meltwater routes inside and outside of the ice streams (calculated simply as total length of meltwater routes per unit area) shows that the two datasets are statistically different ($p = 0.03$). On the bed of the Dubawnt Lake Ice Stream, meltwater routes also occur within less elongate, dendritic networks which also appear to be less continuous and extend further towards the ice divide.
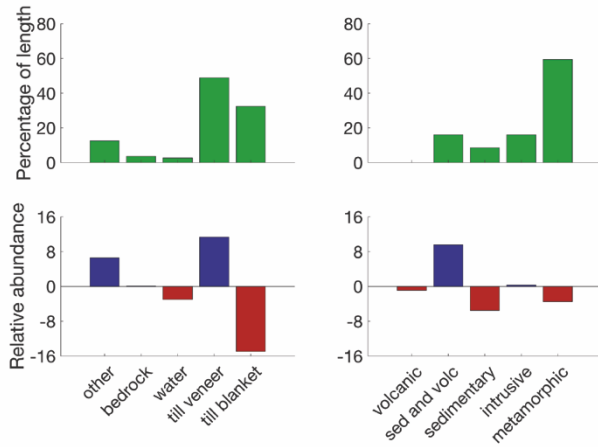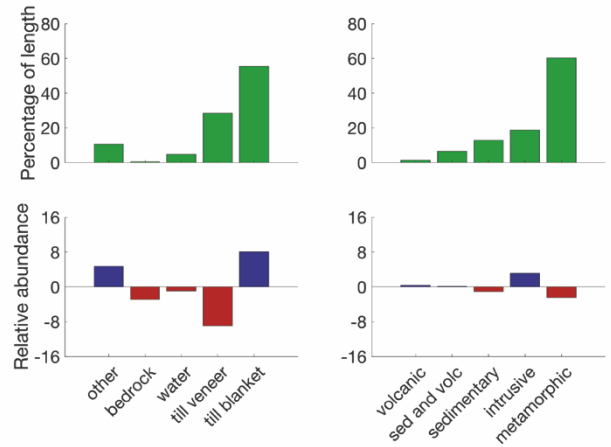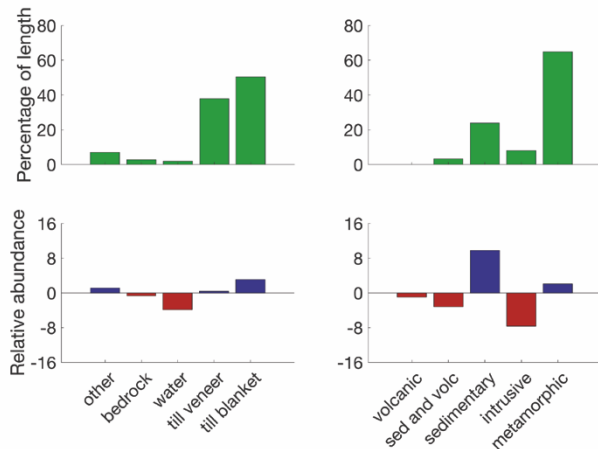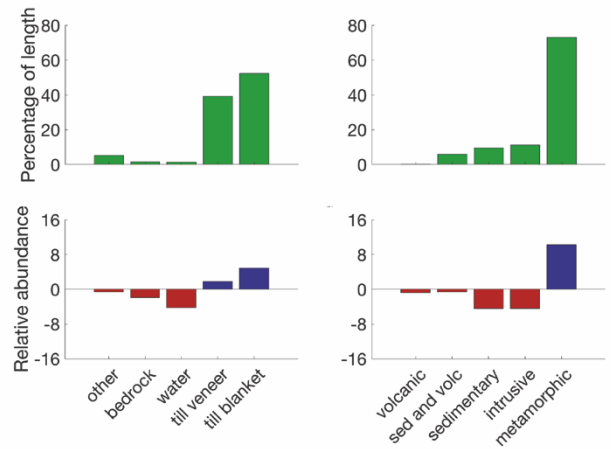
Figure 3.13 Substrate control on geomorphological expression. Occurrence (percentage of length) and relative abundance of different meltwater features over varying surface substrates (Fulton, 1995) and background geology (Wheeler et al. 1996). 'Other' includes marine, lacustrine and glaciofluvial sediments. Blue represents over representation and red represents under representation.
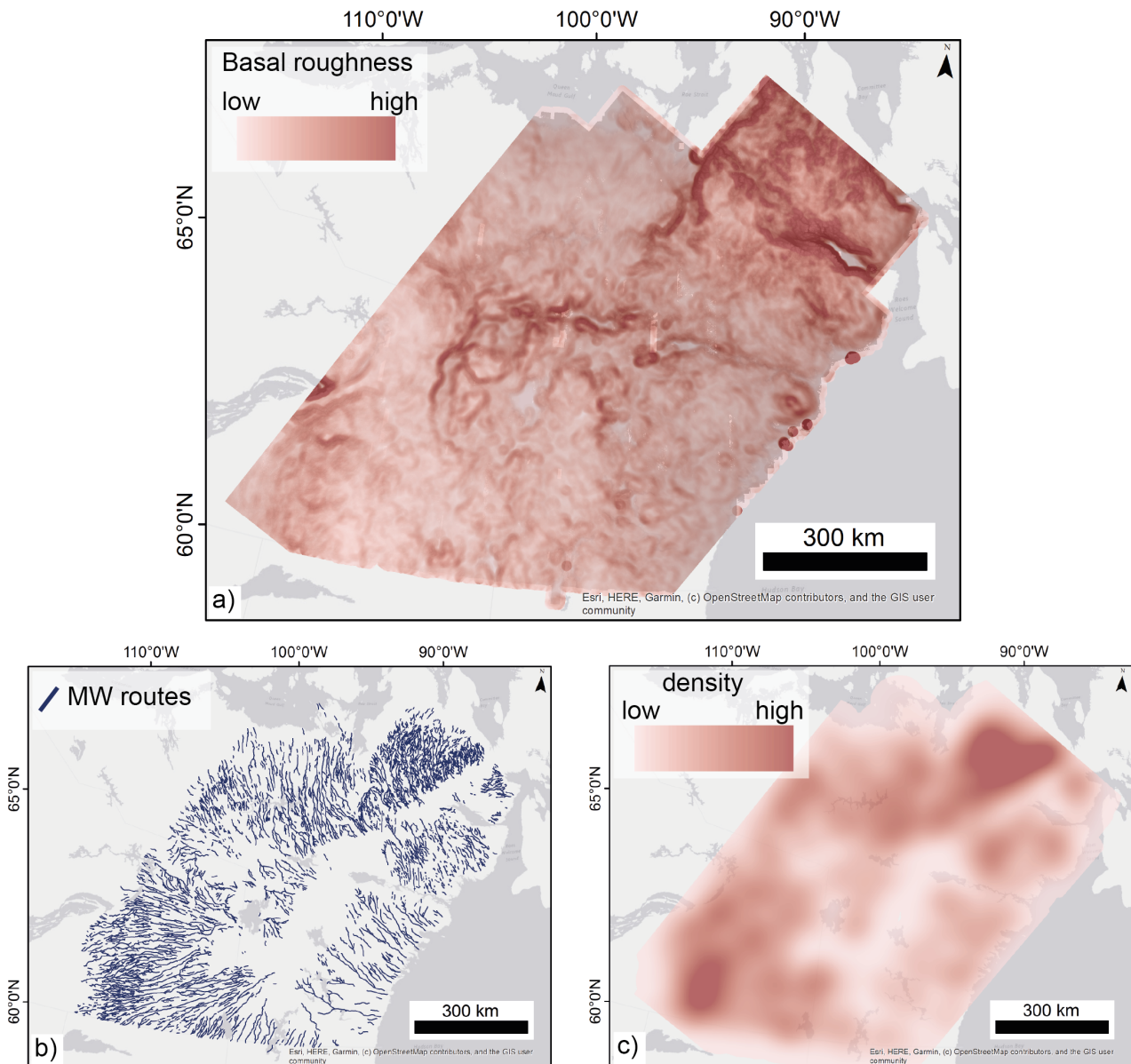
Figure 3.14 a) Local bed roughness (calculated for the approximate wavelength expected to be relevant for the transfer of basal undulations to the ice surface); b) Mapped meltwater routes and; c) Density of meltwater routes. Note the spatial coincidence between the roughest topography in a) and the densest areas of meltwater routes in c).
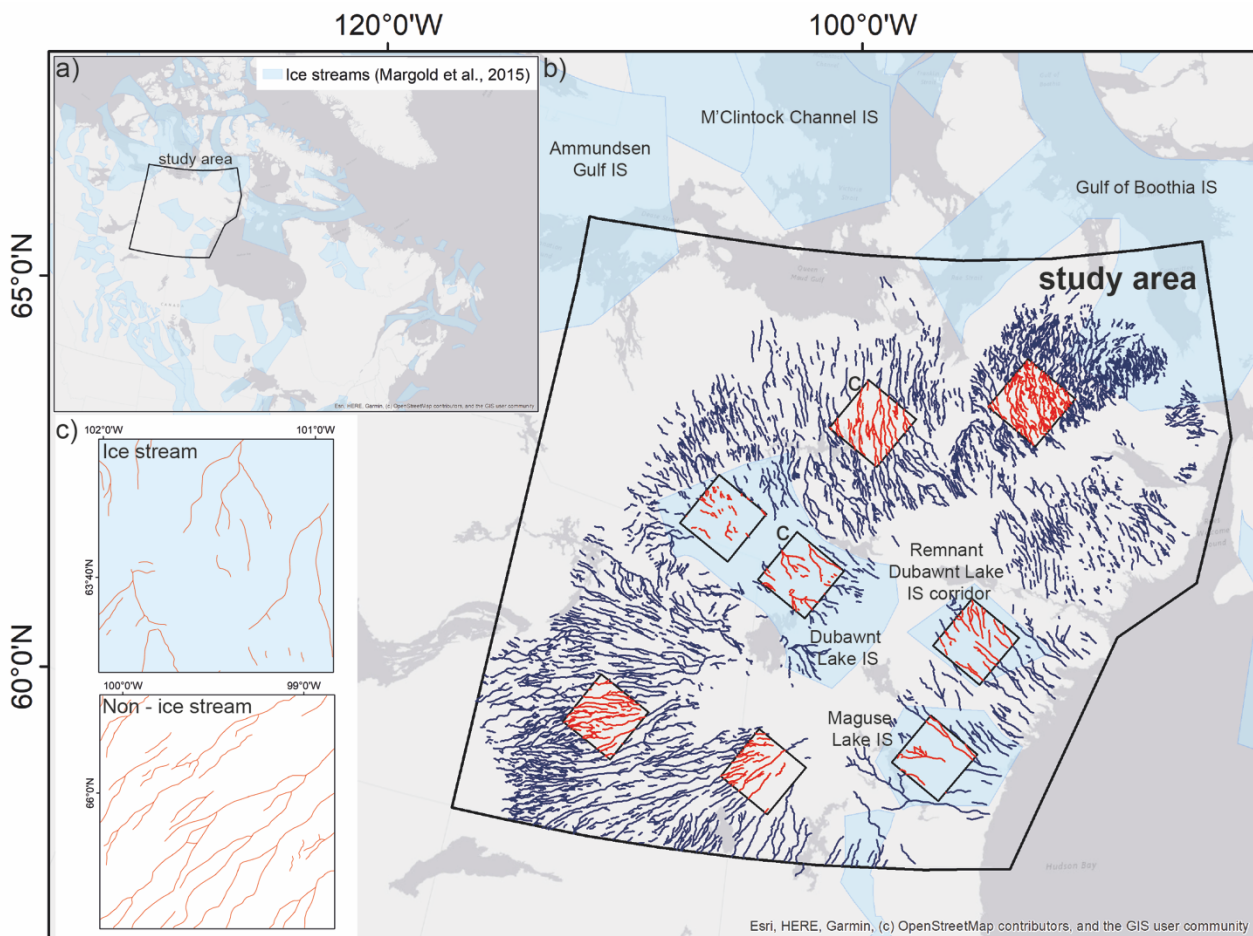
Figure 3.15 a) Comparison of meltwater routes and palaeo-ice streams (Margold et al. 2015); b) Spatial density was calculated for each of the randomly placed sample boxes (100 x 100 km). Ice stream density was compared to the non-ice stream density using a two sample t-test. The null hypothesis is rejected at the 5% significance level (p = 0.03); c) Visual comparison between meltwater routes in ice stream and non-ice stream areas.

To explore potential controls that govern how meltwater landform expression changes with variable background conditions (e.g. substrate, geology, local topography), measurements of width, feature type and substrate were extracted along individual meltwater routes (Fig. 3.16 – 3.19). The meltwater routes exhibit undulating long profiles indicative of a subglacial meltwater origin. Significant variations in elevation were observed to occur along individual meltwater routes with the most significant observed at long profile 2 (Fig. 3.17) where an increase of 187 m (88 %) was recorded.
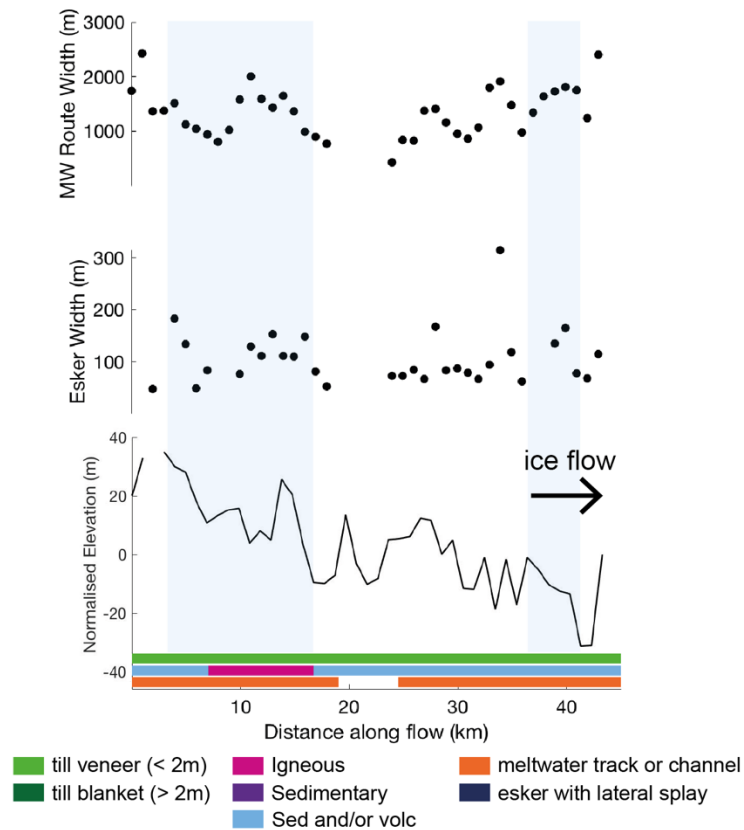
Figure 3.16 Detailed profile 1 exploring local-scale controls on meltwater route width and expression from the ice sheet interior (left) to the exterior (right). The profile was sampled at 1 km intervals along the meltwater route (Fig. 3.6). Elevation is normalised to the downstream end. Blue vertical bars indicate general areas of decreasing slope and red increasing in the direction of the ice flow.

Meltwater routes exhibited considerable variation in width (and elevation) along individual routes with no clear consistent increase or decrease along flow. At long profile 2, an increase in width of > 1000 % was recorded (a minimum width of 191 m and a maximum of 2495 m). Attempts were made to isolate any direct controls on meltwater route width by comparing changes in width with concurrent changes in; a) topography; b) sediment thickness and; c) bed geology. These are described in turn below.
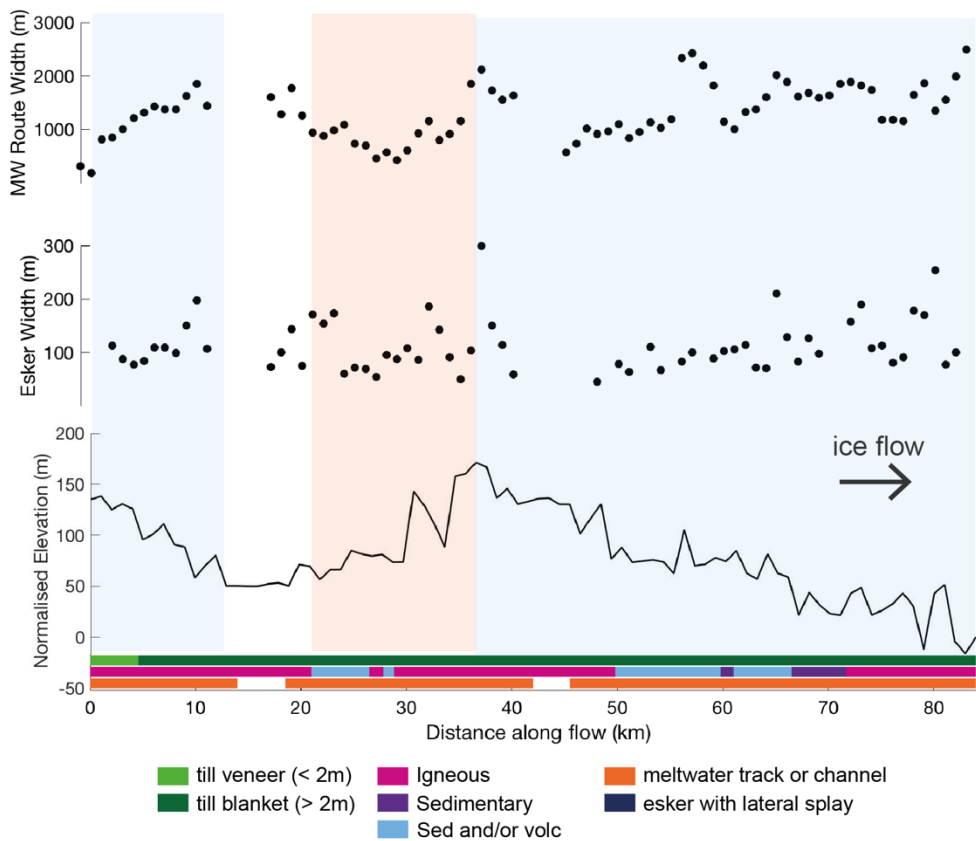
Figure 3.17 Detailed profile 2 – exploring local-scale controls on meltwater route width and expression from the ice sheet interior (left) to the exterior (right). The profile was sampled at 1 km intervals along the meltwater route (Fig. 3.6). Elevation is normalised to the downstream end. Blue vertical bars indicate general areas of decreasing slope and red increasing in the direction of the ice flow.

In terms of local topography, the results are unclear with examples of meltwater routes increasing in width on slopes that ascend and descend in the direction of water flow (e.g. Fig. 3.17 and 3.18). In Fig. 3.16, a large increase in width (883 to 1550 m) is associated with an increase in elevation (~ 70 m over 6 km), which also coincides with a transition from a strongly negative relief feature (a meltwater channel) to a positive relief depositional feature (esker with lateral splay). This sharp transition may be related to the emergence of the meltwater route out of the Thelon sedimentary basin. There are less obvious examples of meltwater routes decreasing in width on ascending slopes (Fig. 3.19). On relatively 'flatter' sections of the long profiles,

113

meltwater width variations of a similar magnitude are still observed (e.g. Fig. 3.18 and 3.19).
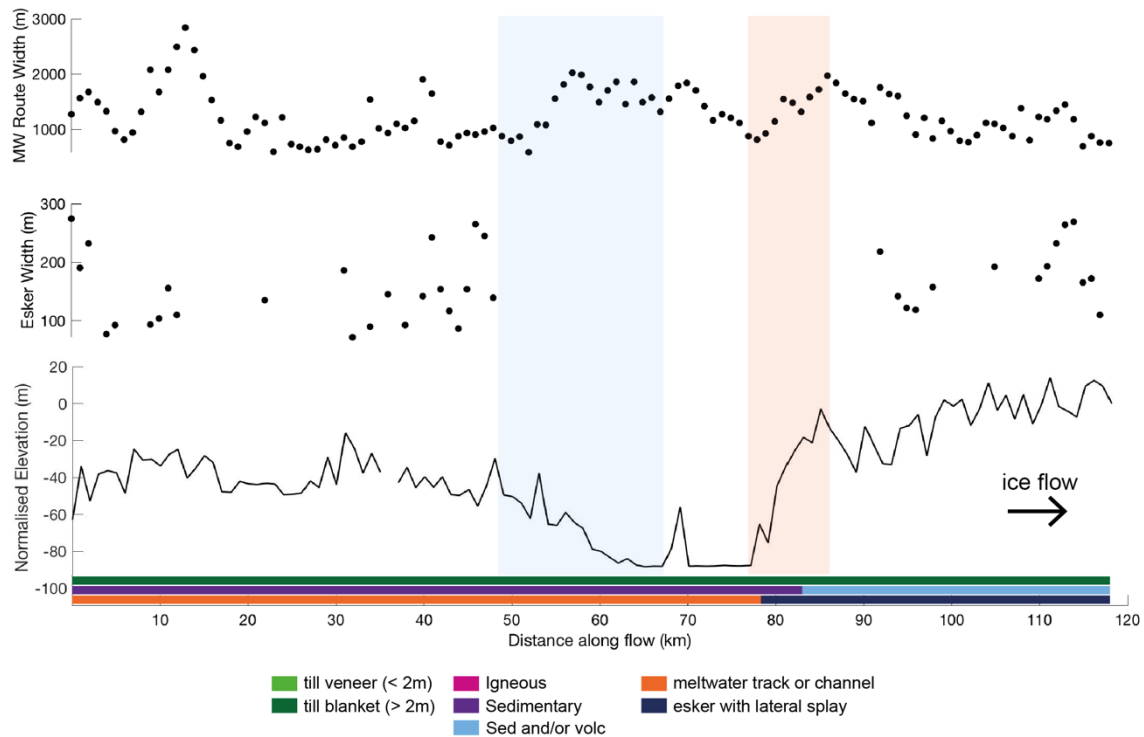
Figure 3.18 Detailed profile 3 – exploring local-scale controls on meltwater route width and expression from the ice sheet interior (left) to the exterior (right). The profile was sampled at 1 km intervals along the meltwater route (Fig. 3.6). Elevation is normalised to the downstream end. Blue vertical bars indicate general areas of decreasing slope and red increasing in the direction of the ice flow.

There does not appear to be a clear relationship between meltwater route width and surface sediment thickness or basal geology. However, these parameters do not vary much and this analysis is hindered by the relatively low resolution of the two background datasets (Fig. 3.3 and 3.4).

Although there is not a consistent ratio between esker width and the associated width of the meltwater track or meltwater channel when measured at the same location, there is a general positive relationship between the two, specifically when following topographic increases or decreases (e.g. Fig. 3.19).
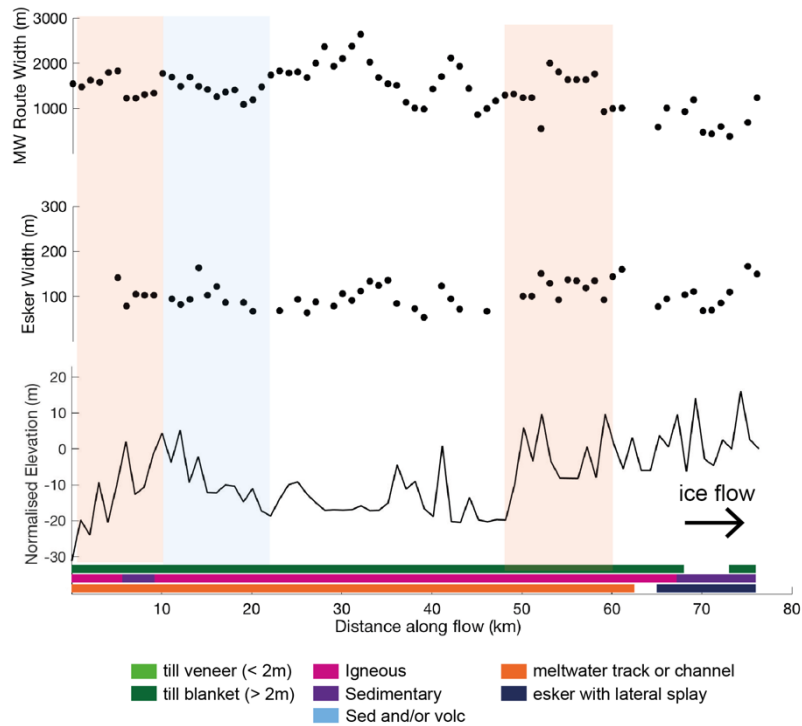
Figure 3.19 Detailed profile 4 – exploring local-scale controls on meltwater route width and expression from the ice sheet interior (left) to the exterior (right). The profile was sampled at 1 km intervals along the meltwater route (Fig. 3.6). Elevation is normalised to the downstream end. Blue vertical bars indicate general areas of decreasing slope and red increasing in the direction of the ice flow.

The absence of predicted lakes at the heads of the meltwater route networks (Fig. 3.20) suggests that the formation of the meltwater route network in general is unlikely to be attributed to large subglacial lake drainage(s). However, individual meltwater routes or small network/(s) may have been formed in this way, either by lakes predicted in figure 3.20 or by the drainage of lakes smaller than the resolution of the existing predictions (5 km resolution), which are expected – from contemporary ice sheets – to be numerous (Dowdeswell and Siegert, 2002; Bowling et al. (2019).
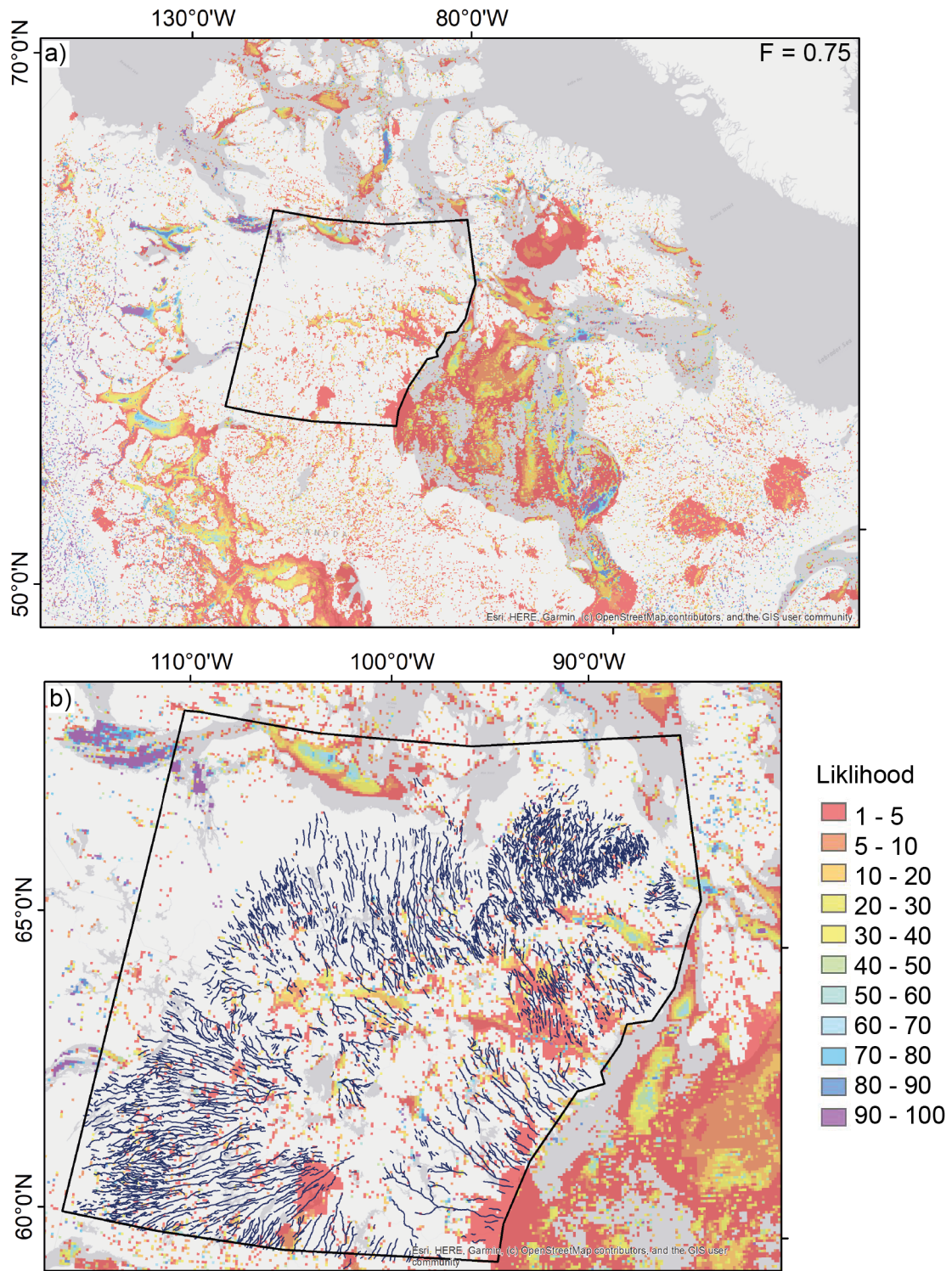
Figure 3.20 Percentage of time subglacial lakes formed when ice covered (predicted by Livingstone et al., (2013)). This is a less conservative estimate using an F value of 0.75 which produced lakes in far greater frequency and magnitude compared to F=1. Almost all significant depressions within the landscape are filled effectively giving an upper bound on depressions capable of hosting lakes.

116

3.4 Discussion
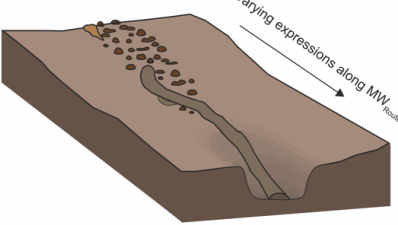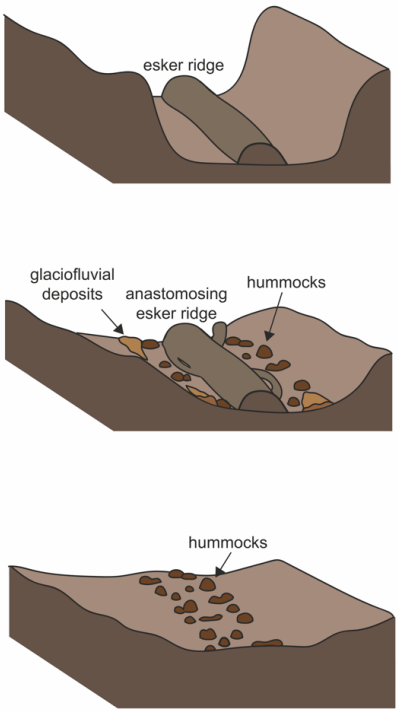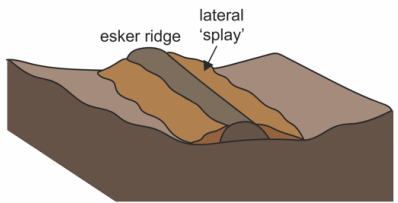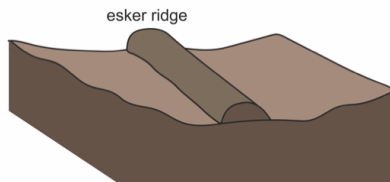
The new meltwater routes map shows that meltwater tracks and meltwater channels, which flank and connect (in an along-flow direction) esker ridges, are a dominant part of the landscape across the former Keewatin sector of the LIS. Holistic mapping of meltwater routes including features cut up into the ice (i.e. eskers), features cut down into the bed and those in-between (i.e. meltwater tracks and meltwater channels) creates a more complete and less fragmented regional representation of drainage compared to maps of individual features (Fig. 3.6) and allows the expressions, distributions and associations between different meltwater landforms, which make up the meltwater routes, to be assessed. The broad scale pattern of palaeo-drainage radiating out from the former Keewatin Ice Divide, which remains noticeably absent of meltwater evidence (Fig. 3.6), is consistent with previous studies (Shilts et al. 1987; Aylsworth and Shilts, 1989; Storrar et al. 2013, 2014a), but mapping here results in a greater density, narrower spacing (Fig. 3.10) and higher number of tributaries.

Mapping all features together as meltwater routes revealed the numerous similarities between meltwater tracks and meltwater channels. While Table 3.1 outlines the geomorphic criteria for mapping meltwater routes, in reality, distinguishing between meltwater tracks and meltwater channels at sample points was often somewhat subjective and difficult to determine based on their geomorphology. Similarities between the two included; width, spacing, association with eskers and occurrence within an integrated network characterised by transitions to and from different expressions along individual meltwater routes (Fig. 3.11). This provides strong evidence that these meltwater landforms are varying expressions of the same phenomenon, caused by the same process(es) creating / leaving behind a variable signature of geomorphic work. This is consistent with previous conceptual work linking meltwater landforms. For example, Sjogren et al. (2002) identify various tunnel valley (meltwater channel) expressions that they attribute to different developmental stages, from discontinuous through to fully developed valleys. Peterson and Johnson (2018) suggest that negative relief hummock corridors (meltwater tracks) are a type of tunnel valley and positive relief hummock corridors are equivalent to 'glaciofluvial corridors' in Canada (e.g. Utting et al. 2009). As a result of the observations within this chapter,

I propose that meltwater tracks and meltwater channels can be grouped under the term 'meltwater corridor' and that this encapsulates all features with widths in the range of 100s – 1000s metres (Table 3.3), which have until now been treated separately.

While recognised previously in local case studies (e.g. St-Onge, 1984; Rampton, 2000; Utting et al. 2009), this work confirms that across this 1 million km^2 area of the former LIS, meltwater corridors of varying geomorphic expression are widespread (captured at 84 % of all sample routes) rather than an isolated phenomenon. Esker ridges are captured at just 43 % of sample locations; however, the presence or absence of an esker at the sample point may not be indicative of the entire length of the meltwater route as in many cases the esker ridges within a meltwater corridor are fragmented. Nonetheless, it is probable that the model of R-channels across the Canadian Shield (e.g. Clark and Walder, 1994) is an oversimplification and may under-represent the modes and thus coverage of drainage in this sector and fail to capture important processes recorded on the bed.

Table 3.3 Proposed classification of subglacial meltwater traces. Meltwater routes encompass all visible evidence and consist of variable relief meltwater corridors with widths in the order 100's of metres and esker ridges with widths in the order of 10's of metres. Examples provided are composite images with eskers likely deposited marginally at a later time.

Proposed Classification	Description	Example
Meltwater route	All visible traces of subglacial meltwater drainage (i.e. all of below)	
Meltwater corridor	- Meltwater channel - Tunnel channel - Tunnel valley - Hummock corridor (negative) (e.g. Peterson and Johnson, 2018 - Erosional corridor (e.g. Burke et al., 2011) - Esker corridor (e.g. Sharpe et al., 2017) - Meltwater corridor (e.g. Rampton, 2000) - Washed zone (e.g. Ward et al., 1997) - Hummock corridor (positive) (e.g. Peterson and Johnson)	
Esker with lateral splay	Esker ridge flanked by lateral splay (e.g. Cummings et al., 2011a)	
Esker ridge	Single, multiple or anastomosing esker ridges	

3.4.1 Controls on meltwater corridor distribution and expression

To interpret palaeo-landforms and reconstruct subglacial meltwater behaviour - i.e. 'glacial inversion' (e.g. Kleman and Borgström, 1996) - an understanding of the processes that formed the landforms is needed. I start to unravel understanding of meltwater corridors by first discussing potential controls on their overall distribution and expression. Various hypotheses have been put forward in the literature to explain the distribution (i.e. where landforms do and do not occur) and the individual feature morphometry (e.g. relative differences in length, width or depth), however, a clear consensus on a universal dominant control(s) remains elusive. Here, I aim to contribute to this discussion by exploring the spatial and temporal associations between varying meltwater landforms and a range of background controls at a large scale.

3.4.1.1   Topography

Variable local scale topography is expected to have a control on meltwater landform distribution and expression with alternating sections of ascending, descending and flat regions (Shreve, 1985) . This is likely to impact relative rates of conduit migration due to a varying strength hydraulic gradient and a complex pressurisation regime as local topographic variations intersect with increasing downstream distances. Results from the four long profiles here do not show a definitive relationship (i.e. a consistent increase or decrease in width associated with a particular bed) (Figs. 3.16 - 3.19); however, this is based on a relatively small sample size.

At a larger scale, there are hints at a possible relationship between areas of high topographic roughness and meltwater route density (Fig. 3.14). While there is a high degree of channelisation across the Keewatin sector of the ice sheet bed, channelisation is not uniform. The increased density of meltwater routes within the 'roughest' areas may be the result of subglacial drainage route fragmentation around bed obstacles, with a greater number of tributaries and broken patterns common in regions of high bed roughness. Basal topography also preconditions the large-scale spatial structure of surface drainage (Ignéczi et al. 2018) and the association between rough areas and dense clusters of meltwater routes could be a response to more

surface water penetrating to the bed as the result of extensive crevassing and the storage and drainage of water in surface lakes. This link to surface melt inputs is consistent with observations of more densely spaced eskers during warmer periods (Storrar et al., 2014a,b) and theory, which suggests greater melt results in more closely spaced meltwater routes (Boulton et al. 2009; Hewitt, 2011). For a typical melt season in west Greenland, crevasses capture a significant amount of surface water – more than moulins or the hydrofracture of surface lakes (Koziol et al. 2017). Surface meltwater inputs are thought to be an important control on the distribution of drainage across the bed (e.g. Gulley et al. 2012; Banwell et al. 2016) and the formation and evolution of subglacial meltwater landforms (e.g. Banerjee and McDonald, 1975; St-Onge, 1984; Hooke and Fastook, 2007; Storrar et al. 2014b; Livingstone et al. 2015; Peterson et al. 2017).

3.4.1.2   Subglacial lakes

The lack of association between meltwater routes and predicted subglacial lake locations (Fig. 3.20) suggests that large subglacial lakes were not the primary source of meltwater for the formation of the meltwater landforms in this area. However, there is evidence to suggest that individual meltwater routes or small networks of routes may have been formed following the drainage(s) of small, subglacial lakes likely near the margin, something which is known to occur at the GrIS (Livingstone et al. 2019). Firstly, there are a number of examples (~ 10 identified) (Fig. 3.21) of the characteristic subglacial lake drainage signature; small flat spots associated with meltwater channels which transition downstream into eskers (beads) (Livingstone et al. 2016). There is also an example of a drainage network (Fig. 3.22) that varies from the majority of others in its vicinity in that it is shorter, converges downflow towards two main routes (potential exit portals) and ends in two large and overlapping (terminal) fans. This suggests that further geomorphic and network analysis is likely to support the formation of at least some meltwater routes in the area as a result of small subglacial lake drainages.
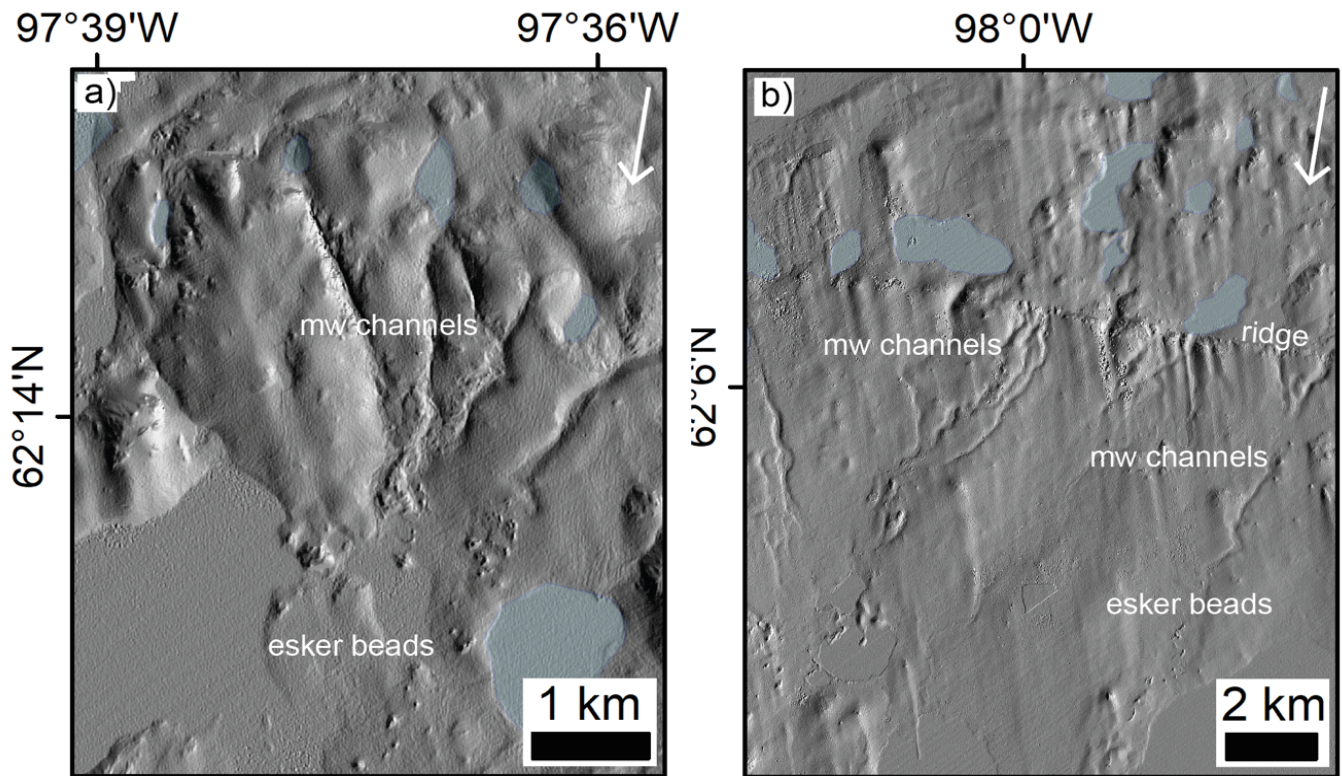
Figure 3.21 – Examples of the geomorphic signature of palaeo subglacial lake drainage i.e. a transition from flat spot -> meltwater channel -> esker (beads) (Livingstone et al. 2016) from within the study area. Light blue polygons represent the flat spots.
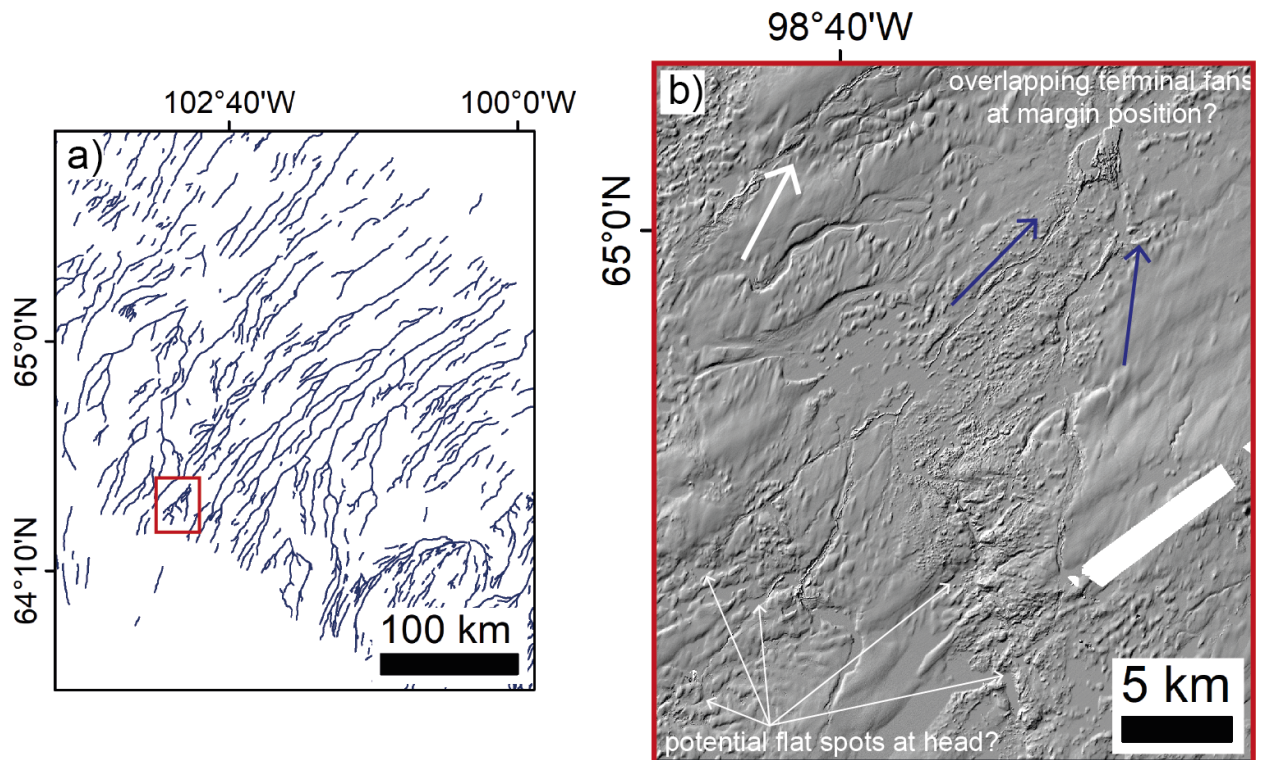
Figure 3.22 Example of how differing network characteristics could be used to help identify meltwater routes formed as a result of lake drainage events. In this example, a series of flat spots trend downstream into meltwater channels, eskers and then terminal fans. The convergence of this meltwater drainage signature differs from the surrounding parallel drainage arrangement.

3.4.1.3   Change in meltwater route spacing/width through time

Although there were no clear trends in meltwater route spacing or width over time (Fig. 3.7 and 3.8), the meltwater routes within this study formed during a period of high and relatively stable atmospheric temperatures (Fig. 3.23) (Storrar et al. 2014b) and thus no significant change in meltwater corridor width or density in response to surface melt inputs is expected. Nonetheless, shorter term variations in surface meltwater delivery to the bed (i.e. daily -> decadal) have been identified as a first order control on subglacial water pressure fluctuations, which drive overlying ice sheet dynamics (Smith et al. 2021) and are thus likely important for the geomorphic processes occurring at the ice-bed interface. This will be explored further in section 3.43.
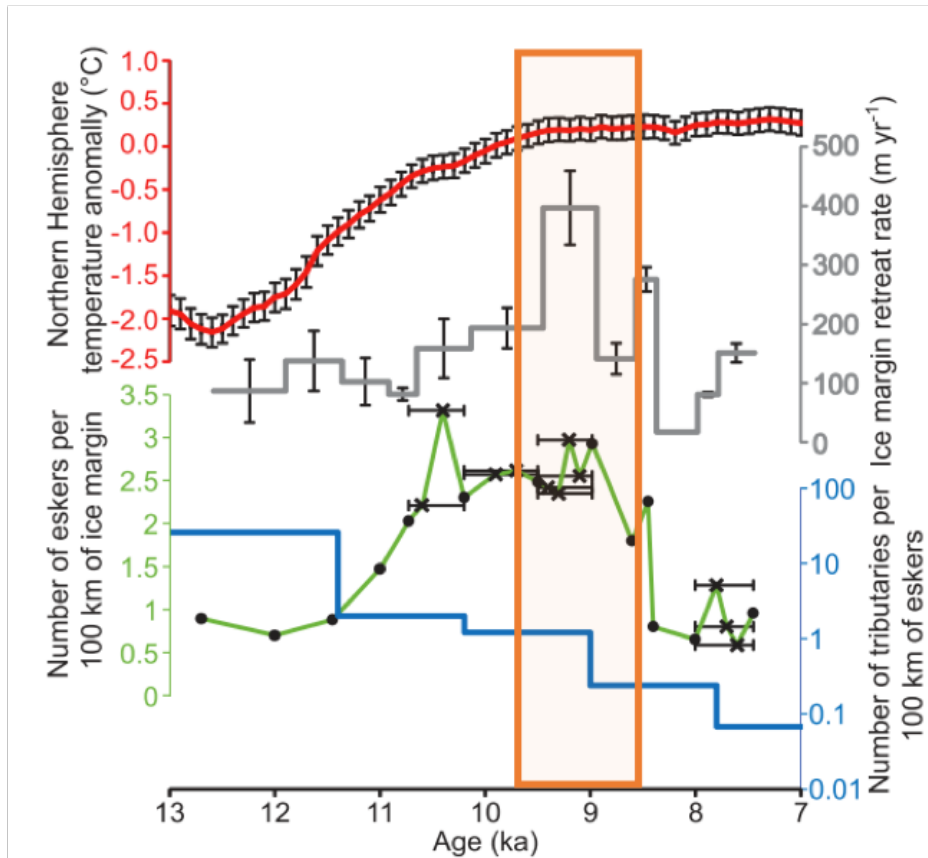
Figure 3.23 Climate and ice margin retreat rate plotted against esker density and tributary number for Keewatin, Canada (Storrar et al., 2014b). The orange box identifies the period of retreat captured by the landforms sampled herein (Fig. 3.6).

3.4.1.4 Ice sheet dynamics

Palaeo-ice stream locations – particularly the Dubawnt Lake Ice Stream are associated with a lower density of meltwater features and differing network patterns (Fig. 3.15). For example, the network pattern of meltwater routes corresponding with the location of the Dubawnt Lake Ice Stream are less elongated and extend further towards the ice divide. Although distributed drainage is favoured beneath ice streams owing to the lower ice surface slopes and thus shallow hydraulic potential gradients (Kamb, 1987; Bell, 2008), where channelised drainage does occur, it is likely to be more dendritic due to enhanced lateral water flow. Fewer meltwater features within ice stream areas is consistent with Livingstone et al. (2015). This may reflect the less

frequent occurrence of channelisation beneath palaeo-ice streams and/ or the lack of preservation potential beneath fast flowing ice (Boulton, 1996).

Dynamic ice mass loss via streaming or surging (and subsequent melting and iceberg calving) has implications for ice sheet stability (e.g. Bell, 2008; Christianson et al. 2014; Christoffersen et al. 2014). The Keewatin sector of the LIS had a relatively low spatial density of ice streams compared to the western and southern margins (Margold et al. 2015; Stokes et al. 2016). This may be partially attributed to the low relief, resistant bed of the shield, which was unable to provide the fine-grained sediments required to lubricate ice flow and the fact that the margin reached the Keewatin sector later during deglaciation when the remaining ice sheet was much smaller (e.g. Margold et al. 2015; Stokes et al. 2016). It may also be that efficient evacuation of meltwater through the dense channelised network, which developed in this region during the final stages of deglaciation, as the climate warmed (Storrar et al. 2014b), inhibited the development of fast flow and potentially contributed to the shut-down of existing ice streams. This is consistent with recent physical modelling (Lelandais et al. 2018) and modern temporal observations that link decadal-scale ice-flow decelerations with more pervasive and efficient drainage channelisation driven by increased surface meltwater inputs to the bed (Sole et al. 2013; Tedstone et al. 2014; van de Wal et al. 2015; Davison et al. 2019) and vice versa (Williams et al. 2020). If this hypothesis is correct, it may be possible to identify this large-scale inverse spatial relationship between channelisation and ice streaming in other palaeo-ice sheet settings by substituting time (from contemporary observations – i.e. higher surface melt versus lower lower surface melt) with space (from landform observations i.e. ice stream vs non ice stream). This potential drainage control on ice-sheet velocity and stability may also influence the pace of deglaciation; slower retreat rates (~ 230 m yr^{-1}) are noted in the northwest of the study area, which coincide with the highest density of meltwater routes, compared to much faster retreat rates (~ 540 m yr^{-1}) associated with the sparsest meltwater routes. This conclusion is tentative given uncertainty in the regions deglacial chronology (Dyke et al. 2003; Dalton et al., 2020) and the many other factors that can influence retreat rate, and thus requires further testing.

3.4.1.5 Sediment thickness and basal geology

Theory suggests that harder beds are more difficult to incise and thus where sediments are sparse, erosion will occur laterally (rather than vertically) resulting in wider corridors. Conversely, areas of thicker sediments (which are relatively softer and easier to erode vertically), will produce narrower but likely deeper corridors. This was explored locally using the long profiles (Fig 3.16 – 3.19). However, the low resolution of the background data precluded the identification of any clear relationship. It is expected however, with higher resolution data, this relationship is likely to be expressed and indeed was the case in Sweden where a higher resolution sediment thickness map was used to show that areas with higher sediment thickness generally exhibited narrower corridors (Peterson et al. 2018).

At a large-scale and looking at variations in landform expression, there is a general tendency for meltwater routes to preferentially form on till, which is more easily eroded than bedrock and where geomorphic evidence is likely to be better developed. Eskers are over-represented on harder, more resistant rock (Fig. 3.7a) where R-channels are more likely to form (Clark and Walder, 1994; Storrar, 2014a), while there is a slight tendency for meltwater channels (i.e. incisional features) to form on the softer, more erodible sedimentary rock (Fig. 3.7c and d). Eskers with lateral splays (i.e. depositional features) appear preferentially on till blankets (Fig. 3.7b) where there is an abundance of sediment that may overwhelm and clog up the conduit (e.g. Burke et al. 2015), while isolated esker ridges favour thin till and are under-represented on thick till. Though detailed long-profiles (Fig. 3.10) hint at local relationships between bed substrate changes and the resultant landform expression, caution must be taken to avoid the assumption that this is a widespread occurrence rather than an isolated coincidence.

3.4.1.6 Summary of controls

Overall, it is difficult to identify a dominant universal control for the large-scale distribution and morphological variations of meltwater routes from this study. While there are hints at local scale relationships (e.g. a transition from an erosional feature to a depositional feature associated with the transition from a soft to hard bed), these

do not seem consistent at the scale investigated here. At the large scale, I speculate that the magnitude of surface meltwater inputted (controlled by the climate) and the location of input points (influenced somewhat by the transfer of basal topographic variation) are likely important contributors to the quasi-regular spacing of the meltwater landforms around the ice sheet divide. Additional further exploration of local scale topography may also reveal important insights into topography as a control on morphological variations.

In summary, there is a physical grounding for the background controls discussed here and it is likely that they do have an effect on the distribution and morphological expression of meltwater pathways; however, their relative contributions are likely to vary over time and space. Furthermore, it is difficult to identify any strong relationships between the background controls and the meltwater features which are likely to have also been strongly influenced by the changing glaciological conditions at the time of their formation (e.g. hydropotential gradient at the bed).

3.4.2 Interpreting meltwater routes

In this section I propose a new model for the formation of meltwater corridors. This has been inspired by the need to explain the following observations from this study;

a) The close spatial association between eskers and meltwater corridors i.e. eskers within meltwater corridors 90 % of the time.
b) The holistic nature of the meltwater routes i.e. variable geomorphic work from strongly erosional (negative relief meltwater corridors) through to depositional features (eskers) likely varying over time and space.
c) The width of meltwater corridors (~ 1 km), which are approximately an order of magnitude greater than the eskers (i.e. the conduits).
d) The lack of association between meltwater corridors and predicted subglacial lake drainages and the likely important role of surface meltwater inputs as a meltwater source.

The proposed model for the formation of meltwater corridors is based on pressure-driven interactions between different elements of the drainage system, driven by highly variable surface meltwater inputs. Linking contemporary observations and modelling of variable pressures within the subglacial hydrological system to support the physical basis behind the proposed model is a key aim of this section.

3.4.3 A proposed model for meltwater corridor formation – repeated pressure-driven drainage interactions

Although hydrological theory dictates that a conduit in steady state will operate at lower pressure than the surrounding distributed system, large or relatively rapid fluctuations in surface meltwater inputs (compared to the rate at which conduits expand from melting caused by turbulent heat dissipation) during the melt season mean the system is rarely in steady-state (Bartholomew et al. 2012).

Once a conduit system has evolved gradually to accommodate high meltwater fluxes (Cowton et al. 2013), it is likely to operate at a lower pressure than the surrounding high-pressure weakly connected system during periods of low meltwater input (e.g. at night and later in the melt season), thus drawing water in (Fig. 3.24 a and c). However, variations in borehole water pressure measurements observed at glaciers in the Alps (e.g. Hubbard et al. 1995; Gordon et al. 1998), Canada (e.g. Rada and Schoof, 2018) and Alaska (e.g. Bartholomaus et al. 2008), ice velocity measurements taken from the Greenland Ice Sheet (e.g. Tedstone et al. 2014) and numerical modelling (e.g. Werder et al. 2013), suggest that large or rapid meltwater inputs can cause spikes in conduit water pressure at a range of temporal scales (Cowton et al. 2013). This temporarily reverses the hydraulic potential gradient and causes water to flow out of the conduit and into the surrounding hydraulically connected distributed drainage system, temporarily connecting the two (Fig. 3.24 b). This process forms the basis for the proposed model.

Although the proposed model envisages an efficient well-developed conduit (Fig. 3.24), a conduit is not required – pressure fluctuations can also occur along an efficient 'core' of linked cavities (e.g. Davison et al. 2019). Nevertheless, this is likely to act in a similar way still interacting and transferring water with the surrounding

hydraulically connected distributed drainage system when its capacity is breached. This may explain why meltwater corridors do not always contain an esker.

A range of drainage structures across the hydraulically connected distributed zone are envisaged to occur in response to conduit over-pressurisation and resulting pressure-driven drainage reorganisation. Based on the wider literature and understanding of the likely drainage structures I suggest potential forms this could take; a) the expansion of linked cavities (e.g. Cowton et al. 2013); b) an anastomosing or braided conduit system (e.g. Walder and Fowler, 1994; Catania & Paola, 2001) or; c) a narrow sheet flood (e.g. Brennand, 1994; Russell et al. 2007). In each of these scenarios, while water flows laterally out of the conduit down the pressure gradient during these high-pressure events, the dominant flow direction is still parallel to the main conduit. The occurrence and frequency of each of these scenarios is likely influenced by factors such as the magnitude of the pressure perturbation, the basal substrate, antecedent drainage conditions and the local hydraulic gradient.

Evidence suggests that cavities are constantly evolving in response to fluctuations in supraglacial meltwater inputs and the extent and capacity of conduits at the bed (Iken et al. 1983; Hoffman et al. 2011; Andrews et al. 2018). Therefore, it seems possible that those cavities surrounding dominant meltwater routes (whether this be an actual conduit or an efficient core) could act like 'overspill' storage when conduits are over-pressurised and water is forced out. These expanded cavities could then merge and develop into conduits in some places forming complex interconnections and patterns.

In areas of thicker sediment, pressure-driven drainage reorganisation may result in braiding (i.e. multiple anastomosing conduits) across the hydraulically connected distributed system (e.g. Clark and Walder, 1994; Catania and Paola, 2001). Indeed, water driven from the conduit into the hydraulically connected distributed system during discrete recharge from moulins has been recognised to form anastomosing conduits at the GrIS (Gulley et al. 2012). This is also consistent with the identification of braided meltwater channels at the base of tunnel valleys in the North Sea (Kirkham et al. 2020b) and the widespread presence of hummocks within / making up meltwater corridors across this study area whose size and shape have led them to be interpreted

as remnants of braided conduits and intervening bars (e.g. Dahlgren, 2013; Peterson et al. 2018).

A large, rapid input in surface meltwater without sufficient time for the subglacial drainage network to evolve, or input into a system that is already at its capacity, could cause the conduit to rupture resulting in temporary localised hydraulic jacking in the areas adjacent to the conduit (e.g. Brennand, 1994). In this way, water may flow over a broader area analogous to when a river bursts its banks during a flood event.

Finally, the possibility of lateral transient migration of an esker-forming conduit should also be considered here. Lateral migration may be in response to changes in ice thickness, subglacial topography and regional and local basal water pressure. This theory has been invoked to explain the formation of some tunnel valleys by the lateral merging of the flow routes of a series of smaller discrete drainage events over time (e.g. Jørgensen and Sandersen, 2006; Kehew et al. 2012; Beaud et al. 2018b) and may be a potential formation mechanism for meltwater corridors approximately an order of magnitude greater than the conduit itself. Nonetheless, lateral migration is more likely to occur in areas with a low hydraulic gradient (i.e. flatter parts of the bed, further inland from the ice sheet margin), which are characterised by quasi-stable conduit configurations and where the water is less restricted and can flow through multiple conduits, which alternate and migrate on multiday timescales (Vore et al. 2019). In contrast, the same research suggests that nearer the margin where the hydraulic gradient is steeper, conduits are relatively stable in space (Vore et al. 2019). This fits with esker sinuosity studies which demonstrate that eskers are often very straight (median sinuosity 1.04 on the Canadian Shield) with esker segments aligning over distances of 10s of km's (Storrar et al. 2014a). If the conduit migrated extensively in the marginal zone, we would expect to find more sinuous eskers or offset esker sections.
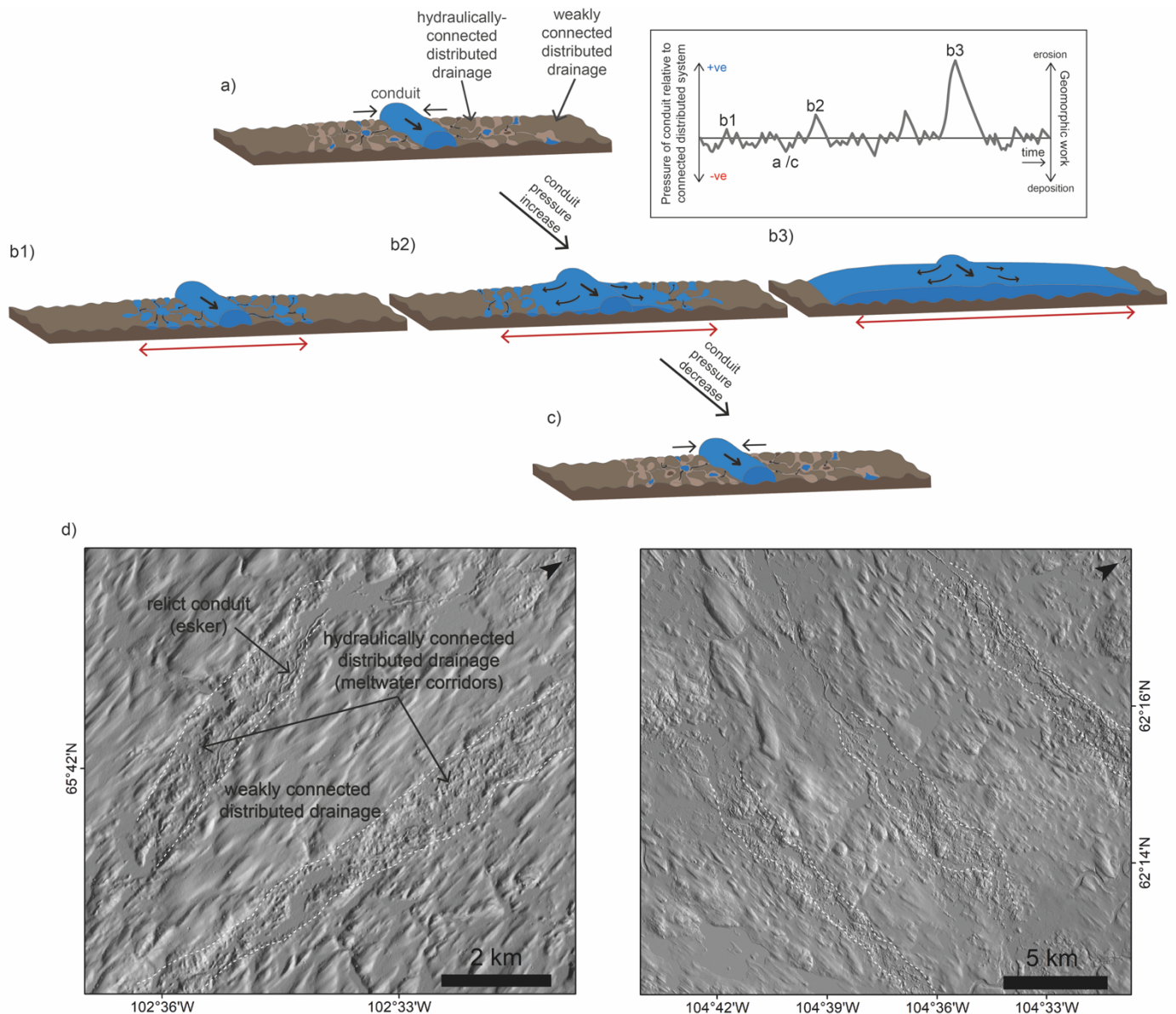
Figure 3.24 Effects of pressure perturbations on the hydraulic conductivity within the conduit connected distributed subsystem: (a) steady state – water is drawn in from across the connected distributed system into the conduit (low pressure) down the pressure gradient, geomorphic work is limited to the conduit, although there may be some lateral sapping (e.g. Boulton and Hindmarsh, 1987); (b) Pressure driven drainage reorganisation occurs as pressurised water is forced out of the conduit and into the surrounding hydraulically distributed drainage system. This may take the form of; a) a narrow sheet flood; b) an anastomosing conduit(s); c) cavity expansion and / or; d) an alternative drainage form. Geomorphic work (erosion and deposition) likely occurs during this phase; (c) Return to steady state as meltwater input decreases or the conduit expands to accommodate a sustained increase in input; (d) Proposed cumulative geomorphic imprint of the process over time, creating the meltwater corridors (white dashed lines) preserved on the landscape today. The inset in the

131

upper right corner demonstrates that pressure perturbations within the conduit fluctuate throughout the melt season and vary in size from regular diurnal fluctuations (e.g. b1) to irregular larger 'events' (e.g. b2 and b3), which may represent precipitation or supra/sub-glacial lake drainages.

I suggest that the model proposed here based on the idea of pressure driven drainage reorganisation taking a range of forms including enlarged linked cavities, anastomosing canal systems (likely within thicker sediments (Clark and Walder, 1994)) and narrow sheet floods, is the simplest explanation for the widespread presence of meltwater corridors. Lateral migration of an esker-forming conduit may occur within this model but alone does not provide such a neat fit because not all meltwater corridors contain evidence of channelised flow (e.g. an esker) and cannot explain the strong width range (Table 3.2). Additionally, the proposed model offers an overarching mechanism (i.e. pressure driven drainage reorganisation resulting in this range of forms) which can explain a variety of meltwater track and channel theories (e.g. St-Onge, 1984; Rampton, 2000; Utting et al. 2009).

3.4.4 Geomorphic work

To add further support for the proposed model and to better link it with the results of this chapter, it is important to consider *how* sediment is accessed, entrained and evacuated in order to generate geomorphic work across the spectrum (i.e. erosional to depositional) within the same integrated drainage system based on the mechanisms outlined above.

The subglacial hydrological system is responsible for transporting the majority of subglacial sediment (e.g. Walder and Fowler, 1994; Richards and Moore, 2003) and the relative amount is influenced by access to sediment (e.g. Willis et al. 1996; Burke et al. 2015) and subglacial water velocity (e.g. Walder and Fowler, 1994; Ng, 2000). Water flow through the distributed system is slow and inefficient with limited sediment mobilisation and restricted transport (e.g. Willis et al. 1990; Alley et al. 1997). As a result, during the 'steady state' phase (Fig. 3.24 a) the geomorphic work in the hydraulically connected distributed drainage system is likely limited by the small cross-

sectional area of passageways and slow water movement (Willis et al. 1990; Alley et al. 1997). However, there could be deformation of finer sediments into the central conduit contributing to gradual lateral channel growth over time; this has been invoked to explain steady state growth of tunnel valleys for example, (e.g. Boulton and Hindmarsh, 1987).

Faster and more turbulent water flow within conduits is more efficient at eroding and transporting sediment and this capability increases rapidly with increased discharge (Alley et al. 1997). However, conduits cover only a small fraction of the bed, which restricts their ability to erode and transport sediment across large areas (Alley et al. 2019). Thus, there is a need for an additional mechanism(s) to access surrounding sediments. Here, I focus on the pressure-driven interaction between the conduit and surrounding hydraulically connected distributed drainage zone (Fig. 3.24 b) as a mechanism to achieve this. This is supported by the wider glacio-fluvial literature, which suggests that pressure reversals which force water out and into the surrounding distributed drainage system increases access to sediment and increases water velocity and therefore its ability to carry sediment (e.g. Swift et al. 2002, 2005b; Gimbert et al. 2016; Delaney et al. 2018).

Subglacial fluvial sediment yield is observed to vary significantly over a range of daily to annual timescales (e.g. Collins, 1990; Bogen, 1996; Bartholomew et al. 2011) with the effects of large meltwater events such as lake drainages or even precipitation (Delaney et al. 2018)) superimposed on the quasi-regular diurnal to seasonal patterns. An extreme example of sediment removal and the resultant geomorphic work of a meltwater event is during the 1996 Icelandic jökulhlaup, when a subglacial flood evacuated sediment creating a large tunnel valley (Russell et al. 2007). Perhaps more in fitting with the scale of the mechanism proposed in this study, Livingstone et al. (2019) identified the drainage of an active subglacial lake < 10 km from the margin of the GrIS. This caused substantial erosion of sediments from beneath the ice sheet, which were deposited in the proglacial outwash plain. This provides an ideal site for detailed geophysical studies which could provide clear, in-situ links between subglacial lake drainage(s) and their geomorphic imprint and therefore act as modern analogue.

In the proposed model meltwater corridor relief across their width is caused by localised turbulent flow enhancing erosion (e.g. Rampton, 2000) during over-pressurisation events in the areas adjacent to the main conduit (Fig. 24 b). As stated above, over-pressurisation events may be driven by regular diurnal to seasonal variations in meltwater input and / or by short term events. The erosive ability of repeated seasonal flows is supported by the modelling work of Beaud et al, (2018) who demonstrate the effectiveness of high frequency, low magnitude events in generating sufficient erosion to from bedrock channels similar in dimension to tunnel valleys. Meltwater is transported to the bed by hundreds of moulins and crevasses and so along the length of a subglacial conduit, there are likely to be multiple meltwater input points. The combined effect of this is a highly dynamic environment even along a single conduit. This makes it likely that the conduit will experience periods of over-pressurisation (significant enough to contribute geomorphic work) variably along its length and supports the hypothesis that low frequency, high magnitude flood events are not required to form subglacial meltwater corridors. Additionally, a key piece of support for the model is that if we assume that a corridor represents a single maximum flow, meltwater corridor widths in this study (0.05 - 3.3 km (mean 0.9 km)) are comparable to measurements of pressure perturbations in contemporary alpine settings (~ 140 m (Hubbard et al. 1995; Gordon et al. 1998)) and modelled ice sheet settings (~ 2 km (Werder et al. 2013)), suggesting that geomorphic activity over that length scale is theoretically plausible.

Sedimentological evidence suggests that hummocks within the corridors occur as a result of both erosional and depositional processes. The proposed model can account for either process, with hummocks forming as a result of: (a) erosion by high energy turbulent water flow along conduits and across the hydraulically connected distributed system (e.g. Rampton, 2000; Peterson et al. 2018); or (b) deposition during waning stages of the flood within cavities either melted up into the overlying ice by turbulent floods (e.g. Utting et al. 2009), or minor conduits and linked cavities alongside the conduit (e.g. Brennand, 1994). Hummocks may also form as a combination of processes akin to the interpretation of triangular shaped landforms ('murtoos'), which are attributed to subglacial till transported by creep and subsequently eroded and shaped by subglacial meltwater (Mäkinen et al. 2017; Ojala et al. 2019).

To summarise the proposed model:

- During periods of over-pressurisation driven by variable surface meltwater inputs, the central conduit or efficient 'core' interacts with the surrounding subglacial hydrological system.
- Flow is no longer through a passive distributed drainage system but somewhere along a continuum from inefficient distributed to efficient channelised. This could theoretically take a range of forms including linked cavities, anastomosing canals, a narrow sheet flood or currently unrecognised drainage structures.
- This mechanism expands the existing drainage systems access to sediments and its ability to entrain them.
- The relative amount and direction (i.e. erosional or depositional) of geomorphic work likely depends on where on this continuum the drainage event occurs (table 3.2).

As meltwater corridors are likely a composite of multiple over-pressurisation events occurring at a range of magnitudes and frequencies, it is difficult to extract clear geomorphic observations (e.g. of braiding, undercutting etc.) to help confirm the occurrence or frequency of particular drainage modes across the hydraulically connected distributed drainage zone and confirm precise details as to exactly how sediment is accessed and entrained. Nonetheless, the proposed model provides the simplest explanation for the results of this study and is grounded by observations and modelling from contemporary ice sheet and alpine sites.

3.4.5 Interpreting a composite drainage signature

This work and earlier studies indicate that esker ridges can be superimposed on hummocks within meltwater corridors, but to date, there are no examples of hummocks overlying eskers (e.g. Peterson et al. 2018). This, along with the fact that eskers are situated in variable positions across meltwater corridors (i.e. rarely within the centre), suggests that the formation of eskers are separated in time from the meltwater corridors in which they often occur (e.g. Beaud et al. 2018a; Hewitt and Creyts, 2019; Livingstone et al. 2020) and supports the notion that palaeo-ice sheet

beds are a composite picture of geomorphic effects, combining different stages and potentially different subglacial drainage regimes (Greenwood et al. 2016).

Using an inland limit of 60 km for subglacial channelisation (e.g. Chandler et al. 2013), and minimum and maximum retreat rates in the study area (~ 230 m yr^{-1} - ~ 540 m yr^{-1}), the time likely spent beneath the channelised zone influenced by surface meltwater inputs can be estimated at between ~ 110 and ~ 260 years. Therefore, it is likely that meltwater corridors reflect the geomorphic work arising from repeated pressure perturbations in the ablation zone (i.e. sub-marginally) over 10s – 100s years. The most significant erosion likely occurred where fluctuating surface meltwater inputs were clustered (e.g. Alley et al. 2019) or where cumulative upstream drainage produced the threshold shear stresses required to erode and transport the substrate, which may have occurred upstream of the peak local meltwater input. While the location of surface meltwater drainage and discrete water input points (crevasses and moulins) are important controls on the distribution of subglacial drainage at the bed (e.g. Decaux et al. 2019), observations suggest that both supraglacial networks (e.g. Koziol et al. 2017) and moulin locations (e.g. Catania and Neumann, 2010) are relatively stable, at least over decadal timescales. Where changes in surface meltwater input areas are observed, this occurs over relatively short distances (~ 300 m^2) with the new routes likely occurring along the same drainage axes and thus not resulting in significant subglacial drainage system reorganisation (Decaux et al. 2019). This is consistent with geomorphological evidence, which reveals a coherent drainage network (Fig. 3.2) with individual meltwater corridors extending 100s km (Table 2.1).

In the proposed model, esker deposition is likely to occur at the margin and is therefore largely separated in time from the formation of the meltwater corridor. Eskers represent the final cast of the conduit in which they formed and thus the common occurrence of eskers within meltwater corridors (90 % of the time in this study), supports the idea that the different landforms are connected and likely part of the same system. There is increasing evidence to support the incremental formation of eskers at a retreating margin (Beaud et al. 2018; Hewitt and Creyts, 2019). Esker splays have similar widths and a close spatial association with meltwater corridors (e.g. transitions along flow or occurring within meltwater corridors). However, it is possible that some or even all of these features were deposited marginally (e.g. Hebrand and Amark,

1989) rather than in subglacial cavities. In fact, marginal deposition is supported by the fact that some of the esker splays align across flow with estimated ice sheet isochrones (Dyke et al. 2003). Nonetheless, it is difficult to constrain their formation from geomorphology alone and further work is needed to better understand how they fit within the propsed model.

3.4.6 Implications

Western sectors of the contemporary Greenland Ice Sheet are broadly analogous to the study area: both are underlain by resistant Precambrian Shield rocks and both experience(d) rapid retreat and high meltwater production rates. This is also similar to southern Sweden, which lay beneath the palaeo Scandinavian Ice Sheet, where similar geomorphic features to those described here, occur extensively (e.g. Peterson et al. 2017; Peterson and Johnson, 2018). This study therefore has potential implications for understanding of the impact of subglacial hydrology on overlying ice dynamics and ice flow regulation of past, current and future ice sheets.

The interaction between a subglacial conduit and the surrounding hydraulically connected distributed drainage system is believed to be widespread in contemporary glaciological settings (e.g. Hubbard et al. 1995; Gordon et al. 1996; Bartholomaus et al. 2008; Werder et al. 2013; Tedstone et al. 2014) and has been identified as key to understanding ice velocity variations and predicting future ice sheet mass loss (Davison et al. 2019). However, the true extent and influence of the hydraulically connected distributed drainage system beneath the Greenland Ice Sheet is unknown due to the challenge of observing contemporary subglacial environments. Palaeo-studies, such as this one, offer the potential to reveal new insights into the nature and configuration of the subglacial hydrological system at an ice sheet scale and potential quantification of how much of the bed and ice surface dynamics were affected by subglacial meltwater.

Based on the proposed model, the coverage of each drainage element across the bed of the Keewatin sector can be estimated. Conduits (i.e. eskers) cover ~ 0.5 % of the bed based on an average esker width of 100 m and spacing of 18.8 km (Storrar et al. 2014a). The coverage of conduits and the surrounding hydraulically connected

distributed drainage system (i.e. meltwater corridors) increases to an average of ~ 13 % using the average width and spacing of meltwater routes in this study, but could realistically vary between 5 % (lower quartile width and upper quartile spacing) and 36 % (upper quartile width and lower quartile spacing). This represents an area 25 times greater than the conduits (eskers) alone, but assumes that all meltwater routes were active at the same time. It is important to note that this remains a minimum estimate as not all meltwater activity will leave geomorphic evidence.

Based on the above and while a significant increase in the area of the bed influenced by surface meltwater inputs is proposed, these findings also fit with the hypothesis that the weakly-connected distributed system covers a large percentage of the subglacial bed (Hoffman et al. 2016). The results suggest that somewhere between 64 - 95 % of the bed existed within the weakly-connected distributed system where there are no traces of subglacial meltwater flow visible in the ArcticDEM. This finding is similar to Hodge (1979) who suggested that 90 % of the bed at the South Cascade Glacier in Washington was hydraulically isolated. Quantifying the relative coverage of the inactive hydraulically isolated regions of the bed and better understanding how they regulate the active drainage regions and modulate basal traction is likely to be important for understanding ice sheet dynamics (Hoffman et al. 2016).

In contemporary settings, the hydraulically connected distributed drainage system is strongly linked to surface meltwater inputs and conduit over pressurisation. The LIS is expected to have exhibited strong surface melting during the period of retreat over this area (estimated at -0.85 m yr^{-1} for 9 ka) with surface ablation accounting for much of this (Carlson et al. 2009). The widespread presence of meltwater corridors across Keewatin thus complements their interpretation and reveals a geomorphic signature of this interaction.

Finally, there are still large uncertainties as to how sediment is accessed by subglacial meltwater and transported to conduits (Alley et al. 2019). It is possible that the over pressurisation of conduits and their interaction with the surrounding hydraulically connected distributed drainage is a key driver of sediment erosion and entrainment within the ablation zone and may help address this question (Swift et al.

2002, 2005a, 2005b). As a result, conduits may be less sediment limited than previously thought and, much like the evolution of the subglacial drainage system (e.g. Schoof, 2010), rates of subglacial fluvial erosion may be strongly controlled by melt supply variability rather than the overall input of meltwater into the system.

3.5 Conclusions

The ArcticDEM was used here to identify and map all visible traces of subglacial meltwater drainage in the Keewatin sector of the former LIS. Meltwater features (meltwater tracks and meltwater channels) with widths in the order of 100's to 1000's m flanking or joining up intervening segments of esker ridges were common. These have previously been termed and described as different features. However, as they form part of the same integrated network and display similarities in spacing and morphometry, a collective grouping of these features under the term meltwater corridor is proposed (Table 3.2). Combing esker ridges and all varying geomorphic expressions of meltwater corridors within a single meltwater routes map has resulted in the creation of the first large-scale holistic map of subglacial meltwater drainage for this area.

Based on observations from this work and modern analogues, a new model is proposed which accounts for the formation and geomorphic variations of meltwater corridors. In this model, a principal conduit (i.e. the esker) interacts with the surrounding hydraulically connected distributed drainage network (i.e. the meltwater corridor) with the extent and intensity of this interaction, determined by the magnitude of water pressure fluctuations within the conduit. The geomorphic expression (i.e. net erosion or deposition), is likely governed by a combination of glaciological (i.e. relative water pressure fluctuation) and background controls (i.e. topography, basal substrate and geology). Eskers likely represent the final depositional imprint of channelised drainage within the large-scale meltwater routes network close to the ice margin, while meltwater corridors represent a composite imprint of drainage formed over 10s - 100s years. If the model is correct, the drainage footprint of the hydraulically connected distributed drainage system in this sector is 25 times greater than previously assumed from eskers alone, which only account for the central conduit.

Results suggest that the overall distribution and pattern of drainage is influenced by background topography, with greater relief resulting in denser channelised networks, possibly due to fragmentation of subglacial drainage around basal obstacles and the result of more spatially distributed meltwater delivery to the bed. Channelised drainage is relatively rare beneath palaeo ice streams, which instead favour distributed drainage configurations due to the lower ice surface slopes and subglacial hydraulic gradients, and likely also exhibit reduced landform preservation potential. The style of meltwater drainage may influence ice dynamics, with the high degree of channelisation observed in the region able to efficiently dewater the bed leading to slower ice-flow and limited ice stream activity.

Finally, the results suggest that conduit over pressurisation events and the subsequent connection between conduits and the surrounding hydraulically connected distributed drainage system may be important for understanding how sediment is accessed and entrained at the bed. While conduits (eskers) alone cover ~ 0.5 % of the bed, the connected distributed drainage system (meltwater corridors), cover 5 - 36 % of the bed, providing a greater area for sediment erosion and likely the high velocity flows required to do so.

Further research should focus on determining how common the proposed interaction between conduits and the surrounding distributed drainage system is beneath other palaeo and contemporary ice sheets and the controls governing its variability. It is possible that where less surface meltwater is delivered to the bed or ice-surface slopes are shallower for instance when the LIS was larger and the climate colder, the geomorphic expression will be less extensive and subtler. This is because conduits are less likely to evolve due to lower hydraulic gradients, and their interaction with the surrounding distributed system is limited because of invariant melt supply. Understanding where this interaction and signature occurs will help confirm or refute the proposed model, and develop understanding of how meltwater drainage evolves and influences ice dynamics and mass balance over long time-scales.

CHAPTER 4: MELTWATER CURIOS

In this chapter I explore a number of serendipitous findings discovered during the mapping of visible meltwater traces (Chapter 3), which have the potential to provide new insight into the palaeo-subglacial hydrological drainage structure and the processes of meltwater landform formation. The ideas presented within this chapter are based on initial exploratory observations from limited sample sites and are therefore understandably speculative in places and require further work before any robust conclusions can be made. While they remain tentative, they do support the concept of a complex mosaic of conditions at the ice sheet bed, which are likely highly variable over time and space. It is likely that the presence / absence of water influences how the bed and ice interact and that this is recorded in the landform record. Results here therefore emphasise the importance of recognising these landform associations and similarities / differences in expression and attempting to link these to the varying processes, which formed them.

4.1 ESKER ASSEMBLAGES ACROSS KEEWATIN

Glaciofluvial sediment deposition can occur in a range of environments including; (a) subglacial conduits; (b) open tunnels (i.e. where a subglacial conduit is at atmospheric pressure near the ice margin); (c) englacially; (d) supraglacially; or beyond the margin into; (e) standing water (subaqueous) or (f) onto land (subaerial). Recent physical modelling supports the time transgressive formation of eskers – i.e. deposition of repeated short segments (say tens to hundreds of metres or more) – behind a retreating margin (e.g. Beaud et al. 2018a; Hewitt and Creyts, 2019). The basic premise of this is that pressurised subglacial water transports sediment towards the margin within conduits where it is subsequently deposited due to a reduction in sediment carrying capacity, likely as a result of reduced pressurisation closer to the margin or by lateral flow expansion and reduced energy (e.g. Banerjee and McDonald, 1975; Warren and Ashley, 1994; Brennand, 2000; Benn and Evans, 2010). Deposition does not always occur as a simple esker ridge and additional associated assemblages have been recognised in detailed small-scale investigations of individual ridges (e.g. Gorrell and Shaw, 1991; Warren and Ashley, 1994; Mäkinen, 2003; Ahokangas and

Mäkinen, 2014; Perkins et al. 2016; Storrar et al. 2020). However, their variation in expression and overall distribution at a large-scale has yet to be addressed.

4.1.1 Published findings (Livingstone et al. 2020)

Multiple aligned 'chains' of esker beads were initially identified in the area either side of Chesterfield Inlet to the west of Hudson Bay. Beads were semi-regularly spaced both along flow and across flow. A close association (1-to-1) was noted between individual beads and v-shaped ridges, interpreted as De Geer moraines, with the bead at the head of the 'v' and the ridges stretching ~ 1 - 2 km either side of it (Livingstone et al. 2020). The chains of beads were hypothesised to have been deposited at the grounding line of a calving ice sheet margin on quasi-annual timescales (Fig. 4.1). Ice marginal formation of esker beads (e.g. De Geer, 1897, 1910; Banerjee and McDonald, 1975; Rust and Romanelli, 1975; Cheel and Rust, 1986; Mäkinen, 2003) was favoured over a subglacial origin (e.g. Gorrell and Shaw, 1991; Brennand, 1994) based on morphological observations. Specifically: (a) some of the beads have a flat top (indicating sedimentation up to the water level); (b) fan-shaped beads were orientated downstream rather than transverse to flow; (c) beads graded into ridges in the up-flow direction; (d) beads were strongly aligned across-flow; and (e) beads exhibited an approximately 1-to-1 association with de Geer moraines (i.e. v-shaped ridges), which indicate formation at the mouth of a subglacial conduit within an embayment (e.g. Hoppe, 1957; Strömberg, 1981; Lindén and Möller, 2005; Bouvier et al. 2015; Dowling et al. 2016; Livingstone et al. 2020). This resulted in the overarching hypothesis that deposition as a series of beads in this area occurred as a result of limited sediment fluxes such that ice sheet margin retreat outpaced sediment backfilling prohibiting the formation of a continuous esker ridge (Livingstone et al. 2020). The applicability of this model will now be tested and discussed in this section using a larger sample size from the Keewatin area.

4.1.2 Methods

The hypothesis presented in Livingstone et al. (2020) was tested by extending the mapping of esker assemblages and further differentiating between different expressions; classifying features as; (a) esker bead; (b) esker fan or; (c) esker net

(Table 4.1). Manual mapping was undertaken in ArcGIS, marking each individual feature as a point and categorising it as one of the above features. Features were distinguished based on morphology (size and shape) with beads typically small, round hill-like features, fans more wedge-shaped and larger and nets typically < 1 km anastomosing sections of esker ridges. Individual beads mapped as polygons in Livingstone et al. (2020) were re-mapped as points to ensure standard mapping throughout and to re-classify any beads that should be categorised as a (small) fan. To explore potential controls on the formation and distribution of these esker assemblages, their distribution was then compared to background controls that may have influenced their depositional environment and thus their likelihood of formation and resulting morphological expression.
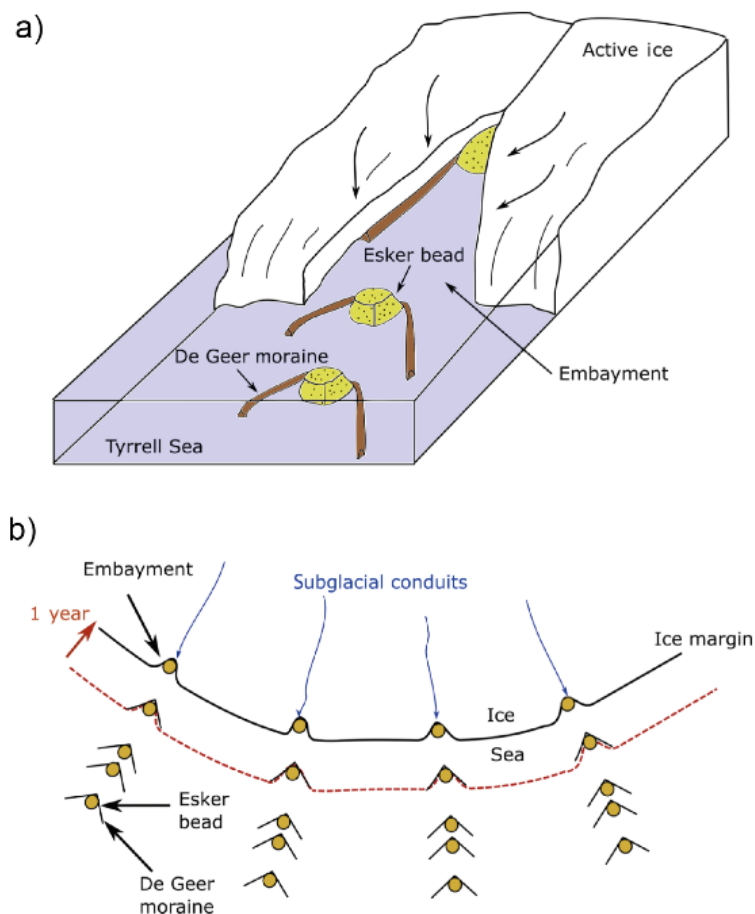
Figure 4.1 Proposed model of quasi-annual subaqueous esker bead and de Geer formation in embayments at marine grounding lines (Livingstone et al. 2020). De Geer formation likely occurred during winter ice re-advance while beads were likely deposited prior to the onset or

after summer retreat from the moraine. The annual deposition of esker beads at the mouth of a retreating ice front creates a 'chain' along flow with spacing affected by the rate of retreat. There is a remarkable consistency in the lateral spacing of the beaded chains (~ 6 – 10 km) which is likely to be a 'true' representation of subglacial conduit spacing, at least near the inferred palaeo-ice margin. The location of the study area in Livingstone et al. (2020) is identified in figure 4.3a.

4.1.3 Observations and interpretations

Mapping across the wider Keewatin area revealed the pervasive presence of esker beads, fans and nets in a range of different settings. A summary of observations of each feature type and existing interpretations of depositional settings from the literature are presented in Table 4.1.
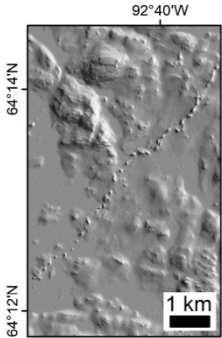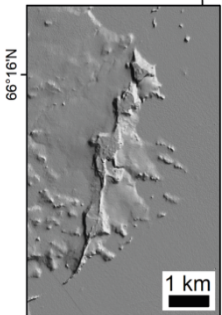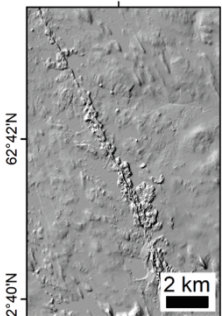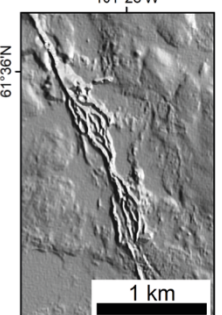
Within the study area, esker beads (n = 11,038) varied in size and shape but were typically identified as distinct mound-like hills. Esker beads were differentiated from fans largely based on size (e.g. Fig. 4.2b) and to some degree on shape with beads typically more rounded than the small fans which exhibited a more wedge-like to fan shaped geometry. Esker beads and fans were often clearly associated with one another – often transitioning between types or occurring within close proximity (e.g. Fig. 4.2b). Formation theories for both beads and terminal fans typically invoke ice marginal deposition into standing water (e.g. De Geer, 1897, 1910; Banerjee and McDonald, 1975; Rust and Romanelli, 1975; Sharpe, 1988; Gorrell and Shaw, 1991; Brennand, 2000) or on land (e.g. Hebrand and Åmark, 1989). Beads - and in many cases terminal fans - were repeated along-flow forming series of successive features spaced at quasi-regular intervals along the same esker (e.g. Fig. 4.2a-c).

Within this study, 'lateral fans' a subset of the features classified as fans, and comprising lateral fan-shaped sediments either side of an esker ridge and 'pads' or beads of sediment attached by small ridges were also identified (e.g. Gorrell and Shaw, 1991; Cummings et al. 2011a, 2011b; Prowse, 2017). A variety of depositional settings have been invoked for these fan features including sedimentation into subglacial cavities alongside a conduit (e.g. Gorrell and Shaw, 1991; Brennand, 1994),

proglacially at the mouth of conduits as a broad fan that prograded into standing water (e.g. Powell, 1990; Hoyal et al. 2003; Cummings et al. 2011b), or supraglacially in a manner analogous to river overbank splay (e.g. Prowse, 2017). Lateral fans represented < 5 % of all fans within this study, and exhibited significant morphological variations. There appears to be a spatial coincidence between lateral fans and esker nets (see below), with most lateral fans forming within the W / SW sector of the study area and often flanking, or occurring alternately along-flow with nets.

Esker nets (n = 962) are anastomosing sections of eskers with two of more ridges (Table 4.1). These typically existed here as short sections, often re-joining down-flow into a single esker ridge and often repeating along the same esker (e.g. Fig. 4.2d). In some places, esker nets appeared to transition into fans at their down-flow end while in others, they appeared to be flat-topped or partially buried and often related to what looked like additional marginal outwash (e.g. Fig. 4.2i). Esker nets commonly occurred at the intersection between two esker ridges (i.e. as a tributary esker joined a 'trunk' esker) (Fig. 4.2g and h).

Table 4.1. Observations and interpretations of esker assemblages.

Landform	Example	Observations	Proposed depositional environment
Esker beads	92°40'W, 64°14'N, 64°12'N, 1 km	- 10's m in diameter - vary in shape from distinct, mound-like hills to wedge and fan-shaped geometries - flat-topped in places - form long chains - can merge into ridges	*Subglacial:* synchronous deposition into conduit adjacent cavities during periods of ice-bed separation in response to high meltwater inputs (Gorrell and Shaw, 1991; Brennand, 1994) *Marginal:* time-transgressive deposition at a conduit mouth in proglacial lacustrine or marine (e.g. de Geer, 1897, 1910, Banerjee and McDonald, 1975; Hebrand and Åmark, 1989; Ashley et al. 1991; Livingstone et al. 2020) or terrestrial setting (Hebrand and Åmark, 1989)
Esker fans (terminal)	97°50'W, 66°16'N, 1 km	- variable size from ~ 100 m to ~ 3 km at widest point - vary in shape including large, flat-topped approx. triangular outwash fans to more irregular mounds - often repeated - can merge along-flow	*Marginal:* deposition onto land or into standing water, recording ice frontal or grounding line sedimentation (e.g. Banerjee and McDonald, 1975; Gorrell and Shaw, 1991; Brennand, 2000)
Esker fans (lateral)	105°30'W, 62°42'N, 62°40'N, 2 km	- typically an order of magnitude wider than the esker ridge - gently sloping outwards - typically flat-topped surface	*Subglacial:* high intensity flow and localised hydraulic jacking (Brennand, 1994) *Marginal:* subaqueous outwash (e.g. Powell, 1990; Hoyal et al. 2003) *Supraglacial:* deposition on adjacent glacier ice akin to overbank splay (e.g. Prowse, 2017)
Esker nets	101°28'W, 61°36'N, 1 km	- typically < 1km - anastomosing sections of esker ridges (mostly > 2) - can re-join downstream into a single esker ridge or merge into fan like deposits	*Subglacial:* sediment choking (e.g. Shilts et al. 1987; Menzies and Shilts, 1996), flow splitting in ascending reaches (e.g. Shreve, 1985) or high-pressure meltwater leakage event (e.g. Gorrell and Shaw, 1991; Brennand, 1994) *Marginal:* high concentration of meltwater and sediment on a flat bed and an evolving drainage system (Storrar et al. 2020). *Supraglacial:* sedimentation within shifting abandoned channels (e.g. Bennett and Glasser, 1996; Bennett et al. 2009)

Esker nets have been hypothesised to form in a range of environments including; (a) supraglacially (e.g. Bennett and Glasser, 1996; Huddart et al. 1999; Bennett et al. 2009); (b) marginally (e.g. Storrar et al. 2020) or; (c) subglacially (e.g. Brennand, 1994). Subglacial formation theories have invoked high flow events, which force open minor channels surrounding the main conduit (Brennand, 1994), or are associated with high sediment loads that choke the main conduit causing additional conduits (i.e. eskers) to form for meltwater to divert around the blockage (e.g. Shilts et al. 1987; Menzies and Shilts, 1996). Shreve (1985) suggested that multi-ridge eskers may form subglacially as a result of pseudo-flow separation in response to ascending flow paths where water is focussed at low points. While Shreve (1985) postulate that this could occur multiple times, thus generating a series of parallel ridge, it is unable to explain complex anabranching patterns. Finally, marginal formation of complex eskers (not dissimilar to the esker nets within this study) has been recently identified by Storrar et al. (2020) in Iceland and Svalbard. Their formation has been linked to a range of ice-marginal processes such as outburst floods, detachment of dead ice, deposition in association with outwash heads or channel abandonment related to changes in base level as a consequence of proglacial channel evolution (Storrar et al. 2020). While they acknowledge a degree of chaos is required in determining where a complex esker will form, they suggest this is more likely in parts of the drainage system with large volumes of meltwater and sediment.

At a number of locations it was somewhat difficult to classify an assemblage as one specific feature. For example, there were cases where esker nets appeared to be flanked by wider sediments and examples where they seemed to transition downflow into terminal fans. This raises the question as to whether spatially coexisting features were deposited synchronously or represent multiple events separated in time and depositional setting (e.g. Ravier et al. 2014).
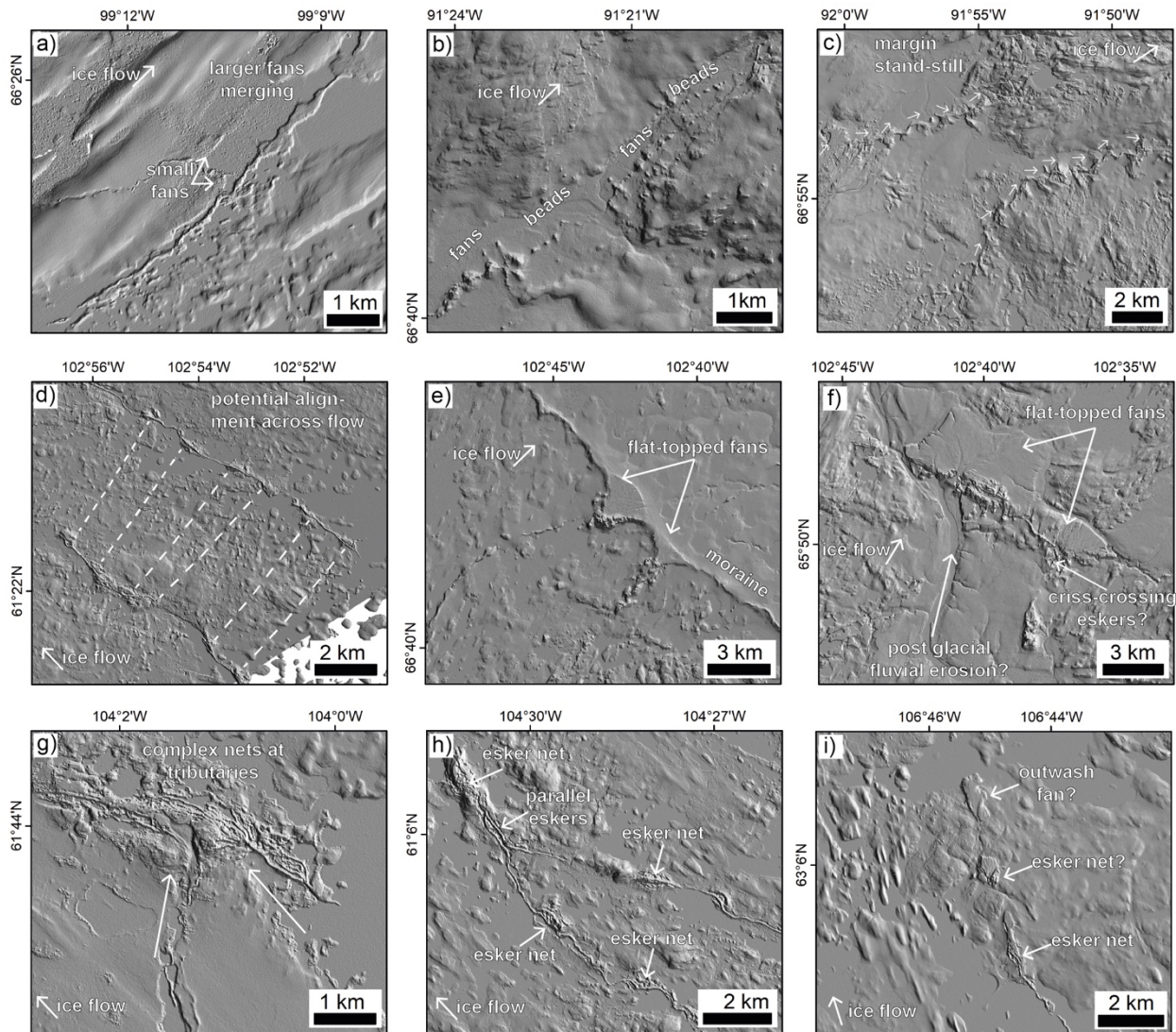
Figure 4.2 Observations of esker assemblages; (a) co-occurrence of small and larger fans, which often merge down-flow (i.e. not always distinct features); (b) transition along-flow from fans to beads; (c) migrating portal at a margin stand-still resulting in multiple fans with slightly different orientations; (d) adjacent esker systems whose nets potentially align across flow (lines drawn that link them); (e and f) large, flat-topped fans at moraine positions; (g) esker nets where an esker tributary joins a trunk esker; (h) eskers joining and aligned parallel prior to net formation and; (i) esker nets with varying definition (e.g. flat topped, transitioning into fans).

Mapping of esker nets, fans and beads revealed differences in their spatial distribution (Fig. 4.3). To investigate potential explanations for this, landform types were compared to a range of controls:

148

149
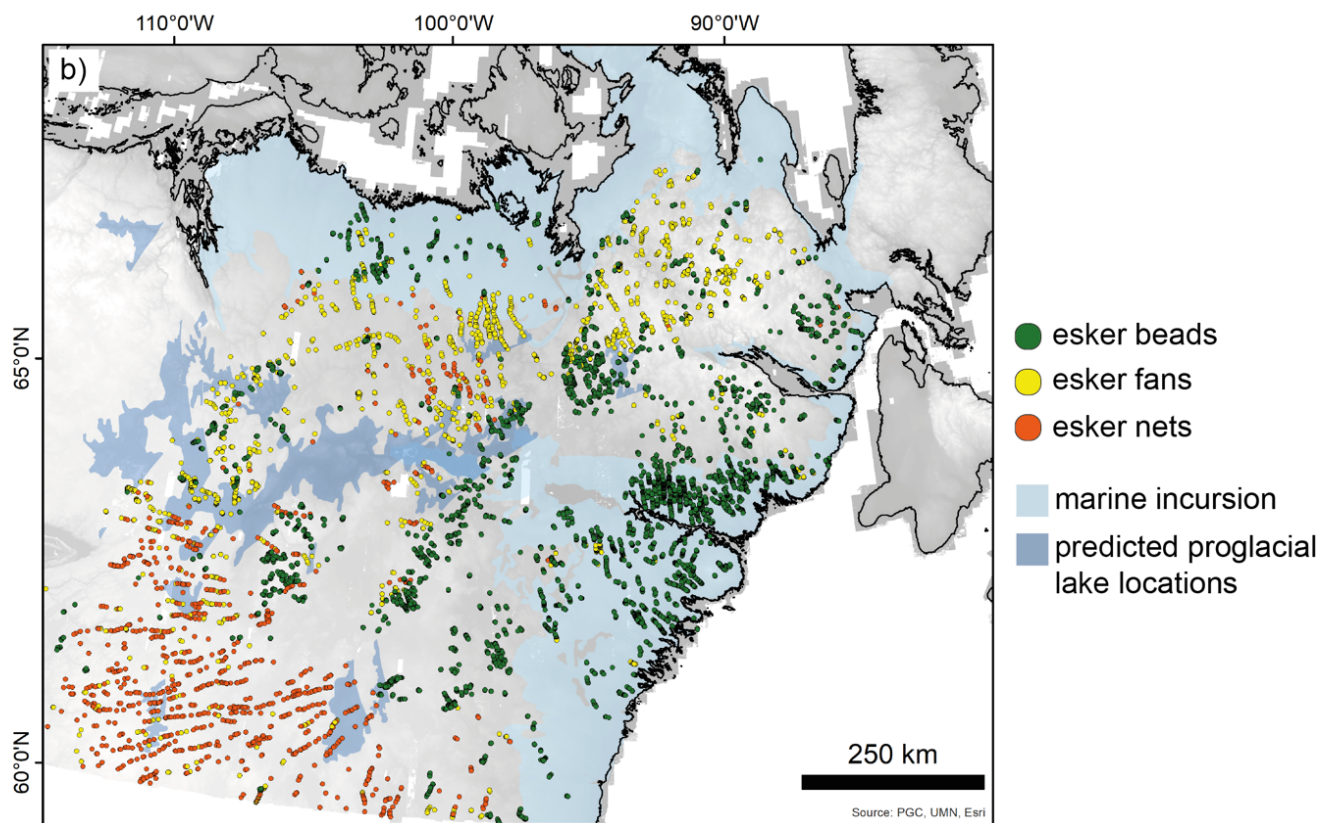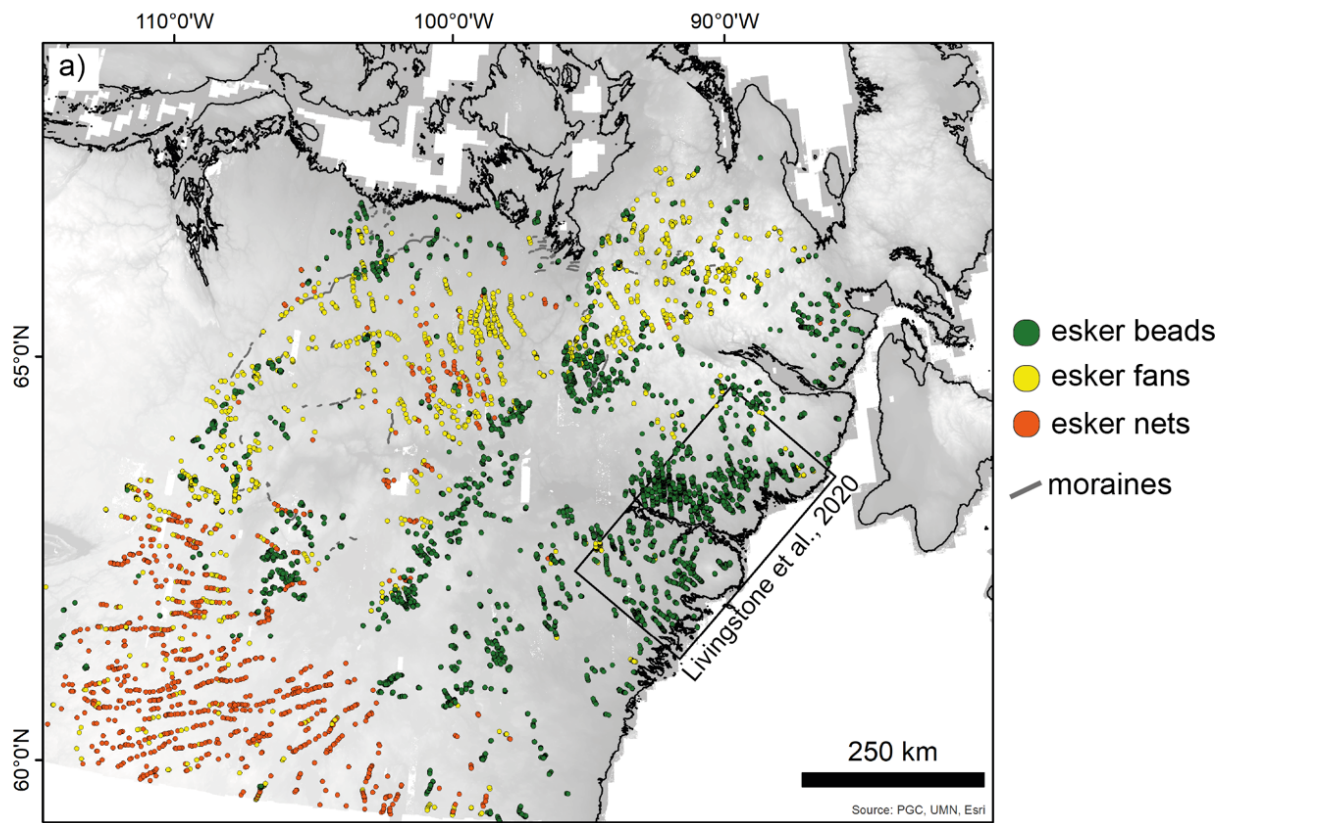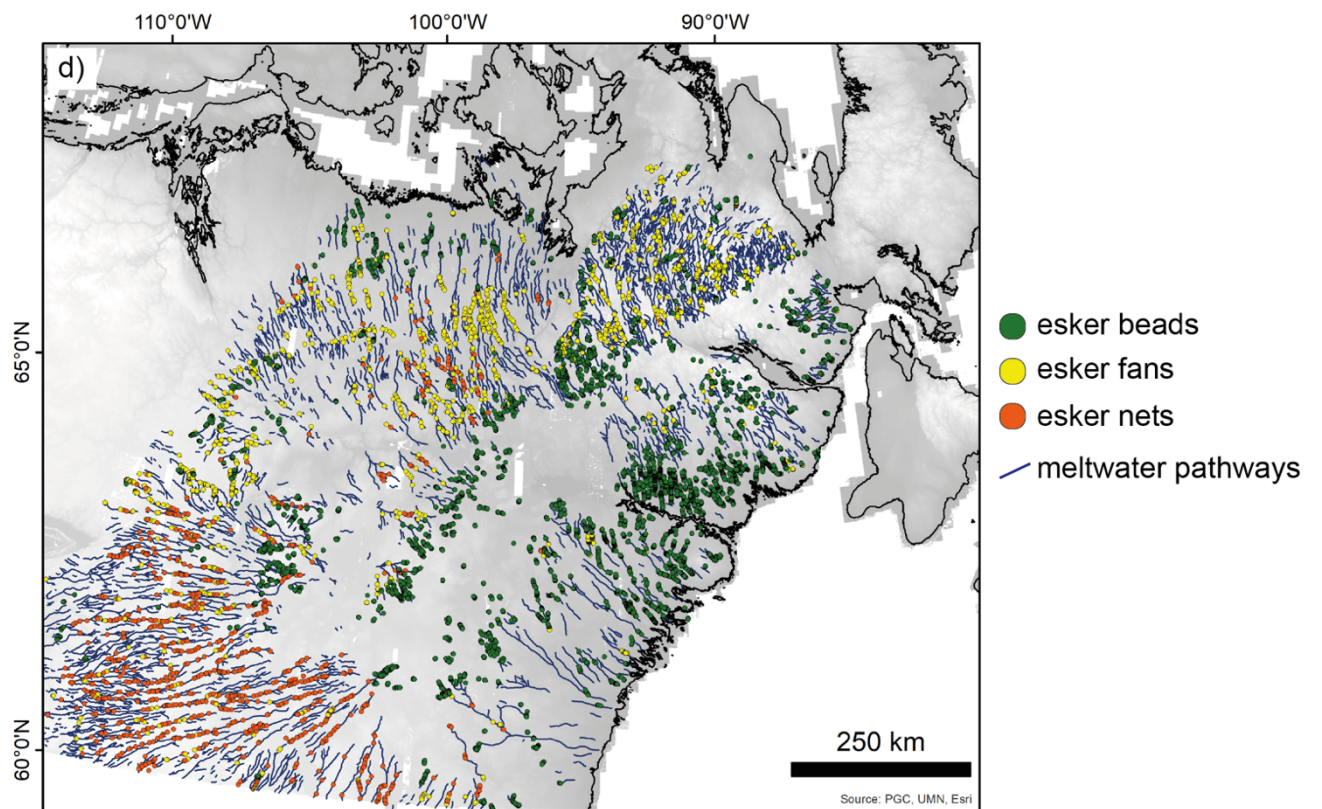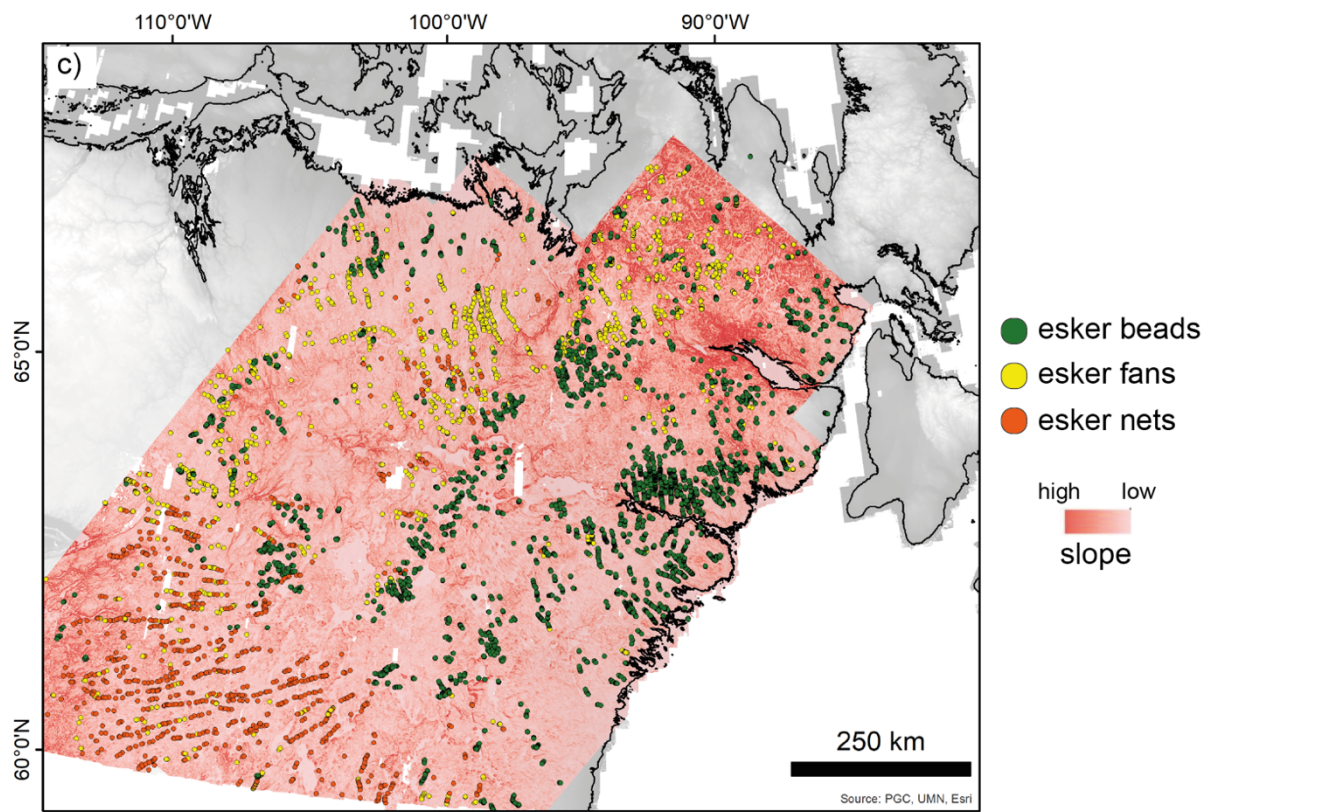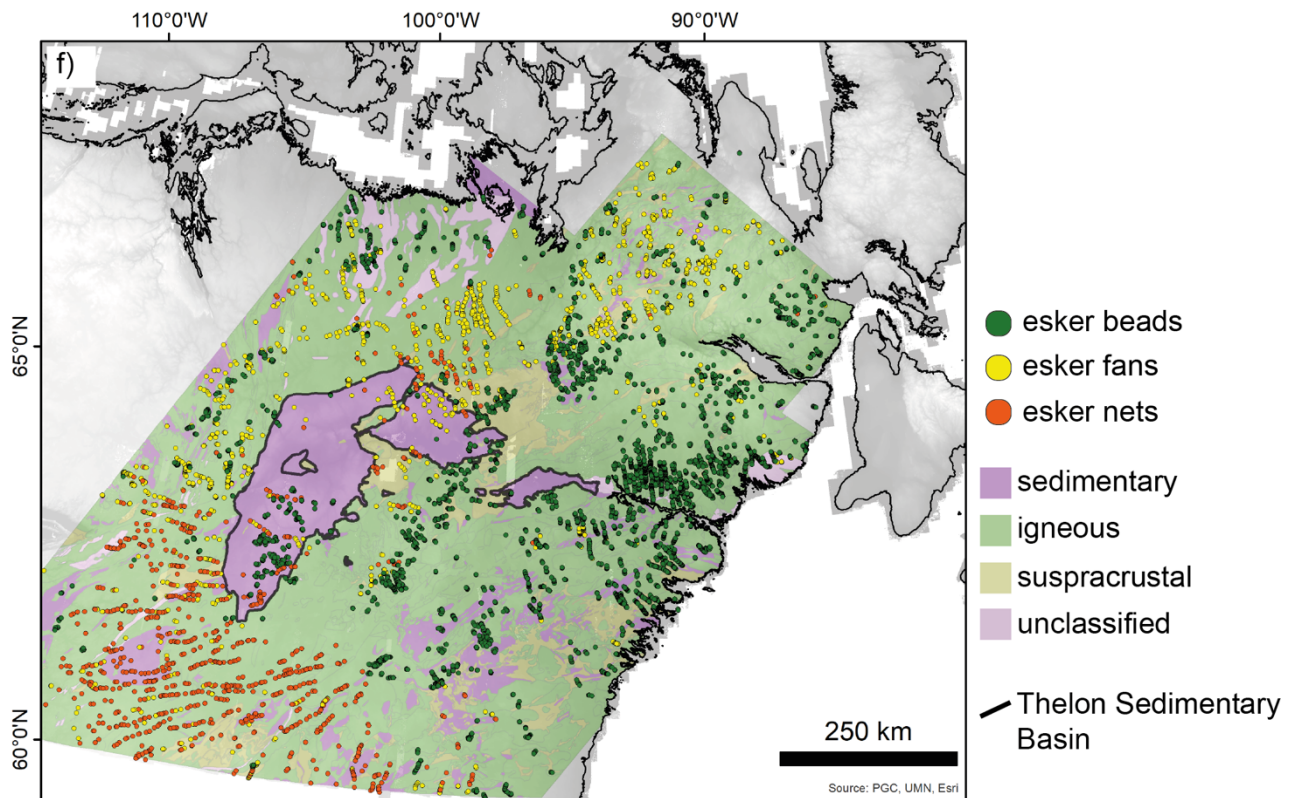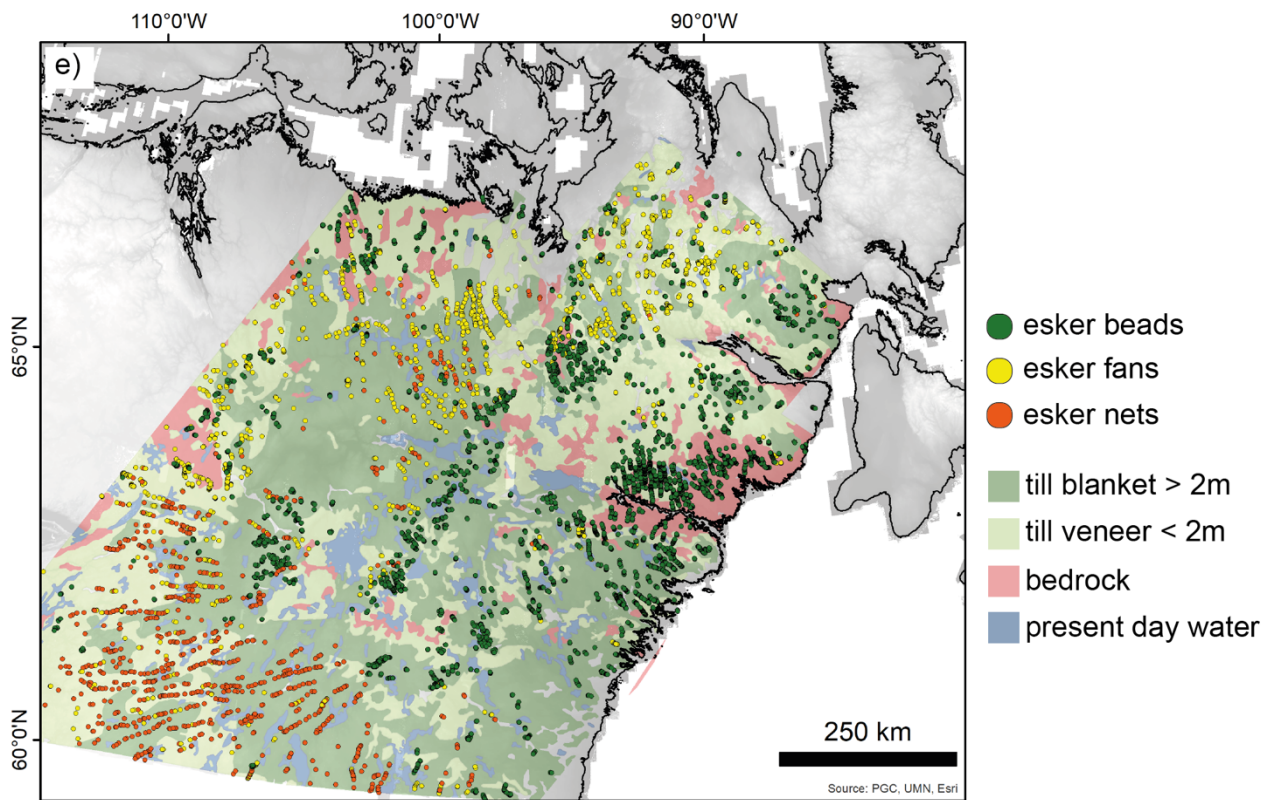
Figure 4.3 (above) Esker beads (green), fans (yellow) and nets (orange) across the study area (a). Distribution of features compared to; (b) marine incursion (Prest et al. 1968) and predicted proglacial lakes (Stokes and Clark, 2003); (c) topographic slope (see page 93 for explanation of how this was calculated); (d) mapped meltwater pathways (Chapter 3); (e) surface substrates (Fulton, 1995) and; (f) bed geology (Wheeler et al. 1996).

a) Former marine incursion and proglacial lakes

Around 50 % of the esker beads were found to occur in areas formerly below sea-level (Fig. 4.3b). In these locations, esker beads were the most common meltwater landform type and the ridge segments that did occur were commonly shorter and narrower than elsewhere and showed evidence of forming from the along-flow merging of multiple beads. While the presence of standing water at the conduit mouth is not a necessity for esker formation – as is indicated by the widespread occurrence of eskers and associated assemblages outside of marine or lacustrine environments (Fig. 4.3b) – chances of preservation are increased here owing to the low energy environment and lack of migrating, braided proglacial streams, which may subsequently erode the esker deposit (e.g. Banerjee and McDonald, 1975; Storrar et al. 2020). This may be particularly important for the preservation of small esker beads. There does not appear to be a clear association between any particular landform and the presence of (predicted) proglacial lakes (Fig. 4.3b) and in fact landforms seem largely absent from parts of the predicted lakes in the west.

b) Local topography

The distribution of features was compared to topographic slope – calculated at 500 m resolution. This suggested that most of the esker assemblages were deposited on relatively flat sections of bed (Fig. 4.3c). The NE sector of the study area exhibits the roughest terrain and here, the dominant features mapped were terminal fans. However, it was also noted that glaciofluvial outwash was common in the area, often constrained within well-developed systems of meltwater corridors, which could have buried eskers and associated deposits preventing their detection.

c) *Relation to meltwater pathways*

The majority of meltwater pathways exhibit one or a range of nets, fans and beads along their course (Fig. 4.3d). Fans and nets most commonly occur as part of the more developed meltwater system while esker beads tend to form further in towards the ice sheet divide than any other subglacial meltwater landform and often at the head of more developed meltwater corridors (Fig. 4.3d). Roughly 6 % of all esker beads occurred within the central 6.5 ka isochrone i.e. during the last stages of deglaciation within this area, with ~ 27 % within the 7 ka, although some of these also coincided with marine inundation areas in the east and south-east.

d) *Basal substrate and geology*

To identify the role of geology in controlling the distribution and expression of complex esker assemblages, they were compared to a surficial deposit and thickness map (Fulton, 1995) (Fig. 4.3e) and a basal geology map (Wheeler et al. 1996) (Fig. 4.3f). There was no clear large-scale spatial coincidence between the esker assemblages and basal substrate or geology.
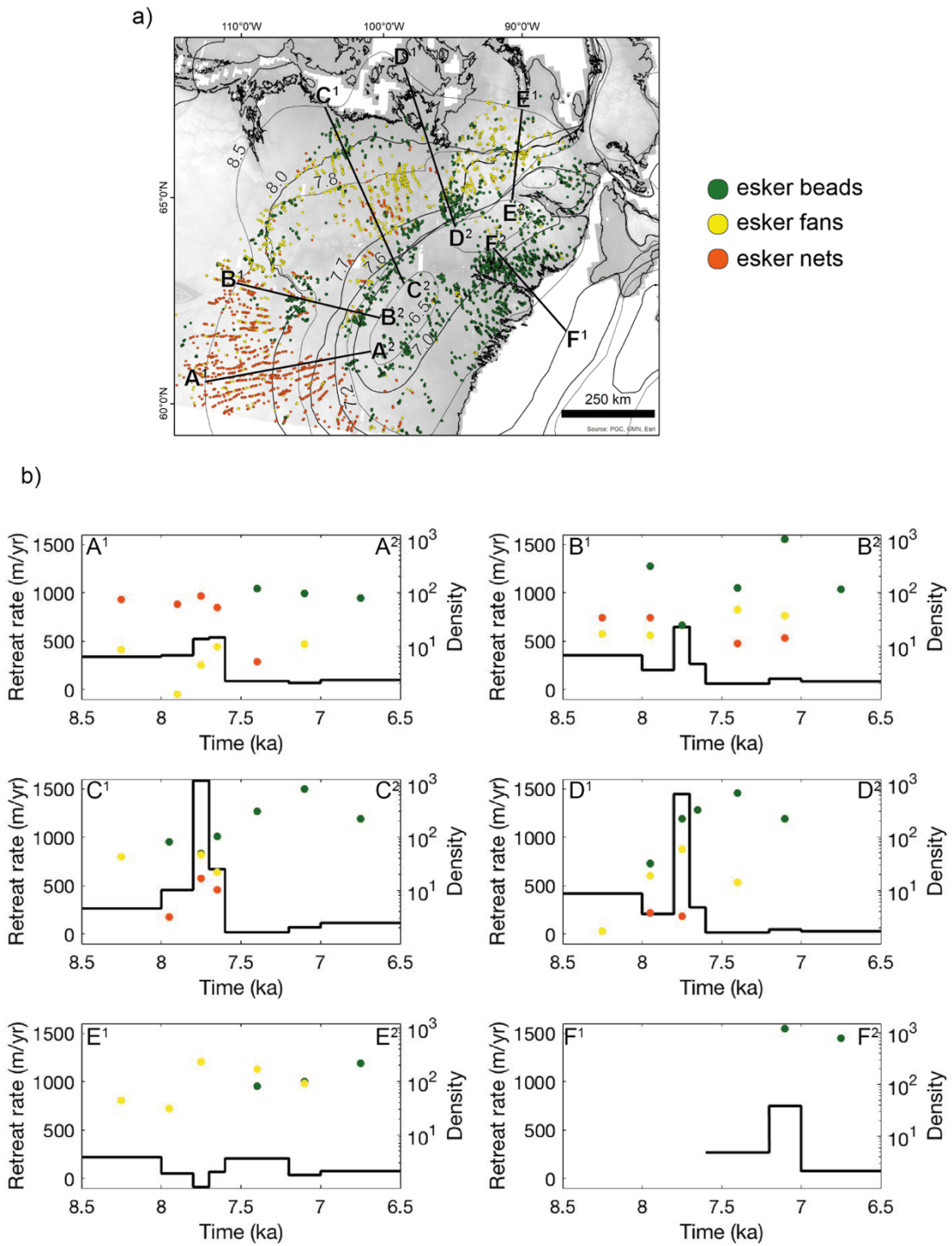
Figure 4.4 Ice sheet retreat rates for transects (a) approximately evenly spaced normal to retreat isochrons (Dalton et al. 2020) around the Keewatin ice sheet divide compared to local (within ~ 100 km) esker assemblage density.

e) Ice sheet retreat rates

The density of esker assemblages was compared to retreat rates along 6 profiles around the ice sheet (Fig. 4.4). These profiles showed clear variation in retreat rate around the ice divide but less obvious trends in the density of esker assemblages associated with these. The highest density of esker beads occurred at ~ 7 ka in the north and east and slightly earlier in the west / north-west, and tended to be associated with a slower period of retreat except for in transect F. Esker fans occur in high density in the north (transect E) in association with slow retreat rates (Fig.4.4), which are likely to have created numerous closely spaced fans (Fig. 4.2c). However, this pattern was not apparent in the other transects. Although the largest fans are observed to occur at known stand-still positions (e.g. Fig. 4.2e), with their glaciofluvial material contributing to the construction of large arcuate moraines, this is difficult to identify from the profiles (~ 8 ka in transect C) as it is likely the stand-still generated one large fan rather than several smaller ones thus contributing to a lower density. Caution must be taken when interpreting these results as the retreat rate calculated between each isochrone is an average and it is not known whether there was steady retreat throughout the period or more sporadic behaviour, e.g. rapid retreat followed by a period of slow retreat / a stand-still.

4.1.4 Discussion

The model proposed in Livingstone et al. (2020) links esker deposition at the margin to; (a) sediment availability and; (b) margin retreat rate, which together influence the relative amount of backfilling and thus whether the resultant esker forms a continuous ridge or fragmented ridge segments or beads / fans with gaps (e.g. Fig. 4.5). This idea is explored further here by investigating whether different esker assemblages form preferentially under particular geologic contexts (e.g. substrate thickness, basal geology etc.) or glaciological (e.g. ice sheet retreat rates, likely magnitude and duration of surface meltwater inputs and subsequent access and entrainment of sediments, thermal regime etc.) conditions. Extending from the ideas in Livingstone et al. (2020), the hypothesis here is that in an idealised scenario:

1) *Esker beads form preferentially in areas with limited sediment availability and rapid retreat rates, which results in low backfilling.*

2) *Esker ridges form in areas where the match between sediment availability and retreat rate is intermediate between 1) and 3).*

3) *Large, terminal esker fans form in areas with abundant sediment availability and slow to no margin retreat.*

These ideas will be tested here by discussing the general settings of esker beads and fans and the likely processes influencing them. As it was noted above that 50 % of esker beads and 80 % of esker fans occurred in subaerial (above inferred palaeo-water level) settings, the two scenarios (marine/lacustrine vs subaerial) will not be treated separately in the initial discussion but examples from each will be used later.

4.1.4.1   Esker beads

Livingstone et al. (2020) hypothesise that beads occur commonly within their study area (Fig. 4.3a) as a result of limited sediment availability and rapid retreat rates. This is supported by observations that the bed is predominantly bedrock and till veneer (< 2 m) (Fig. 4.3f) and indicators of rapid deglaciation up to and > 400 m/yr from annually spaced De Geer moraines (Livingstone et al. 2020) and ice sheet retreat isochrones produced from an updated radiocarbon inventory (Dalton et al. 2020: Fig. 4.4 – transect F).

I show that at a larger-scale esker beads form at a similar time during late stage deglaciation (~ 7 ka) but are not consistently associated with marine inundation or rapid retreat rates. This therefore requires other potential controls on formation to be considered. Esker beads occur commonly within the inner zone of the Keewatin sector, which is characterised by an absence of eskers and ribbed moraine and generally low occurrence of streamlined features with small, low rounded hummocks covering much of the bed (Aylsworth and Shilts, 1989). Ice flow is expected to have been slow, with low rates of erosion and sediment entrainment occurring beneath the small remnant ice cap (Aylsworth and Shilts, 1989). Atmospheric temperatures

remained high during final deglaciation (relatively consistent between 10 ka and 7 ka) (Shakun et al. 2012) so it is likely that surface melt continued to occur. However, as with contemporary ice caps (Barnes and Devon) and glaciers in the Canadian Arctic, the ice bed is likely to have become polythermal (Blatter, 1987; Copland and Sharp, 2001; Gilbert et al. 2016) instead of predominantly warm based as the ice thinned and slowed. This may have influenced the surface and subglacial hydrology (e.g. Boon and Sharp, 2003; Ryser et al. 2013; Yang et al. 2019).

In particular, slow flow and low strain rates will likely limit the potential for crevassing and hydrofracture (e.g. Chandler et al. 2013). This is supported by recent finding by Yang et al. (2019) from the Devon and Barnes Ice Caps (remnant LIS) that moulins are typically restricted to very marginal areas (~ 5 km), suggesting that only a relatively small area of the bed is hydraulically connected with the surface. Furthermore, Boon and Sharp (2003) suggest that subglacial drainage under polythermal glaciers may be hindered by re-freezing and that the formation of sustained surface-to-bed connections is likely to be initiated by a number of preliminary drainage events where re-refreezing results in ice warming and a positive feedback that favours the formation of permanent routes during subsequent drainage events. Therefore, the difference in thermal regime could have had an impact on; (a) the location of surface meltwater inputs which are likely restricted to marginal regions (< 5 km (Yang et al. 2019)); (b) the frequency and magnitude of meltwater at the bed as a result of the lower chance of surface meltwater (organised into discrete channels) intersecting the limited number of moulins, potential re-freezing and lower basal melt production and; (c) the development of widespread conduit-hydraulically connected distributed drainage.

Furthermore, at a large scale, there is a less clear relationship between esker assemblages and basal substrate and geology with beads and fans occurring variably over till blanket, till veneer and bedrock. However, it is commonly accepted that for typical conditions during ice sheet retreat, where there is an abundance of surface meltwater accessing the bed in the summer, sediment transport within subglacial hydrological systems is not limited by the ability of the water to carry sediment but by its ability to access and entrain it (e.g. Gimbert et al. 2016). Thus, the overall occurrence of sediment (often > 2 m till (Fig. 4.2h)), is likely less important than the

magnitude and duration of subglacial flow and the frequency of connections between the conduit and surrounding hydraulically-connected distributed drainage system (see model in Chapter 3), which determines how much sediment can actually be entrained. The areal extent of this effect has been observed to vary in width from ~ 140 m in alpine glacier settings (Hubbard et al. 1995) to a few kilometres in ice sheet settings (e.g. Werder et al. 2013) with modelling predicting up to 10 km (Hewitt, 2011). This highlights the need to consider all parts of the system including glaciofluvial erosion, transport and deposition.

Combined, I hypothesise that a shrinking ice sheet resulted in short subglacial conduits with limited catchment areas formed close to the ice sheet margin with limited access to sediments and much of the water present at the surface flowing off at the margin instead of through the glacier to the bed. This would have limited the potential for meltwater corridors to form and thus for meltwater to access and entrain sediment to backfill conduits.
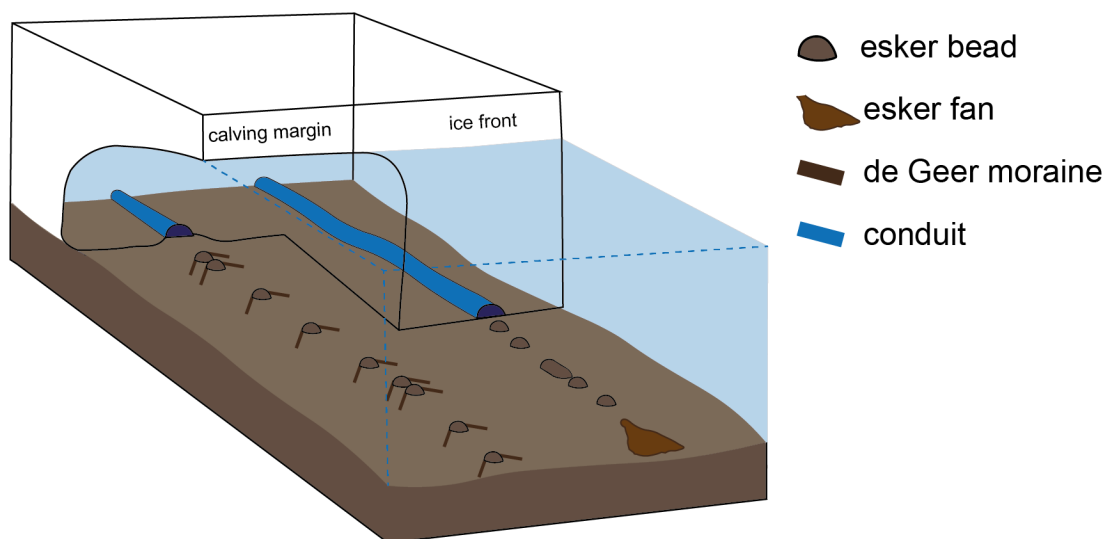
Figure 4.5 A range of landforms observed in subaqueous depositional environments at a); a calving margin and b) an ice front. At the calving ice margin, de Geer moraines may also be forming in embayments at the conduit mouth during periods of rapid retreat resulting in a 1-to-1 association with individual beads (see Livingston et al. 2020 and Fig. 4.1). At an ice front, a variety of landforms may form depending on the stability of the margin; beads form during periods of rapid retreat, slower retreat may result in the along-flow merging of beads into ridge-like features while temporal margin stability will result in the build-up of a fan.

4.1.4.2 Large terminal esker fans

Large terminal esker fans in the study area are noted to occur in association with moraine systems, in particular, the MacAlpine moraine. Moraines are rare across the Keewatin sector, suggesting limited periods of extensive stand-stills, and where they do occur are largely made up of glaciofluvial sediments (e.g. Aylsworth and Shilts, 1989). At margin stand-stills, it is likely that sediment delivered was continuously transported onto and across the fan, building it up over the duration of the stand-still. Water flux may be a key control here in determining whether sediment is either deposited at the mouth of the conduit, and subsequently builds up an esker through backfilling or whether sediment is continuously flushed out contributing to the build-up of a fan. Hewitt and Creyts (2019) suggest this is influenced by conduit size, with larger conduits and greater water discharges more likely to carry a greater proportion of the sediment out into the proglacial environment. Marginal fans can enhance ice sheet stability, resulting in a positive feedback on their formation (Powell, 1990), and the temporal stability of the ice sheet margin is expected to have facilitated the evolution of well-developed subglacial drainage corridors back from the margin into the ablation area. With regular high-pressure perturbations within the conduit forcing a connection with the surrounding hydraulically connected distributed drainage zone, the bed is likely to have experienced enhanced removal of sediments contributing to the build-up of the fans.

4.1.4.3   A potential landform continuum

These findings potentially support the idea of a continuum between esker beads and large terminal esker fans. In this model (Fig. 4.6), esker beads form at one end of the spectrum associated with rapid retreat rates and limited sediment coverage or low sediment and water fluxes as a consequence of a shrinking ice sheet and reduced catchment area. At the opposite end, large terminal esker fans are able to build up in areas with high water flux and sediment delivery, likely facilitated by well-developed conduit – distributed drainage system connections which increase access to sediment at the bed and provides sufficient flow velocities to erode and entrain it. This is supported by earlier research into fan deposition at a marine terminating ice margin in Svalbard where a range of depositional features are linked to variations in retreat rate

and margin stability and sediment concentration (Dowdeswell et al. 2015). Their observations suggest that the development of well-defined outwash fans require stability over years to decades – as also observed by the development of a fan at the margin of Muir Glacier in Alaska over ~ 20 years (Seramur et al. 1997) – while a retreating terminus with only short stand-stills will result in the deposition of small sediment lobes at the mouth of conduit portals (analogous to esker beads). It is also supported by mathematical modelling, which shows that margin retreat rates affect the size of esker deposits with smaller eskers in areas of more rapid retreat and larger eskers where margins are more stable (Hewitt and Creyts, 2019).
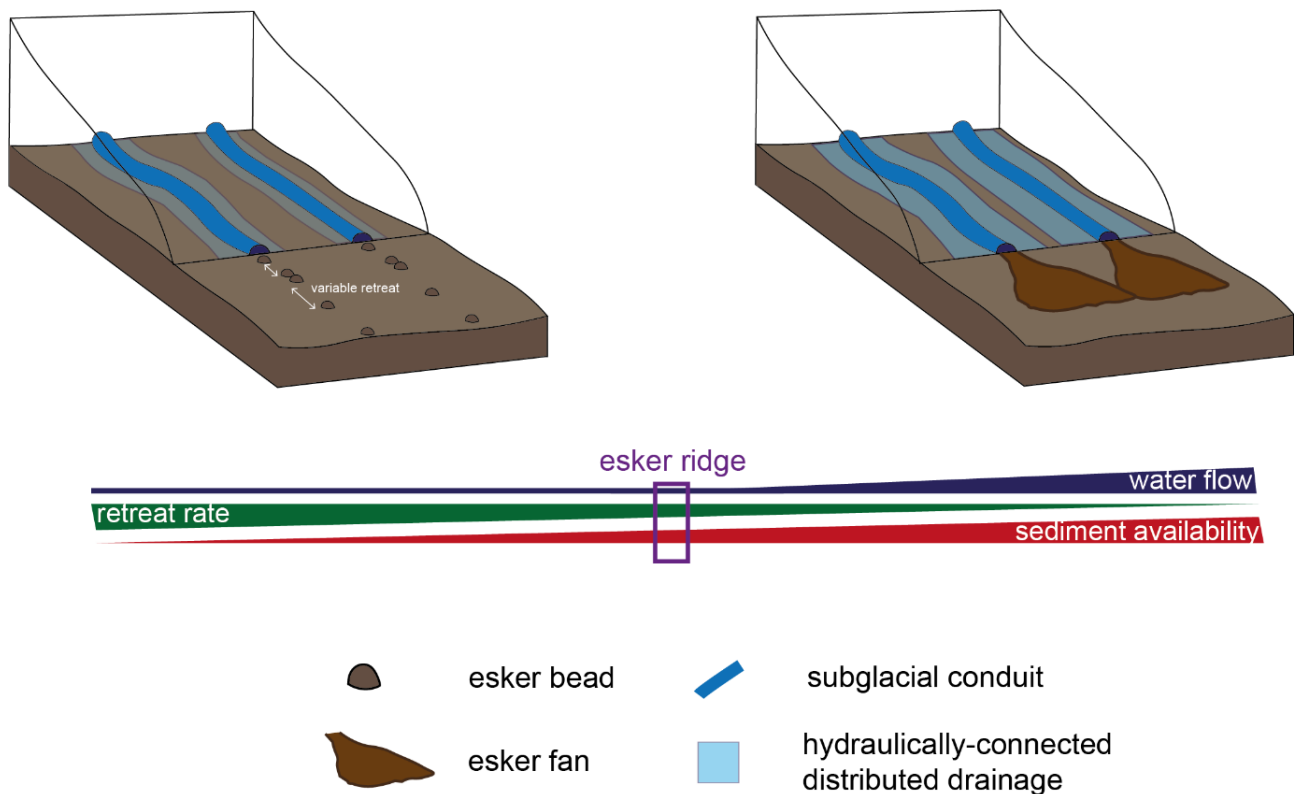
Figure 4.6 Proposed depositional scenarios for the deposition of; (a) esker beads and; (b) esker fans with the resultant landform expression dependent on sediment availability, retreat rate and water flow, which determines whether sediment can build up within the conduit to form an esker ridge (low) or is washed out beyond the margin (high). Conduit size (and interaction with the surrounding hydraulically connected distributed drainage system) is likely to vary between settings, becoming larger and better established in areas with a high water flux and greater temporal stability.

Work in this thesis suggests that between these two end members a range of landform morphologies can exist; for example, beads merging into ridges in areas where retreat rate is slower and beads are not clearly separated by large gaps and successive small fans where retreat rate may be rapid and sediment availability is higher. Together, this supports the idea that landform expression (i.e. size of deposit and resultant morphology) is complex but may reflect the balance between water flux, sediment access and delivery to the margin and the ice margin retreat rate (Fig. 4.6).

4.1.4.4   Broader implications

a) Esker formation

Eskers have long been hypothesised to form in segments (e.g. Banerjee and McDonald, 1975; Hebrand and Åmark, 1989; Ashley et al. 1991; Bolduc, 1992; Hooke and Fastook, 2007) that build up to form long ridges as the ice margin retreats (i.e. time-transgressive formation). This is supported by repeated sedimentological sequences along eskers (e.g. Hebrand and Åmark, 1989) and recent modelling studies that suggest that a bottleneck in sediment transport near the margin is an inherent property of subglacial channelised flow if enough sediment is present (e.g. Beaud et al. 2018a). The work in Livingstone et al. (2020) and this study adds further support to widespread time-transgressive esker formation. It also offers a potential approach to approximate a minimum estimate of how many of the eskers in the region formed time transgressively through the identification of fans and beads. Conversely eskers / meltwater pathways which do not contain these signatures may have formed synchronously, for example during an outburst flood, and could be targeted for detailed sedimentological investigations (e.g. Burke et al. 2010).

b) Palaeo-ice sheet retreat

Additional inferences can be made about the nature of ice sheet retreat, the palaeo-hydrological system and proglacial environment based on the morphology of the esker beads, fans and nets. For example, large, flat-topped fans at ice margin positions may be used as an indicator for the depth of proglacial lakes which formed in front of them. Furthermore, the presence of subaqueous landforms in areas outside

of the marine inundated sectors could be used as an indication of the presence of small proglacial lakes below the resolution of the data used for making predictions in Stokes and Clark (2004).

Livingstone et al. (2020) demonstrated the potential to exploit the association between esker beads and de Geer moraines to generate a high-resolution retreat chronology spanning ~ 350 years. This is really useful given the lack of moraines in the area and the remoteness of the location, which has resulted in limited geochronological constraints (e.g. Dalton et al. 2020). The fact that many of the beads, fans and nets align with one another across flow, broadly perpendicular to the direction of moraines and margin isochrones, raises the potential for these features to be used similarly to reconstruct high resolution retreat patterns in other parts of the ice sheet.

c) Palaeo-subglacial drainage

I suggest that subglacial drainage sufficient to mobilise sediment occurred further in towards the ice sheet interior and for a longer period of the ice sheets life than has previously been indicated from studies of esker ridges alone (e.g. Aylsworth and Shilts, 1989; Storrar et al. 2013). As the remaining ice sheet was likely polythermal by this point, the main source of water is likely to have been from the surface and restricted to near the margin. It is possible that the transition from meltwater pathways and esker ridges and fans to predominantly esker beads represents a switch from warm based to polythermal associated with a shrinking ice cap.

d) Esker nets

This proposed model does not account for all features and a clear omission to the discussion thus far are esker nets. While I do not attempt to fit these into the model at this point, there are a number of interesting observations to make about their distribution and morphology. Observations of esker nets in this study do not conclusively support a single typical setting for their formation and instead, a range of possible scenarios (e.g. subglacial and marginal) may be supported. For example, sometimes esker nets appear to align across ice flow (e.g. Fig. 4.2d). If conduits were active at different times, a spatial control would be the most likely cause (e.g. local

increase in slope or a change in the glaciological conditions). However, there is no clear indication of a visible spatial change associated with examples here. Contemporaneously active adjacent subglacial conduits may explain the formation of locally aligned nets across flow if there was a temporal control, such as a still-stand or large sediment pulse perhaps linked to an extreme melt event. A subglacial origin is supported by the re-joining of the multi-ridge sections into a single esker ridge, which is difficult to account for in a marginal setting. However, a marginal setting may be invoked to explain alignment over larger areas with the esker nets formed at the ice front. This latter interpretation is supported by their often flat-topped surface (indicative of deposition under atmospheric pressure or into standing water, e.g. Russell et al. 2001; Delaney, 2001) and their association with lateral deposits and potential down-flow transitions into terminal fans.

There is a strong spatial coincidence between esker nets and well-developed fields of ribbed moraine in the S / SW of the study area, which may be worth further exploration. Eskers and nets are exclusively found superimposed over the ribbed moraine (i.e. no observations of ribbed moraine over eskers), suggesting they were formed after the ribbed moraine. The preservation of ribbed moraines has been linked to stagnant ice (Aylsworth and Shilts, 1989) and / or spatial variations in thermal or hydrological conditions at the bed (e.g. Trommelen et al. 2014).

Finally, esker nets are almost entirely absent from the NW sector. The NW sector is broadly characterised as having fewer well-developed esker systems (e.g. Fig. 3.4) but widespread erosional meltwater corridors. The meltwater corridors are more densely spaced in this area than other parts of the study area and, in Chapter 3, this was linked to high basal roughness and the potential for this to be transferred to the surface (e.g. Ignéczi et al. 2018) resulting in the presence of numerous surface lakes which subsequently drained to the bed. While there are fewer esker ridges in this area, there is an abundance of glaciofluvial outwash, often occurring as tabular sheets within meltwater corridors indicating that sediment was not in short supply but that perhaps marginal deposition (subaerial) occurred differently due to the expected high velocity, dynamic meltwater flows and the topographic variations of the bed which prevented sediment being washed further away.

4.1.5 Conclusions

This work has demonstrated the widespread occurrence of esker assemblages around the Keewatin Ice Sheet Divide – in both subaerial and subaqueous locations - which have the potential to provide a wealth of information on palaeo-ice sheet retreat, hydrology and landform genesis. Work in Livingstone et al. (2020) reveals a strong relationship between abundant esker beads and low sediment availability and high retreat rates. However, at an ice sheet scale this relationship is less clear. This could be the result of other more influential controls, or because the coarse resolution and averaging of the retreat rate data fails to capture short periods of rapid retreat potentially ~ 7 ka. Nonetheless, results here support the idea of a potential continuum between esker beads and large terminal fans with a variety of morphologies (e.g. coalesced beads, esker ridges etc.) in between. The morphology of esker assemblages are likely to be influenced by a range of factors including margin stability (e.g. large fans building-up during stand-stills), water fluxes (e.g. high water fluxes resulting in esker fan progradation rather than conduit backfilling) and the subglacial drainage systems ability to access and entrain sediment. This depends on the interplay of variables such as basal substrate and meltwater supply, which is able to drive conduit-distributed drainage system interactions (Chapter 3) and thus access to the sediment, topography etc. and is expected to be influenced by the shrinking ice sheet and resulting transition in thermal regime.

To support these conclusions more robust, higher resolution data (e.g. sediment thickness maps and predicted proglacial lakes locations) are required and ideally a field campaign to sample esker sediments to investigate the conditions under which they were deposited using sedimentological and stratigraphical criteria (e.g. Brennand, 2000; Ravier et al. 2014). A potentially more feasible progression of this work is the testing of the proposed depositional scenarios using a numerical model for esker formation.

4.2 IS DRUMLIN LENGTH INFLUENCED BY SUBGLACIAL HYDROLOGY?

Drumlins are oval-shaped hills, largely made up of glacial drift and tend to occur grouped together in 'fields' where individual drumlins are aligned in the direction of ice flow (Clark et al. 2009). They are considered to be a geomorphic signature of ice-bed coupling and thus are important for enhancing understanding of subglacial ice sheet processes (e.g. Clark et al. 2009). While they are known to form subglacially, their exact formation mechanism is still debated (see Clark, 2010, Stokes et al. 2011, Möller and Dowling, 2018 or Sookhan et al. 2016 for a review of proposed formation methods which are not discussed fully here).

Drumlins vary in size, with typical lengths in the order of 1 km and up to 50 m in relief (Clark et al. 2009). In addition to the 'classic' drumlin shape, they can comprise spindle-like features, two-tailed features (similar to barchan dunes) and more rounded features with a low elongation ratio (Clark et al. 2009). Drumlins within the same local area tend to exhibit a similar long-axis orientation and morphology (Clark et al. 2009), but can vary in size, due to variations in developmental stage and external controls (e.g. Ely et al. 2018).

Conditions at the ice-bed interface are key in controlling whether bedforms are able to develop and the physical forms they take (Greenwood and Clark, 2010). Variations in the expression of drumlins have been linked to a range of controlling factors, including basal thermal regime, ice velocity, consistency of ice flow direction, sediment thickness and rheology and hydrological regime (e.g. Clark, 1993; Hart, 1999; Clark and Stokes, 2001; Rattas and Piotrowski, 2003; Stokes and Clark, 2002; Piotrowski, 2004; Briner, 2007; Hess and Briner, 2009; Maclachlan and Eyles, 2013). For example, drumlins and mega-scale glacial lineations have been widely correlated with areas of fast palaeo-ice velocities (e.g. Clark, 1993; Hart, 1999) and used as diagnostic criteria for the identification of palaeo-ice streams (e.g. Stokes and Clark, 1999). These factors have been explored at a range of spatial scales. At a local-scale, Rattas and Piotrowski (2003) explored the influence of bedrock characteristics and till texture on drumlin morphology in Estonia, suggesting that drumlin form could be related to the permeability of the substratum and grain size within the till. However, at a larger-scale Greenwood and Clark (2010) found no systematic relationship between

drumlin incidence, density or size and substrate properties and highlight the importance of scale-dependence when examining such relationships. They suggest that only under certain (currently unknown) local conditions is this relationship expressed dominantly over other controls (e.g. ice dynamics and topography).

During mapping for chapter 3, I noticed an area where drumlin length appeared to qualitatively increase with distance away from the meltwater tracks. This motivated me to explore the potential influence of hydrology on drumlin formation. Does subglacial drainage of water influence drumlin development?

4.2.1 Methods

Drumlin length was used as a simple indicator of morphologic variation. Drumlins were mapped at three test sites from around the former Keewatin Ice Divide (Fig. 4.7). Mapping for test sites 2 and 3 was produced by manual digitisation of drumlin long axis in ArcGIS using multi-hillshaded ArcticDEM tiles. Mapping for test site 1 was taken from Stokes and Clark (2003a) who used Landsat imagery to map streamlined features on the bed of the Dubawnt Lake Ice Steam. Test sites were selected with uniform background geology and sediment thickness to try and reduce the influence of other variables (apart from ice velocity) on drumlin lengths. The frequency distribution of drumlin lengths was then explored at each test site using histograms and basic descriptive statistics (e.g. min, max, mean and standard deviation) (Figs. 4.8 - 4.10). The shortest distance of each drumlin (polyline) to the edge of a meltwater corridor (polygon) was calculated automatically in ArcGIS using the 'Near' function.
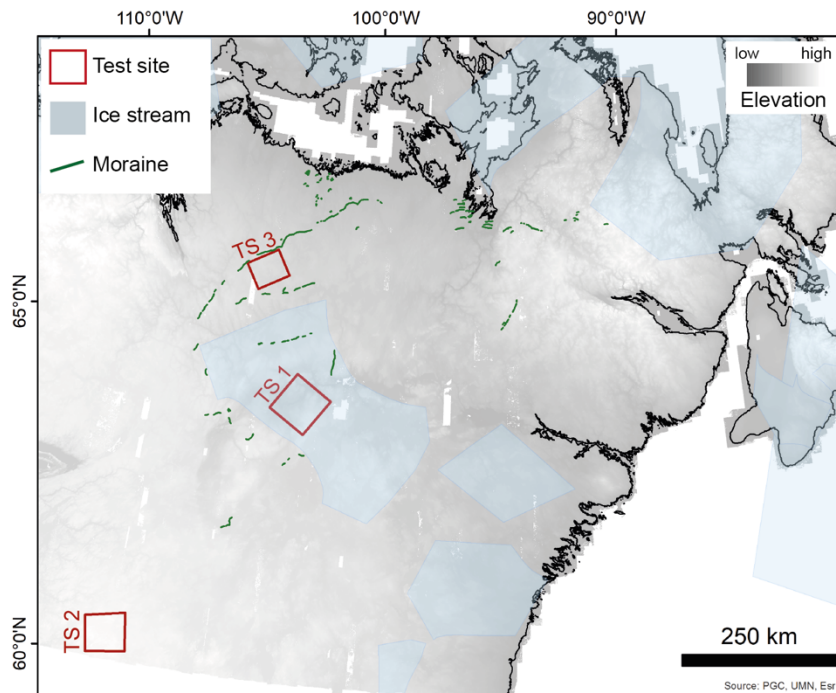
Figure 4.7 Locations of test sites (TS) 1 – 3 (red) selected for manual drumlin mapping, with the location of ice streams (blue) (Margold et al. 2015) and moraines (green) identified.

Drumlin length was automatically calculated and recorded for each polyline. To assess the relationship between drumlin length and proximity to meltwater corridors, length was first plotted against distance as a scatter graph. The relationship was further quantified by sorting the data into 200 m width bins (between 0 - 3,000 m length) and 500 m bins (> 3,000 m long) and the mean of each plotted as a bar graph.

4.2.2 Observations

Test site 1 (Fig. 4.8) covers a 5490 km^2 section of bed influenced by the presence of the Dubawnt Lake Ice Stream, which was likely active for around 250 years between ~ 9.3 and ~ 9.05 ka (Margold et al. 2018). Thus, the drumlins here probably formed under fast flow. Drumlins in this area are long, with a maximum of 17,207 m and mean of 1,720 m. They appear more densely spaced in the western part of the image, thinning towards the east. There is a high degree of parallel conformity amongst the drumlins and other streamlined bedforms but not between the

drumlins and meltwater corridors which can be seen cross-cutting the drumlins at an oblique angle. Meltwater corridors are noticeably sparse in this area in comparison to the surrounding areas outside of the palaeo-ice stream (see Chapter 3). The frequency distribution (Fig. 4.8b) reveals a positive skew as is common for drumlin populations (e.g. Clark et al. 2009). There is no clear relationship between drumlin length and distance from meltwater corridors (Fig. 4.8c).
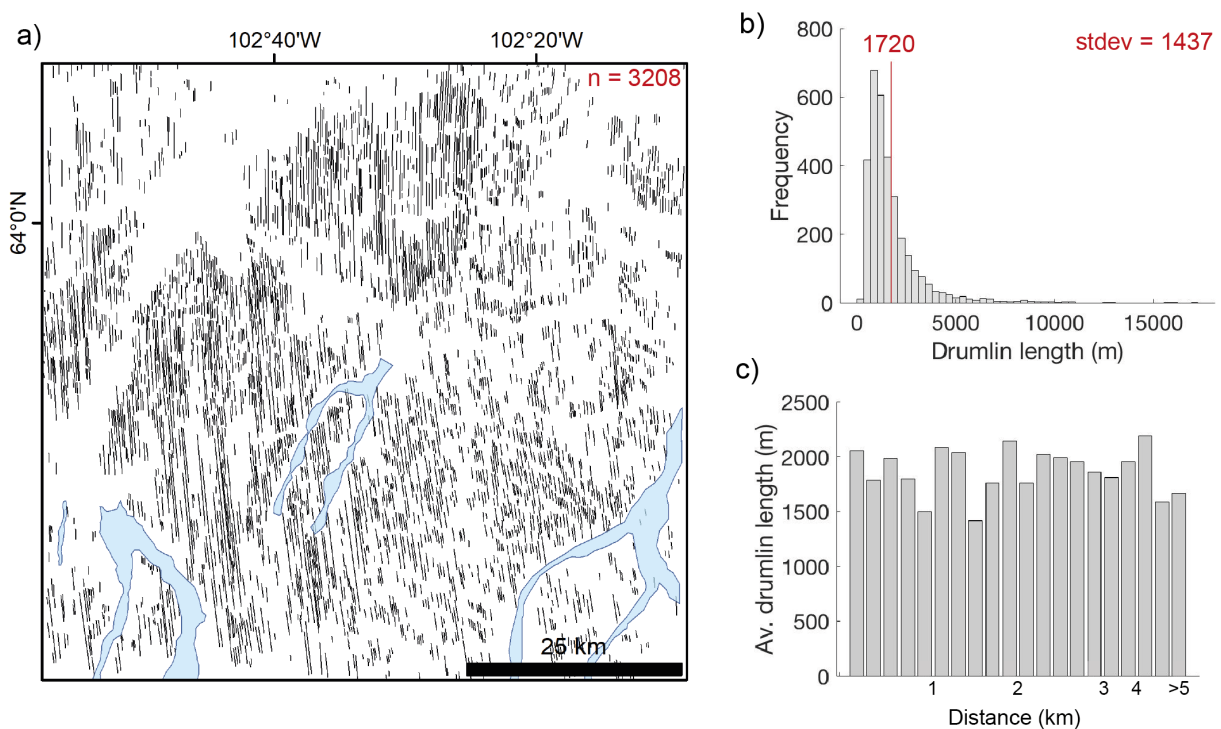
Figure 4.8 Drumlins (black lines) (Stokes and Clark, 2003) and meltwater corridors (blue polygons) in test site 1 (a); frequency distribution of drumlin lengths (b); drumlin lengths plotted against distance from meltwater corridors (c).Ice flow is from the bottom to the top of the image.

Test site 2 (Fig. 4.9) occurs outside of an ice stream (Margold et al. 2018) in an area with typical retreat rates of ~ 350 myr^{-1} and covers 4483 km^2. Drumlins are approximately evenly distributed across the site and exhibit a high degree of parallel conformity, perhaps diverging slightly downflow. Drumlins here vary in length from 108 to 3,849 m (mean 1,211 m). The more uniform frequency distribution (Fig. 4.9b) is different than at the other two sites. There are meltwater corridors throughout the area

but no relationship between drumlin length and distance from the meltwater corridors is found (Fig. 4.9c). Geomorphic evidence (Fig. 4.13) supports this with observations of meltwater corridors superimposed on and cutting through drumlins, suggesting that they occurred later in time.
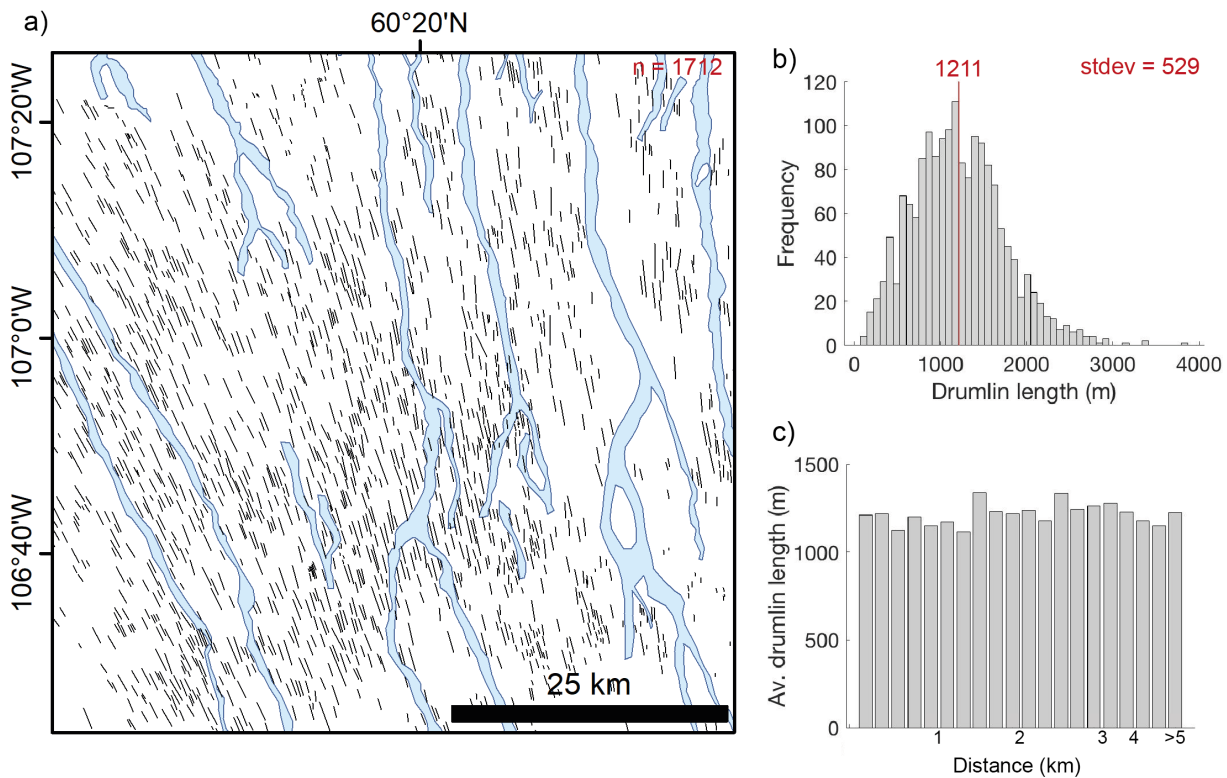
Figure 4.9 Drumlins (black lines) and meltwater corridors (blue polygons) in test site 2 (a); frequency distribution of drumlin lengths (b); drumlin lengths plotted against distance from meltwater corridors (c). Ice flow is from the bottom to the top of the image.

Test site 3 (Fig. 4.10) covers 2,730 km^2 and also occurs outside of an ice stream. The site is located less than a few kilometres upstream of the MacAlpine Moraine (Fig. 4.7), which delineates an ice sheet stand-still (e.g. Aylsworth and Shilts, 1989). There are more drumlins than at the other two sites (n = 5,384) despite the smaller area and they are less evenly distributed and appear to be somewhat grouped by average size. The frequency distribution of drumlin lengths is similar in shape to the population at test site 1, but an order of magnitude smaller (Fig. 4.10 b). Drumlin length varies from a minimum of 39 m to a maximum of 2,355 m (on average 373 m). This is at the lower

end of what is commonly observed in the literature (see Clark et al. 2009). Meltwater corridors are common in this area, spaced approximately 5 km apart. There are possible examples of drumlins orientated towards the meltwater corridor (e.g. NW of study site) and qualitatively, it looks as though drumlins surrounding the meltwater corridors (or potential areas of flow where a geomorphological signature is less well developed / not recorded (the light polygons in Fig. 4.10 a)) are shorter than drumlins further away (Fig. 4.14). While there does not seem to be a correlation between individual drumlin length and distance from a corridor, a relationship can be seen when the mean drumlin length is considered at increasing distance intervals from the meltwater corridors (Fig. 4.10 c. This shows a gradual increase in average drumlin length from immediately adjacent to the meltwater corridor up to ~ 1.6 km after which drumlin length appears to fluctuate. There is also geomorphic evidence to suggest either the formation of small drumlins or the streamlining of hummocks within the meltwater corridors and there is no evidence of drumlins (at least the small ones) being cut by meltwater corridors.
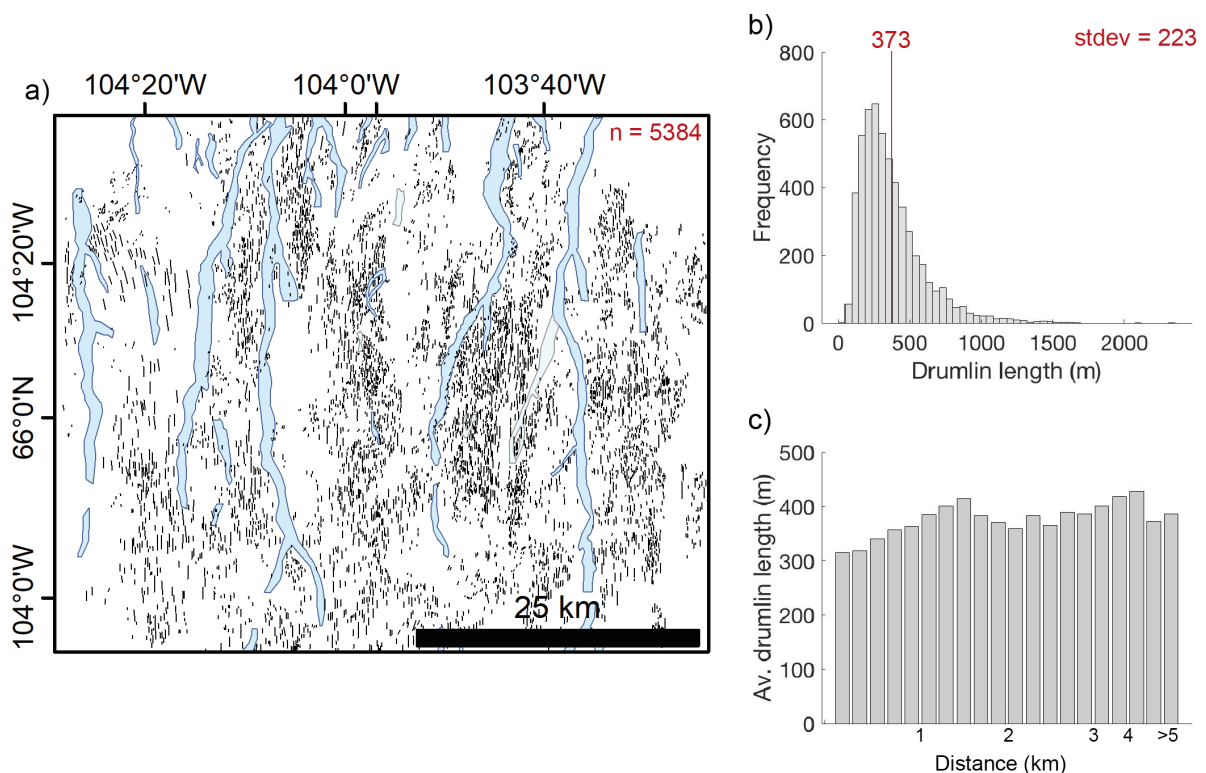
Figure 4.10 Drumlins (black lines) and meltwater corridors (blue polygons) in test site 3 (a); frequency distribution of drumlin lengths (b); and drumlin lengths plotted against distance from meltwater corridors (c). Ice flow is from the bottom to the top of the image.

To further explore the relationship between mean drumlin length and distance, I investigated the relationship along a cross-profile (Fig. 4.11). This revealed considerable variability in drumlin length across test site 3. There are potentially examples of 'v-shaped' drumlin length distributions either side of meltwater corridors (identified by the red dashed lines in Fig. 4.11b). However, this is not clear at all of the meltwater corridors and it is not certain whether this relationship is due to chance, nor does there seem to be a preference for a 'stronger' or 'weaker' relationship associated with meltwater corridor, which may or may not reflect the magnitude of flow during drumlin formation.
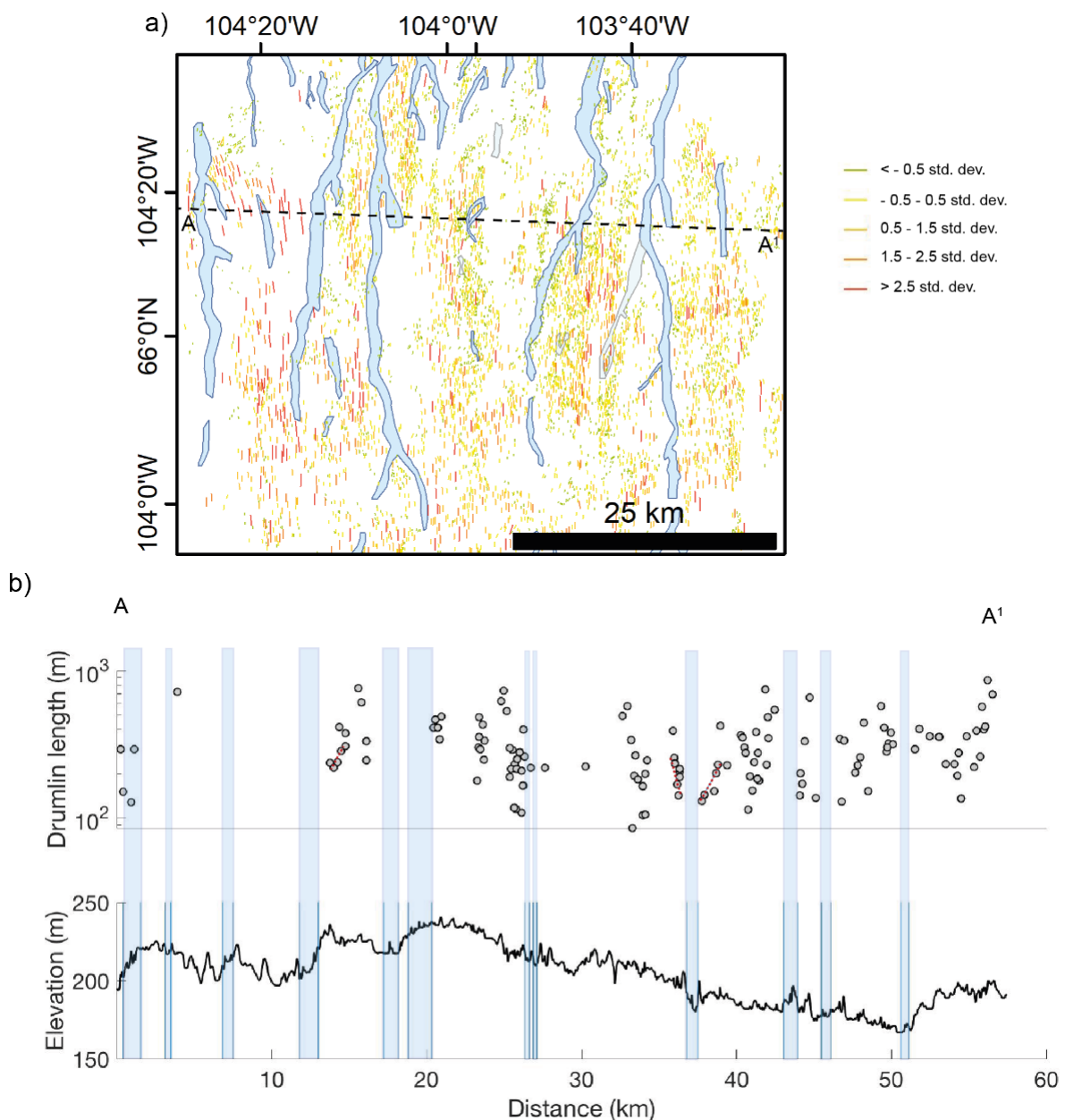
Figure 4.11 (above) Drumlins coloured by length (a) with an example profile across drumlins and meltwater corridors (light blue) (b). Ice flow is from the bottom to the top of the image. A single profile was sampled owing to time constraints and this was selected in an area which exhibited dense drumlins so as to best capture length variations.

4.2.3 Discussion

4.2.3.1 Theoretical support for a hydrological control on drumlin length

The character and evolution of the subglacial hydrological system in space and time acts as an important control not only on ice sheet dynamics but also till and land forming processes (e.g. Boulton et al. 2001). Subglacial deformation is thought to be widespread and accounts for a significant amount of ice sheet movement (Alley et al. 1986; Boulton and Hindmarsh, 1987; Clarke, 1987; Alley et al. 1987a, 1987b; Alley, 1989a, 1989b). Deformation rates are affected by the water content, and the composition and thickness of sediments at the ice bed (Evans et al. 2006) with differences in these influenced by the distribution and evolution of the subglacial hydrological system (e.g. Boulton et al. 2001). If the presence of drumlins at the bed is a record of ice-bed interactions and subglacial deformation (e.g. Boulton and Hindmarsh, 1987), it is therefore logical to expect that drumlin length may reflect this.

Water pressure within subglacial sediments is a major control on the likelihood and rate of sediment deformation (Boulton et al. 2001). Here, I suggest that drumlin length will reflect this, with shorter drumlins occurring near conduits in areas of alternating high and low basal water pressure, while longer drumlins will occur further from the conduits in areas which experience more consistent high water pressure (Fig. 4.12). Based on the model proposed in Chapter 3, the hydraulically-connected distributed drainage zone adjacent to subglacial conduits will be affected by; (a) conduit over-pressurisation and resultant decoupling of the ice-bed interface as water is flushed out of the conduit and into the surrounding hydraulically connected distributed system causing either cavity expansion or a localised sheet flood (e.g. Fig. 3.11) and (b) the development of efficient drainage which draws in water from the surrounding hydraulically connected distributed system, lowering the pressure and

forming stiffer, more rigid tills (Boulton and Hindmarsh, 1987; Clark and Walder, 1994; Boulton et al. 2001). Drumlins are thought less likely to form within or immediately adjacent to meltwater corridors where frequent ice-bed separations limit the time for the ice to act on the bed (ice is sliding instead of deforming) and / or the till is more rigid and difficult to deform when water is draining into the conduit. The model proposed in chapter 3 suggests that these effects can occur repeatedly each melt season over tens to hundreds of years within the ablation area, therefore increasingly affecting the conditions at the bed.

The action of subglacial drainage is also likely to remove till below and surrounding the conduit. Boulton (1976) first saw evidence of creep into subglacial tunnels leading to the proposition that this was an effective mechanism for removing till at the bed (Boulton and Hindmarsh, 1987). Alley (1992) developed this idea, suggesting that this would result in a thin or absent deforming till layer immediately surrounding a conduit in as little as a single melt-season. While this mechanism was only proposed to affect small distances (on the scale of one to several metres), a similar effect is likely to occur as a result of repeated connections between the conduit and surrounding distributed drainage system (see Chapter 3), whereby pressure variations enhance erosion and the hydraulic connection (along with proposed conduit migration), offer a potential mechanism for till entrainment and removal.

Further from the conduits, the bed is less affected by surface meltwater inputs and conditions are more conducive for deformation and drumlin formation owing to consistently high water pressures (e.g. Alley et al. 1986; Boulton et al. 2001; Bennett, 2003). Despite their distance from surface meltwater inputs, conditions in these sections are unlikely to be uniform over time and space and can still be influenced by variations in the channelised system (Andrews et al. 2014). For example, the expansion and increased efficiency of the subglacial drainage system in response to sustained meltwater inputs is thought to cause slow seasonal drainage from isolated regions into the connected system and thus dewatering over large areas (e.g. Tedstone et al. 2015). This will alter basal properties and is likely to affect the areas closest to the conduits most significantly and decrease with distance laterally outwards. This idea of spatially varying water content and till properties is consistent with the idea of a transient mosaic of bed conditions (Piotrowski, 2004; Lee and

Phillips, 2008). Furthermore, the co-existence of stable and deforming beds (linked to difference in water content and till properties) have been observed to occur beneath the contemporary AIS (e.g. Smith et al. 2009). Here a drumlin was inferred to have developed over 7 years or less, with the potential water required for the deformation sourced from an adjacent area which was observed to experience de-watering and sediment compaction (and thus reduced deformation) indicating that sections of the bed can be mobilised or inactivated in response to changes in porosity, water content and changes of water pressure (Smith et al. 2007).
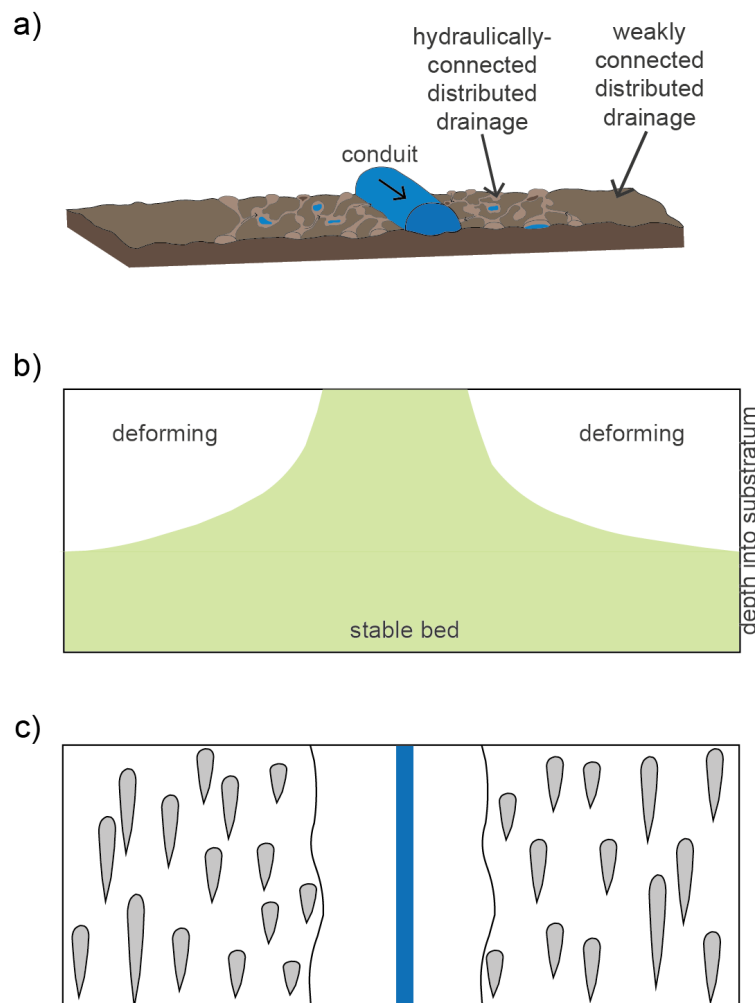
Figure 4.12 Model of how drumlin length is expected to vary with distance from a subglacial conduit. Deformation is limited within the hydraulically-connected distributed drainage system because: (i) High magnitude over pressurisation events, typically earlier in the melt season, cause ice-bed separation and basal sliding and (ii) later on in the melt season, efficient subglacial conduits result in a well-drained bed. Deformation rates are higher within the

weakly-connected distributed drainage system where high-pressure conditions dominate. (b) shows a cross-section of how deformation rates may vary surrounding a conduit and (c) shows a plan-form view of how this may be expressed in terms of drumlin incidence and length surrounding a central conduit (blue) within a meltwater corridor (black outline) (Schematics not to scale).

4.2.3.2 Assessment of hydrological controls on drumlin length in Keewatin

In this section I assess the relationship between drumlins and meltwater corridors in light of the following possible formation scenarios; (a) the drumlins formed before the meltwater corridors; (b) drumlins and meltwater corridors formed contemporaneously (i.e. the scenario outlined above) and; (c) the drumlins formed after the meltwater corridors. I consider the third scenario unlikely given that there is no widespread evidence of drumlins within meltwater corridors and because channelised subglacial drainage is likely to have occurred close to the margin during deglaciation. Here, I explore the evidence to support the alternative two scenarios at each of the test sites:

1) *Drumlins formed before the meltwater corridors*

The highly elongate drumlins and MSGLs at test site 1 (Fig. 4.13 c and d) are interpreted to have formed prior to the development of channelised subglacial meltwater drainage. This is based on the noticeably different orientations between the two landforms, suggesting that the meltwater corridors formed subsequent to the drumlins when the ice-flow geometry has shifted. Similarly, test site 2 (Fig. 4.13 a and b) shows no evidence to support the contemporaneous formation of drumlins and meltwater corridors. In fact, there is geomorphic evidence to suggest that channelised meltwater drainage occurred after the formation of drumlins with corridors and eskers superimposed on drumlins and corridors clearly truncating drumlins located immediately adjacent to the corridors.
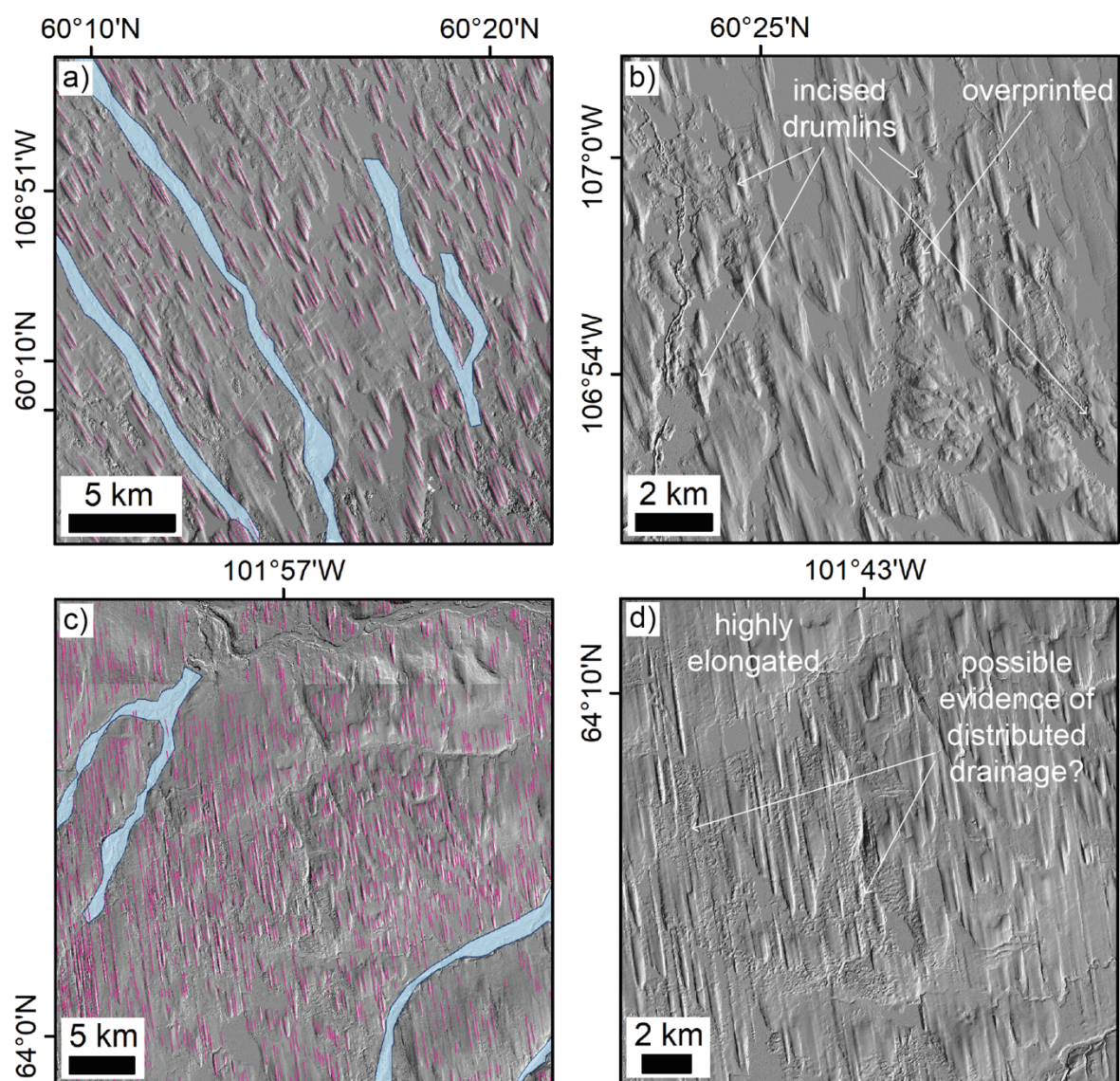
Figure 4.13 Examples of geomorphology from test sites 2 (a and b) and 1 (c and d) where there is not expected to be relationship between drumlins and meltwater corridors. Ice flow is from the lower right to upper left of the image.

Subglacial hydrology is expected to play a significant role in ice stream dynamics (e.g. Bell, 2008; Christianson et al. 2014) with the probability of ice streaming higher in areas with high subglacial water flux (e.g. Livingstone et al. 2015). Eskers and meltwater corridors are noticeably rarer on the bed of the Dubawnt Lake Ice Stream than the surrounding non-ice stream area (Fig. 3.15) and this has been linked to the dominance of distributed drainage beneath ice streams - linked to widespread

deformation and high velocities (e.g. Kamb, 1987; Bell, 2008) – and the fact that any meltwater landforms developed under fast ice are unlikely to have been preserved (e.g. Boulton, 1996; Livingstone et al. 2015). Nonetheless, geomorphological evidence (e.g. of ribbed moraines in the onset region) supports the hypothesis that the Dubawnt Lake Ice Stream shut down during deglaciation (Stokes et al. 2006) and this could be linked to changes in subglacial hydrology. Physical modelling supports the role of an evolving subglacial hydrological system in both initiating and shutting down ice streaming, with the latter a result of channelisation enhancing ice stability and causing deceleration of the ice (Lelandais et al. 2018). Furthermore, contemporary observations in both Greenland and Antarctica indicate that re-routing of water at the bed can influence ice stream velocities (e.g. Alley et al. 1984; Anandakrishnan and Alley, 1997; Vaughan et al. 2008; Carter et al. 2013; Chu et al. 2016); the shut-down of the Kamb Ice Stream has been attributed to reduced basal lubrication associated with a switch from distributed to channelised drainage (Catania et al. 2006). Thus, it is possible that the formation of efficient subglacial conduits that formed after the drumlins contributed to the shut-down of the Dubawnt Lake Ice Stream.

2) *Contemporaneous formation of drumlins and meltwater corridors*

The good match between drumlin and meltwater corridor orientations at test site 3 (Fig. 4.14) suggests contemporaneous formation and thereby facilitates an assessment of the main hypothesis regarding drumlin length and drainage. Specifically; (a) drumlins and meltwater corridors exhibit a high degree of parallel conformity; (b) there are no clear examples of drumlins being cut by meltwater features and; (c) distribution of drumlin lengths does not look random with a visual perception of some spatial control on their variation.

Although drumlins within a field can exhibit variations in length, it is not known whether this is due to different generations co-existing (i.e. shorter drumlins are younger) or the influence of an external control(s) (e.g. Ely et al. 2018). There is considerable spatial variability in drumlin lengths within site 3 (Fig. 4.10). However, length does not appear to vary systematically in a downstream direction or to occur randomly. Rather, there appears to be some relation to the positioning of meltwater corridors. Dowling et al. (2016) suggest that shorter drumlins in their study site are

younger, having formed within 5 - 35 years and evidence from beneath contemporary ice suggests similar short formation times of ~ 5 - 7 years (Smith et al. 2007). This would suggest that 'new' drumlins are forming across the site in areas with favourable conditions (e.g. sediment availability) and may explain why the smallest drumlins can be seen to occur across most of the site. Observations show that average drumlin length gradually increases up to ~ 1.6 km away from the meltwater corridors (Fig. 4.10 c), after which the distance effect is negligible. This suggests that drumlin formation in the hydrologically weakly-connected parts of the bed may be affected by the presence of subglacial meltwater over distances in the order of 1 - 2 km. This site is situated just upstream of the MacAlpine moraine system, a major still-stand position of the LIS (Aylsworth and Shilts, 1989). Thus, if we assume a similar ablation area to the GrIS today (~ 50 km), the entirety of this site is likely to have experienced significant surface meltwater inputs for a long period of time and drumlins are unlikely to have been time limited. Instead, the persistent subglacial drainage corridors within this site are likely to have 'stunted' the growth of drumlins because of the factors outlined above in Section 4.2.3.1. The limited number of larger drumlins located close to the meltwater corridors, in this interpretation, are likely to have formed during an early period of flow when this area was not so close to the margin, therefore suggesting the occurrence of multiple generations of drumlins. Results here indicating the effects of a conduit on the surrounding bed are within the modelled range outlined by Hewitt (2011) who demonstrate how the pressure within a channel is 'felt' by the surrounding distributed drainage over distances in the order of ~ 10 km. Here, the stability of the ice sheet margin and thus likely repeated meltwater flows down the same pathways likely resulted in an increasingly efficient drainage system and well-drained bed year-on-year. This would enhance ice-bed coupling and thus reduce local ice flow and may explain why drumlin lengths are generally much lower here than elsewhere (i.e. the presence of the conduit is felt across the whole area as conduits are spaced less than the 10 km distance identified by Hewitt (2011), but the impact may decrease with distance from the conduit).

In general, there is a high degree of conformity between drumlin long axes and meltwater corridor orientation and this is supported by the fact that there are no examples of drumlins (at least the small ones) being cut by meltwater corridors. Potential deviations in drumlin long axis orientation towards the meltwater corridors

can be detected in places; however, a similar phenomenon was noticed by Dowling et al. (2016) around eskers at a marine terminating margin in Sweden. They attributed changes in long-axis orientation to the presence of subglacial conduits, which contributed to the formation of embayments at the margin, locally altering ice flow towards the location of the eskers. The smaller 'younger' drumlins were hypothesised to have formed under these conditions over 5 - 35 years within ~ 5 - 7 km of the margin.
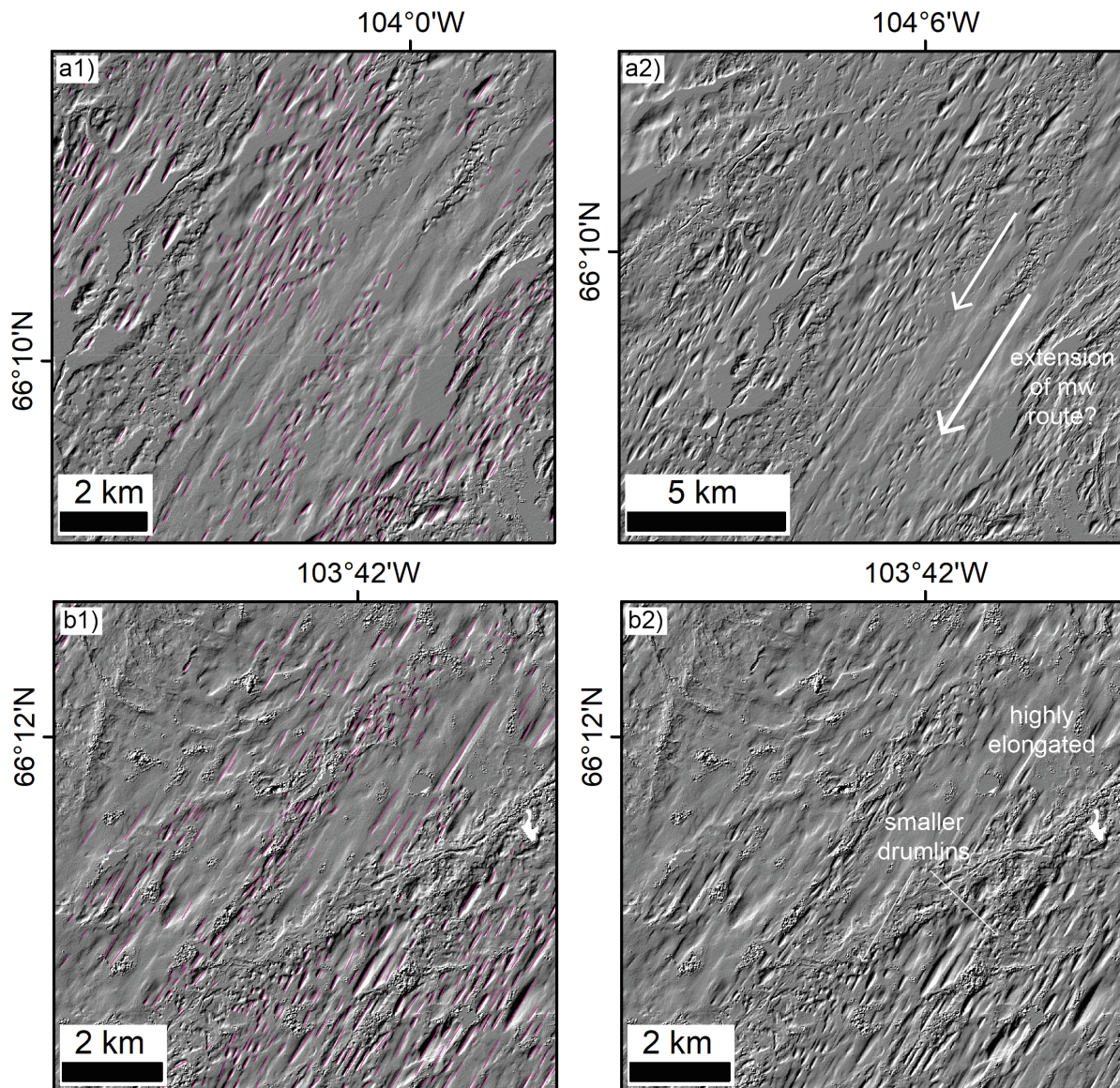
Figure 4.14 – Examples of geomorphology and drumlin mapping (a1 and b1) from test site 3 where there is a possible contemporaneous formation of drumlins and meltwater corridors. Ice flow is from the lower left to upper right of the image in a and b.

Despite these observations, not all of the meltwater corridors in the area show a relationship and the strength of this apparent relationship may vary between different meltwater conduits. For example, it is possible that only one / some of the meltwater corridors within this area formed contemporaneously with the drumlins and that corridors – and in fact individual drumlins – were not all actively forming at the same time. Subglacial hydrology is highly variable over space and time and geomorphic evidence often represents a composite picture of these temporal changes.

4.2.4. Conclusions

Although not conclusive, results here suggest a possible controlling relationship between drumlin length and distance from subglacial meltwater corridors which sheds some light on possible interactions at the bed between (a) ice streaming and channelisation of the drainage system, perhaps contributing to ice stream shut down and; (b) local ice dynamics (and drumlin formation) and hydrology when they are thought to co-exist. However, despite being hinted at, the relationships demonstrated here were not significant and more work is required to expand the population and to explore additional areas before anything conclusive can be said. By upscaling and looking at different regions, a better understanding of the temporal relationship between drumlins and meltwater and the effect of any contemporaneous relationship is likely to be obtained. It may be that effects on drumlin formation only occur under specific conditions, for example when the margin is stable for long enough to have a significant effect on the geomorphology of a region.

4.3 RIBBED MORAINE TRACTS

Ribbed moraines occur commonly on the Canadian Shield owing to the low relief and unconstrained topography (Trommelen et al. 2014) and tend to be situated close to former ice divides (Prest, 1968; Aylsworth and Shilts, 1989; De Angelis, 2007; Kleman et al. 2010). Numerous hypotheses exist for their formation largely grouped around the ideas of; (a) fracture and extension (e.g. Hättestrand and Kleman, 1999; Sarala, 2006); (b) subglacial modification of pre-existing ridges of hummocks (e.g. Boulton, 1987; Lundqvist, 1989; 1997b; Möller, 2006); (c) natural instability (e.g. Hindmarsh, 1998; Dunlop et al. 2008; Fowler, 2009; Chapwanya et al. 2011) or; (d) shear and stack (e.g. Shaw, 1979; Stokes et al. 2008). They frequently exist alongside other subglacial landforms, likely corresponding to a multi-phase formation history which complicates their interpretation (Aylsworth and Shilts, 1989; Stokes et al. 2008; Vérité et al. 2020).

The characteristics of individual ribbed moraines and the fields they exist in can vary significantly (Dunlop and Clark, 2006). Of particular interest here are the occurrence of ribbed moraine organised into narrow tracts parallel with ice flow (e.g. Aylsworth and Shilts, 1989; Dunlop and Clark, 2006). In Canada, these tracts are observed to vary in length from 12 - 45 km and in width from several hundreds of metres to several kilometres (Dunlop and Clark, 2006). Within the study area they are widespread and their relationship with subglacial meltwater traces is examined here.

4.3.1 Observations and interpretations

Mapping of meltwater corridors (Chapter 3) revealed the widespread occurrence of ribbed moraine tracts in the SW of the study area (Fig. 4.15 a and d). In this area I decided to undertake initial exploratory mapping to better understand their frequency and distribution and their spatial coincidence with meltwater corridors. This was achieved by approximately mapping their centrelines with a polyline directly into ArcGIS. Previous mapping of ribbed moraines (e.g. Aylsworth & Shilts, 1989; Wagner, 2014) confirmed the common occurrence of ribbed moraine within this sector surrounding the ice sheet; some of these ribbed moraine are noted to form elongate tracts (Fig. 4.15 b and c).

a)

meltwater route
ribbed moraine

300 km

Esri, HERE, Garmin, (c) OpenStreetMap contributors, and the GIS user community

b)

(Aylsworth & Shilts, 1989)

ribbed moraine
lineations
drift poor areas
glaciofluvial material

c)

(Wagner, 2014)

Ribbed moraine field boundaries

Shaw et al. 2010*

This study**

* Mapped from 15 m (pansharpened) 2,4,7 FCC Landsat 7 ETM+ imagery at ~1:100,000 scale and 90 m SRTM DEMs at ~1:250,000 scale

** Mapped from 10 m SPOT 4/5 panchromatic band imagery, various 15 m (pansharpened) Landsat 7 ETM+ multi-band combinations, and ~20 m CDED DEMs at scales between ~1:10,000 - 1:150,000

100 km

182

Figure 4.15 Ribbed moraine tracts mapped in this study (a and d) and within the wider literature (b and c) across the Keewatin area. Ribbed moraine tracts appear to occur relatively commonly here and exhibit a close spatial association with meltwater routes (d) – ice flow is from the right to left of the image.

Mapping here reveals the occurrence of at least 40 ice flow parallel ribbed moraine tracts typically < 5 km in width (Fig. 4.15 d). The areas lacking ribbed moraine tracts within this area were often covered by widespread ribbed moraine fields (e.g. centre north of the study area (Fig. 4.15 d and Fig. 4.16 d)). The areas in between the ribbed moraine tracts typically exhibit smooth and streamlined terrain (Fig. 4.16 a and b). Within this area there is a clear spatial association between ribbed moraine tracts and meltwater landforms (Fig 4.15 d and Fig. 4.16). It is estimated that > 2/3rds of the meltwater corridors (on average ~ 1 km in width) within the SW study area occur within ribbed moraine tracts. From initial exploratory observations, meltwater corridors within ribbed moraine tracts do not appear morphologically dissimilar to those outside in other areas. Unlike the drumlins in section 4.2, which I suggest may increase in length with increasing distance from the esker, individual ribs do not appear to exhibit any

systematic variation in size. However, those close to the meltwater corridors potentially exhibit evidence of 'washing' i.e. ribs closer to the conduits appear more well defined, perhaps indicative of the surrounding sediment being removed (Fig. 4.16 a).
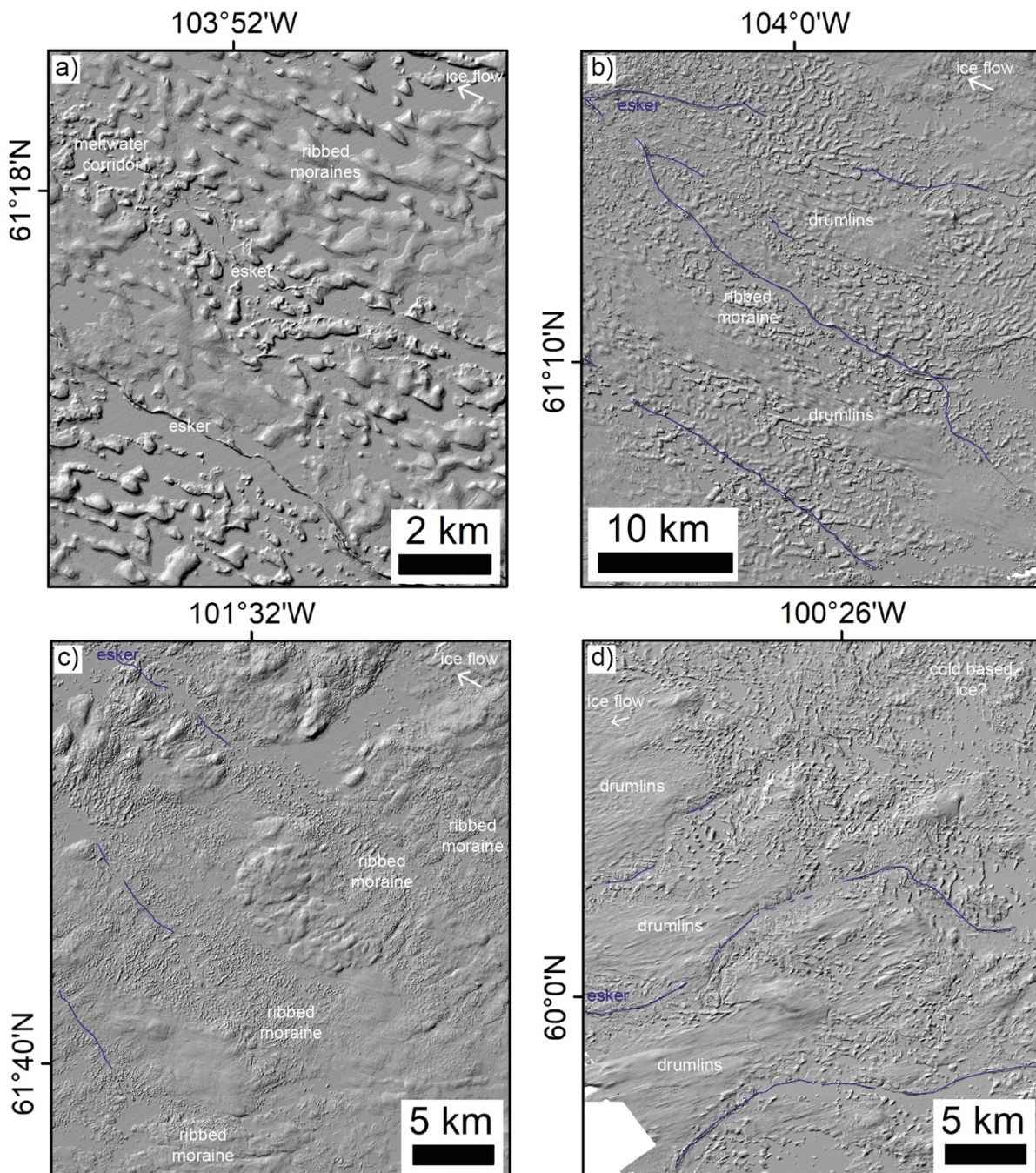
Figure 4.16 Examples of esker, meltwater corridor and ribbed moraine associations; (a) an esker within a meltwater corridor within a narrow tract of ribbed moraines; (b) lateral transitions from ribbed moraine tracts (containing eskers and meltwater corridors) to drumlins with some seemingly superimposed on the ribbed moraines beneath; (c) possible example of ribbed

moraine tracts which could represent the up-ice extension of subglacial meltwater flow in an area where eskers were not formed or preserved and; (d) alternating drumlins and ribbed moraine tracts (with eskers) and a transition into a broad drumlin field. This may suggest a broader-scale switch in basal conditions (e.g. cold ice based).

The fact that there is a clear spatial coincidence between ribbed moraine tracts and meltwater corridors supports the idea that their formation is linked and that spatially variable drainage at the bed acts as an important control on landform formation. This begs the question: how can the occurrence of meltwater corridors within ribbed moraine tracts and their relative absence from the areas in-between be explained? Below I discuss two possible scenarios;

a) Meltwater corridors and ribbed moraine tracts formed contemporaneously and thus exist as part of the same meltwater drainage signature.

b) Ribbed moraines were formed first across a wide area of the bed; focussed meltwater drainage preferentially preserved the ribbed moraine close to the main drainage axis while ribbed moraine further away were modified or overprinted.

4.3.2 Discussion

An association between ribbed moraines and streamlined bedforms (e.g. drumlins and flutes) has been widely discussed in the literature with common observations of along flow transitions between ribs and drumlins resulting in the concept of a bedform continuum (e.g. Aario, 1977; Boulton, 1987; Stokes et al. 2013; Ely et al. 2016). Less frequently observations have been made of lateral transitions between ribbed moraine fields and drumlins (e.g. Shilts, 1977; Trommelen et al. 2014; Wagner, 2014). Within this area (Fig. 4.15 d), meltwater corridors (on average ~ 1 km wide) are almost exclusively located within tracts of ribbed moraine (typically < 5 km wide) (Fig. 4.15 d and Fig. 4.16). Areas in between the ribbed moraine tracts are typically smooth and streamlined (Fig. 4.16). These observations hint at a

systematically varying pattern of landforms with increasing distance from an inferred conduit location (i.e. an esker).

In Chapter 3 meltwater corridors are proposed to record repeated interactions between a central conduit and the surrounding hydraulically connected distributed drainage system driven by over-pressurisation events. Within the three-system drainage model (Fig 3.24 a), the hydraulically connected distributed drainage zone (represented by the meltwater corridor) transitions laterally into the weakly connected distributed drainage zone (e.g. Andrews et al. 2014; Davison et al. 2019). While the hydraulically connected distributed drainage zone immediately adjacent to the conduit is regularly and strongly affected by variable meltwater inputs and pressure fluctuations, the area beyond this - prior to the transition into the isolated distributed drainage zones which is largely cut off from the larger hydrological system - is still affected by meltwater activity but to a lesser extent (e.g. Andrews et al. 2014; Davison et al. 2019). While this zone may be connected to surface inputs following occasional particularly large over-pressurisation events, the net flow of water within the weakly connected drainage zone is likely to have been down the hydraulic gradient into the hydraulically connected distributed drainage zone and conduit. As a result of gradual dewatering, this zone would have exhibited an overall decrease in pressure and an increase in effective pressure, enhancing ice bed coupling (e.g. Sole et al. 2013; Tedstone et al. 2015; Hoffman et al. 2016). These variable conditions across the bed are likely to have been key to processes which determined both landform formation (as outlined in section 4.2.3.1) and preservation.

4.3.2.1   Contemporaneous formation

In terms of contemporaneous formation (i.e. meltwater corridors and ribbed moraine tracts forming at the same time), recent physical modelling by Vérité et al. (2020) supports the idea of variable conditions and landforming potential at the bed controlled by proximity to drainage pathways. They suggest that ribbed moraines are more likely to form in areas of elevated basal shear stress such as in proximity to efficient drainage pathways which reduce basal water pressure. In contrast, their formation is likely to be inhibited in poorly developed drainage areas that experienced high water pressure, ice-bed decoupling and basal sliding (Vérité et al. 2020). In other

words the areas dominated by distributed drainage and high pressure in-between the main drainage routes. If meltwater corridors and ribbed moraine tracts formed contemporaneously, meltwater corridors could represent the areas of more focussed meltwater flow with the surrounding – laterally more distant - ribbed moraines tracts affected to a lesser extent by the presence of major meltwater drainage. Those which do not contain clear evidence of a meltwater corridor and / or esker may have formed where the drainage existed as an 'efficient core' (Davison et al. 2019) rather than as an esker-forming conduit. The SW study area (Fig. 4.15 d) is generally conducive to ribbed landform formation – as evidenced by its widespread occurrence within ribbed moraine fields in figure 4.15 b – while other regions may not have been. This may explain why not all meltwater corridors occur within ribbed moraine tracts.

4.3.2.2 Preferential preservation

Alternatively, the ribbed moraine could have formed before the meltwater corridors during an earlier stage of glaciation, perhaps shortly after the LGM (Trommelen et al. 2014). This is based on the fact that meltwater corridors and eskers are superimposed on top of the ribs with no evidence of the alternative. In this scenario, I suggest – similarly to above – that the presence of meltwater drainage routes at the bed affects the processes which occur across an area wider than the corridors themselves. This is expected to have influenced; a) how well ribbed moraines are preserved and; b) to what extent ribs can be modified or additional landforms (i.e. drumlins) be formed with increasing distance from the drainage routes.

Within the wider literature till dewatering and consequent stiffening are identified as potential mechanisms for ribbed moraine preservation (e.g. Boulton et al. 2009; Tylmann et al. 2013). In contrast, areas further away from the channelised flow are likely to have been characterised by consistently high-pressure inefficient drainage systems (e.g. Boulton et al. 2001; Bennett, 2003; Rada & Schoof, 2018) which favour greater rates of sediment deformation and thus greater rates of rib modification or overprinting by drumlins.

The diminishing lateral influence of a conduit on the surrounding basal conditions and how these relate to potential switch in geomorphic work or landforming

potential are poorly understood. In both of the discussed hypotheses above (section 4.3.2.1 and 4.3.2.2), the lateral effects of the presence of the conduit on the surrounding bed is estimated to be < 5 km (i.e. the width of the ribbed moraine tracts). This fits with the findings from section 4.2 which suggest that the total area of the bed around a conduit that appeared to be influenced by till dewatering was ~ 4 km based on an average meltwater corridor width of ~ 1 km and an increase in drumlin length of ~ 1.6 km either side. These estimates are both lower than the 10 km distance predicted by Hewitt (2011); however, my results are likely a minimum estimate that just captures the region of the bed that was modified sufficiently to leave a landform imprint. Additional research could explore this relationship further to determine over what length-scales this occurs and what factors determine the relatively abrupt switch between ribbed moraines and drumlins.

4.3.3 Conclusions

Observations of well-preserved ribbed moraine tracts in close association with signatures of channelised drainage add further support to the idea of a complex mosaic of bed conditions strongly influenced by sediment water content. I suggest that variations in sediment water content can control both the formation of landforms when occurring contemporaneously and/ or their preservation when drainage occurs at a later stage. This may be informative for understanding the relationship between drumlins and ribbed moraine as these observations potentially support the idea that a landform continuum is not necessary to explain the close associations between drumlins and ribbed moraines, instead suggesting that they can form under different conditions at different times (e.g. Trommelen et al. 2014).

CHAPTER 5: CONCLUSIONS

5.1 Summary of key achievements

This thesis contributes methodological developments and enhances understanding of interactions between subglacial hydrology, ice sheet dynamics and landform formation. Key achievements are summarised as follows in the order that they occurred within the thesis:

- *First fully automated method for detecting and mapping subglacial meltwater tracks from high-resolution digital elevation data.* This methodological development allows for the rapid identification of subglacial meltwater tracks at an ice sheet scale from high-resolution ArcticDEM data. Accuracy assessments reveal that it successfully captures the general configuration, morphometry (length and width) and location of meltwater tracks. The code is freely available at: doi.org/10.15131/shef.data.7999445.

- *Improved understanding of the large-scale distribution of meltwater tracks in Canada.* Meltwater tracks have been studied before in relatively localised studies; however, I confirm their widespread occurrence across the LIS bed. Large-scale mapping also provides insight into the distribution of these features and their association with other meltwater landforms (i.e. tunnel valleys and eskers) and background controls (i.e. geology and sediment thickness).

- *First large-scale holistic map of subglacial drainage networks (meltwater pathways) in Keewatin, Canada.* This study is the first to apply a holistic meltwater mapping approach across a large (~ 1 million km^2) area. It demonstrates the clear spatial associations between 'different' meltwater landforms and confirms the need to consider this in future mapping endeavours and when attempting to explain their formation. Mapping of the meltwater pathways is freely available at: doi.org/10.15131/shef.data.12752987.v1.

- *Exploration of meltwater landform distribution, expression and controls.* Meltwater corridors are the most common meltwater landform recorded,

identified at 84 % of all sample points while eskers were only recorded at 43 % (often occurring within meltwater corridors). Meltwater corridors are an order of magnitude wider than the eskers they often contain. Combining all expressions of meltwater drainage results in an average spacing of 8 km, which is at the lower end of what is predicted in the literature using esker ridges alone. Meltwater pathways are most prolific where basal topography is roughest and scarcest in areas coincident with palaeo-ice streams. At a study-wide scale, eskers occur most commonly on harder rock and meltwater corridors on sedimentary rock.

- *A new model of meltwater corridor formation.* Based on the geomorphological observations of the holistic drainage map and the known occurrence of processes in contemporary settings, a new model for meltwater corridor formation is proposed. This is founded on the idea that variable surface meltwater inputs cause the repeated over-pressurisation of subglacial conduits within an ice sheet's ablation zone, forcing the conduit to periodically connect and interact with the surrounding hydraulically-connected distributed drainage zone either side. Repeated interactions (i.e. expansion of linked cavities, localised sheet floods or lateral conduit migration) are hypothesised to result in the observed geomorphic work (i.e. formation of corridors) with the lateral extent influenced by the duration, magnitude and frequency of the water pressure perturbations. This theory provides an overarching mechanism and brings together previously disparate theories based on morphological and sedimentological work, which suggest a range of erosional and depositional processes (e.g. St-Onge, 1984; Rampton, 2000; Utting et al. 2009). The model is supported by observations from contemporary and modelling studies.

- *Estimate of the spatial impact of meltwater drainage on the ice sheet bed*. The interaction between a conduit and the surrounding hydraulically-connected distributed drainage system has been identified in contemporary settings but a lack of direct observations means that the reality of this connection – its spatial and temporal occurrence, its expression, and its impact – remains speculative. An ice sheet's palaeo-bed offers potential to contextualise limited spatio-temporal contemporary observations to address these issues. If we assume the

model is correct, it suggests that between 5 - 36 % of the bed experienced meltwater interactions within the ablation zone, which is 25 times greater than estimates using eskers alone. This may help explain the large impact conduits have on overlying ice sheet dynamics relative to their dimensions.

- *Widespread identification of a mechanism for conduits to scavenge sediment from their surroundings.* The model proposed in Chapter 3 supports the idea that conduit overpresurisation and the subsequent interaction with the surrounding distributed drainage system (e.g. Hubbard et al. 1995; Swift et al. 2005a) can erode and entrain sediment at the bed, beyond the width of the conduit, to produce the meltwater corridor imprint. The variability of surface meltwater delivery to the bed, which influences this interaction, may therefore be more important for determining how much sediment is available for landform construction at the margin than the sediment coverage.

- *First large-scale mapping of esker beads, nets and fans.* Mapping of these different esker assemblages facilitates the detection of clear spatial patterns in their distribution. This suggests the potential of a landform continuum between esker beads (formed in areas with rapid retreat and low sediment delivery rates to the margin) and terminal esker fans (formed in areas of ice margin stand-still and high sediment delivery rates to the margin).

- *Insight into the time-transgressive formation of eskers.* Landform studies have to consider the possibility of equifinality when interpreting the characteristics of a particular feature. While morphological criteria have been developed (e.g. Fig. 1.6 (Brennand, 2000)), it is often difficult to determine whether a landform formed as a result of time-transgressive versus synchronous formation using morphology alone. As esker beads and fans have been identified as indicators of time transgressive formation, mapping these may be useful for separating out landforms formed in this way. Furthermore, the widespread occurrence of these indicators confirms that many eskers within the study area formed time-transgressively at the margin. This also offers the potential to obtain high resolution margin retreat positions when features align across flow.

- *Potential links between subglacial meltwater and a) landform formation and b) ice sheet dynamics.* Observations in Chapter 4 suggest that drumlins may develop contemporaneously with meltwater pathways and that their length may reflect variable deformation conditions at the bed caused by the presence of a meltwater corridor with this effect decreasing with distance from the meltwater corridor. This supports the idea of a complex mosaic of conditions at the bed as has been identified beneath contemporary ice sheets. In another example, it is clear the channelised drainage occurred after drumlin formation due to a mismatch in flow orientations and meltwater corridors overprinted on drumlins. This occurs within an area that was previously beneath the Dubawnt Ice Stream and I hypothesise that the development of channelised drainage may have contributed to ice stream shut down owing to the large-scale dewatering of the bed and subsequent enhanced ice-bed coupling.

- *Discovery of palaeo-subglacial lakes and their drainage signatures.* Geomorphic criteria for the identification of subglacial lakes have been proposed in the literature (e.g. flat spot associated with a meltwater channel, which transitions downstream into an esker (Livingstone et al. 2016)) and I was able to identify potential examples of this within the study area. This could be helpful for separating drainage signatures formed as a result of discrete outburst events from those formed time-transgressively. The possible identification of flat spots associated with meltwater channels which then transition into esker beads towards the centre of the ice divide, may also provide insight into the signature of repeated drainages of small ice marginal lakes and potential sediment yields per event.

5.2 Limitations

Throughout this thesis a number of limitations were considered. These are outlined in detail here. There are a number of limitations associated with automatic landform mapping. For example, testing revealed that while efforts were made to reduce the impact of non-glacial land surface features, results were impacted by confounding influences (i.e. geology and human structures), resulting in falsely identified meltwater landforms. Additionally, sensitivity analysis in Chapter 2 suggested that narrower

meltwater tracks and those with more subdued topographic expressions were more likely to be missed. Nonetheless, the impact of this was mitigated within this thesis by viewing the automatic output as a first pass map and using it as a guide for more detailed manual mapping.

An implicit limitation of using meltwater landforms to make inferences about the palaeo-meltwater drainage system is the fact that we are still not entirely sure what each meltwater landform represents, i.e. what controls its absence or presence and its morphological variation (see Greenwood et al. 2016 for a review). While efforts were made here to explore underlying controls (e.g. substrate thickness, basal geology etc.) with the motivation of addressing this uncertainty, hydrological and glaciological conditions that would have also influenced the form of the hydrological system and affected the relative direction and magnitude of geomorphic work remain poorly constrained. Many of the large-scale datasets for the remote and understudied area considered in this thesis have significantly lower spatial resolution than the DEMs (e.g. geology and basal sediment maps and predicted proglacial lake locations) and are thus unlikely to facilitate the detection of small-scale changes, which may have been important. Furthermore, the widespread occurrence of meltwater features across the Keewatin sector of the LIS is likely a reflection of widespread melting conditions and therefore care must be taken not to assume that this is representative of drainage conditions earlier on in the ice sheet's life-cycle.

While the recent release of high spatial resolution DEMs has enabled the detection of additional meltwater signatures which have been proposed to represent the signature of distributed drainage (e.g. Mäkinen et al. 2017), much of the work on palaeo-hydrological systems thus far has focussed on channelised systems. While the model proposed in Chapter 3 – linking conduits with the surrounding-connected distributed drainage system – accounts for 2 of 3 modes of drainage within the 3-part drainage system (e.g. Andrews et al. 2014; Hoffman et al. 2016), the distribution and expression of drainage outside of this region, within the weakly-connected distributed, system remains unknown. Estimates from within this thesis indicate that it covers a large proportion of the bed (64 – 95 %) in agreement with its hypothesised significant impact on overlying ice sheet dynamics (e.g. Hoffman et al. 2016).

This thesis takes a large-scale morphological approach. While this has its benefits, such as the provision of a large dataset which captures a range of morphological variations and background conditions, it also has limitations. Firstly, large-scale work necessitates a degree of generalisation due to the large area covered and ultimately a sacrifice in detail to obtain knowledge on the overall pattern and distribution of landforms and processes. Meltwater pathways were mapped as centrelines (long profiles) instead of polygons that could have provided more information on the area of these features. Sampling of measurements (e.g. lateral spacing, width) along meltwater corridors was also less frequent than would have been possible for a small sample area which may have may have led to some of the more local-scale variations being missed.

While the ArcticDEM represents significant progress in the provision of free, widespread, high resolution data, it is confined to beyond 60° north (Fig. 1.12). This restricted the spatial extent of the work in this thesis. For example, previous mapping revealed the widespread presence of eskers across the Hudson Bay surrounding the Labrador Ice Dome and further south in Canada to ~ 50° north (Storrar et al. 2014a). As a result, at present, I am not able to assess the existence of meltwater tracks into this lower latitude region, in locations which are likely to exhibit different background and geological conditions. Furthermore, the study area in this thesis represents ~ 1,000 years of ice margin evolution and thus does not capture the ice sheet's complete deglaciation. As such, it is difficult to extract temporal patterns associated with a shrinking ice mass (e.g. Storrar et al. 2014b) and no clear trend is observed in metrics such as meltwater corridor width or spacing.

Finally, there is a limit to how much information can be extracted from morphological studies without additional fieldwork to confirm spatial associations or to sample sediments. Studying the sediments of these features may be key for confirming how the landforms are produced and potentially inferring additional meltwater flow conditions such as meltwater velocity or magnitude (e.g. Brennand, 2000).

5.3 Future work

There are a number of avenues of research which have been opened up by this thesis, which are summarised here. The automatic landform detection and mapping method developed in Chapter 2 could be applied to different areas of the palaeo-bed. Work from Sweden reveals the occurrence of meltwater tracks beneath the former Fennoscandian Ice Sheet (e.g. Peterson et al. 2017) and my method could be used to expand this mapping to surrounding areas (e.g. Norway, Finland or the Kola peninsula) to test how widespread they are. Additionally, it could be applied to other landforms with similar geomorphic characteristics (e.g. a high parallel conformity and a definable size range) to facilitate rapid and objective first pass mapping over large areas. Initial experimentation has revealed for instance, how this method could be applied to identify eskers.

Chapter 3 provides a large dataset of meltwater corridor distribution as well as information on the occurrence of different morphological expressions, widths, lengths and spacings. This could be useful for constraining and testing subglacial hydrology models. In particular, the results of the holistic mapping are likely to be more representative of the complete hydrological system than single landforms. It is also hoped that this thesis inspires model developments to test various hypothesis and ideas put forward here. For example, a possible positive relationship was identified between basal topographic roughness and subglacial meltwater corridor density. This could occur as a result of increased hydrological network fragmentation or due the presence of more supraglacial lakes within this area because of enhanced transfer of basal undulations (Ignéczi et al. 2018). While subglacial meltwater landforms are linked to surface meltwater delivery here and in numerous earlier studies, comparing meltwater pathways to the predicted locations of palaeo-supraglacial lakes (e.g. using methods in Ignéczi et al. (2018) but developed for palaeo-ice sheets) could help confirm this. Furthermore, detailed long-profiles hinted at a local scale control on feature expression, additional mapping and higher resolution data (substrate thickness and basal geology) are required to confirm this.

Chapter 3 proposes a model for the formation of meltwater corridors based on the idea that they represent the repeated interaction of a conduit with the surrounding

hydraulically-connected distributed drainage system over 10s – 100s of years within the ablation zone. It would be interesting to see if a model could be developed to test the role of subglacial meltwater pressure fluctuations in contributing geomorphic work and whether erosional features wider than the conduit could be created over decades to centuries using a range of likely surface meltwater inputs. This would help to address questions about the duration and magnitude of flow required for landform formation.

In Chapter 4, the presence of esker beads, ridges and fans is linked to the balance between sediment access and ice-margin retreat rate, which together are hypothesised to determine the relative rate and amount of conduit backfilling. Esker depositional models could be used to explore the impact of varying these parameters on the resultant landform. It would also be insightful to investigate how the relative magnitude and frequency of the upstream connection between the conduit and the surrounding hydraulically-connected distributed system controls sediment access and erosion and thus ultimately is key to determining sediment availability at the margin.

As well as model developments, a number of additional observations in this thesis could benefit from further research through the expansion of mapping or the identification of contemporary analogues. This is particularly true for the serendipitous findings in Chapter 4 where additional mapping will help to assess the proposed relationships hinted at within this thesis. For example, distributed drainage is generally expected to form beneath ice streams (e.g. Kamb, 1987; Bell, 2008). This is supported in this thesis by the relative sparsity of meltwater corridors beneath palaeo-ice streams (Chapter 3) and the observation that highly elongated drumlins and MSGLs beneath a section of the Dubawnt Lake palaeo-ice stream in Chapter 4 show no relationship with the sparse meltwater pathways, suggesting that channels formed later than the streaming and may have played a role in ice stream shut-down. This has been shown to occur in physical modelling experiments by Lelandais et al. (2018) and it is clear from contemporary ice streams that hydrological routing is key to the initiation and shut-down of streaming (e.g. Alley et al. 1986; Anadakrishnan and Alley, 1997; Bell, 2008). Thus, there is a clear need for additional research into the role of subglacial hydrology at palaeo-ice streams, for example mapping of hydrological signatures – particularly in the onset zone (e.g. eskers or meltwater pathways or subglacial lakes)

– and a better understanding of when each landform formed (i.e. drumlins and MSGLs versus evidence of channelised drainage). The abundance of palaeo-ice streams in Canada and the availability of the ArcticDEM makes this a good place to explore these issues.

It would be useful to see how common meltwater corridors are in different settings. In Chapter 3, I hypothesise that where less surface meltwater is delivered to the bed or ice surface slopes are shallower, the geomorphic expression of the interaction between the conduit and surrounding hydraulically connected distributed drainage system will be less extensive and more indistinct as conduits are less likely to evolve due to lower hydraulic gradients and are less likely to be over pressurised due to invariant meltwater supply. Understanding where these signatures are present / absent will help confirm or refute this theory.

Identifying modern analogues, which allow observation of these processes occurring in contemporary settings (e.g. the formation of erosional channels following a lake drainage, accurately quantifying sediment erosion rates in response to repeated pressure fluctuations over a season and identifying typical subglacial conduit migration rates) may help support the physical plausibility of the model and confirm the long-suspected importance of transient surface meltwater inputs to the bed in contributing to both ice sheet dynamics and geomorphic work. It is becoming increasingly possible to address these questions with new technologies such as on-ice passive seismology (e.g. Gimbert et al. 2016; Nanni et al. 2020) and improved satellite data (e.g. Bowling et al. 2019), which are facilitating increasingly high spatial and temporal resolution research and permitting larger areas of the contemporary ice sheet bed to be explored and monitored.

CHAPTER 6: REFERENCES

Aario, R. Associations of flutings, drumlins, hummocks and transverse ridges. Geojournal. 1(6) : 65-72. 1977.

Ahokangas, E. Mäkinen, J. Sedimentology of an ice lobe margin esker with implications for the deglacial dynamics of the Finnish Lake District lobe trunk. Boreas. 2014.

Alley, R.B. Water-pressure coupling of sliding and bed deformation : I. Water system. Journal of Glaciology. 35(119) : 108-18. 1989a.

Alley, R.B. Water-pressure coupling of sliding and bed deformation : II. Velocity-depth profiled. Journal of Glaciology. 35(119) : 119-29. 1989b.

Alley, R.B. How can low-pressure channels and deforming tills exist subglacially? Journal of Glaciology. 38(128). 1992.

Alley, R.B. Anandakrishnan, S. Bentley, C.R. Lord, N. A water-piracy hypothesis for the stagnation of ice stream C, Antarctica. Annals of Glaciology. 20 : 187-94. 1994.

Alley, R.B. Blankenship, D. Bentley, C. Rooney, S. Deformation of till beneath Ice Stream B, West Antarctica. Nature. 322 : 57-59. 1986.

Alley, R.B. Blankenship, D. Bentley, C. Rooney, S. Deformation of till beneath Ice Stream B. 3. Till deformation : evidence and implications. Journal of Geophysical Research. 92(B9) : 8921-29. 1987a.

Alley, R.B. Blankenship, D.D. Rooney, S.T. Bentley, C.R. Till beneath Ice Stream B. 4. A coupled ice-till flow model. Journal of Geophysical Research. 92(B9) : 8931-40. 1987b.

Alley, R.B. Cuffey, K.M. Evenseon, E.B. Strasser, J.C. Lawson, D.E. Larson, G.J. How glaciers entrain and transport basal sediment : physical constraints. Quarternary Science Reviews. 16 : 1017-38. 1997.

Alley, R.B. Cuffey, K.M. Zoet, L.K. Glacial erosion : status and outlook. Annals of Glaciology. 60(80) : 1-13. 2019.

Alley, R.B. Dupont, T.K. Parizek, B.R. Anandakrishnan, S. Access of surface meltwater to beds of sub-freezing glaciers : preliminary insights. Annals of Glaciology. 40(1) : 8-14. 2005.

Anandakrishnan, S. Alley, R.B. Stagnation of ice stream C, West Antarctica by water piracy. Geophysical Research Letters. 24 : 265-68. 1997.

Andrews, L.C. Catania, G.A. Hoffman, M.J. Gulley, J.D. Lüthi, M.P. Ryser, C. et al. Direct observations of evolving subglacial drainage beneath the Greenland Ice Sheet. Nature, 514(7520). 80–83. 2014.

Arrell, K. Wise, S. Wood, J. Donoghue, D. Spectral filtering as a method of visualising and removing striped artefacts in digital elevation data. Earth Processes and Landforms. 33(6): 943-61. 2008.

Ashley, G.M. Boothroyd, J.C. Borns, H.W. Sedimentology of late Pleistocene (Laurentide) deglacia-phase depostis, eastern Maine; an example of temperate marine grounded ice-sheet margin. in Anderson, J.B. and Ashley, G.M. eds. Glacial Marine Sedimentation: Palaeoclimatic Signficance: Geological Society of Americal Special Paper 261: 107-25. 1991.

Ashmore, D.W. Bingham, R.G. Antarctic subglacial hydrology: current knowledge and future challenges. Antarctic Science. 26(6). 758-73. 2014.

Attig, J.W. Mickelson, D.M. Clayton, L. Late Wisconsin landform distribution and glacier-bed conditions in Wisconsin. Sedimentary Geology. 62: 399-405. 1989.

Aylsworth, J. M. and Shilts, W. W. Glacial features around the Keewatin Ice Divide: Districts of Mackenzie and Keewatin. Geological Survey of Canada, Map 24-1987. 1:1,000,000. 1989.

Aylsworth, J.M. Shilts, W.W. Russel, H.A.J. Pyne, D.M. Eskers around the Keewatin Ice Divide: Northwest Territories and Nunavut. Geological Survey of Canada, Open File, 7047. 2012.

Baatz, M. Schäpe, A. Multiresolution Segmentation: An Optimization Approach for High Quality Multi-Scale Image Segmentation. In: Strobl, J. Blaschke, T. and Griesbner, G. Eds., Angewandte Geographische Informations-Verarbeitung, XII, Wichmann Verlag, Karlsruhe, Germany, 12-23. 2000.

Bamber, J.L. Aspinall, W.P. An expert judgement assessment of future sea level rise from the ice sheets. Nature Climate Change. 3: 424-27. 2013.

Bamber, J.L. Siegert, M.J. Griggs, J.A. Marshall, S.J. Spada, G. Paleofluvial mega-canyon beneath the central Greenland Ice Sheet. Science. 341. 2013.

Banerjee, I. McDonald, B.C. Nature of esker sedimentation. In: Jopling, A.V. McDonald, B.C. (Eds.), Glaciofluvial and Glaciolacustrine Sedimentation, vol

23. Society of Economic Palaeonologists and Mineralogists. Special Publication. 304-20. 1975.

Banwell, A.F. Arnold, N.S. Willis, I.C. Tedesco, M. Ahlstrøm, A.P. Modelling supraglacial water routing and lake filling on the Greenland Ice Sheet. Journal of Geophysical. Research. 117. 2012.

Banwell, A. Hewitt, I. Willis, I. Arnold, A. Moulin density controls drainage development beneath the Greenland ice sheet. Journal of Geophysical Research: Earth Surface. 121: 2248-69. 2016.

Banwell, A.F. MacAyeal, D.R. Sergienko, O.V. Breakup of the Larsen B Ice Shelf triggered by chain reaction drainage of supraglacial lakes. Geophysical Research Letters. 40: 5872-76. 2013b.

Banwell, A.F. Willis, I.C. Arnolod, N.S. Modeling subglacial water routing at Paakitsoq, W Greenland. Journal of Geophysical Research. Earth. 118: 1282-95. 2013a.

Bartholomaus, T.C., Anderson, R.S. Anderson, S.P. Response of glacier basal motion to transient water storage. Nature Geoscience, 1. 33–37. 2008.

Bartholomew, I. Nienow, P. Sole, A. Mair, D. Cowton, T. King, M.A. Short-term variability in Greenland ice sheet motion forced by time varying meltwater drainage: Implications for the relationship between subglacial drainage system behaviour and ice velocity. Journal of Geophysical Research. 117. 2012.

Bartholomew, I. Nienow, P. Mair, D. Cowton, T. Palmer, S. Wadham, J. Supraglacial forcing of subglacial draiange in the ablation zone of the Greenland ice sheet. Geophysical Rsearch Letters. 38. 2011.

Bartholomew, I. Nienow, P. Mair, D. Hubbard, A. King, M.A. Sole, A. Seasonal evolution of subglacial drainage and acceleration in Greenland outlet glacier. Nature Geoscience. 3: 408-11. 2010.

Beaud, F. Flowers, G. Venditti, J.G. Modeling sediment transport in ice-walled subglacical channels and its implications for esker formation and proglacial sediment yields. Journal of Geophysical Research: Earth Surface. 123: 3206-27. 2018a.

Beaud, F. Venditti, J.G. Flowers, G.E. Koppes, M. Excavation of subglacial bedrock channels by seasonal meltwater flow. Earth Surface Processes and Landforms. 2018b.

Bell, R.E. The role of subglacial water in ice-sheet mass balance. Nat. Geosci. 1(5): 297-304. 2008.

Benn, D.I. Evans, D.J.A. Glaciers and Glaciation, 2 ed. Hodder Eductation, Euston Road, London, UK. 2010.

Bennett, M.R. Ice streams as the arteries of an ice sheet: their mechanics, stability and significance. Earth Science Reviews. 61: 309-39. 2003.

Bennett, G.L. Evans, D.J.A. Carbonneau, P. Twigg, D.R. Evolution of a debris-charged glacier landsystem, Kvíárjökull, Iceland. Journal of Maps. 6: 40-67. 2010.

Bennett, M.R. Glasser, N.F. Glacial Geology: Ice Sheets and Landfroms. Wiley, Chichester. 364. 1996.

Bennett, M.R. Huddart, D. Thomas, G.S.P. The Newbigging esker system, Lanarkshire, Southern Scotland: a model for composite tunnel, subaqueous fan and supraglacial esker sedimentation. Glacial Sedimentary Processes and Products: Special Publication 39 of the IAS, John Wiley and Sons, Incorporated, Hokoken. 177-202. 2009.

Bindscahlder, R.A. The importance of pressurized subglacial water in seperation and sliding at the glacier bed. Journal of Glaciology. 57: 929-41. 1983.

Bingham, R.G. Nienow, P.W. Sharp, M.J. Boon, S. Subglacial drainage processes at a High Arctic polythermal valley glacier. Journal of Glaciology. 51(172): 15-24. 2005.

Bingham, R.G. Hubbard, A.L. Nienow, P.W. Sharp, M.J. An investigation into the mechanisms controlling seasonal speedup events at a High Arctic glacier. Journal of Geophysical Research. 113. 2008.

Bishop, M.P. Allan James, L. Shroder, J.F. Walsh, S.J. Geospatial technologies and digital geomorphological mapping: Concepts, issues and research. Geomorphology. 137: 5-26. 2012.

Björnsson, H. Subglacial lakes and jökulhlaups in Iceland. Global and Planetary Change. 35: 255-71. 2003.

Blatter, H. On the thermal regime of an Arctic valley glacier: A study of White Glacier, Axel, Heiberg Island, NWT, Canada. Journal of Glaciology. 33(114). 200-11. 1987.

Bouchard, M.A. Subglacial landforms and deposits in central and northern Quebec, Canada, with emphasis on Rogen moraines. Sedimentary Geology. 62: 293-308. 1989.

Bougamont, M. Tulaczyk, S. Joughin, I. Response of subglacial sediments to basal freeze-on 2. Application in numerical modeling of the recent stoppage of Ice Stream C, West Antarctica. Journal of Geophysical Research. Solid Earth. 2003.

Bolduc, A.M. The formation of eskers based on their morphology, stratigraphy and lithologic composition, Labrador, Canada (Unpublished Ph.D thesis). Lehigh University. 1992.

Boon, S. Sharp, M. The role of hydrologically-driven ice fracture in drainage system evolution on an Arctic glacier. Geophysical Research Letters. 30(18). 2003.

Bougamont, M. Tulaczyk, S. Joughin, I. Response of subglacial sediments to basal freeze-on -2. Application in numerical modlling of the recent stoppage of Ice Stream C, West Antarctica. Journal of Geophysical Research. Solid Earth. 108(B4). 2003.

Boulton, G.S. The origin of glacially fluted surface – observations and theory. Journal of Glaciology. 17(76): 287-309. 1976.

Boulton, G.S. Theory of glacial erosion, transport and deposition as a consequence of subglacial sediment deformation. Journal of Glaciology. 42. 1996.

Boulton, G. S., Caban, P. E. and Van Gijssel, K. Groundwater flow beneath ice sheets: part I - large scale patterns. Quaternary Science Reviews, 14, 545-562. 1995.

Boulton, G.S. Clark, C.D. A highly mobile Laurentide Ice Sheet revealed by satellite images of glacial lineations. Nature. 346: 813-17. 1990.

Boulton, G.S. Dobbie, K.E. Zatsepin, S. Sediment deformation beneath glaciers and its coupling to the subglacial hydraulic system. Quaternary International. 86: 3-28. 2001.

Boulton, G. S., Hagdorn, M., Maillot, P. B. and Zatsepin, S. Drainage beneath ice sheets: groundwater-channel coupling, and the origin of esker systems from former ice sheets. Quaternary Science Reviews, 28, 621-638. 2009.

Boulton, G.S. Hindmarsh, R.C.A. Sediment deformation beneath glaciers: rheology and geological consequences. Journal of Geophysical Research. 92. 9059-82. 1987.

Boulton, G.S. Lunn, R. Vidstrand, P. Zatspein, S. Subglacial drainage by groundwater-channel coupling, and the origin of esker systems: Part I – Glaciological observaations. Quaternary Science Reviews. 26(7–8). 1067-90. 2007a.

Boulton, G.S. Lunn, R. Vidstrand, P. Zatspein, S. Subglacial drainage by groundwater-channel coupling, and the origin of esker systems: Part II - Theory and simulation of a modern system. Quaternary Science Reviews. 26(7–8). 1091–105. 2007b.

Bouvier, V. Johnson, M.D. Påsse, T. Distribution, genesis and annual-origin of De Geer moraines in Sweden: insights revealed by LiDAR. GFF. 137. 2015.

Bowling, J.S. Livingstone, S.J. Sole, A.J. Chu, W. Distribution and dynamics of Greenland subglacial lakes. Nature Communications. 2019.

Boyd, R. Scott, D.B. Douma, M. Glacial tunnel valleys and Quaternary history of the outer Scotian Shelf. Nature. 333: 61-64. 1988.

Brennand, T.A. Macroforms, large bedforms and rhythmic sedimentary sequences in subglacial eskers, south-central Ontario: implications for esker genesis and meltwater regime. Sedimentary Geology. 91(1). 9-55. 1994.

Brennand, T.A. Deglacial meltwater drainage and glaciodynamics: Inferences from Laurentide eskers, Canada. Geomorphology. 32(3–4). 263–93. 2000.

Brennand, T.A. Shaw, J. Tunnel channels and associated landforms, south-central Ontario: their implication for ice-sheet hydrology. Canadian Journal of Earth Sciences. 31. 505-22. 1994.

Brennand, T.A. Shaw, J. The Harricana glaciofluvial complex, Abitibi region, Quebec: its genesis and implications for meltwater regime and ice-sheet dynamics. Sedimentary Geology. 102(3-4). 221-62. 1996.

Briner, J.P. Supporting evidence from the New York drumlin field that elongate subglacial bedforms indicate fast ice flow. Boreas. 36(2): 143-47. 2007.

Burke, M.J. Brennand, T.A. Perkins, A.J. Erosional corridor evolution in south-central British Columbia: insights from ground-penetrating radar surveys. Proceedings of Geohydro 2011. 2011.

Burke, M.J. Brennand, T.A. Perkins, A.J. Evolution of the subglacial hydrologic system beneath the rapidly decaying Cordilleran Ice Sheet by ice-dammed lake

drainage: implications for meltwater-induced ice acceleration. Quaternary Science Reviews. 50: 125-40. 2012.

Burke, M.J. Brennand, T.A. Sjogren, D.B. The role of sediment supply in esker formation and ice tunnel evolution. Quaternary Science Reviews. 115: 50-77. 2015.

Burke, M.J. Woodward, J. Russell, A.J. Fleisher, P.J. Structural controls on englacial esker sedimentation: Skeidarárjökull, Iceland. Annals of Glaciology. 50: 85-92. 2009.

Burke, M.J. Woodward, J. Russell, A.J. Fleisher, P.J. Bailey, P.J. Controls on the sedimentary architecture of a single event englacial esker: Skeidarárjökull, Iceland. Quaternary Science Reviews. 27: 1829-47. 2008.

Burke, M.J. Woodward, J. Russell, A.J. Fleisher, P.J. Bailey, P.J. The sedimentary architecture of outburst flood eskers: a comparison of ground-penetrating radar data from Bering Glacier, Alaska and Skeirarárjökull. Iceland Geological Society AM. Bull. 122: 1637-45. 2010.

Capps, D.M. Rabus, B. Clague, J.L. Shugar, D.H. Identification and characterisation of alpine subglacial lakes using interferometric synthetic aperture radar (inSAR): Brady Glacier, Alaska, USA. Journal of Glaciology. 56(199). 2010.

Carlson, A.E. Anslow, F.S. Obbink, E.A. LeGrande, A.N. Ullman, D.J. Licciardi, J.M. Surface melt driven Laurentide Ice Sheet retreat during the early Holocene. Geophysical Research Letters. 36. 2009.

Carlson, A.E. Clark, P.U. Ice sheet sources of sea level rise and freshwater discharge during the last deglaciation. Reviews of Geophysics. 50(4). 2012.

Carlson, A.E. Legrande, A.N. Oppo, D.W. Came, R.E. Schmidt, G.A. Anslow, F.S. Licciardi, J.M. Obbink, E.A. Rapid early Holocene deglaciation of the Laurentide ice sheet. Nature Geoscience. 1(9): 620-24. 2008.

Carrivick, J.L. Quincey, D.J. Progressive increase in number and volume of ice-marginal lakes on the western margin of the Greenland Ice Sheet. Global Planetary Change. 116: 156-63. 2014.

Carter, S.P. Fricker, H.A. Siegfried, M.R. Antarctic subglacial lakes drain through sediment floored canals: theory and model testing on real and idealized domains. The Cryosphere. 11(1): 381-405. 2017.

Carter, S.P. Blankenship, D.D. Young, D.A. Peters, M.E. Holt, J.W. Siegert, M.J. Dynamic distributed drainage implied by the flow evolution of the 1996-1998 Adventure Trench subglacial lake discharge. Earth and Planetary Science Letters. 283: 24-37. 2009.

Carter, S.P. Fricker, H.A. Siegfried, M.R. Evidence of rapid subglacial water piracy under Whillans Ice Stream, West Antarctica. Journal of Glaciology. 59(218). 2013.

Catania, G.A. Neumann, T.A. Persistent englacial drainage features in the Greenland Ice Sheet. Geophysical Research Letters. 37. 2010.

Catania, G.A. Neumann, T.A. Price, S.F. Characterizing englacial drainage in the ablation zone of the Greenland ice sheet. Journal of Glaciology. 54(187): 567-78. 2008.

Catania, G. Paola, C. Braiding under glass. Geology. 29(3): 259-62. 2001.

Catania, G.A. Scambos, T.A. Conway, H. Raymond, C.F. Sequential stagnation of Kamb Ice Stream, West Antarctica. Geophysical Research Letters. 33. 2006.

Cazenave, A. Llovel, W. Contemporary sea level rise. Ann. Rev. Mar. Sci. 2: 145-73. doi: 10.1146/annurev-marine-120308-081105. 2010.

Chandler, B. M. P., Lovell, H., Boston, C. M., Lukas, S., Barr, I. D., Benn, D. I., Clark, C. D., Darvill, C. M., Evans, D. J. A., Ewertowski, M., Loibl, D., Margold, M., Otto, J., Roberts, D. H., Stokes, C. R., Storrar, R. D. and Stroeven, A. Glacial geomorphological mapping: a review of approaches and frameworks for best practice. Earth-Science Reviews, 185, 806-846. 2018.

Chandler, D.M. Wadham, J.L. Lis, G.P. Cowton, T. Sole, A. Bartholomew, I. Telling, J. Nienow, P. Bagshaw, E.B. Mair, D. Vinen, S. Hubbard, A. Evolution of the subglacial drainage system beneath the Greenland Ice Sheet revealed by tracers. Nature Geoscience. 6: 195-98. 2013.

Chapwanya, M. Clark, C.D. Fowler, A.C. Numerical computations of a theoretical model of ribbed moraine formation. Earth Surface Processes Landforms. 36: 1101-12. 2011.

Cheel, R.J. The depositional history of an esker near Ottawa, Canada. Canadian Journal of Earth Sciences. 19: 1417-27. 1982.

Cheel, R.J. Rust, B.R. A sequence of soft-sediment deformation (dewatering) structures in Late Quaternary subaqueous outwash near Ottawa, Canada. Sedimentary Geology. 47: 77-93. 1986.

Christianson, K. Peters, L.W. Alley, R.B. Anandakrishnan, S. Jacobel, R.W. Riversman, K.W. Muto, A. Keisling, B.A. Dilatant till facilitates ice-stream flow in northeast Greenland. Earth Planet. Sci. Lett. 401: 57-69. 2014.

Christoffersen, P. Bougamont, M. Carter, S.P. Fricker, H.A. Tulaczyk, S. Significant groundwater contribution to Antarctic streams hydrologic budget. Geophysical Research Letters. 41. 2003-10. 2014.

Christoffersen, P. Tulaczyk, S. Wattrrus, N.J. Peterson, J. Quintana-Krupinski, N. Clark, C.D. Sjunneskog, C. Large subglacial lake beneath the Laurentide Ice Sheet inferred from sedimentary sequences. Geology. 36(7): 563-66. 2008.

Chu, W. Creyts, T.T. Bell, R.E. Rerouting of subglacial water flow between neighbouring glaciers in West Greenland. Journal of Geophysical Research: Earth Surface. 121(5). 2016.

Chudley, T.R. Christoffersen, P. Doyle, S.H. Bougamont, M. Schoonman, C.M. Hubbard, B. James, M.R. Supraglacial lake drainage at a fast-flowing Greenlandic outlet glacier. PNAS. 116(51): 25468-77. 2019.

Clapperton, C.M. Channels formed by the superimposition of glacial meltwater streams, with special reference to the East Cheviot Hills, north-west England. Geographical Annals Series A. Physical Geography. 207-20. 1968.

Clark, C.D. Mega-scale glacial lineations and cross-cutting ice-flow landforms. Earth Surface Processes Landforms. 18: 1-29. 1993.

Clark, C.D. Emergent drumlins and their clones: from till dilatancy to flow instabilities. Journal of Glaciology. 56: 1011-25. 2010.

Clark, C.D. Evans, D.J.A. Khatwa, A. Bradwell, T. Jordan, C.J. Marsh, S.H. Mitchell, W.A. Bateman, M.D. Map and GIS database of glacial landforms and features related to the British Ice Sheet. Boreas. 33: 359-75. 2004.

Clark, C.D. Hughes, A.L.C. Greenwood, S.L. Jordan, C. Sejrup, H.P. Pattern and timing of retreat of the last British-Irish Ice Sheet. Quaternary Science Reviews. 44: 112-46. 2012.

Clark, C.D. Hughes, A.L.C. Greenwood, S.L. Spagnolo, M. Ng, F.S.L. Size and shape characteristics of drumlins, derived from a large sample, and associated scaling laws. Quaternary Science Reviews. 28: 677-92. 2009.

Clark, C.D. Stokes, C.R. Extent and basal characteristics of the M'Clintock Channel Ice Stream. Quaternary Internations. 86(1): 81-101. 2001.

Clark, P.U. Walder, J.S. Subglacial drainage, eskers, and deforming beds beneath the Laurentide and Eurasian ice sheets. Geol. Soc. Am. Bull. 106: 304 – 14. 1994.

Clarke, G.K.C. Fast glacier flow: Ice streams, surging and tidewater glaciers. Journal of Geophysical Research. 92:8835-41. 1987.

Clarke, G.K.C. Subglacial processes. Annual Review of Earth and Planetary Sciences. 33: 299-313. 2005.

Clason, C.C. Mair, D.WF. Nienow, P.W. Bartholomew, I.D. Sole, A. Palmer, S. Schwanghart, W. Modelling the transfer of supraglacial meltwater to the bed of Leverett Glacier, Southwest Greenland. The Cryosphere. 9: 123-38. 2015.

Clayton, L. Attig, J.W. Mickelson, D.M. Tunnel channels formed in Wisconsin during the last glaciation. In: Mickelson, D.M. Attig, J.W. (eds.), Glacial Processes Past and Present. Geological Society of America, Special Paper. 337: 69-82. 1999.

Colgan, W. Rajaram, H. Anderson, R. Steffen, K. Phillips, T. Joughin, I. Abdalati, W. The annual glaciohydrology cycle in the ablation zone of the Greenland ice sheet: Part 1. Hydrology model. Journal of Glaciology. 57(204): 697-709. 2012.

Colgan, W. Steffen, K. McLamb, W.S. Abdalati, W. Motyka, R. Phillips, T. Anderson, R. An increase in crevasse extent, West Greenland: Hydrologic implications. Geophysical Research Letters. 38(18). 2011.

Collins, D.N. Seasonal development of subglacial drainage and suspended sediment delivery to meltwater beneath an Alpine glacier. Annals of Glaciology. 13: 45-50. 1989.

Collins, D.N. Seasonal and annual variations of suspended sediment transport in meltwaters draining from an Alpine glacier. International Association of Hydrological Sciences Publication. 193: 439-46. 1990.

Cook, S.J. Swift, D.A. Kirkbride, M. Knight, P.G. Waller, R.I. The empirical basis for modelling glacial erosion rates. Nature Communications. 2020.

Cooley, S.W. Christoffersen, P. Observation bias correction reveals more rapidly draining lakes on the Greenland Ice Sheet. Journal of Geophysical Research. Earth Surface. 122: 1867-81. 2017.

Copland, L. Sharp, M. Mapping thermal and hydrological conditions beneath a polythermal glacier with radio-echo sounding. Journal of Glaciology. 47(157): 232-42. 2001.

Cowton, T. Nienow, P. Sole, A. Wadham, J. Lis, G. Bartholomew, I. et al. Evolution of drainage system morphology at a land-terminating Greenlandic outlet glacier. Journal of Geophysical Research. Earth Surface Processes. 118. 29-41. 2013.

Cowton, T. Nienow, P. Sole, A. Bartholomew, I. Mair, D. Variability in ice motion at a land-terminating Greenlandic outlet glacier: the role of channelized and distributed drainage systems. Journal of Glaciology. 62(233): 451-66. 2016.

Cowton, T. Nienow, P. Bartholomew, I. Sole, A. Mair, D. Rapid erosion beneath the Greenland ice sheet. Geology. 40: 343:46. 2012.

Crozier, J. Karlstrom, L. Yang, K. Basal control of supraglacial meltwater catchments on the Greenland Ice Sheet. Cryosphere. 12: 3383-407. 2018.

Cummings, D.I. Kjarsgaard, B.A. Russell, H.A.J. Sharpe, D.R. Eskers as mineral exploration tools. Earth Science Reviews. 109: 32-43. 2011a.

Cummings, D.I. Gorrell, G. Guillbault, J-P. Hunter, J.A. Logan, C. Ponomarenko, D. Pugin. A. J-M. Pullan, S.E. Russell, H.A.J. Sharpe, D.R. Sequence stratigraphy of a glaciated basin fill, with a focus on esker sedimentation. Geological Society of American Bulletin. 2011b.

Cutler, P.M. Colgan, P.M. Mickelson, D.M. Sedimentological evidence for outburst floods from the Laurentide Ice Sheet margin in Wisonsin, USA: implications for tunnel-channel formation. Quaternary Internationl. 90. 23-40. 2002.

Dahlgren, S. Subglacially meltwater eroded hummocks. MSc Thesis. Department of Earth Sciences, University of Gothenburg. 2013.

Dalton, A.S. Margold, M. Stokes, C.R. Tarasov, L. Dyke, A.S. et al. An updated radiocarbon-based ice margin chronology for the last deglaciation of the North American Ice Sheet Complex. Quaternary Science Reviews. 234. 2020.

Das, S.B. Joughin, I. Behn, M.D. Howat, I.M. King, M.A. Lizarralde, D. Bhatia, M.P. Fracture propagation to the base of the Greenland Ice Sheet during supraglacial lake drainage. Science. 320 (5877). 963-64. 2008.

Davison, B.J. Sole, A.J. Livingstone, S.J. Cowton, T.W. Nienow, P.W. The influence of hydrology on the dynamics of land-terminating sectors of the Greenland Ice Sheet. Front. Earth Sci. 7:10. 2019.

De Angelis, H. Glacial geomorphology of the east-central Canadian Arctic. Journal of Maps. 323-41. 2007.

Decaux, L. Grabiec, M. Ignatiuk, D. Jania, J. Role of discrete water recharge from supraglacial drainage systems in modelling patterns of subglacial conduits in Svalbard glaciers. The Cryosphere. 13: 735-52. 2019.

de Fleurian, B. Morlighem, M. Seroussi, H. Rignot, E. van den Broeke, M.R. Kuipers Munneke, P. Mouginot, J. Smeets, P.C.J.P. Tedstone, A.J. A modelling study of the effect of runoff variability on the effective pressure beneath Russell Glacier, West Greenland. Journal of Geophysical Research: Earth Surace. 121(10). 2016.

De Geer, G. Om rullstensåsarnas bildningssätt, Geologiska Föreningen i Stockholm Förhandlingar. 19: 366-88. 1897.

De Geer, G. Geochronolgie der letzten 12 000 Jahre, The 11th International Geological Congress in Stockholm. 457-71. 1910.

Delaney, C.A. Morphology and sedimentology of the Rooskagh Esker, Co. Roscommon. Irish Journal of Earth Sciences. 19: 5-22. 2001

Delaney, I. Bauder, A. Werder, M.A. Farinotti, D. Regional and annual variability in subglacial sediment transport by water for two glaciers in the Swiss Alps. Frontiers in Earth Science. 6: 175. 2018.

Diemer, J.A. Subaqueous outwash deposits in the Ingraham ridge, Chazy, New York. Canadian Journal of Earth Sciences. 25: 1384-96. 1988.

d'Oleire-Oltmanns, S. Eisank, C. Dragut, L. Blaschke, T. An object-based workflow to extract landforms at multiple scales from two distinct data types. IEEE Geoscience and Remote Sensing Letters. 10(4): 947-51. 2013.

Dow, C.F. Kulessa, B. Rutt, I.C. Doyle, S.H. Hubbard, A. Upper bounds on subglacial channel development for interior regions of the Greenland ice sheet. Jounral of Glaciology. 60(224). 2014.

Dow, C.F. Kulessa, B. Rutt, I.C. Tsai, V.C. Pimentel, S. Doyle, S.H. van As, D. Lindbäck, K. Pettersson, R. Jones, G.A. Hubbard, A. Modeling of subglacial hydrological development following rapid supraglacial lake drainage. Journal of Geophysical Research: Earth Surface. 120: 1127-47. 2015.

Dowdeswell, J.A. Hogan, K.A. Arnold, N.D. Mugford, R.I. Wells, M. Hirst, P.P. Decalf, C. Sediment-rich meltwater plumes and ice-proximal fans at the margins of modern and ancient tidewater glaciers: observations and modelling. Sedimentology. 62: 1665-92. 2015.

Dowdeswell, J.A. Siegert, M.J. The physiography of modern Antarctic subglacial lakes. Global and Planetary Change. 35: 221-36. 2002.

Dowling, T.P.F. Möller, P. Spagnolo, M. Rapid subglacial streamlined bedform formation at a calving bay margin. Journal of Quaternary Science. 31(8). 879-92. 2016.

Downs, J.Z. Johnsson, J.V. Harper, J.T. Meierbachtol, T. Werder, M.A. Dynamic hydraulic conductivity reconciles mismatch between modeled and observed winter subglacial water pressure. Journal of Geophysical Research: Earth Surface. 123: 818-36. 2018.

Doyle, S.H. Hubbard, A.L. Dow, C.F. Jones, G.A. Fitzpatrick, A. Gusmeroli, A. Kulessa, B. Lindback, K. Pettersson, R. Box, J.E. Ice tectonic deformation during the rapid in situ drainage of a supraglacial lake on the Greenland Ice Sheet. The Cryosphere. 7: 129-40. 2013.

Doyle, S.H. Hubbard, A. Fitzpatrick, A.A.W. van As, D. Mikkelsen, A.B. Pettersson, R. et al. Persistent flow acceleration within the interior of the Greenland ice sheet. Geophysical Research Letters. 41: 899-905. 2014.

Doyle, S.H. Hubbard, A. Van De Wal, R.S. van As, D. Scharrer, K. Meierbachtol, T.W. et al. Amplified melt and flow of the Greenland ice sheet driven by late-summer cyclonic rainfall. Nature Geoscience. 8: 647-53. 2015.

Dredge, L. Nixon, F. Richardson, R. Surficial Geology, Northwestern Manitoba: Geological Survey of Canada, 'A' Series Map 1608A, 1: 500 000. 1985.

Drews, R. Pattyn, F. Hewitt, I.J. Ng, F.S.L. Berger, S. Matsuoka, K. Helm, V. Bergeot, N. Favier, L. Neckel, N. Actively evolving subglacial conduits and eskers initiate ice shelf channels at an Antarctic grounding line. Nature Communications. 2017.

Dungan, J.L. Toward a comprehensive view of uncertainty in remote sensing analysis. In Uncertainty in Remote Sensing and GIS, G.M. Foody and P.M. Atkinson (Eds). 25-35. (Chichester, UK: Wiley). 2002.

Dunlop, P. Clark, C.D. The morphological characteristics of ribbed moraine. Quaternary Science Reviews. 25: 1668-91. 2006.

Dunlop, P. Clark, C.D. Hindmarsh, R.C.A. Bed ribbing instability explanation: testing a numerical model of ribbed moraine formation arising from coupled flow of ice and subglacial sediment. Journal of Geophysical Research. 113(15). 2008.

Dyke, A.S. Moore, A. Robertson, I. Deglaciation of North America. Geological Survey of Canada. Open File, 1574. 2003.

Dyke, A.S. Prest, V.K. Late Wisconsinan and Holocene history of the Laurentide ice sheet. Geog. Phys. Quat. 41: 237-64. 1987.

Ehlers, J. Linke, G. The origin of deep buried channels of Elsterian age in Northwest Germany. Journal of Quaternary Science. 4(3): 255-65. 1989.

Eisank, C. Smith, M.J. Hillier, J.K. Assessment of multiresolution segmentation for delimiting drumlins in digital elevation models. Geomorphology. 214: 452-64. 2014.

Ely, J.C. Clark, C.D. Spagnolo, M. Hughes, A.L.C. Stokes, C.R. Using the size and position of drumlins to understand how they grow, interact and evolve. Earth Surface Processes and Landforms. 43: 1073-87. 2018.

Ely, J.C. Clark, C.D. Spagnolo, M. Stokes, C.R. Greenwood, S.L. Anna, L.C. Hughes, Dunlop, P. Hess, D. Do subglacial bedforms comprise a size and shape continuum? Geomorphology. 257(15): 108-119. 2016.

Engelhardt, H. Harrison, W. Kamb, B. Basal sliding and conditions at the glacier bed as revealed by bore-hole photography. Journal of Glaciology. 20: 469-508. 1978.

Engelhardt, H. Kamb, B. Basal hydraulic system of a West Antarctic ice stream: constraints from basal observations. 43(144): 207-30. 1997.

Evans, D.J.A. Clark, C.D. Mitchell, W.A. The last British Ice Sheet: a review of the evidence utilised in the compilation of the Glacial Map of Britain. Earth Science Reviews. 70: 253-12. 2005.

Evans, D.J.A. Phillips, E.R. Hiemstra, J.F. Auton, C.A. Subglacial till: Formation, sedimentary characteristics and classification. Earth-Science Reviews. 78: 115-76. 2006.

Evans, I.S. Geomorphometry and landform mapping: what is a landform? Geomorphology. 137: 94-106. 2012.

Evatt, G.W. Fowler, A.C. Clark, C.D. Hutton, N.R.J. Subglacial floods beneath ice sheets. Philosophical Transactions of The Royal Society A. 364. 2006.

Fisher, T.G. Jol, H.M. Boudreau, A.M. Saginaw Lobe tunnel channels (Laurentide Ice Sheet) and their significance in south-central Michigan, USA. Quaternary Science Reviews. 24(22): 2375-91. 2005.

Fitzpatrick, A.A.W. Hubbard, A.L. Box, J.E. Quincey, D.J. van As, D. Mikkelsen, A.P.B. et al. A decade (2002-2012) of lake volume estimates across Russell Glacier, West Greenland. Cryosphere. 8: 107-21. 2014.

Flament, T. Berthier, E. Remy, F. Cascading water underneath Wilkes Land, East Antarctic ice sheet, observed using altimetry and digital elevation models. The Cryosphere. 8(2): 673-87. 2014.

Flowers, G.W. Modelling water flow under glaciers and ice sheets. Proceedings Royal Society A. 471. 2015.

Foroutan, M. Zimbelman, J.R. Semi-automatic mapping of linear-trending bedforms using 'Self-Organising Maps' algorithm. Geomorphology. 293(A): 156-66. 2017.

Forster, R.R. Box, J.E. van den Broeke, M.R. Miège, C. Burgess, E.W. van Angelen, J.H. Lenaerts, J.T.M. Koenig, L.S. Paden, J. Lewis, C. Prasad Gogineni, S. Leuschen, C. McConnel, J.R. Extensive liquid meltwater storage in firn within the Greenland ice sheet. Nature Geoscience. 7: 95-98. 2014.

Fountain, A. Borehole water-level variations and implications for the subglacial hydraulics of South Cascade Glacier, Washington State, USA. Journal of Glaciology. 40(135): 293-304. 1994.

Fountain, A.G. Walder, J.S. Water flow through temperate glaciers. Rev. Geophys. 36: 299-328. 1998.

Fowler, A. Sliding with cavity formation. Journal of Glaciology. 33: 131-41. 1987.

Fowler, A.C. Instability modelling of drumlin formation incorporating lee-side cavity growth. Proc. Royal Soc. Lond. Ser. A Math. Phys. Eng. Sci. 465: 2681-702. 2009.

Freeze, R.A. Cherry, J.A. Groundwater. Prentice Hall, Englewoods Cliffs, NJ. 1979.

Fricker, H.A. Scambos, T. Bindschadler, R. Padman, L. An active subglacial water system in West Antarctica mapped from space. Science. 315(5818). 2007.

Fricker, H.A. Siegfried, M.R. Carter, S.P. Scambos, T.A. A decade of progress in observing and modelling Antarctic subglacial water systems. Philosophical Transactions of the Royal Society A. 374(2059). 2016.

Fudge, T.J. Humphrey, N.F. Harper, J.T. Pfeffer, W.T. Diurnal fluctuations in borehole water levels: configuration of the drainage system beneath Bench Glacier, Alaska, USA. Journal of Glaciology. 54(185). 2008.

Fulton, R.J. Surficial materials of Canada. Geological Survey of Canada, 'A' Series Map 1880A. 1:5,000,000. 1995.

Gilbert, A. Flowers, G.E. Miller, G.H. Rabus, B.T. Van Wychen, W. Gardner, A.S. Copland, L. Sensitivity of Barnes Ice Cap, Baffin Island, Canada, to climate state and internal dynamics. Journal of Geophysical Research: Earth Surface. 121: 1516-39. 2016.

Gillet-Chaulet, F. Gagliardini, O. Seddik, H. Nodet, M. Durand, G. Ritz, C. et al. Greenland ice sheet contribution to sea-level rise from a new-generation ice sheet model. Cryosphere. 6: 1561-76. 2012.

Gimbert, F. Tsai, V.C. Amundson, J.M. Bartholomaus, T.C. Walter, J.I. Subseasonal changes observed in subglacial channel pressure, size and sediment transport. Geophysical Research Letters. 43: 3786-94. 2016.

Goeller, S. Steinhage, D. Thoma, M. Grosfeld, K. Assessing the subglacial lake coverage of Antarctica. Annals of Glaciology. 57: 109-17. 2016.

Gordon, S. Sharp, M. Hubbard, B. Smart, C. Ketterling, B. Willis, I. Seasonal reorganization of subglacial drainage inferred from measurements in boreholes. Hydrological Processes. 12. 105-33. 1998.

Gorrell, G. Shaw, J. Deposition in an esker, bead and fan complex, Lanark, Ontario, Canada. Sedimentary Geology. 72(3-4): 285-314. 1991.

Greenwood, S.L. Clark, C.D. Subglacial bedforms of the Irish Ice Sheet. Journal of Maps. 4(1): 325-57. 2008.

Greenwood, S.L. Clark, C.D. The sensitivity of subglacial bedform size and distribution to substrate lithological control. Sedimentary Geology. 232: 130-44. 2010.

Greenwood, S.L. Clason, C.C. Helanow, C. Margold, M. Theoretical, contemporary observational and palaeo-perspectives on ice sheet hydrology: Processes and products. Earth Science Reviews. 155: 1-27. 2016.

Glasser, N.F. Sambrook Smith, G.H. Glacial meltwater erosion of the Mid-Cheshire Ridge: implications for ice dynamics during the Late Devensian glaciation of northwest England. Journal of Quaternary Science. 14: 703-10. 1999.

Gudmundsson, G.H. Transmission of basal variability to a glacier surface. Journal of Geophysical Research: Solid Earth. 108(B5). 2003.

Gulley, J.D. Grabiec, M. Martin, J.B. Jania, J. Catania, G. Glowacki, P. The effect of discrete recharge by moulins and heterogenity in flow-path efficiency at glacier beds on subglacial hydrology. Journal of Glaciology. 58(211). 2012.

Gustavson, T.C. Boothroyd, J.C. A depositional model for outwash, sediment sources, and hydrologic characteristics, Malaspine Glacier, Alaska: a modern analog of the southeastern margin of the Laurentide Ice Sheet. Bulletin of the Geological Society of America. 99: 187-200. 1987.

Haiblen, A.M. Glacial history and landform genesis in the Lac de Gras Area, Northwest Territories. MSc Thesis. Department of Earth Sciences, Simon Fraser University. 2017.

Hall, D.K. Comiso, J.C. DiGirolamo, N.E. et al. Variability in the surface temperature and melt extent of the Greenland ice sheet from MODIS. Geophysical Research Letters. 40: 1-7. 2013.

Haralick, R. Shapiro, L. Image segmentation techniques. Computer Vision, Graphics and Image Processing. 29: 100-32. 1985.

Hart, J.K. Identifying fast ice flow from landform assemblages in the geological record: a discussion. Annals of Glaciology. 28: 59-66. 1999.

Hättestrand, C. Kleman, J. Ribbed moraine formation. Quaternary Science Review.18: 43-61. 1999.

Hebrand, M. Amark, M. Esker formation and glacier dynamics in eastern Skane and adjacecnt areas, southern Sweden. Boreas. 18(1): 67-81. 1989.

Helm, V. Humbert, A. Miller, H. Elevation and elevation change of Greenland and Antarctica derived from CryoSat-2. Cryosphere. 8: 1539-59. 2014.

Hess, D.P. Briner, J.P. Geospatial analysis of control on subglacial bedform morphometry in the New York Drumlin Field – implications for Laurentide Ice Sheet dynamics. Earth Surface Processes Landforms. 34: 1126-35. 2009.

Hewitt, I.J. Modelling distributed and channelized subglacial drainage: the spacing of channels. Journal of Glaciology. 57(202). 2011.

Hewitt, I.J. Seasonal changes in ice sheet motion due to melt water lubrication. Earth and Planertary Science Letters. 371-72. 16-25. 2013.

Hewitt, I.H. Creyts, T.T. A model for the formation of eskers. Geophysical Research Letters. 46. 2019.

Hillier, J.K. Smith, M. Residual relief separation: digital elevation model enhancement for geomorphological mapping. Earth Surface Processes and Landforms. 33: 2266-76. 2008.

Hillier, J.K. Smith, M. Armugam, R. Barr, I. Boston, CM. Clark, C.D. Ely, J. Fankl, A. Greenwood, S.L. Gosselin, L. Hättestrand, C. Hogan, K. Hughes, A.L.C. Livingstone, S.J. Lovell, H. McHenry, M. Muñoz, Y. Pellicer, X.M. Pellitero, R. Robb, C. Roberson, S. Ruther, D. Spagnolo, M. Standell, M. Stokes, C.R. Storrar, R. Tate, N.J. Wooldridge, K. Manual mapping of drumlins in synthetic landscapes to assess operator effectiveness. Journal of Maps. 11(5): 719-29. 2015.

Hillier, J.K. Watts, A.B. "Plate-like" subsidence of the East Pacific Rise-South Pacific superswell system. Geomagnetism and Palaeomagnetism / Marine Geology and Geophysics. 109(B10). 2004.

Hindmarsh, R.C.A. Drumlinisation and drumlin-forming instabilities: viscous till mechanisms. Journal of Glaciology. 44(147): 293-314. 1998.

Hodge, S.M. Direct measurements of basal water pressures: progress and problems. Journal of Glaciology. 23, 309-19. 1979.

Hoffman, M.J. Andrews, L.C. Price, S.A. Catania, G.A. Neumann, T.A. Luthi, M.P. et al. Greenland subglacial drainage evolution regulated by weakly connected regions of the bed. Nature Communications. 7: 13903. 2016.

Hoffman, M.J. Catania, G.A. Neumann, T.A. Andrews. L.C. Rumrill, J.A. Links between acceleration, melting, and supraglacial lake drainage of the western Greenland Ice Sheet. Journal of Geophysical Research. 116. 2011.

Hoffman, M.J. Neumann, T. Catania, G.A. Andrews, L.C. Links between acceleration, melting and supraglacial lake drainage at the western Greenland Ice Sheet. AGUFM. 2010.

Hoffman, M.J. Price, S.F. The roles of channelisation and parameter sensitivity on feedbacks between subglacial hydrology and glacier dynamics. AGUFM. 2013.

Hooke, R.L. On the role of mechanical energy in maintaining subglacial water conduits at atmospheric water pressure. Journal of Glaciology. 30(105). 1984.

Hooke, R.L. Fastook, J. Thermal conditions at the bed of the Laurentide ice sheet during deglaciation: implications for esker formation. Journal of Glaciology. 53(183). 2007.

Hooke, R.L. Jennings, C.E. On the formation of the tunnel valleys of the southern Laurentide ice sheet. Quaternary Science Reviews. 25(11–12). 1364–72. 2006.

Hooke, R. LeB. Laumann, T. Kohler, J. Subglacial water pressures and the shape of subglacial conduits. Journal of Glaciology. 36 (122). 67-71. 1990.

Hooke, R.L. Wold, B. Hagen, J.O. Subglacial hydrology and sediment transport at Bondhusbreen, southwest Norway. Geological Society of American Bulletin. 96: 388-97. 1985.

Hoppe, G. Problems of glacial morphology and the Ice Age, Geogr. Annaler. 39. 1-18. 1957.

Horgan, H.J. Anderson, B. Alley, R.B. Chamberlain, C.J. Dykes, R. Kehrl, L.M. Townend, J. Glacier velocity variability due to rain-induced sliding and cavity formation. Earth and Planetary Science Letters. 432: 273-82. 2015.

Howarth, P.J. Investigations of two eskers at eastern Breidamerkurjökull, Iceland. Arctic and Alpine Research. 3: 305-18. 1971.

Howat, I.M. de la Peńa, S. van Angelen, J.H. Lenaerts, J.T.N. van den Broeke, M.R. Expansion of meltwater lakes on the Greenland Ice Sheet. The Cryosphere. 7: 201-4. 2013.

Hoyal, D.C.J.D. Van Wagoner, J.C. Adair, N.L. Deffenbaugh, M. Li, D. Sun, T. Huh, C. Griffin, D.E. Sedimentation from jets: A depositional model for clastic deposits of all scales and environments: Salt Lake City, Utah, Search and Discovery Article No. 40082, American Association of Petroleum Geologists Annual Meeting, May 14, 2003, 10.

Hubbard, B.P. Nienow, P. Alpine subglacial hydrology. Quaternary Science Reviews. 16: 939-55. 1997.

Hubbard, B.P. Sharp, M.J. Willis, I.C. Nielsen, M.K. Smart, C.C. Borehole water-level variation and the structure of the subglacial hydrological system of Haut Glacier d'Arolla, Valais, Switzerland. Journal of Glaciology. 41(139). 572–83. 1995.

Huddart, D. Bennett, M.R. Glasser, N.F. Morphology and sedimentology of a high-arctic esker system: Vegbreen, Svalbard. Boreas. 28(2). 1999.

Hughes, A. Clark, C.D. Jordan, C. Subglacial bedforms of the last British ice sheet. Journal of Maps. 543-63. 2010.

Ignéczi, A. Sole, A.J. Livingstone, S.J. Leeson, A.A. Fettweis, X. Selmes, N. et al. Northeast sector of the Greenland Ice Sheet to undergo the greatest inland expansion of supraglacial lakes during the 21st century. Geophysical Research Letters. 43: 9729-38. 2016.

Ignéczi, A. Sole, A.J. Livingstone, S.J. Ng, F.S.L. Yang, K. Greenland ice sheet surface topography and draiange structure controlled by transfer of basal variability. Frontiers in Earth Science. 6: 101. 2018.

Iken, A. Bindschadler, R.A. Combined measurements of subglacial water pressure and surface velocity of Findelengletscher, Switzerland: conclusions about drainage system and sliding mechanisms. Journal of Glaciology. 32: 101-19. 1986.

Iken, A. Truffe, M. The relationship between subglacial water pressure and velocity of Findelengletscher, Switzerland, during its advance and retreat. Journal of Glaciology. 43: 328-38. 1997.

Iken, A. Rothlisberger, H. Flotron, A. Harberli, W. The uplift of Unteraargletscher at the beginning of the melt season – a consequnce of water sorage at the bed? Journal of Glaciology. 29: 28-47. 1983.

IPCC. Climate Change 2013: The Physical Science Basis. Cambridge University Press, Cambridge, UK. 2013.

Irvine-Fynn, T.D.L. Hodson, A.J. Moorman, B.J. Vatne, G. Hubbard, A.L. Polythermal glacier hydrology: a review. Rev. Geophys. 49. 2011.

Iverson, N.R. Baker, R.W. Hooke, R.L. Hanson, B. Jansson, P. Coupling between a glacier and a soft bed: I. A relation between effective pressure and local shear stress determined from till elasticity. Journal of Glaciology. 45: 31-40. 1999.

Jansen, J.D. Codilean, A.T. Stroeven, A.P. Fabel, D. Hättestrand, C. Kleman, J. Harbor, J.M. Heyman, J. Kubik, P.W. Xu, S. Inner gorges cut by subglacial meltwater during Fennoscandian ice sheet decay. Nature Communications. 5(3815): 1-7. 2014.

Jansson, P. Dynamics and hydrology of a small polythermal valley glacier. Geografiska Annaler: Series A, Physical Geography. 78(2-3). 1996.

Janszen, A. Spaak, M. Moscariello, A. Effects of the substraum on the formation of glacial tunnel valleys: an example from the Middle Pleistocene of the southern North Sea Basin. Boreas. 41(4): 629-43. 2012.

Jordan, G. Schott, B. Application of wavelet analysis to the study of spatial pattern of morphotectonic lineaments in digital terrain models. A case study. Remote Sensing Environment. 94: 31-38. 2005.

Jorge, M.G. Brennand, T.A. Semi-automated extraction of longitudinal subglacial bedforms from digital terrain models – Two new methods. Geomorphology. 288: 148-63. 2017.

Jørgensen, F. Sandersen, P.B.E. Buried and open tunnel valleys in Denmark – erosion beneath multiple ice sheets. Quaternary Science Reviews. 25(11-12): 1339-63. 2006.

Joughin, I. Das, S.B. Flowers, G.E. Behn, M.D. Alley, R.B. King, M.A. Smith, B.E. Bamber, J.L. van den Broeke, M.R. van Angelen, J.H. Influence of ice-sheet geometry and supraglacial lakes on seasonal ice-flow variability. The Cryosphere. 7: 1185-92. 2013.

Joughin, I. Das, S.B. King, M. Smith, B.E. Howat, I.M. Moon, T. Seasonal speedup along the western flank of the Greenland Ice Sheet. Science. 320: 781-83. 2008.

Kamb, B. Glacier surge mechanism based on linked cavity configuration of the basal water conduit system. Journal of Geophysical Research, Solid Earth. 92(B9). 9038-100. 1987.

Karlsson, N.B. Dahl-Jensen, D. Response of the large-scale subglacial drainage system of Northwest Greenland to surface elevation changes. The Cryosphere. 9: 1465-79. 2015.

Karlstrom, L. Gajjar, P. Manga, M. Meander formation in supraglacial streams. Journal of Geophysical Research: Earth Surface. 118: 1897-907. 2013.

Karlstrom, L. Yang, K. Fluvial supraglacial landscape evolution on the Greenland Ice Sheet. Geophysical Research Letters. 43: 2638-92. 2016.

Kehew, A.E. Beukema, S.P. Bird, B.C. Kozlowski, A.L. Fast flow of the Lake Michigan Lobe: evidence from sediment-landform assemblages in south-western Michigan, USA. Quaternary Science Reviews. 24: 2335-53. 2005.

Kehew, A.E. Nicks, L.P. Straw, W.T. Palimpsest tunnel valleys: evidence for relative timing of advances in an interlobate area of the Laurentide ice sheet. Ann. Glaciol. 28: 47 – 52. 1999.

Kehew, A.E., Piotrowski, J.A. and Jørgensen, F. Tunnel valleys: Concepts and controversies - A review. Earth-Science Reviews. 113(1–2). .33–58. 2012.

Kerr, D. Knight, R. Sharpe, D. Cummings, D. Reconnaissance surficial geology, Lynx Lake, Northwest Territories, NTS 75-J: Geological Survey of Canada, 1: 125 000. 2014a.

Kerr, D. Knight, R. Sharpe, D. Cummings, D. Reconnaissance surficial geology, Walmsley Lake, Northwest Territories, NTS 75-N, Canadian Geoscience Map-140: Geological Survey of Canada, 1:125 000. 2014b.

King, E.C. Pritchard, H.D. Smith, A.M. Subglacial landforms beneath Rutford Ice Stream, Antarctica: detailed bed topography from ice-penetrating radar. Earth System Science. 8: 151-58. 2016.

King, E.C. Woodward, J. Smith, A.M. Seismic and radar observations of subglacial bed forms beneath the onset zone of Rutford Ice Stream, Antarctica. Journal of Glaciology. 53(183). 2007.

Kingslake, J. Ely, J.C. Das, I. Bell, R.E. Widespread movement of meltwater onto and across Antarctic ice shelves. Nature. 544: 349-52. 2017.

Kingslake, J. Ng, F. Sole, A. Modelling channelised surface drainage of supraglacial lakes. Journal of Glaciology. 61(225): 185-99. 2015.

Kirkham, J. Hogan, K.A. Larter, R.D. Arnold, N.S. Nitsche, F.O. Kuhn, G, Gohl, K. Anderson, J.B. Dowdeswell, J.A. Morphometry of bedrock meltwater channels on Antarctic inner continental shelves: Implications for channel development and subglacial hydrology. Geomorphology. 370. 2020a.

Kirkham, J. Hogan, K. Larter, R. Self, E. Games, K. Huuse, M. Stewart, M. Ottesen, D. Arnold, N. Dowdeswell, J. New insights into North Sea tunnel valley infill and genesis from high-resolution 3D seismic data. EGU General Assembly 2020, Online 2020, Online 4-8 May, 2020. EGU2020-118. 2020b.

Kleman, J. The palimpsest glacial landscape in north-west Sweden. Geografiska. 74A: 306-25. 1992.

Kleman, J. Applegate, P.J. Durations and propagation patterns of ice sheet instability events. Quaternary Science Reviews. 92: 32-39. 2014.

Kleman, J. Borgström, I. Reconstruction of palaeo-ice sheets: the use of geomorphological data. Eart Surface Processes and Landforms. 21(10): 893-909. 1996.

Kleman, J. Glasser, N.F. The subglacial thermal organisation (STO) of ice sheets. Quaternary Science Reviews. 26(5-6): 585-97. 2007.

Kleman, J. Hättestrand, C. Stroeven, A.P. Jansson, K.N. De Angelis, H. Borgström, I. Reconstruction of palaeo-ice sheets – inversion of their glacial geomorphological record. P.G. Knight (Ed.), Glacier Science and Environmental Change. Chapter 38. Blackwell Science Ltd, Oxford. 2006.

Kleman, J. Jansson, K.N. De Angelis, H. Stroeven, A. Hättestrand, C. Alm, G. Glasser, N.F. North American Ice Sheet build up during the last glacial cycle, 115-21 kyr. Quaternary Science Reviews. 29: 2036-51. 2010.

Knight, J. McCabe, A.M. Identification and significance of ice-flow-transverse subglacial ridges (Rogen moraines) in northern central Ireland. Journal of Quaternary Science. 12: 519-24. 1997.

Koziol, C. Arbold, A. Pope, A. Colgan, W. Quantifying supraglacial meltwater pathways in the Paakitsoq region, West Greenland. Journal of Glaciology. 63(239): 464-76. 2017.

Koziol, C.P. Arnold, N. Modelling seasonal meltwater forcing of the velocity of land terminating margins of the Greenland Ice Sheet. The Cryosphere. 12: 971-91. 2018.

Krabill, W. Hanna, E. Huybrechts, P. Abdalati, W. Cappelen, J. Csatho, B. Frederick, E. Manizade, S. Martin, C. Sonntag, J. Swift, R. Thomas, R. Yungel, J. Greenland Ice Sheet: Increased coastal thinning. Geophysical Research Letters. 31. 2004.

Krawczynski, M.J. Behn, M.D. Das, S.B. Joughin, D.I. Constraints on the lake volume required for hydrofracture through ice sheets. Geophysical Research Letters. 36(10). 2009.

Krüger, J. Gletscheren og landskabet – i nutid og istid. Geografiske temahæfter. Gyldendal, Nordisk For-lag, Copenhagen. 77. 1989.

Kuhn, G. Hillenbrand, C.D. Kasten, S. Smith, J.A. Nitsche, F.O. Frederichs, T. Wiers, S. Ehrmann, W. Klages, J. P. Mogollón, J.M. Evidence for palaeo-subglacial lake on the Antarctic continental shelf. Nature Communications. 2017.

Kuipers Munneke, P. Ligtenberg, S.R.M. van den Broeke, M.R. van Angelen, J.H. Forster, R.R. Explaining the presence of perennial liquid water bodies in the firn of the Greenland Ice Sheet. Geophysical Research Letters. 41(2): 476-83. 2014.

Langley, E.S. Leeson, A.A. Stokes, C.R. Jamieson, S.S.R. Seasonal evolution of supraglacail lakes on an East Antarctic outlet glacier. Geophysical Research Letters. 43(16): 8563-71. 2016.

Lee, H.A. Craig, B.G. Fyles, J.G. Keewatin ice divide. Geol. Soc. Am. Bull. 68: 1760-61. 1957.

Lee, J.R. Phillips, E.R. Progressive soft sediment deformation within a subglacial shear zone – a hybrid mosaic-pervasive deformation model for Middle Pleistocene glaciotectonised sediments from easter England. Quaternary Science Reviews. 27: 1350-62. 2008.

Lelandais, T. Ravier, E. Pochat, S. Bourgeois, O. Clark, C. Mourgues, R. Strzerzynski, P. Modelled subglacial floods and tunnel valleys control the life cycle of transitory ice streams. The Cryosphere. 12: 2759-72. 2018.

Lenaerts, J.T.M. Lhermitte, S. Drews, R. Ligtenberg, S.R.M. Berger, S. Helm, V. Smeets, C.J.P.P. van den Broeke, M.R. van de Berg, W.J. van Meijgaard, E. Eijkelboom, M. Eisen, O. Pattyn, F. Meltwater produced by wind-albedo interaction stored in an East Antarctic ice shelf. Nature Climate Change. 7: 58-62. 2017.

Lewington, E.L.M. Livingstone, S.J. Sole, A.J. Clark, C.D. Ng, F. An automated method for mapping geomorphological expressions of former subglacial meltwater pathways (hummock corridors) from high resolution digital elevation data. Geomorphology. 339: 70-86. 2019.

Lewington, E.L.M. Livingstone, S.J. Clark, C.D. Sole, A.J. Storrar, R.D. A model for interaction between conduits and surrounding hydraulically connected distributed drainage based on geomorphological evidence from Keewatin, Canada. The Cryosphere. 14: 2949-76. 2020.

Lewis, S.M. Smith, L.C. Hydrologic drainage of the Greenland Ice Sheet. Hydrological Processes. 23(14). 2009.

Liestøl, O. Storbreen Glacier in Jotunheimen, Norway. Norsk Polarinstitutt Skrifter. 141. 1967.

Lindbäck, K. Pettersson, R. Hubbard, A.L. Doyle, S.H. van As, D. Mikkelsen, A.B. Fitzpatrick, A.A. Subglacial water drainage, storage, and piracy beneath the Greenland ice sheet. Geophysical Research Letters. 42: 7606-14. 2015.

Lindén, M. Möller, P. Marginal formation of De Geer moraines and their implictions to the dynamics of grounding-line recession. Journal of Quaternary Sciences. 20: 113-33. 2005.

Livingstone, S.J. and Clark, C.D. Morphological properties of tunnel valleys of the southern sector of the Laurentide ice sheet and implications for their formation. Earth Surface Dynamics. 4. 567–89. 2016.

Livingstone, S.J. Clark, C.D. Tarasov, L. Modelling North American palaeo-subglacial lakes and their meltwater drainage pathways. Earth and Planetary Science Letters. 375: 13-33. 2013.

Livingstone, S.J. Lewington, E.L.M. Clark, C.D. Storrar, R.D. Sole, A.J. McMartin, I. Dewald, N. Ng, F.. A quasi-annual record of time-transgressive esker formation: implications for ice sheet reconstruction and subglacial hydrology. The Cryosphere. 14: 1989-2004. 2020.

Livingstone, S.J Storrar, R.D. Hillier, J.K. Stokes, C.R. Tarasov, L. An ice-sheet scale comparison of eskers with modelled subglacial drainage routes. Geomorphology. 246. 104–12. 2015.

Livingstone, S.J. Utting, D.J. Ruffell, A. Clark, C.D. Pawley, S. Atkinson, N. Fowler, A.C. Discovery of relict subglacial lakes and their geometry and mechanism of drainage. Nature Communications. 7. 11767. 2016.

Lliboutry, L. General theory of subglacial cavitation and sliding of temperate glaciers. Journal of Glaciology. 7. 21-58. 1968.

Lundqvist, J. Rogen (ribbed) moraine – identification and possible origin. Sedimentary Geology. 62: 281-92. 1989.

Lundqvist, J. Structure and rhythmic pattern of glaciofluvial deposits north of Lake Vänern, south-central Sweden. Boreas. 26: 127-40. 1997a.

Lundqvist, J. Rogen moraine – an example of two-step formation of glacial landscapes. Sedimentary Geology. 111: 27-40. 1997b.

Lundqvist, J. Periodical sedimentation in Scandinavian eskers. GFF. 121(3): 175-81. 1999.

MacDonald, R.G. Alexander, J. Bacon, J.C. Cooker, M.J. Flow patterns, sedimentation and deposit architecture under a hydraulic jump on a non-eroding bed: defining hydraulic jump unit bars. Sedimentology 56: 1346-67. 2009.

Maclachlan, J.C. Eyles, C.H. Quantitative geomorphological analysis of drumlins in the Peterborough drumlin field, Ontario, Canada. Geografiska Annaler: Series A, Physical Geography. 95(2). 2013.

Mair, D. Nienow, P. Sharp, M. Wohlleben, T. Willis, I. Influences of subglacial drainage system evolution on glacier surface motion: Haut Glacier d'Arolla, Switzerland. Journal of Geophysical Research: Solid Earth. 107(B8): 8 -13. 2002.

Mair, D. Willis, I. Fischer, U.H. Hubbard, B. Nienow, P. Hubbard, A. Hydrological controls on patterns of surface, internal and basal motion during three "spring events": Haut Glacier d'Arolla, Switzerland. Journal of Glaciology. 49(167): 555-67. 2003.

Mäkinen, J. Time-transgressive deposits of repeated depositional sequences within interlobate glaciofluvial (esker) sediments in Köyliö, SW Finalnd. Sedimentology 50. (2): 337-60. 2003.

Mäkinen, J. Kajutti, K. Palmu, J-P. Ojala, A. Ahokangas, E. Triangular-shaped landforms reveal subglacial drainage routes in SW Finland. Quaternary Science Reviews. 164. 37–53. 2017.

Marcott, S.A. Shakun, J.D. Clark, P.U. Mix, A.C. A reconstruction of regional and global temperature for the past 11,300 years. Science. 339: 1198-201. 2013.

Margold, M. Jansson, K.N. Kleman, J. Stroeven, A.P. Clague, J.J. Retreat pattern of the Cordilleran Ice Sheet in central British Columbia at the end of the last glaciation reconstructed from glacial meltwater landforms. Boreas. 42: 830-47. 2013.

Margold, M. Stokes, C.R. Clark, C.D. Ice streams in the Laurentide Ice Sheet: Identification, characteristics and comparison to modern ice sheets. Earth Science Reviews. 143. 117-46. 2015.

Margold, M. Stokes, C.R. Clark, C.D. Reconciling records of ice streaming and ice margin retreat to produce a palaeographic reconstruction of the deglaciation of the Laurentide Ice Sheet. Quaternary Science Reviews. 189: 1-30. 2018.

Marshall, S.J. Tarasov, L. Clarke, G.K.C. Peltier, W.R. Glaciological reconstruction of the Laurentide Ice Sheet: physical processes and modelling challenges. Canadian Journal of Earth Sciences. 37: 769-93. 2000.

Martini, I.P. Pleistocene glacial fan deltas in southern Ontario, Canada. In: Colella, A, Prior, D. (Eds.), Coarse-grained delates. Int. Assoc. Sedimentol., Spec. Publ. 10: 281-95. 1990.

McMartin, I. Henderson, P. J. Evidence from Keewatin (central Nunavut) for paleo-ice divide migration. Géographie physique et Quaternaire, 58, 163-186. 2004.

Meierbachtol, T. Harper, J. Humphrey, N. Basal drainage system response to increasing surface melt on the Greenland Ice Sheet. Science. 341. 2013.

Menzies, J. Shilts, W.W. Subglacial environments. in Menzies, J. (Ed.), Past Glacial Environments: Sediments, Forms and Techniques. Butterworth-Heinemann, Oxford. 1996.

Middleton, M. Nevalainen, P. Hyvönen, E. Heikkonen, J. Sutinen, R. Pattern recognition of LiDAR data and sediment anisotropy advocate polygenetic subglacial mass-flow origin for the Kemijärvi hummocky moraine field in northern Finland. Geomorphology. 362. 2020.

Möller, P. Rogen moraine: an example of glacial reshaping of pre-existing landforms. Quaternary Science Reviews. 25: 362-89. 2006.

Möller, P. Dowling, T.P.F. Streamlined subglacial bedforms on the Närke plain, south-central Sweden – Areal distribution, morphometrics, internal architecture and formation. Quaternary Science Reviews. 146: 182-215.

Möller, P. Dowling, T.P.F. Equifinality in glacial geomorphology: instability theory examined via ribbed moraine and drumlins in Sweden. GFF. 140(2). 2018.

Mooers, H.D. On the formation of the tunnel valleys of the Superior Lobe, Central Minnesota. Quaternary Research. 32: 24 – 35. 1989.

Moussavi, M. Pope, A. Halberstadt, A.R.W. Trusel, L.D. Cioffi, L. Abdalati, W. Antarctic supraglacial lake detection using Landsat 8 and Sentinel-2 imagery: towards continental generation of lake volumes. Remote Sensing. 12(1): 134. 2020.

Munch, B. Trtik, P. Marone, F. Stampanoni, M. Stripe and ring artefact removal with combined wavelet – Fourier filtering. Optic Express. 17(10): 8567-91. 2009.

Nanni, U. Gimbert, F. Vincent, C. Graff, D. Walter, F. Piard, L. Moreau, L. Quantification of seasonal and diurnal dynamics of subglacial channels using seismic observations on an Alpine glacier. The Cryosphere. 14: 1475-96. 2020.

Ng, F.S.L. Canals under sediment-based ice sheets. Annals of Glaciology. 30. 2000.

Ng, F. Ignéczi, A. Sole, A.J. Livingstone, S.J. Response of surface topography to basal variability along glacial flowlines. Journal of Geophysical Research: Earth Surface. 123: 2319-40. 2018.

Nick, F.M. Vieli, A. Andersen, M.L. Joughin, I. Payne, A. Edwards, T.L. et al. Future sea-level rise from Greenland's main outlet glacier in a warming climate. Nature. 497: 235-38. 2013.

Nienow, P. Sharp, M. Willis, I. Velocity-discharge relationships derived from dye-tracer experiments in glacial meltwaters: implications for subglacial meltwater flow conditions. Hydrological Processes. 10: 1411-26. 1996.

Nienow, P. Sharp, M. Willis, I. Seasonal changes in the morphology of the subglacial drainage system, Haut Glacier d'Arolla, Switzerland. Earth Surface Processes and Landforms. 23: 825-84. 1998.

Nienow, P.W. Sole, A.J. Slater, D.A. Cowton, T.R. Recent advances in our understanding of the role of meltwater in the Greenland Ice Sheet system. Current Climate Change Reports. 3: 330-44. 2017.

Nitsche, F.O. Gohl, K. Larter, R.D. Hillenbrand, C.-D. Kuhn, G. Smith, J.A. Jacobs, S. Anderson, J.B. Jakobsson, M. Palaeo ice flow and subglacial meltwater dynamics in Pine Island Bay, West Antarctica. The Cryosphere. 7: 249-62. 2013.

Noh, M.J. Howat, I.M. Automated stereo-photogrammetric DEM generation at high latitudes: Surface Extraction with TIN-based Search-space Minimisation (SETSM) validation and demonstration over glaciated regions. GISci. Remote Sens. 52(2), 198-217. 2015.

Nordmann, V. Beskrivele til Geologisk kort over Danmark. Kortbladet Fredericia. AL Kvartære aflejringer. Geological Survey of Denmark (Series I). 22-A. 1-125. 1958.

Nye, J. Water at the bed of a glacier. IASH Publications 95. (Symposium at Cambridge 1969 – Hydrology of Glaciers). Pp. 189-194. 1973.

Nye, J.F. Frank, F.C. Hydrology of the intergranular veins in a temperate glacier. Symposium on the Hydrology of Glaciers. 95: 157-61. 1973.

Ó Cofaigh, C. Tunnel valley genesis. Progress in Physical Geography. 20. 1-19. 1996.

Ojala, A.E.K. Peterson, G. Mäkinen, J. Johnson, M.D. Kajutti, K. Palmu, J-P. Ahokangas, E. Öhrling, C. Ice-sheet scale distribution and morphometry of triangular shaped hummocks (murtoos): a subglacial landform produced during rapid retreat of the Scandinavian Ice Sheet. Anals of Glaciology. 1-12. 2019.

Otsu, N. A threshold selection method from gray-level histograms. IEEE Transactions on Systems, Man, and Cybernetics. SMC-9. 1979.

Ottesen, D. Stokes, C.R. Rise, L. Olsen, L. Quaternary ice-sheet dynamics and ice streaming along the coastal parts of northern Norway. Quaternary Science Reviews. 27: 19. 2008.

Parizek, B.P. Alley, R.B. Implications of increased Greenland surface melt under global-warming scenarios: ice-sheet simulations. Quaternary Science Reviews. 23(9-10): 1013-27. 2004.

Perkins, A.J., Brennand, T.A. Burke, M.J. Towards a morphogenetic classification of eskers: Implications for modelling ice sheet hydrology. Quaternary Science Reviews. 134. 19–38. 2016.

Peterson, G. Johnson, M.D. Hummock corridors in the south-central sector of the Fennoscandian ice sheet, morphometry and pattern. Earth Surface Processes and Landforms. 43: 919-29. 2018.

Peterson, G. Johnson, M.D. Smith, C.A. Glacial geomorphology of the south swedish uplands – focus on the spatial distribution of hummock tracts. Journal of Maps. 13(2): 534 – 44. 2017.

Peterson, G. Johnson, M.D. Dahlgren, S. Passe, T. Alexanderson, H. Genesis of hummocks found in tunnel valleys: an example from Horda, southern Sweden. GFF. 140(2): 189 – 544. 2018.

Phillips, T. Rajaram, H. Colgagn, W. Steffan, K. Abdalati, W. Evaluation of cryo-hydrologic warming as an explanation for increased ice velocities in the wet snow zone, Sermeq Avannarleq, West Greenland. Journal of Geophysical Research. Earth Surface. 118: 1241-56. 2013.

Piotrowski, J.A. Tunnel-valley formation in north west Germany – geology, mechanisms of formation and subglacial bed conditions for the Bornhoved tunnel valley. Sedimentary Geology. 89. 107-41. 1994.

Piotrowski, J.A. Channelized subglacial drainage under soft-bedded ice sheets: evidence from small N-channels in Central European lowland. Geol. Q. 43(2): 153-62. 1999.

Piotrowski, J.A. Reflections on soft subglacial beds as a mosaic of deforming and stable spots. Quaternary Science Reviews. 23: 993-1000. 2004.

Poinar, K. Dow, C.F. Andrews, L.C. Long-term support of an active subglacial hydrologic system in southeast Greenland by firn aquifers. Geophysical Research Letters. 46. 4772-81. 2019.

Poinar, K. Joughin, I. Das, S. Behn, M.D. Lenaerts, J.T.M. van den Broeke, M.R. Limits to future expansion of surface-melt-enhanced ice flow into the interior of western Greenland. Geophysical Research Letters. 42(6). 1800-7. 2015.

Porter, C., Morin, P., Howat, I., Noh, M.J., Bates, B., Peterman, K., Keesey, S., Schlenk, M., Gardiner, J., Tomko, K. Willis, M., et al. ArcticDEM. Harvard Dataverse, V1. 2018.

Powell, R.D. Glacimarine processes at grounding-line fans and their growth to ice-contact deltas. Geological Society, London, Special Publications, 53(1): 53-73. 1990.

Praeg, D. Seismic imaging of mid-Pleistocene tunnel valleys in the North Sea Basin – high resolution from low frequencies. Journal of Applied Geophysics. 53 273-298. 2003.

Pratomo, J. Kuffer, M. Martinez, J. Kohli, D. Coupling uncertainties with accuracy assessment in object-based slum detection case study: Jakarta, Indonesia. Remote Sensing. 9(11). 2017.

Prest, V.K. Grant, D.R. Rampton, V.N. Glacial map of Canada. Geological Survey of Canada. Map 1253A. 1:5,000,000. 1968.

Price, R.J. Eskers near the Casement glacier, Alaska. Geografiska Annaler. Series A. Physical Geography. 48: 111-25. 1966.

Price, R.J. Moraines, sandar, kames and eskers near Breiomerkurjökull, Iceland. Transactions of the Institute of British Geographers. 46: 17-43. 1969.

Price, S.F. Payne, A.J. Catania, G.A. Neumann, T.A. Seasonal acceleration of inland ice via longitudinal coupling to marginal ice. Journal of Glaciology. 54: 213-19. 2008.

Pritchard, H.D. Arthern, R.J. Vaughan, D.G. Edwards, L.A. Extensive dynamic thinning on the margins of the Greenland and Antarctic ice sheets. Nature. 491(7266): 971-75. 2009.

Prowse, N.D. Morphology and Sedimentology of Eskers in the Lac de Gras Area, Northwest Territories, Canada. PhD Thesis. Carleton University. Ottawa, Canada. 2017.

Punkari, M. Glacial and glaciofluvial deposits in the interlobate areas of the Scandinavian Ice Sheet. Quaternary Science Reviews, 16, 741-753. 1997.

Rada, C. Schoof, C. Channelized, distributed, and disconnected: subglacial drainage under a valley glacier in the Yukon. The Cryosphere. 12: 2609-36. 2018.

Rampton, V.N. Large-scale effects of subglacial meltwater flow in the southern Slave Province, Northwest Territories, Canada. Canadian Journal of Earth Sciences. 37(1). 81–93. 2000.

Rattas, M. Piotrowski, J.A. Influence of bedrock permeability and till grain size on the formation of the Saadjärve drumlin field, Estonia, under an east-Baltic Weichselian ice stream. Boreas 2: 167-77. 2003.

Ravier, E. Buoncristiani, J.F. Guiarud, M. Menzies, H. Clerc, S. Goupy, B. Portier, E. Porewater pressure control on subglacial soft sediment remobilisation and tunnel valley formation: a case study from the Alnif tunnel valley (Morocco). Sedimentary Geoogy. 304: 71-95. 2014.

Rennermalm, A.K. Moustafa, S.E. Mioduszewski, J. Chu, V.W. Forster, R.R. Hagedorn, B. Harper, J.T. Mote, T.L. Robinson, D.A. Shuman, C.A. Smith, L.C. Tedesco, M. Understanding Greenland ice sheet hydrology using an integrated multi-scale approach. Environmental Research Letters. 8. 2013.

Richards, G. Moore, R.D. Suspended sediment dynamics in a steep, glacier-fed mountain stream, Place Creek, Canada. Hydrological Processes. 17: 1733-53. 2003.

Rignot, E. Velicogna, I. van den Broeke, M.R. Monaghan, A. Lenaerts, J.T.M Acceleration of the contribution of the Greenland and Antarctic ice sheets to sea level rise. Geophysical Research Letters. 38. 2011.

Ringrose, S. Depositional processes in the development of esker in Manitoba. in Davidson-Arnott, R.nickling, W. and Fahey, B.D. eds. Research in Glaciofluvial and Glaciolacustrine Systems: Norwich, Geo Books. 117-38. 1982.

Rothlisberger, H. Water pressure in Intra- and Subglacial Channels. Journal of Glaciology. 11: 177-203. 1972.

Russell, A.J., Gregory, A.R., Large, A.R., Fleisher, P.J. and Harris, T.D. Tunnel channel formation during the November 1996 jökulhlaup, Skeiðarárjökull, Iceland. Annals of Glaciology, 45, 95-103. 2007.

Russell, A.J. Knudson, Ó. Fay, H. Marren, P.M. Heinz, J. Tronicke, J. Morphology and sedimentology of a giant supraglacial, ice-walled, GLOF channel Skeisarárjökull, Iceland: implications for esker genesis. Global and Planetary Change. 28: 193-216. 2001.

Rust, B.R. Romanelli, R. Late quaternary subaqueous outwash deposits near Ottawa, Canada. A.V. Jopling, B.C. McDonald (Eds.), Glaciofluvial and Glaciolacustrine Sedimentation, Soc. Econ. Paleontol. Mineral., Spec. Publ. 177-92. 1975.

Rutishauser, A. Blankenship, D.D. Sharp, M. Skidmore, M.L. Greenbaum, J.S. Grima, C. Schroeder, D.M. Dowdeswell, J.A. Young, D.A. Discovery of a hypersaline subglacial lake complex beneath Devon Ice Cap, Canadian Arctic. Science Advances. 4(4). 2018.

Ryherd, S. Woodcock, C.E. Combining spectral and texture data in the segmentation of remotely sensed images .Photogrammetric Engineering and Remote Sensing. 62(2): 181-94. 1996.

Ryser, C. Lüthi, M. Blindow, N. Suckro, S. Funk, M. Bauder, A. Cold ice in the ablation zone: its relation to glacier hydrology and ice water content. Journal of Geophysical Research Earth Surface. 118: 693-705. 2013.

Saha, K. Wells, N.A. Munro-Stasiuk, M. An object-orientated approach to automated landform mapping: A case study of drumlins. Computers and Geosciences. 37(9): 1324-36. 2011.

Sarala, P. Ribbed moraine stratigarphy and formation in Southern Finnish Lapland. Journal of Quaternary Science. 21: 387-98. 2006.

Saunderson, H.C. The sliding bed facies in esker sands and gravels: a criterion for full pipe (tunnel) flow? Sedimentology. 24: 623-38. 1977.

Scambos, T.A. Bohlander, J.A. Shuman, C.A. Skvarca, P. Glacier acceleration and thinning after ice shelf collapse in the Larsen B embayment, Antarctica. Geophysical Research Letters. 31. 2004.

Scambos, T.A. Huble, C. Fahnestock, M. Bohlander, J. The link between climate warming and break-up of ice shelves in the Antarctic Peninsula. Journal of Glaciology. 46(154). 2000.

Schoof, C. Ice sheet acceleration driven by melt supply variability. Nature. 468: 803-806. 2010.

Seramur, K.C. Powell, R.D. Carlson, P.R. Evaluation of conditions along the grounding line of temperate marine glaciers: an example from Muir Inlet, Glacier Bay, Alaska. Mar. Geol. 140: 307-27. 1997.

Sergienko, O. V. Glaciological twins: Basally controlled subglacial and supraglacial lakes. Journal of Glaciology. 59(213). 3–8. 2013.

Shaw, J. Genesis of the Sveg tills and Rogen moraines of central Sweden: a model of basal melt out. Boreas. 8: 409-26. 1979.

Shaw, J. The meltwater hypothesis for subglacial bedforms. Quaternary International. 90(1). 5-22. 2002.

Shaw, J. In defence of the meltwater (megaflood) hypothesis for the formation of subglacial bedform fields. Journal of Quaternary Science. 25(3). 249-60. 2010.

Shackleton, C. Patton, H. Hubbard, A. Winsborrow, M. Kingslake, J. Estevas, M. Andreassen, K. Greenwood, S.L. Subglacial water storage beneath the Fennoscandian and Barents Sea ice sheets. Quaternary Science Reviews, 201: 13-28. (2018).

Shakun, J.D. Clark, P.U. He, F. Marcott, S.A. Mix, A.C. Liu, Z. Otto-Bliesner, B. Schmittner, A. Bard, E. Global warming preceded by increasing carbon dioxide concetrations during the last deglaciation. Nature. 484: 49-54. 2012.

Sharpe, D.R. Glaciomarine fan deposition in the Champlain Sea. in Gadd, N.R. ed. The Late Quaternary Development of the Champlain Sea Basin: Geological Association of Canada Special Paper 35: 312. 1988.

Sharpe, D., Kjarsgaard, B. Knight, R.D. Russell, H.A.J. Kerr, D.E. Glacial dispersal and flow history, East Arm area of Great Slave Lake, NWT, Canada. Quaternary Science Review. 165: 49 – 72. 2017.

Shepherd, A. Hubbard, A. Nienow, P. King, M. McMillan, M. Joughin, I. Greenland ice sheet motion coupled with daily melting in lare summer. Geophysical Research Letters. 36: 2-5. 2009.

Shilts, W.W. Esker sedimentation models, Deep Rose Lake map area, District of Keewatin; in Current Research, Part B, Geological Survey of Canada, Paper 84-1B: 217-22. 1984.

Shilts, W.W. Aylsworth, J.M. Kaszycki, C.A. Klasson, R.A. Canadian Shield. In: Graf, W.L. (Ed.), Geomorphic Systems of North America. Geological Society of America, Boulder, Colorado. pp. 119-61. Centennial Special Volume 2. 1987.

Shoemaker, E.M. Subglacial hydrology for an ice sheet resting on a deformable aquifer. Journal of Glaciology. 32(110). 1986.

Shreve, R.L. Movement of water in glaciers. Journal of Glaciology. 11(62). 205–14. 1972.

Shreve, R.L. Esker characteristics in terms of glacial physics, Katahdin esker system, Maine. Geol. Soc. Am. Bull. 96, 639 – 46. 1985.

Siegert, M.J. Dowdeswell, J.A. Gorman, M.R. McIntyre, N.F. An inventory of Antarctic subglacial lakes. Antarctic Science. 8(3): 281-86. 1996.

Siegert, M.J. Ross, N. Le Brocq, A.M. Recent advances in understanding Antarctic subglacial lakes and hydrology. Philosophical Transactions A. 374. 2016.

Siegfried, M.R. Fricker, H.A. Thirteen years of subglacial lake activity in Antarctica from multi-mission satellite altimetry. Annals of Glaciology. 59(76): 42-55. 2018.

Siegfried, M.R. Fricker, H.A. Carter, S.P. Tulaczyk, S. Episodic ice velocity fluctuations triggered by a subglacial flood in West Antarctica. Geophysical Research Letters. 43(6): 2640-48. 2016.

Simkins, L.M. Anderson, J.B. Greenwood, S.L. Gonnermann, H.M. Prothro, L.M. Ruth, A. Halberstadt, W. Stearns, L.A. Pollard, D. Deconto, R.M. Anatomy of a meltwater drainage system beneath the ancestral East Antarctic ice sheet. Nature Geoscience. 10: 691-98. 2017.

Sissons, J.B. A subglacial drainage system by the Tinto Hills, Lankashire. Trans Edinb. Geol. Soc. 18: 175 – 92. 1961.

Sjogren, D.B. Fisher, T.G. Taylor, L.D. Jol, H.M. Munro-Stasiuk, M.J. Incipient tunnel channels. Quaternary International. 90. 41–56. 2002.

Smed, P. Studier over den fynske øgruppes glaciale landskabsformer. Medd. Dansk Geologisk Forening. 15 : 1-74. 1962.

Smed, P. Die Entstehung der dänischen und norddeutschen Rinnentäler (Tunneltäler) – Glaziologische Gesichtspunkte. Eiszeitalter und Gegenwart. 48 : 1-18. 1998.

Smith, L.C. Chu, V.W. Yang, K. Gleason, C.J. Pitcher, L.H. Rennermalm, A.K. Legleiter, C.J. Behar, A.E. Overstreet, B.T. Moustafa, S.E. Tedesco, M. Forster, R.R. LeWinter, A.L. Finnegan, D.C. Sheng, Y. Balog, J. Efficient meltwater draiange through supraglacial streams and rivers on the southwest Greenland ice sheet. PNAS. 112(4) : 1001-6. 2015.

Smith, M.J. Clark, C.D. Methods for the visualisation of digital elevation models for landform mapping. Earth Surface Processes and Landforms. 30(7) : 885-900. 2005.

Smith, A.M. Murray, T. Bedform topography and basal conditions beneath a fast-flowing West Antarctic ice stream. Quarternary Science Reviews. 28 : 584-96. 2009.

Smith, A.M. Murray, T. Nicholls, K.W. Makinson, K. Aoalgeirsdóttir, G. Behar, A.E. Vaughan, D.G. Rapid erosion, drumlin formation, and changing hydrology beneath an Antarctic ice stream. Geology. 35(2) : 127-30. 2007.

Sole, A.J. Mair, D.W.F. Nienow, P.W. Bartholomew, I.D. King, M.A. Burke, M.J. Joughin, I. Seasonal speedup of a Greenland marine-terminating outlet glacier forced by surface melt-induced changes in subglacial hydrology. Journal of Geophysical Research. Earth Surface. 116(F3). 2011.

Sole, A. Nienow, P. Bartholomew, I. Mair, D. Cowton, T. Tedstone, A. et al. Winter motion mediates dynamic response of the Greenland Ice Sheet to warmer summers. Geophysical Research Letters. 40(15). 3940–44. 2013.

Sookhan, S. Eyles, N. Putkinen, N. LiDAR-based volume assessment of the origin of the Wadena drumlin field, Minnesota, USA. Sedimentary Geology. 338: 72-83. 2016.

Spagnolo, M. Bartholomaus, T.C. Clark, C.D. Stokes, C.R. Atkinson, N. Dowdeswell, J.A. Ely, J.C. Graham, A.G.C. Hogan, K.A. King, E.C. Larter, R.D. Livingstone, S.J. Pritchard, H.D. The periodic topography of ice stream beds: Insights from the Fourier spectra of mega-scale glacial lineations. Journal of Geophysical Research: Earth Surface. 122(7): 1355-1373. 2017.

Stearns, L.A. Smith, B.E. Hamilton, G.S. Increased flow speed on a large East Antarctic outlet glacier caused by subglacial floods. Nature Geoscience. 1: 837-31. 2008.

Stehman, S.V. Wickham, J.D. Pixels, blocks of pixels, and polygons: Choosing a spatial unit for thematic accuracy assessment. Remote Sensing of the Environment. 115(12): 3044-55. 2011.

Stevens, L.A. Behn, M.D. Das, S.B. Joughin, I. Noel, B.P. Broeke, M.R. Herring, T. Greenland Ice Sheet flow response to runoff variability. Geophys. Res. Lett. 43: 11295-303. 2016.

Stevens, L.A. Behn, M.D. McGuire, J.J. Das, S.B. Joughin, I. Herring, T. Shean, D.E. King, M.A. Greenland supraglacial lake drainages triggered by hydrologically induced basal slip. Nature. 522: 73-76. 2015.

Stokes, C.R. Clark, C.D. Geomorphological criteria for identifying Pleistocene ice streams. Annals of Glaciology. 28: 67-74. 1999.

Stokes, C.R. Clark, C.D. Are long subglacial bedforms indicative of fast ice flow? Boreas. 31(3): 239-49. 2002.

Stokes, C.R. Clark, C.D. The Dubawnt Lake palaeo-ice stream: evidence for dynamic ice sheet behaviour on the Canadian Shield and insights regarding the controls on ice-stream location and vigour. Boreas. 32(1): 263-79. 2003a.

Stokes, C.R. Clark, C.D. Laurentide ice streaming on the Canadian Shield: A conflict with the soft-bedded ice stream paradigm? Geology. 31(4): 347-50. 2003b.

Stokes, C.R. Clark, C.D. Evolution of late glacial ice-marginal lakes on the northwestern Canadian Shield and their influence on the location of the Dubawnt Lake palaeo-ice stream. 215: 155-71. 2004.

Stokes, C.R. Clark, C.D. Lian, O.B. Tulaczyk, S. Geomorphological map of ribbed moraines on the Dubawnt Lake Palaeo-Ice Stream bed: A signature of Ice Stream shut-down? Journal of Maps (2:1): 1-9. 2006.

Stokes, C.R. Tarasov, L. Blomdin, R. Cronin, T.M. Fisher, T.G. Gyllencreutz, R. Hättestrand, C. Heyman, J. Hindmarsh, R.C.A. Hughes, A.L.C. Jakobsson, M. Kirchner, N. Livingstone, S.J Margold, M. Murton, J.B. Noormets, R. Peltier, W.R. Peteet, D.M. Piper, D.J.W. Preusser, F. Renssen, H. Roberts, D.H. Roche, D.M. Saint-Ange, F. Stroeven, A.P. Teller, J.T. On the reconstruction of palaeo-ice sheets: Recent advances and future challenges. Quaternary Science Reviews. 125: 15-49. 2015.

Stokes, C.R. Lian, O.B. Tulaczyk, S. Clark, C.D. Superimposition of ribbed moraines on palaeo-ice stream bed: implications for ice stream dynamics and shutdown. Earth Surface Processes and Landforms. 33: 593-609. 2008.

Stokes, C. R., Margold, M., Clark, C. D. Tarasov, L. Ice stream activity scaled to ice sheet volume during Laurentide Ice Sheet deglaciation. Nature, 530: 322-326. 2016.

Stokes, C.R. Sanderson, J.E. Miles, B.W.J. Jamieson, S.S.R. Leeson, A.A. Widespread distribution of supraglacial lakes around the margin of the East Antarctic Ice Sheet. Scientific Reports. 9. 2019.

Stokes, C.R. Spagnolo, M. Clark, C.D. The composition and internal structure of drumlins: Complexity, commonality, and implications for a unifying theory of their formation. Earth Science Reviews. 107(3-4): 398-422. 2011.

Stokes, C.R. Spagnolo, M. Clark, C.D. Ò Cofaigh, C. Lian, O.B. Dunstone, R.B. Formation of mega-scale glacial lineation on the Dubawnt Lake Ice Stream bed: 1. Size, shape and spacing from a large remote sensing dataset. Quaternary Science Reviews. 77: 190-209. 2013.

St-Onge, D.A. Surficial deposits of the Redrock Lake area, District of Mackenzie; in Current Research, Part A, Geological Survey of Canada, Paper 84 (1A). 271-78. 1984.

Storrar, R. D., Ewertowski, M., Tomczyk, A., Barr, I. D., Livingstone, S. J., Ruffell, A., Stoker, B. Evans, D. J. A. Equifinality and preservation potential of complex eskers. Boreas. 2020.

Storrar, R.D. Livingstone, S.J. Glacial geomorphology of the northern Kivalliq region, Nunavut, Canada, with an emphasis on meltwater drainage systems. J. Maps. 13: 153-64. 2017.

Storrar, R.D. Stokes, C.R. Evans, D.J.A. A map of large Canadian eskers from Landsat imagery. Journal of Maps. 3: 456-73. 2013.

Storrar, R.D. Stokes, C.R. Evans, D.J.A. Morphometry and pattern of a large sample (> 20,000) of Canadian eskers and implications for subglacial drainage beneath ice sheets. Quaternary Science Reviews. 105: 1 – 25. 2014a.

Storrar, R.D., Stokes, C.R. Evans, D.J.A. Increased channelization of subglacial drainage during deglaciation of the Laurentide Ice Sheet. Geology. 42(3). 239–42. 2014b.

Stroeven, A. P., Hättestrand, C., Kleman, J., Heyman, J., Fabel, D., Fredin, O., Goodfellow, B. W., Harbor, J. M., Jansen, J. D., Olsen, L., Caffee, M. W., Fink, D., Lundqvist, J., Rosqvist, G. C., Strömberg, B. Jansson, K. N. Deglaciation of Fennoscandia. Quaternary Science Reviews, 147, 91-121. 2016.

Strömberg, B. Calving bays, striae and moraines at Gysinge-Hedesunda, central Sweden. Geogr. Annaler. A. 63: 149-54. 1981.

Sugden, D.E. Denton, G.H. Marchant, D.R. Subglacial meltwater channels systems and ice sheet overriding, Asgard Range, Antarctica. Geographical Annals Series A Physical Geography. Physical Geography. 73(2): 109-21. 1991.

Swift, D.A. Nienow, P.W. Spedding, N. Hoey, T,B, Geomorphic implications of subglacial drainage configuration: rates of basal sediment evacuation controlled by seasonal drainage system evolution. Sedimentary Geology. 149. 5-19. 2002.

Swift, D.A. Nienow, P.W. Hoey, T.B. Basal sediment evacuation by subglacial meltwater: suspended sediment transport from Haut Glacier d'Arolla, Switzerland. Earth Surface Processes and Landforms. 30: 867-83. 2005a.

Swift, D.A. Nienow, P.W. Hoey, T.B. Mair, D.W.F. Seasonal evolution of runoff from Haut Glacier d'Arolla, Switzerland and implications for glacial geomorphic processes. Journal of Hydrology. 309: 133-48. 2005b.

Tedesco, M. Willis, I.C. Hoffman, M.J. Banwell, A.F. Alexander, P. Arnold, N.S. Ice dynamic response to two modes of surface lake drainage on the Greenland ice sheet. Environmental Research Letters. 8(3). 2013.

Tedstone, A.J. Nienow, P.W. Gourmelen, N. Dehecq, A. Goldberg, D. Hanna, E. Decadal slow-down of a land-terminating sector of the Greenland Ice Sheet despite warming. Nature. 526: 692 – 95. 2015.

Tedstone, A.J. Nienow, P.W. Gourmelen, N. Sole, A.J. Greenland ice sheet annual motion insensitive to spatial variations in subglacial hydraulic structure. Geophysical Research Letters. 41: 8910-17. 2014.

Tedstone, A.J. Nienow, P.W. Sole, A.J. Mair, D.W. Cowton, T.R. Bartholomew, I.D. et al. Greenland ice sheet motion insensitive to exceptional meltwater forcing. Proceedings of the National Academy of Sciences of the United States of America. 110(49). 19719–24. 2013.

Trommelen, M.S. Ross, M. Ismail, A. Ribbed moraines in northern Manitoba, Canada: characteristics and preservation as part of a subglacail bed mosaic near the core regions of ice sheets. Quaternary Science Reviews. 87: 135-55. 2014.

Tsai, D.M. Hsieh, C.Y. Automated surface inspection for directional textures. Image and Vision Computing. 18:49-62. 1999.

Tuckett, P.A. Ely, J.C. Sole, A.J. Livingstone, S.J. Davison, B.J. Melchior van Wessem, J. Howard, J. Rapid accelerations of Antarctic Peninsula outlet glaciers driven by surface melt. Nature Communications. 10:4311. 2019.

Tulaczyk, S. Kamb, B.W. Engelhardt, H.F. Basal mechanics of Ice Stream B, West Antarctica 2. Undrained plastic bed model. Journal of Geophysical Research. 105: 483-94. 2000.

Tylmann, K. Piotrowski, J.A. Wysota, W. The ice/bed interface mosaic: deforming spots intervening with stable areas under the fringe of the Scandinavian Ice Sheet at Samplawa, Poland. Boreas. 42. 428-41. 2013.

Utting, D.J., Ward, B.C. Little, E.C. Genesis of hummocks in glaciofluvial corridors near the Keewatin Ice Divide, Canada. Boreas. 38(3). 471–481. 2009.

Van Buren, D. Fourier removal of stripe artefacts in IRAS images. Astronomical Journal. 94: 1092- 94. 1987.

van der Veen, C.J. Fracture mechanics approach to penetration of surface crevasses on glaciers. Cold Regions Science and Technology. 27(1): 31-47. 1998.

van der Veen, C.J. Fracture propagation as means of rapidly transferring surface meltwater to the base of glaciers. Geophysical Research Letters. 34. 2007.

van der Vegt, P., Janszen, A. Moscariello, A. Tunnel valleys: current knowledge and future perspectives. Geological Society, London, Special Publications. 368(1). 75–97. 2012.

van de Wal, R.S.W. Boot, W. Van den Broeke, M.R. Smeets, C.J.P.P. Reijmer, C.H. Donker, J.J.A. et al. Large and rapid melt-induced velocity changes in the ablation zone of the Greenland Ice Sheet. Science. 321. 111-13. 2008.

van de Wal, R.S.W. Smeets, C.J.P.P. Boot, W. Stoffelen, M. van Kampen, R. Doyle, S.H. Wilhelms, F. van den Broeke, M.R. Reijmer, C.H. Oerlemans, J. Hubbard, A. Self-regulation of ice flow varies across the ablation area in south-west Greenland. Cryospehre. 9: 603-11. 2015.

Vaughan, D.G. Relating the occurrence of crevasses to surface strain rates. Journal of Glaciology. 39(132). 1993.

Vaughan, D.G. Corr, H.F.J. Smith, A.M. Pritchard, H.D. Shepherd, A. Flow-switching and water piracy between Rutford Ice Stream and Carlson Inlet, West Antarctica. Journal of Glaciology. 54(184). 2008.

Vérité, J. Ravier, É. Bourgeois, O. Pochat, S. Lelandais, T. Mourgues, R. Clark, C.D. Bessin, P. Peigné, D. Atkinson, N. Ribbed bedforms in palaeo-ice streams reveal shear margin positions, lobe shutdown and the interaction of meltwater drainage and ice velocity patterns. The Cryosphere Discuss. [preprint]. In review, 2020.

Vore, M.E. Bartholomaus, T.C. Winberry, J.P. Walter, J.I. Amundson, J.M. Seismic tremor reveals spatial organisation and temporal changes of subglacial water system. Journal of Geophysical Research. 124: 427-46. 2019.

Wagner, K. Ribbed moraines and subglacial geomorphological signatures of interior-sector palaeo-ice sheet dynamics. MSc Thesis. Department of Earth Sciences, Brock University, Ontario. 2014.

Walder, J.S. Stability of sheet flow of water beneath temperate glaciers and implications for glacier surging. Journal of Glaciology. 28(99): 273-93. 1982.

Walder, J.S. Hydraulics of subglacial cavities. Journal of Glaciology. 32(112). 439-445. 1986.

Walder, J.S. Fowler, A. Channelized subglacial drainage over a deformable bed. Journal of Glaciology. 40(134). 1994.

Ward, B.C. Dredge, L.A. Kerr, D.E. Surficial geology, Lac de Gras, District of Mackenzie, Northwest Territories (NTS 76-D): Geological Survey of Canada, 1:125 000. 1997.

Warren, W.P. Ashley, G.M. Origins of the ice-contact stratified ridges (eskers) of Ireland. Journal of Sedimentary Research. 64(3a). 433-49. 1994.

Weertman, J. General theory of water flow at the base of a glacier or ice sheet. Reviews of Geophysics and Space Physics. 10. 287-333. 1972.

Weertman, J. Birchfield, G. Stability of sheet water flow under a glacier. Journal of Glaciology. 29(103): 374-82. 1983.

Werder, M.A. Hewitt, I.J Schoof, C.G. Flowers, G.E. Modeling channelized and distributed subglacial drainage in two dimensions. Journal of Geophysical Research: Earth Surface. 118(4). .2140–58. 2013.

Wessel, P. An empirical method for optimal robust regional-residual separation of geophysical data. Journal of Mathematical Geology. 30(4): 391-408. 1998.

Wheeler, J.O. Hoffman, P.F. Card, K.D. Davidson, A. Sanford, B.V. Okulitch, A.V. Roest, W.R. Geological Map of Canada. Geological Survey of Canada, map 1860A. 1996.

Williams, C. O'Leary, M. Luckman, A. Jóhannesson, T. Murray, T. Automated crevasse mapping: assisting with mountain and glacier hazard assessment. Geophysical Research Abstracts. Vol. 20. EGU2018-5137. 2018.

Williams, J.J. Gourmelen, N. Nienow, P. Dynamic response of the Greenland ice sheet to recent cooling. Scientific Reports. 10: 1647. 2020.

Willis, I.C. Richards, K.S. Sharp, M.J. Links between proglacial stream suspended sediment dynamics, glacier hydrology and glacier motion at Midtdalsbreen, Norway. Hydrological Processes. 10: 629-48. 1996.

Willis, I.C. Sharp, M.J. Richards, K.S. Configuration of the drainage system of Midtdalsbreen, Norway, as indicated by dye-tracing experiments. Journal of Glaciology. 36(122): 89-101. 1990.

Wilson, J.T. Eskers northeast of Great Slave Lake. In: Transactions of the Royal Society of Canada. 119-30. 1939.

Wilton, D.J. Jowett, A. Hanna, E. Bigg, G.R. van den Broeke, M.R. Fettweis, X. et al. High resolution (1 km) positive degree-day modelling of Greenland ice sheet surface mass balance, 1870-2012 using reanalysis data. Journal of Glaciology. 63: 76-193. 2017.

Wingfield, R. The origin of major incision within the Pleistocene deposits of the North Sea. Marine Geology. 91: 31-52. 1990.

Wingham, D.J. Siegert, M.J. Shepherd, A. Muir, A.S. Rapid discharge connects Antarctic subglacial lakes. Nature Letters. 440(2). 2006.

Wolovick, M.J. Bell, R.E. Creyts, T.T. Frearson, N. Identification and control of subglacial water networks under Dome A, Antarctica. Journal of Geophysical Research: Earth Surface. 118)1). 2013.

Wright, H.E. Tunnel valleys, glacial surges and subglacial hydrology of the Superior Lobe, Minnesota. In: Black, R.F. Goldthwait, R.P. and Willman, H.B. (eds.) The Wisconsian Stage. Geological Society of America, Memoir. 136: 251-76. 1973.

Wright, A. Siegert, M. A fourth inventory of Antarctic subglacial lakes. Antarctic Science. 24(6): 659-64. 2012.

Yang, K. Smith, L.C. Sole, A. Livingstone, S.J. Cheng, X. Chen, Z. Li, M. Supraglacial rivers on the northwest Greenland Ice Sheet, Devon Ice Cap, and Barnes Ice Cap mapped using Sentinel-2 imagery. International Journal of Applied Earth Observation and Geoinformation. 78: 1-13. 2019.

Yu, P. Eyles, N. Sookhan, S. Automated drumlin shape and volume estimation using high resolution LiDAR imagery (Curvature Based Relief Separation): A test from the Wadena Drumlin Field, Minnesota. Geomorphology. 246: 589-601. 2015.

Zhang, X. Feng, X. Xiao, P. He, G. Zhu, L. Segmentation quality evaluation using region-based precision and recall measures for remote sensing. ISPRS Journal of Photogrammetry and Remote Sensing. 102: 73-84. 2015.

Zwally, H.J. Abdalati, W. Herring, T. Larson, K. Saba, J. Steffen, K. Surface melt induced acceleration of the Greenland Ice Sheet flow. Science. 297. 218-22. 2002.